

6-7-2018

Evolutionary and Population Dynamics of Crustaceans in the Gulf of Mexico

Laura Timm

Florida International University, ltimm004@fiu.edu

DOI: 10.25148/etd.FIDC006826

Follow this and additional works at: <https://digitalcommons.fiu.edu/etd>

 Part of the [Biology Commons](#), [Evolution Commons](#), [Genomics Commons](#), [Marine Biology Commons](#), [Molecular Genetics Commons](#), and the [Population Biology Commons](#)

Recommended Citation

Timm, Laura, "Evolutionary and Population Dynamics of Crustaceans in the Gulf of Mexico" (2018). *FIU Electronic Theses and Dissertations*. 3807.

<https://digitalcommons.fiu.edu/etd/3807>

This work is brought to you for free and open access by the University Graduate School at FIU Digital Commons. It has been accepted for inclusion in FIU Electronic Theses and Dissertations by an authorized administrator of FIU Digital Commons. For more information, please contact dcc@fiu.edu.

FLORIDA INTERNATIONAL UNIVERSITY

Miami, Florida

EVOLUTIONARY AND POPULATION DYNAMICS OF CRUSTACEANS IN THE
GULF OF MEXICO

A dissertation submitted in partial fulfillment of

the requirements for the degree of

DOCTOR OF PHILOSOPHY

in

BIOLOGY

by

Laura E. Timm

2018

To: Dean Michael R. Heithaus
College of Arts, Sciences and Education

This dissertation, written by Laura E. Timm, and entitled Evolutionary and Population Dynamics of Crustaceans in the Gulf of Mexico, having been approved in respect to style and intellectual content, is referred to you for judgment.

We have read this dissertation and recommend that it be approved.

Jose Eirin-Lopez

Mauricio Rodriguez-Lanetty

Eric von Wettberg

Wensong Wu

Heather Bracken-Grissom, Major Professor

Date of Defense: June 7, 2018

The dissertation of Laura E. Timm is approved.

Dean Michael R. Heithaus
College of Arts, Sciences and Education

Andrés G. Gil
Vice President for Research and Economic Development
and Dean of the University Graduate School

Florida International University, 2018

© Copyright 2018 by Laura E. Timm

All rights reserved.

DEDICATION

This dissertation is dedicated to all my teachers, most especially my mother (who began teaching me at birth and has not stopped yet). My teachers are many and most are neither teachers nor mentors by profession. A few of them are blood relatives; a few others will always be my family, regardless of the genetic distance. They range in age and background and most do not play nice. Six of them did not live to see this come to fruition. This is for all of them.

And it is paltry repayment for what they gave me.

ACKNOWLEDGMENTS

This dissertation would not have been possible without the input and assistance of many people. My advisor, Dr. Heather Bracken-Grissom provided tireless support as a mentor, role model, and scientist. Moreover, she taught me how to do these things for myself, as well as countless other skills spanning the realms of research, writing, and thinking; for which she has my sincerest gratitude. I also thank the member of my committee: Dr. Eirin-Lopez, who taught me the basics of epigenetics and the importance of considering its effects when interpreting results; Dr. Mauricio Rodriguez-Lanetty, who provided valuable insight into transcriptomics and the other directions my research could take; Dr. Eric von Wettberg, whose guidance in the realm of population genetics was always timely and helpful; and Dr. Wensong Wu, who provided some of the best statistical instruction I have ever encountered. I am grateful to Dr. Joan Browder, Mr. Tom Jackson, Ms. Shaina Simon, and Dr. Ian Zink for their contributions to Chapter III. Chapter IV was made possible by specimen donation from Dr. Michael Heithaus and Dr. Dean Grubbs, and assistance from Dr. Diana Churchill and Ms. Barbara Moahamad. I also extend thanks to the Deep Pelagic Nekton Dynamics of the Gulf of Mexico (DEEPEND) consortium. I count the opportunity to work with this collection of world-class researchers, who contributed advice and earnest feedback, as one of the best parts of my graduate school experience. I learned to be a scientist in DEEPEND. Specifically, the research presented in Chapter V would not have been possible without the mentorship of Dr. Tammy Frank, who taught me to identify midwater Gulf crustaceans at sea. Dr. Tracey Sutton, Ms. April Cook, Dr. Matt Johnston, and Dr. Rosanna Milligan were instrumental in keeping me oriented in the wealth of metadata resulting from each

DEEPEND cruise, as well as navigating the Gulf of Mexico Research Initiative's Information & Data Cooperative, for which they deserve special recognition here. Likewise, the members of the Point Sur crew and Mr. Gray Lawson, the MOC10 net operator, provided the necessary support to collect the specimens used in Chapter V. Across all chapters of this dissertation, Dr. Emily Warschefsky and my CRUSTOMICS lab mates provided support, advice, and encouragement. Bioinformatics advice was provided by Mr. Joseph Ahrens and Mr. Jordon Rahaman in the Siltberg-Liberles' lab, and computational support for FIU's High Performance Computing Cluster was readily provided by Dr. Cassian D'Cunha. My lab assistants, Ms. Barbara Moahamad and Ms. Lys Isma, were invaluable assets in the lab. They contributed greatly to this work through their dedication and hard work. I thank the Gulf of Mexico Research Initiative, which funded the majority of my research through the DEEPEND consortium. Moreover, the annual Gulf of Mexico Oil Spill and Ecosystem Sciences Conference provided me an international audience with whom to share my research. Finally, I thank Florida International University. Through fellowships and travel grants, FIU has nurtured my career and provided me the space, time, and resources to pursue my passion for science without starving. Thank you.

ABSTRACT OF THE DISSERTATION
EVOLUTIONARY AND POPULATION DYNAMICS OF CRUSTACEANS IN THE
GULF OF MEXICO

by

Laura E. Timm

Florida International University, 2018

Miami, Florida

Professor Heather Bracken-Grissom, Major Professor

Evolution occurs and can be conceptualized along a spectrum, bounded on one extreme by the relationships between deep lineages – such as phyla, classes, and orders – and on the other by the molecular dynamics of operational taxonomic units within a species, defined as population genetics. The purpose of this dissertation was to better understand the evolutionary and population dynamics of crustaceans within the Gulf of Mexico. In the second chapter of my dissertation, I provide a guide to best phylogenetic practice while reviewing infraordinal relationships within Decapoda, including the promise held by next-generation sequencing (NGS) approaches such as Anchored Hybrid Enrichment. Chapter III is a phylogenetic study of species relationships within the economically important shrimp genus, *Farfantepenaeus*, targeting three mitochondrial genes and uncovering an intriguing pattern of latitudinal speciation. As the first inclusive molecular phylogeny of the genus, we find support for the newly described species *F. isabellae*, but a lack of support for the species status of *F. notialis*. Additionally, our results suggest the existence of two distinct subspecies of *F. brasiliensis*. Chapter IV investigates the relative impacts of habitat heterogeneity and the presence of a possible glacial refugium in

determining population dynamics of the Giant Deep-Sea Isopod, *Bathynomus giganteus* in the northern Gulf of Mexico. Through hybrid population genetics/genomics analyses and Bayesian testing of population models, we find strong evidence for habitat heterogeneity determining population dynamics for this charismatic deep-sea invertebrate. Chapter V further investigates the role of environment in determining and maintaining genetic diversity and population connectivity, specifically focused on establishing biological baselines with which we can diagnose health and resilience of the Gulf of Mexico. This was accomplished through a comparative NGS population genomics study of three species of mesopelagic crustaceans: *Acanthephyra purpurea*, *Systellaspis debilis*, and *Robustosergia robusta*. While diversity and connectivity differs in each species, the comparative results bespeak the importance of access to the Gulf Loop Current in determining and maintaining population dynamics. Overall, my work significantly contributes to our knowledge of Crustacea at the phylogenetic- and population genetic-level.

TABLE OF CONTENTS

CHAPTER	PAGE
PREFACE	1
I. INTRODUCTION	3
LITERATURE CITED	10
II. THE FOREST FOR THE TREES: EVALUATING MOLECULAR PHYLOGENIES WITH AN EMPHASIS ON HIGHER-LEVEL DECAPODA	17
ABSTRACT	18
INTRODUCTION: ENTER THE DECAPODA	19
PART I: A BRIEF HISTORY OF DECAPOD CLASSIFICATION AND PHYLOGENY AS DETERMINED BY MORPHOLOGY	20
PART II: THE DAWN OF MOLECULAR METHODS AND EVALUATING THE FOREST OF TREES	22
PART III: A REVIEW OF HIGHER-LEVEL DECAPOD MOLECULAR PHYLOGENIES	35
FUTURE DIRECTIONS	42
CONCLUSIONS	44
ACKNOWLEDGEMENTS	45
LITERATURE CITED	46
Tables	63
Figure Captions	74
Figures	75
Appendices Captions	78
Appendices	79
III. A TREE MONEY GROWS ON: THE FIRST INCLUSIVE MOLECULAR PHYLOGENY OF ECONOMICALLY IMPORTANT PINK SHRIMP (DECAPODA: FARFANTEPENAEUS) REVEALS CRYPTIC DIVERSITY	84
ABSTRACT	85
INTRODUCTION	86
METHODS	89
RESULTS	94
DISCUSSION	98
CONCLUSIONS	107
FUTURE WORK	108
ACKNOWLEDGEMENTS	108
LITERATURE CITED	109
Tables	115

Figure Captions	118
Figures.....	119
Appendices Captions	123
Appendices.....	124
IV. BATHYNOMUS GIGANTEUS (ISOPODA: CIROLANIDAE) AND THE CANYON: A POPULATION GENETICS ASSESSMENT OF DE SOTO CANYON AS A GLACIAL REFUGIUM FOR THE GIANT DEEP-SEA ISOPOD	132
ABSTRACT.....	133
INTRODUCTION	134
METHODS	138
RESULTS	143
DISCUSSION.....	147
CONCLUSIONS.....	153
ACKNOWLEDGEMENTS	154
LITERATURE CITED	155
Tables.....	163
Figure Captions.....	169
Figures.....	171
Appendices Captions	175
Appendices.....	176
V. EFFECTS OF DIEL VERTICAL MIGRATION AND THE GULF LOOP CURRENT ON POPULATION DYNAMICS OF MESOPELAGIC SHRIMPS IN THE GULF OF MEXICO	184
ABSTRACT.....	185
INTRODUCTION	185
METHODS	191
RESULTS	197
DISCUSSION.....	201
CONCLUSIONS.....	207
ACKNOWLEDGEMENTS	207
LITERATURE CITED	208
Tables.....	213
Figure Captions.....	218
Figures.....	222
Appendices Captions	231
Appendices.....	232
VI. CONCLUSIONS AND FUTURE DIRECTIONS.....	242
LITERATURE CITED	248
VITA.....	251

LIST OF TABLES

TABLE		PAGE
 CHAPTER II		
1	The gene markers and out-group(s) used in higher-level (Infraorder) decapod phylogeny studies to date.....	63
 CHAPTER III		
1	Number of individuals included in the study, including the total number and the number of de novo sequences generated (reported in parentheses).....	115
2	The primer pairs and annealing temperatures associated with PCR amplification of three mitochondrial genes used in this study	116
3	Genetic distances between species are presented for a lumped analysis (below the diagonal), in which <i>F. brasiliensis</i> is analyzed as a single species, and a split analysis (above the diagonal), in which <i>F. brasiliensis</i> is divided into the two subclades suggested by the concatenated phylogram. Values are from COI data. Values below 0.03 are indicated with *	117
 CHAPTER IV		
1	Custom-made, sample-specific barcoded adapters used in the study. The first column lists the two individual specimens associated with each barcode, differentiated by Illumina i7 internal index. Both strands of each adapter are given (1.1 and 1.2) in the 5' to 3' direction. These strands are annealed prior to ligation to the ddRADseq fragments. The barcode section of the adapter is underlined	163
2	Sampling effort for each data type and region. The number of individuals (N), number of single nucleotide polymorphisms (SNPs), and haplotypes are given for De Soto Canyon (DC) and the regions lying east and west of the canyon (eDC and wDC, respectively)	164
3	Results of the hierarchical AMOVAs conducted to characterize genetic variation among individuals ($F_{IT} = 98.5\%$), among individuals within populations ($F_{IS} = 0\%$), and among populations ($F_{ST} = 1.5\%$). The Infinite Allele Model was used with 999 permutations to assess statistical significance. Any missing data was replaced with randomly drawn alleles determined by the overall allele frequencies of the data set. The Concatenated Sanger AMOVA yielded statistically significant results ($p = 0.048$). AMOVA results indicate the vast majority of variance is due to differences between individuals (F_{IT}), regardless of the region from which they were sampled. * indicates $p\text{-value} < 0.05$	165

4	Inter-population genetic distances between the De Soto Canyon (DC), and the regions lying east and west of the canyon (eDC and wDC, respectively) are reported below the diagonal. P-values are reported above the diagonal.....	166
5	Diversity metrics, nucleotide diversity (π) and haplotype diversity (h), and Tajima's D and significance value for each population in each dataset. * indicates p-values <0.05; ** indicates p-values < 0.01 (Dsim < Dobs, 1000 simulations). Diversity values from previous studies of molecular diversity in marine invertebrates, specifically bivalves, are also reported. For these previous studies, the sample size (N) is given in place of "region"	167
6	Models tested in MIGRATE-N and their associated thermodynamically integrated log marginal likelihood (lmL). Results presented here are from the 20,000-step runs. Populations are put in parentheses and the symbols between them indicate the direction of migration (<, >, or <>) or its absence (x). The direction listed before (wDC) indicates direction between eDC and wDC. When two populations are listed within the same set of parentheses, e.g. (wDC+DC), it means that individuals collected from these two regions are treated as a single population. Models are listed in order of decreasing lmL.....	168

CHAPTER V

1	The primer pairs and annealing temperatures associated with PCR amplification of two mitochondrial genes targeted for DNA barcoding of samples included in the ddRADseq library preparations.....	213
2	Details of ddRADseq protocol for each species, including enzymes, custom-made barcoded-adapter sequences, and size selection schemes. Both strands of each adapter are given (1.1 and 1.2) in the 5' to 3' direction. These strands are annealed prior to ligation to the ddRADseq fragments. The barcode section of the adapter is underlined. Note that the overhang in the 1.1 strands differs between the "oplo" and the "flex" adapters. Illumina i7 adapters were also used, specifically index 1, 3, 7, 12, 13, 16, 21, 24, 29, 37, 42, and 43.....	214
3	Diversity indices, including the inbreeding coefficient (Gis), observed heterozygosity (Ho), and expected heterozygosity (He), for the three targeted species: <i>Acanthephyra purpurea</i> , <i>Systellaspis debilis</i> , and <i>Robustosergia robusta</i>	216
4	Results of testing for correlation between surface/epipelagic abundance ("SA", here defined as above 600m) and three diversity metrics: inbreeding coefficient (Gis), expected heterozygosity (He), and observed heterozygosity (Ho) . R ² is taken from the trendline and has been discussed in a previous figure. Pearson's index ranges from -1 (strong negative/indirect correlation) to 1 (strong positive/direct correlation) with values closer to 0 indicating	

weak correlation. However, Pearson is a parametric test. As our data are not normally distributed, Spearman's r_s and Kendall's τ (non-parametric tests) were also carried out. Spearman's r_s is interpreted in the same way as Pearson's index, but when $|r_s| > 0.5$, the correlation is considered strong. Here, this is indicated with *. Kendall's τ is compared to a critical value. When $|\tau| >$ critical value, correlation is not significant ("Not sig", in table). When $|\tau| \leq$ critical value, correlation is significant ("Sig").....217

LIST OF FIGURES

FIGURE		PAGE
CHAPTER II		
1	Phylogenetic trees of infraordinal decapod phylogeny including: A, Dixon et al. (2003) morphological analysis; B, Scholtz and Richter (1995) meta-analysis. Major molecular studies include: C, Crandall et al. (2003) analysis of 18S; D, Ah Yong and O’Meally (2004) analysis of 16S, 18S, 28S, and morphological characters; E, Porter et al. (2005) analysis of 16S, 18S, 28S, and H3; F, Tsang et al. (2008a) analysis of PEPCCK and NAK; G, Bracken et al. (2009a) analysis of 16S, 18S, 28S, and H3; H, Toon et al. (2009) analysis of 12S, 16S, 18S, 28S, H3, EF-2, EPRS, and TM9sf4; I, Bracken et al. (2010) analysis of 16S, 18S, 28S, and H3; J, Qian et al. (2011) analysis of whole mt-genome; K, Bybee et al. (2011a) analysis of 12S, 16S, 18S, 28S, H3, and COI; L, Shen et al. (2013) analysis of whole mt-genome.....	74
2	An illustration of a species tree (depicted with double-lines) compared to four arbitrary single-gene trees. While the true species tree is always the same, the gene trees recapitulate different relationships when samples from the same species groups	74
3	An illustration of long-branch attraction (LBA), in which distantly related taxa have accrued so many differences that they cluster together. In this figure, species A and D are truly distantly-related (left tree), but cluster together due to LBA (right tree). Figure adapted from Forterre and Philippe (1999).....	74
CHAPTER III		
1	For each species, the thelycum (left) and petasma (right) are shown. Species’ name colors correspond to colors used on gene trees, distribution maps, and the phylogeny. Illustrations are adapted from the FAO key (FAO, 1983) and Tavares & Gusmão, 2017	118
2	Commonly used morphological features for identifying species of <i>Farfantepenaeus</i> : A) overhead view of carapace dorsal surface, B) lateral view of one half of petasma, C) overhead view of sternites XIII and XIV and thelycum (specimen from Little Bahama Bank), C’) thelycum as viewed in C (specimen from Brazil), D) lateral view posterior 6 th pleonite (i.e., abdominal somite) posterior margin (specimen from Camocin, Brazil), and D’) lateral view of 6 th pleonite posterior (specimen from Saint Augustine, Florida, USA). Highlighted anatomical characters described in the text: 1) dexter adrostral sulcus, 2) rostrum, 3) postrostral crest, 4) adrostral carina, 5) epigastric tooth,	

- 6) terminus of ventral costa, 7) ventrolateral lobe, 8) distomarginal spines, 9) median lobe, 10) distomeduab projection, 11) proxomedian projection of the median lobe, 12) lateral plates, 13) posterior process, 14) anterior process (hidden by lateral plates), 15) median carina, 16) dorsolateral sulcus, and 17) dorsomedian keel. Depicted specimen is *F. brasiliensis*, the selected type specimen for the genus (Burukovsky 1997). Illustrations adapted from Pérez-Farfante (1988). Scales: A = 10 mm, B-D' = 3 mm118
- 3 Bayesian phylogram based on concatenated molecular data (12S+16S+COI). Vertical colored bars represent species and the black vertical bar denotes outgroups. Clades are designated by gray brackets which connect to color-coded distribution maps. Support values (Bayesian posterior probabilities/maximum likelihood bootstrap) are noted above each branch118
- 4 From left to right: Single-gene phylograms for 12S, 16S, and COI, including an expanded view of the *Farfantepenaeus brasiliensis* N and S clades from the COI tree. Nodes supported by Bayesian posterior probabilities >0.9 and bootstrap support >70 are denoted with * above each branch118

CHAPTER IV

- 1 A bathymetric map of sampling sites. Warmer colors denote shallower depths. Collection sites are marked with white points and circles indicate grouping of collection sites across three geographic areas: western De Soto, De Soto Canyon, and eastern De Soto. This map was derived from the “Bathymetry of the Gulf of Mexico and Adjacent Areas of the Caribbean Sea and Atlantic Ocean in Shaded Relief” figure within the International Bathymetric Chart of the Caribbean Sea and Gulf of Mexico (IBCCA) map set, under the National Oceanic and Atmospheric Administration’s National Geophysical Data Center (NOAA NGDC).....169
- 2 Multi-dimensional scaling plots as heat maps built from MAFFT-aligned concatenated Sanger data (left); as well as the plot rendered from 2380 SNPs identified with ddRADseq (right). See Supplementary Materials for Methods and Results of ddRADseq. In the heat maps, higher density of individuals is denoted with warmer colors. In both plots, individuals are clustered based on genetic distance. Note the difference in scale between plots. Across plots, we do not see evidence of genetic differentiation169
- 3 Percent of shared haplotypes (found across regions) and endemic haplotypes (number of unique endemic haplotypes/total number of haplotypes) found within the study area are presented in the bar chart on the left. Note that East De Soto Canyon contains the highest percent of endemic haplotypes across

loci. Shared haplotypes are further divided in the pie chart to the right. The 13 shared haplotypes found in the data are expressed as percentages shared between: all regions (wDC-DC-eDC = 6), West De Soto Canyon and De Soto Canyon (wDC-DC = 0), De Soto Canyon and East De Soto Canyon (DC-eDC = 6), and West De Soto Canyon and East De Soto Canyon (wDC-eDC = 1)169

- 4 On the left are Tajima’s D values for each species. * indicates $p < 0.05$. ** indicates $p < 0.01$. All values indicate population growth and, with the exception of wDC, all are statistically significant. To the right of the Tajima’s D graph are four Extended Bayesian Skyline Plots (EBSPs) generated in BEAST. Top to bottom: West De Soto Canyon + De Soto Canyon + East De Soto Canyon, West De Soto Canyon, De Soto Canyon, and East De Soto Canyon. The horizontal axis describes time (in thousands of years) and the vertical axis measures population size. In these visual representations of the EBSP posterior samples for each analysis: the solid lines define the 95% central posterior density (CPD) and the dotted line traces the median value over time. Note that all regions experienced population growth, individually and overall (in agreement with the Tajima’s D values). Population growth was most dramatic in the analysis of all samples (ALL, top), which was expected. By region, population growth was fastest in the east (EDC, bottom) and slowest in the west (WDC, second from the top).....170

CHAPTER V

- 1 The general route of the Gulf Loop Current in the Gulf of Mexico. Image taken from NASA’s Earth Observatory/U.S. Naval Research Laboratory. Arrows indicate direction of flow and colors represent speed with warmer colors denoting faster speeds (see legend).....218
- 2 Results taken from Timm & Judkins et al., 2018. TOP: the targeted species, from left-to-right, *Cranchia scabra* Leach, 1817, *Pyroteuthis margaritifera* (Rüppell, 1884), and *Vampyroteuthis infernalis* Chun, 1903 (Photo credit: Dr. Danté Fenolio). MIDDLE: relative abundance, indicated by bar length, is plotted by depth (in meters) and solar cycle (“Day” is represented by gray or white bars to the left; “Night” is represented by black bars to the right). BOTTOM: results of Principal Component Analyses are presented for each species. For the species with high surface abundance (*C. scabra* and *P. margaritifera*), individuals form a single cluster within the PCA. However, *V. infernalis*, which has low surface abundance forms two non-basin-specific clusters218
- 3 TOP: from left-to-right, three species of mesopelagic shrimp targeted in this study, including the oplophorids *Acantheephyra purpurea* A. Milne-Edwards,

	1888 and <i>Systellaspis debilis</i> (A. Milne-Edwards, 1888), and the sergestid <i>Robustosergia robusta</i> (Smith, 1882) (Photo credit: Dr. Danté Fenolio). BOTTOM: relative abundance, indicated by bar length, is plotted by depth (in meters) and solar cycle (“Day” is represented by gray or white bars to the left; “Night” is represented by black bars to the right)218	
4	A map of sites sampled over the course of four Deep Pelagic Nekton Dynamics of the Gulf of Mexico (DEEPEND) cruises which took place in 2015 and 2016.....219	
5	This graph depicts the different diversity indices (observed heterozygosity in blue, expected heterozygosity in green, and inbreeding coefficient in grey) for <i>Acanthephyra purpurea</i> , <i>Systellaspis debilis</i> , and <i>Robustosergia robusta</i>219	
6	Across the top, diversity (reported as expected heterozygosity) is compared between basins (Atlantic in grey, Florida Straits in blue, and Gulf of Mexico in pink) for <i>Acanthephyra purpurea</i> , <i>Systellaspis debilis</i> , and <i>Robustosergia robusta</i> . Below, three diversity indices (observed heterozygosity, expected heterozygosity, and inbreeding coefficient) are given for each basin. The red-themed graph depicts interbasin diversity for <i>A. purpurea</i> , blue-themed for <i>S. debilis</i> , and purple-themed for <i>R. robusta</i>219	
7	Results of the hierarchical AMOVAs conducted to characterize genetic variation among individuals ($F_{IT} = 71.9\%-83.9\%$), among individuals within populations ($F_{IS} = 11.9\%-19.4\%$), and among populations ($F_{ST} = 0\%-16.2\%$). The Infinite Allele Model was used with 999 permutations to assess statistical significance, which is reported in parentheses. Any missing data was replaced with randomly drawn alleles determined by the overall allele frequencies of the data set. AMOVA results indicate the vast majority of variance is due to differences between individuals (F_{IT}), regardless of the region from which they were sampled. * indicates p-value < 0.05219	
8	DISTRUCT plots, Principal Component Analyses (PCAs), and multidimensional scaling (MDS) heat maps for <i>Acanthephyra purpurea</i> , <i>Systellaspis debilis</i> , and <i>Robustosergia robusta</i> . TOP: Population membership plots built on k-means clustering analyses of (from left to right) <i>A. purpurea</i> , <i>S. debilis</i> , and <i>R. robusta</i> . The <i>A. purpurea</i> and <i>S. debilis</i> plots are divided into samples collected from the Atlantic, Florida Straits, and Gulf of Mexico. The <i>R. robusta</i> plot does not include any individuals from the Florida Straits. Using STRUCTURE, k = 1-7 were tested ten times each, with 20,000 generations of burn-in and an additional 200,000 MCMC generations. After analysis, the optimal k was chosen using Evanno and deltaK in STRUCTURE HARVESTER. The optimal k value is reported alongside the DISTRUCT plot. MIDDLE: PCAs plotted in R using the adegenet package. Here, we see individuals of <i>A. purpurea</i> and <i>S. debilis</i> each form a single	

cluster. Individuals of *R. robusta* form two basin-specific clusters: a cluster of individuals from the Atlantic and a cluster from the Gulf of Mexico. BOTTOM: MDS plots built on genetic distance between individuals of (from left to right) *A. purpurea*, *S. debilis*, and *R. robusta*. Plots are colored with heat maps, in which similarity is colored with warmer colors and distance is colored with colder colors. These heat maps strongly agree with the PCAs: individuals of *A. purpurea* and *S. debilis* are assigned to large single-clusters while individuals of *R. robusta* are arranged in two clusters220

- 9 TOP: species included in testing for correlation in increasing order of surface/epipelagic abundance. From left to right: *Vampyroteuthis infernalis*, *Robustosergia robusta*, *Pyroteuthis margaritifera*, *Cranchia scabra*, *Acanthephyra purpurea*, and *Systellaspis debilis*. UPPER MIDDLE: T-plots of discrete depth abundances for each species, divided by solar cycle (day to the left and night to the right). LOWER MIDDLE: Principal Component Analyses for each species. BOTTOM: graph relating genetic diversity (inbreeding coefficient [*Gis*] in blue, expected heterozygosity [*He*] in red, and observed heterozygosity [*Ho*] in purple) to abundance in the surface/epipelagic (here, we define this as above 600m). We find an indirect relationship, with diversity decreasing as the percent of individuals found in the surface/epipelagic increases. This correlation is strongest in *Ho* ($R^2=0.87$) compared to *He* ($R^2=0.49$) and *Gis* ($R^2=0.073$).....221

PREFACE

The following chapters have been or will be submitted for publication and are formatted according to journal specifications:

CHAPTER II

Timm, L. E., and Bracken-Grissom, H. D. 2015. The forest for the trees: evaluating molecular phylogenies with an emphasis on higher-level Decapoda. *Journal of Crustacean Biology*, 35, 577-592.

CHAPTER III

Timm, L. E., Browder, J., Simon, S., Jackson, T., Zink, I, and Bracken-Grissom, H. D. Submitted. A tree money grows on: the first inclusive molecular phylogeny of the economically important pink shrimp (Decapoda, *Farfantepenaeus*) reveals cryptic diversity. Submitted to *Invertebrate Systematics*.

CHAPTER IV

Timm, L. E., Moahamed, B., Churchill, D. A., and Bracken-Grissom, H. D. 2018. *Bathynomus giganteus* (Isopoda: Cirolanidae) and the canyon: a population genetics assessment of De Soto canyon as a glacial refugium for the giant deep-sea isopod. *Hydrobiologia*, 1-15.

CHAPTER V

Timm, L. E., Isma, L., & Bracken-Grissom, H. D. In prep. Effects of diel vertical migration and the Gulf Loop Current on the population dynamics of mesopelagic shrimps in the Gulf of Mexico.

CHAPTER I
INTRODUCTION

Evolution occurs along a spectrum, bounded on one extreme by the relationships between deep lineages – such as phyla, classes, and orders – and bounded on the other extreme by the molecular dynamics of operational taxonomic units within a species, defined as population genetics (Brito & Edwards, 2009; Brumfield et al., 2003). This dissertation sought to increase our understanding of crustacean evolution, specifically the impacts of the marine environment on the evolutionary history and population dynamics of decapod crustaceans, largely focusing within the Gulf of Mexico.

Order Decapoda encompasses approximately 15,000 extant species and over 3000 extinct species (De Grave et al., 2009). Morphologically, decapods are highly diverse, including crabs, lobsters, shrimp, barnacles, and hermit crabs, among others. This diversity is in part a result of the age of the order: Decapoda is hypothesized to have originated, at the earliest, in the early Cambrian and have since colonized nearly every aquatic habitat on Earth (Martin & Davis, 2001; Bracken-Grissom et al., 2013, 2014). Given the high economic importance of decapods to many global fisheries, as well as their critical role in ecosystem functions, a robust understanding of evolution in this order is crucial.

The second chapter of my dissertation serves as a guide to best phylogenetic practice while reviewing the current and historically inferred relationships between the infraorders of Decapoda Latreille, 1802 (Crustacea, Malacostraca). I particularly emphasize the power of next-generation sequencing (NGS) methods to resolve these relationships. In Chapter 3, I present a phylogenetic study of the economically important penaeid shrimp genus, *Farfantepenaeus* Burukovsky, 1997 (Decapoda, Penaeidae), targeting three mitochondrial genes. The fourth chapter of this work focuses on the

population dynamics of the Giant Deep-Sea Isopod, *Bathynomus giganteus* A. Milne-Edwards, 1879 (Isopoda, Cirolanidae), a cirolanid isopod common to the northern Gulf of Mexico. The primary goal of the study was to evaluate the status of De Soto Canyon as a glacial refugium during the last glacial maximum, while also investigating the role of habitat heterogeneity in determining population dynamics. Chapter 5 was perhaps the most ambitious undertaking described in this dissertation: this comparative population genomics study focused on using the genomic proxies genetic diversity and population connectivity to diagnose health and resilience in mesopelagic crustaceans common to the Gulf of Mexico, specifically *Acantheephyra purpurea* A. Milne-Edwards, 1881 (Decapoda, Oplophoridae), *Systemaspis debilis* (A. Milne-Edwards, 1881) (Decapoda, Oplophoridae), and *Robustosergia robusta* (Smith, 1882) (Decapod, Sergestidae). This was primarily motivated by a need to evaluate the ecological fallout of the Deepwater Horizon Oil Spill. However, in pursuit of this goal, we uncovered an intriguing negative correlation between surface/epipelagic abundance and genetic diversity.

The forest for the trees: reviewing the literature on infraordinal relationships within Decapoda

As we seek to build a comprehensive Tree of Life, many relationships lack phylogenetic resolution and different analyses recapitulate different relationships, resulting in substantial conflict among phylogenetic studies. Decapoda is no exception. Since studies of decapod phylogeny began in the late 1800s, consensus has been elusive (Calman, 1904; Dixon et al., 2003; Schram, 2003; Scholtz & Richter, 1995; Schram, 1986; Schram & Dixon, 2004; Siewing, 1963). Nearly 200 years later, emerging

molecular methods have significantly improved our understanding of the evolutionary relationships within this large, diverse group, but infraordinal relationships remain unclear (Abele, 1991; Ahyong & Meally, 2010; Bracken et al., 2009; Crandall et al., 2000; Kim & Abele, 1990; Porter et al., 2005; Qian et al., 2011; Tsang et al., 2008). In reviewing the literature, it seems this lack of resolution may be attributable to differences in four aspects of phylogenetic systematics: sampling effort, marker selection, data-recycling, and analysis. Therefore, the foundation on which a tree was built, specifically in relation to these four aspects, must be carefully evaluated prior or in concert with result interpretation (Timm & Bracken-Grissom, 2015). In the literature review presented in Chapter II, I summarize the early morphological studies of infraordinal relationships within Decapoda, identify potential sources of disagreement in molecular studies, provide a best-practices guide for phylogenetic analysis including suggestions for evaluating trees, and review the previous molecular studies. Finally, I turn my attention to NGS methods and their potential to reach the “Holy Grail” of decapod phylogeny: a phylogeny informed by and in agreement with the classification system (Schram, 2001).

A tree money grows on: the first inclusive molecular phylogeny of Farfantepenaeus

Worldwide, the penaeid shrimp genus *Farfantepenaeus*, collectively known as pink shrimp, represent a large percentage of economically important shrimp compiled NMFS Landings query, 2/28/2018), necessitating management of many species within the genus. Policy-driven species management is most effective when informed by a comprehensive understanding of the evolutionary forces driving biodiversity among and within taxa, such as that imparted by a robust phylogenetic framework (Bernatchez,

1995). In Chapter III, I present the first fully-inclusive molecular phylogeny of *Farfantepenaeus*. Gene trees were built from three targeted mitochondrial genes (12S, 16S, and cytochrome c oxidase subunit I) and a phylogeny was inferred using frequentist (maximum likelihood) and Bayesian approaches. Given the high economic importance of many species within *Farfantepenaeus*, the phylogeny constitutes a robust improvement in understanding each species' evolutionary history, which is critical for proper management.

Bathynomus giganteus and the canyon: a hybrid population genetics/genomics assessment of De Soto Canyon as glacial refugium

Earth experienced its last glacial maximum 20,000 years ago, lowering sea levels by 120m (Richmond & Fullerton, 1986). In the northern Gulf of Mexico, this left much of the continental shelf exposed (Sager et al., 1992) and greatly decreased the geographic range of many benthic species. However, the De Soto Canyon, with its maximum depth of 2100m (Coleman et al., 2014), remained connected to the greater Gulf. Chapter IV began as a population genetics effort to evaluate the potential role of De Soto Canyon as a glacial refugium in the northern Gulf of Mexico. Population genetics has gained popularity as a method to evaluate putative glacial refuge in the terrestrial realm (reviewed in Avise, 1992; Beck et al., 2008; Bernatchez & Dodson, 1991; Bernatchez & Wilson, 1998; Hewitt, 2004; Hewitt, 1996; Knowles, 2001; Lewis & Crawford, 1995; Nesbø et al., 1999; Petit, 2003; Provan & Bennett, 2008; Taberlet et al., 1998; Trewick & Wallis, 2001) and is beginning to be applied to the marine realm (Campo et al., 2009; Dömel et al., 2015; García-Merchán et al., 2012; Kearsse et al., 2012; Maggs et al., 2008;

Mäkinen & Merilä, 2008; Médail & Diadema, 2009; Palero et al., 2008; Provan & Bennett, 2008; Provan et al., 2005; Thatje et al., 2005; Zemplak et al., 2008). However, as Chapter IV developed, I began to consider the role that habitat heterogeneity, which has been identified as a key determinant in genetic diversity (Levin et al., 2001; Vanreusel et al., 2010), in maintaining population dynamics in the benthic abyss. The goal of this study was to determine whether population dynamics of the giant deep-sea isopod, *Bathynomus giganteus*, were better explained by habitat diversity or by the past presence of a marine glacial refugium in De Soto Canyon. To accomplish this I 1) measured genetic diversity in De Soto Canyon and adjacent regions, 2) characterized gene flow and connectivity between these regions, and 3) investigated historical changes to population size. In addition to the traditional Sanger sequencing approach, I also performed a next-generation sequencing pilot study using double digest Restriction site-Associated DNA sequencing (Timm et al., 2018). Overall, Chapter IV investigates population dynamics in a charismatic benthic marine invertebrate and characterizes these dynamics in terms of the current and historical environment.

Effects of diel vertical migration and the Gulf Loop Current on population dynamics of mesopelagic shrimps in the Gulf of Mexico

The Gulf of Mexico is a unique biogeographic region, distinct from adjacent basins (Backus et al., 1977; Gartner, 1988). Specifically, the mesopelagic (200m-1000m) has been described as hyper-diverse (Sutton et al., 2017), but not been well-studied (Davison et al., 2015; Robinson et al., 2010; St. John et al., 2016; Webb et al., 2010). Filling this data gap has been given high priority in recent years because of the high rate

of perturbations, both natural (Hurricane Ike and Hurricane Harvey) and anthropogenic (the Deepwater Horizon and Shell oil spills), as we seek to assess the impacts of these disturbances. In collaboration with the Deep Pelagic Nekton Dynamics of the Gulf of Mexico (DEEPEND) consortium, I aimed to inventory natural genetic variability in mesopelagic shrimp common to the Gulf midwater. To establish this “reference state” of population dynamics in the Gulf midwater, I performed a comparative population genomics study, targeting genetic diversity as a proxy for species health (Cowen & Sponaugle, 2009; Danovaro et al., 2008; Hughes & Stachowicz, 2004) and population connectivity as a proxy for species resilience (Cowen & Sponaugle, 2009; Hellberg et al., 2002). Focusing on these proxies in Chapter V, I establish biological baselines for three species of mesopelagic shrimp (*Acanthephyra purpurea*, *Systellaspis debilis*, and *Robustosergia robusta*). Additionally, I layout a hypothetical relationship between population dynamics and the Gulf Loop Current, which serves as the major avenue of transport in the eastern Gulf. Generally, Chapter V inventories natural variability and establishes biological baselines within populations and species of midwater crustacean with the long-term goal of better understanding the impacts of ecological disturbances on the Gulf ecosystem as a whole.

Intellectual Merit

My work significantly contributes to our knowledge of Crustacea at the phylogenetic- and population genetic-level. The literature review distilled the state of the field in evaluating and testing evolutionary relationships between the infraorders of Decapoda and presented a concise guide to good phylogenetic practice. This guide was

put into practice in the first comprehensive molecular phylogeny of the species within the genus *Farfantepenaeus*, an economically important target of fisheries internationally. My work in population genetics began with an investigation of the role of the unique environment and complex topography of the Gulf of Mexico on the current and historical population dynamics of the charismatic giant deep-sea isopod. This work accomplished two novel objectives: it interrogates the De Soto Canyon as a potential glacial refugium for this abyssal species, which would have important implications for the species; it also tests for an association between habitat diversity and genetic diversity. The comparative population genomics study further explores the larger, ecological implications of the population dynamics of its resident species. This chapter seeks to establish biological baselines in response to realized and future anthropogenic threats. It also infers environmental health and resilience from genomic proxies. Finally, these inferences are contextualized in terms of individual species behaviors and life histories, testing for correlations between surface abundance, genetic diversity, and ecosystem properties. Overall, my dissertation greatly furthers our understanding of evolution within Crustacea.

LITERATURE CITED

- Abele, L. G. (1991). Comparison of morphological and molecular phylogeny of the Decapoda. *Memoirs of the Queensland Museum*, 31, 101–108.
- Ahyong, S. T., & Meally, D. O. (2010). The Raffles Bulletin of Zoology 2004 Phylogeny of the Decapoda Reptantia: resolution using three molecular loci and morphology, 52(2), 673–693.
- Avise, J. C. (1992). Molecular population structure and the biogeographic history of a regional fauna: a case history with lessons for conservation biology. *Oikos*, 63, 62–76.

- Backus, R. H., Craddock, J. E., Haedrich, R. L., & Robison, B. H. (1977). Atlantic mesopelagic zoogeography. In *Memoirs of the Sears Foundation for Marine Research*, 26-286.
- Beck, J. B., Schmuths, H., & Schaal, B. A. (2008). Native range genetic variation in *Arabidopsis thaliana* is strongly geographically structured and reflects Pleistocene glacial dynamics. *Molecular Ecology*, 17, 902–915.
- Bernatchez, L. (1995). A role for molecular systematics in defining evolutionarily significant units in fishes. In *American Fisheries Society Symposium*.
- Bernatchez, L., & Dodson, J. J. (1991). Phylogeographic structure in mitochondrial DNA of the Lake Whitefish (*Coregonus clupeaformis*) and its relation to Pleistocene glaciations. *Evolution*, 45, 1016–1035.
- Bernatchez, L., & Wilson, C. C. (1998). Comparative phylogeography of Nearctic and Palearctic fishes. *Molecular Ecology*, 7, 431–452.
- Bracken, H. D., Toon, A., Felder, D. L., Martin, J. W., Finley, M., Rasmussen, J., ... Crandall, K. A. (2009). The decapod tree of life: Compiling the data and moving toward a consensus of decapod evolution. *Arthropod Systematics & Phylogeny*, 67, 99–116.
- Bracken-Grissom, H. D., Ahyong, S. T., Wilkinson, R. D., Feldmann, R. M., Schweitzer, C. E., Breinholt, J. W., Bendall, M., Palero, F., Chan, T.-Y., Felder, D. L., Robles, R., Chu, K.-H., Tsang, L.-M., Kim, D., Martin, J. W., & Crandall, K. A. (2014). The emergence of the lobsters: phylogenetic relationships, morphological evolution and divergence time comparisons of an ancient group (Decapoda: Achelata, Glypheidea, Polychelida). *Systematic Biology*, 63, 457-479.
- Bracken-Grissom, H. D., Cannon, M., Cabezas, P., Feldmann, R. M., Schweitzer, C. E., Ahyong, S. T., Felder, D. L., Lemaitre, R., & Crandall, K. A. (2013). A comprehensive and integrative reconstruction of evolutionary history for Anomura (Crustacea: Decapoda). *BMC Evolutionary Biology*, 13, 1-28.
- Brito, P., & Edwards, S. (2009). Multilocus phylogeography and phylogenetics using sequence-based markers. *Genetica*, 135, 439-455.
- Brumfield, R., Beerli, P., Nickerson, D. A., & Edwards, S. V. (2003). The utility of single nucleotide polymorphisms in inferences of population history. *Trends in Ecology and Evolution*, 18, 249-256.
- Calman, W. D. (1904). On the classification of the Crustacea Malacostraca. *Annals and Magazine of Natural History*, 13, 144–158.

- Campo, D., Molares, J., Garcia, L., Fernandez-Rueda, P., Garcia-Gonzalez, C., & Garcia-Vazquez, E. (2009). Phylogeography of the European stalked barnacle (*Pollicipes pollicipes*): Identification of glacial refugia. *Marine Biology*, *157*, 147–156.
- Coleman, F. C., Chanton, J. P., & Chassinger, E. P. (2014). Ecological connectivity in northeastern Gulf of Mexico - The Deep-C Initiative. *International Oil Spill Conference Proceedings, 2014*, 1972–1984.
- Cowen, R. K., & Sponaugle, S. (2009). Larval dispersal and marine population connectivity. *Annual Review of Marine Science*, *1*, 443–466.
- Crandall, K. A., Harris, D. J., & Fetzner, J. W. (2000). The monophyletic origin of freshwater crayfish estimated from nuclear and mitochondrial DNA sequences. *Proceedings of the Royal Society B: Biological Sciences*, *267*, 1679–1686.
- Danovaro, R., Gambi, C., Dell'Anno, A., Corinaldesi, C., Fraschetti, S., Vanreusel, A., ... Gooday, A. J. (2008). Exponential decline of deep-sea ecosystem functioning linked to benthic biodiversity loss. *Current Biology*, *18*, 1–8.
- Davison, P., Lara-Lopez, A., & Koslow, J. A. (2015). Mesopelagic fish biomass in the southern California current ecosystem. *Deep-Sea Research Part II: Topical Studies in Oceanography*, *112*, 129–142.
- De Grave, S., Pentcheff, N. D., Ahyong, S. T., Chan, T.-Y., Crandall, K. A., Dworschak, P. C., Felder, D. L., Feldmann, R. M., Fransen, C. H. J. M., Goulding, L. Y. D., Lemaitre, R., Low, M. E. Y., Martin, J. W., Ng, P. K. L., Schweitzer, C. E., Tan, S. H., Tshudy, D., & Wetzer, R. (2009). A classification of living and fossil genera of decapod crustaceans. *Raffles Bulletin of Zoology*, *21*, 1–109.
- Dixon, C. J., Ahyong, S. T., & Schram, F. R. (2003). A new hypothesis of decapod phylogeny. *Crustaceana*, *76*, 935–975.
- Dömel, J. S., Convey, P., & Leese, F. (2015). Genetic data support independent glacial refugia and open ocean barriers to dispersal for the Southern Ocean sea spider *Austropallene cornigera* (Möbius, 1902). *Journal of Crustacean Biology*, *35*, 480–490.
- García-Merchán, V. H., Robainas-Barcia, A., Abelló, P., Macpherson, E., Palero, F., García-Rodríguez, M., ... Pascual, M. (2012). Phylogeographic patterns of decapod crustaceans at the Atlantic-Mediterranean transition. *Molecular Phylogenetics and Evolution*, *62*, 664–672.
- Gartner, J. V. (1988). The lanternfishes (Pisces: Myctophidae) of the eastern Gulf of Mexico. *Fishery Bulletin*, *85*, 81–98.

- Hellberg, M. E., Burton, R. S., Neigel, J. E., & Palumbi, S. R. (2002). Genetic assessment of connectivity among marine populations. *Bulletin of Marine Science*, 70, 273–290.
- Hewitt, G. M. (1996). Some genetic consequences of ice ages, and their role in divergence and speciation. *Biological Journal of the Linnean Society*, 58, 247–276.
- Hewitt, G. M. (2004). Genetic consequences of climatic oscillations in the Quaternary. *Philosophical Transactions of the Royal Society of London. Series B, Biological Sciences*, 359, 183–195.
- Hughes, A. R., & Stachowicz, J. J. (2004). Genetic diversity enhances the resistance of a seagrass ecosystem to disturbance. *Proceedings of the National Academy of Sciences of the United States of America*, 101, 8998–9002.
- Kearse, M., Moir, R., Wilson, A., Stones-Havas, S., Cheung, M., Sturrock, S., ... Drummond, A. (2012). Geneious Basic: an integrated and extendable desktop software platform for the organization and analysis of sequence data. *Bioinformatics*, 28, 1647–1649.
- Kim, W., & Abele, L. G. (1990). Molecular phylogeny of selected decapod crustaceans based on 18S rRNA nucleotide sequences. *Journal of Crustacean Biology*, 10, 1–13.
- Knowles, L. (2001). Did the Pleistocene glaciations promote divergence? Tests of explicit refugial models in montane grasshoppers. *Molecular Ecology*, 10, 691–701.
- Levin, L. A., Etter, R. J., Rex, M. A., Gooday, A. J., Smith, C. R., Pineda, J., ... Pawson, D. (2001). Environmental influences on regional deep-sea species diversity. *Annual Review of Ecology and Systematics*, 32, 51–93.
- Lewis, P. O., & Crawford, D. J. (1995). Pleistocene refugium endemics exhibit greater allozymic diversity than widespread congeners in the genus *Polygonella* (Polygonaceae). *American Journal of Botany*, 82(2), 141–149.
- Maggs, C. A., Castilho, R., Foltz, D., Henzler, C., Jolly, M. T., Kelly, J., ... Wares, J. (2008). Evaluating signatures of glacial refugia for North Atlantic benthic marine taxa. *Ecology*, 89, S108–S122.
- Mäkinen, H. S., & Merilä, J. (2008). Mitochondrial DNA phylogeography of the three-spined stickleback (*Gasterosteus aculeatus*) in Europe—Evidence for multiple glacial refugia. *Molecular Phylogenetics and Evolution*, 46, 167–182.

- Martin, J. W., & Davis, G. E. (2001). An updated classification of the recent Crustacea. *Natural History Museum of Los Angeles County Science Series*, 39, 1-124.
- Médail, F., & Diadema, K. (2009). Glacial refugia influence plant diversity patterns in the Mediterranean Basin. *Journal of Biogeography*, 36, 1333–1345.
- Nesbø, C. L., Fossheim, T., Vøllestad, L. A., & Jakobsen, K. S. (1999). Genetic divergence and phylogeographic relationships among European perch (*Perca fluviatilis*) populations reflect glacial refugia and postglacial colonization. *Molecular Ecology*, 8, 1387–1404.
- Palero, F., Abelló, P., Macpherson, E., Gristina, M., & Pascual, M. (2008). Phylogeography of the European spiny lobster (*Palinurus elephas*): Influence of current oceanographical features and historical processes. *Molecular Phylogenetics and Evolution*, 48, 708–717.
- Petit, R. J. (2003). Glacial refugia: hot spots but not melting pots of genetic diversity. *Science*, 300, 1563–1565.
- Porter, M. L., Pérez-Losada, M., & Crandall, K. A. (2005). Model-based multi-locus estimation of decapod phylogeny and divergence times. *Molecular Phylogenetics and Evolution*, 37, 355–369.
- Provan, J., & Bennett, K. D. (2008). Phylogeographic insights into cryptic glacial refugia. *Trends in Ecology and Evolution*, 23, 564–571.
- Provan, J., Wattier, R. A., & Maggs, C. A. (2005). Phylogeographic analysis of the red seaweed *Palmaria palmata* reveals a Pleistocene marine glacial refugium in the English Channel. *Molecular Ecology*, 14, 793–803.
- Qian, G., Zhao, Q., Wang A., Zhu, L., Zhou, K., & Sun, H. (2011). Two new decapod (Crustacea, Malacostraca) complete mitochondrial genomes: bearings on the phylogenetic relationships within the Decapoda. *Zoological Journal of the Linnean Society*, 162, 471–481.
- Richmond, G. M., & Fullerton, D. S. (1986). Summation of Quaternary glaciations in the United States of America. *Quaternary Science Reviews*, 5, 183–196.
- Robinson, C., Steinberg, D. K., Anderson, T. R., Arístegui, J., Carlson, C. A., Frost, J. R., ..., Zhang, J. (2010). Mesopelagic zone ecology and biogeochemistry – a synthesis. *Deep-Sea Research Part II: Topical Studies in Oceanography*, 57, 1504-1518.
- Sager, W. W., Schroeder, W. W., Laswell, J. S., Davis, K. S., Rezak, R., & Gittings, S. R. (1992). Mississippi-Alabama outer continental shelf topographic features formed

- during the late Pleistocene-Holocene transgression. *Geo-Marine Letters*, 12, 41–48.
- Scholtz, G., & Richter, S. (1995). Phylogenetic systematics of the reptantian Decapoda (Crustacea, Malacostraca). *Zoological Journal of the Linnean Society*, 113, 289–328.
- Schram, F. R. (1986). *Crustacea*. New York: Oxford University Press.
- Schram, F. R. (2001). Phylogeny of decapods: Moving towards a consensus. *Hydrobiologia*, 449, 1–20.
- Schram, F. R., & Dixon, C. J. (2004). Decapod phylogeny: addition of fossil evidence to a robust morphological cladistic data set. *Bulletin of the Mizunami Fossil Museum*, 31, 1–19.
- Siewing, R. (1963). Studies in malacostracan morphology: Results and problems. In H. B. Whittington & W. D. I. Rolfe (Eds.), *Phylogeny and Evolution of Crustacea* (pp. 85–103). Cambridge, MA: Museum of Comparative Zoology.
- St. John, M. A., Borja, A., Chust, G., Heath, M., Grigorov, I., Mariani, P., Martin, A. P., ..., Santos, R. S. (2016). A dark hole in our understanding of marine ecosystems and their services: perspectives from the mesopelagic community. *Frontiers in Marine Science*, 3, 1-7.
- Sutton, T. T., Clark, M. R., Dunn, D. C., Halpin, P. N., Rogers, A. D., Guinotte, J., ... Heino, M. (2017). A global biogeographic classification of the mesopelagic zone. *Deep-Sea Research Part I: Oceanographic Research Papers*, 126, 85–102.
- Taberlet, P., Fumagalli, L., Wust-Saucy, A.-G., & Cossons, J.-F. (1998). Comparative phylogeography and postglacial colonization. *Molecular Ecology*, 7, 453–464.
- Thatje, S., Hillenbrand, C.-D., & Larter, R. (2005). On the origin of Antarctic marine benthic community structure. *Trends in Ecology & Evolution*, 20, 534–540.
- Timm, L., & Bracken-Grissom, H. D. (2015). The forest for the trees: evaluating molecular phylogenies with an emphasis on higher-level Decapoda. *Journal of Crustacean Biology*, 35, 577–592.
- Timm, L. E., Moahamed, B., Churchill, D. A., & Bracken-Grissom, H. D. (2018). *Bathynomus giganteus* (Isopoda: Cirolanidae) and the canyon: a population genetics assessment of De Soto Canyon as a glacial refugium for the giant deep-sea isopod. *Hydrobiologia*, 1-15.

- Trewick, S. A., & Wallis, G. P. (2001). Bridging the “beech-gap”: New Zealand invertebrate phylogeography implicates Pleistocene glaciation and Pliocene isolation. *Evolution*, *55*, 2170–2180.
- Tsang, L. M., Ma, K. Y., Ahyong, S. T., Chan, T. Y., & Chu, K. H. (2008). Phylogeny of Decapoda using two nuclear protein-coding genes: Origin and evolution of the Reptantia. *Molecular Phylogenetics and Evolution*, *48*, 359–368.
- Vanreusel, A., Fonseca, G., Danovaro, R., Da Silva, M. C., Esteves, A. M., Ferrero, T., ... Galeron, J. (2010). The contribution of deep-sea macrohabitat heterogeneity to global nematode diversity. *Marine Ecology*, *31*, 6–20.
- Webb, T. J., Berghe, E. V., & O’Dor, R. (2010). Biodiversity’s big wet secret: the global distribution of marine biological records reveals chronic under-exploration of the deep pelagic ocean. *PLoS One*, *5*, e10223.
- Zemlak, T. S., Habit, E. M., Walde, S. J., Battini, M. A., Adams, E. D. M., & Ruzzante, D. E. (2008). Across the southern Andes on fin: glacial refugia, drainage reversals and a secondary contact zone revealed by the phylogeographical signal of *Galaxias platei* in Patagonia. *Molecular Ecology*, *17*, 5049–5061.

CHAPTER II

THE FOREST FOR THE TREES: EVALUATING MOLECULAR PHYLOGENIES

WITH AN EMPHASIS ON HIGHER-LEVEL DECAPODA

ABSTRACT

Since the late 1800s, several infraordinal relationships have been proposed for Decapoda; however, reaching a consensus among higher-level relationships is proving difficult. Molecular methods were first applied to higher-level decapod phylogenetics in the 1990s and have significantly contributed to our understanding of the group: sampling is becoming more thorough, a greater number of phylogenetically informative characters are being sequenced, and analysis procedures are becoming more consistent between studies. However, relationships among the deep lineages of Decapoda remain unclear. Several phylogenetic hypotheses have been suggested, and while there is some agreement among studies, an ultimate consensus among higher-level relationships has yet to be reached. This is largely the result of differences in sampling effort, marker selection, data-recycling, and analysis. Because most studies have generated conflicting phylogenetic hypotheses, the foundation on which the tree was built (data and analysis procedures) must be considered and evaluated. In this review, we summarize the early morphological decapod studies, address common problems that are causing a lack of consensus in molecular studies, provide suggestions for evaluating molecular trees, offer tips for good phylogenetic practice, review the previous molecular studies of infraordinal decapod phylogeny, and discuss the future directions of the field, with special attention paid to next-generation sequencing (NGS) techniques.

KEY WORDS: Decapoda, data-recycling, infraorder, insufficient sampling, marker selection, molecular phylogeny, next-generation sequencing, out-group selection

INTRODUCTION: ENTER, THE DECAPODA

Decapoda Latreille, 1802 is an immense order, containing ~15,000 extant and ~3,000 extinct species, including crabs, lobsters, hermit crabs, crayfish, and shrimp (De Grave et al., 2009). The order contains a morphologically diverse group of organisms inferred to have originated in the early Cambrian, possibly earlier (Martin and Davis, 2001; Bracken-Grissom et al., 2013, 2014), and evolving over ~400 million years to colonize and exploit almost every aquatic habitat on Earth. This evolutionary experimentation has resulted in perhaps the greatest diversity in body plan, size, and habitat preference (Monod and Laubier, 1996) present in any group of crustaceans (Martin and Davis, 2001, Bracken-Grissom et al. 2013). Because of this diversity, the “propinquity of descent” (Darwin, 1859) within Decapoda is obscured.

Carcinologists continue their search for what Schram (2001) described as the “Holy Grail:” To arrive at a phylogeny that recapitulates the classification system and vice versa. Many approaches have been used to determine the origin and evolution of decapod infraorders, and morphological methods based on similarity and cladistics have generated a variety of trees (Calman, 1904; Siewing, 1963; Schram, 1986; Scholtz and Richter, 1995 – Fig. 1B; Dixon et al., 2003 – Fig. 1A). The 1990s saw the dawn of molecular phylogenetics for Decapoda; researchers began to use genetic sequence data to infer evolutionary relationships among major lineages (Kim and Abele, 1990; Abele, 1991). Molecular studies have advanced our understanding of Decapoda, but have not yet led to a consensus. Marker selection, realized sampling effort, data-recycling, and analysis ambiguities have contributed to a lack of resolution and confusion over what

constitutes a reliable phylogeny. Next-Generation Sequencing (NGS) methods, such as Targeted Amplicon Sequencing (TAS) and Anchored Hybrid Enrichment (AHE), have the potential to provide new, genome-wide perspectives on the evolution of decapods (Qian et al., 2011; Bybee et al., 2011a; Lemmon et al., 2012; Shen et al., 2013). The current NGS methods are bringing us closer to an inclusively hierarchical phylogeny, which will provide evolutionary insight into decapod biogeography, biodiversity, ecology, character evolution, reproduction, and development.

The aims of this review are to: 1) briefly summarize the morphological studies of decapods; 2) identify common analysis problems that can cause a lack of consensus; 3) present a means of evaluating the strengths and weaknesses of molecular phylogenies; 4) offer suggestions for good phylogenetic practice; 5) review the literature on higher-level decapod molecular phylogenies while evaluating them as described; 6) discuss the future directions of decapod phylogeny with specific focus on next-generation sequencing methods; and 7) compile and present a table of past and current higher taxonomic ranks of Decapoda from the literature.

PART I: A BRIEF HISTORY OF DECAPOD CLASSIFICATION AND PHYLOGENY AS DETERMINED BY MORPHOLOGY

Efforts to classify decapods began in the 1800s and resulted in two schemes of division. Milne Edwards (1834) and Boas (1880) proposed a phenetic division based on primary mode of locomotion: the benthic Reptantia and the swimming Natantia. Huxley (1878) divided the lobster and lobster-like taxa (presently recognized as Achelata Scholtz and

Richter, 1995, Astacidea Latreille, 1802, Axiidea de Saint Laurent, 1979, Gebiidea de Saint Laurent, 1979, and Polychelida Scholtz and Richter, 1995) into two groups based on gill and branchiostegite morphology: Trichobranchiata and Phyllobranchiata. At the turn of the century, Boas' system was still recognized. In a much-cited publication, Borradaile (1907) retained the Reptantia-Natantia subgroups, but revised the taxa comprising each. However, neither the Reptantia-Natantia classification system nor the Trichobranchiata-Phyllobranchiata classification system had been devised to include many fossil representatives. A study by Beurlen and Glaessner (1930), which included data from taxa represented only in the fossil record, proposed a new system. To accommodate the fossilized taxa, Trichelida and Heterochelida were introduced as the suborders within Decapoda. For the next three decades, studies focused primarily on elucidating the lower-level divisions of families and genera.

In 1963, Burkenroad published a study proposing a major restructuring of the higher-level taxonomy of Decapoda. Investigating the gill morphology evident in the eumalacostracan fossil record, he concluded that all previously proposed classification systems exhibited some degree of polyphyly. Noting "peneids" (a name used by Burkenroad to refer to non-brooding shrimp) as one of two major branches within Decapoda, he proposed Dendrobranchiata Bate, 1888 as a suborder to include this group. The second major group he proposed, which contained the majority of decapod infraorders, was Pleocyemata Burkenroad, 1963. These two groups were divided primarily by gill morphology and brooding behavior. Carcinologists have long accepted the Dendrobranchiata-Pleocyemata division, and while Natantia is no longer recognized,

Reptantia still serves as an unranked group containing crawling/walking lineages (see Boas, 1880 for full definition) (on-line Supplementary Table 1).

Several approaches have attempted to further elucidate relationships within Pleocyemata: adult morphology (Martin and Davis, 2001), larval morphology (Clark, 2009), spermiocladistics (Martin and Davis, 2001), eye morphology (Porter and Cronin, 2009), ontogeny (Martin and Davis, 2001), and parasite proxies (Boyko and Williams, 2009), to name a few. As early as the 1970s, molecular methods made thousands of characters available for analysis. Since then, molecular phylogenetic analyses have proven informative at many levels of decapod phylogeny, while also uncovering new areas of investigation.

PART II: THE DAWN OF MOLECULAR METHODS AND EVALUATING THE FOREST OF TREES

As molecular methods were adapted to elucidate decapod phylogeny, many studies proposed different evolutionary hypotheses (Fig. 1). This conflict requires standards by which phylogenies can be evaluated. The field of decapod phylogenetics, along with many other groups, is frequently subject to several potential pitfalls in study design and analysis. These pitfalls, resulting from variability or ambiguity in procedure or analysis, are often overlooked, but are very important to the strength and reliability of results. Here, we identify four such ambiguities: marker selection, realized sampling effort, data-recycling, and analysis ambiguity; and offer suggestions to navigate them.

Markers: Inappropriate or Insufficient

The traditional molecular approaches, and some next-gen methods, require the selection of genetic markers targeted and sequenced from representative taxa. Markers can originate from the mitochondrial genome or from the nuclear genome (mtDNA and nDNA, respectively; see Table 1). Both mtDNA and nDNA have advantages and disadvantages that are nontrivial.

Advantages of mtDNA.— Mitochondrial DNA generally mutates faster than nDNA (Brown et al., 1979), making mtDNA markers most informative at lower taxonomic levels, e.g., genus and species (Moore, 1995). These markers are relatively easy to amplify, as universal primers are available for many taxa (Simon et al., 1994) and encoded genes are strictly orthologous (Qian et al., 2011). Because mtDNA is haploid, recombination is rare (Birky, 2001; Elson and Lightowers, 2006). Whole mt-genomes have gained some popularity in studies of deep-level phylogeny (Fenn et al., 2008), such as in Insecta (Talavera and Vila, 2011), because nucleotide sequence, gene order (Boore and Brown, 1998), gene insertion and deletion (Rokas and Holland, 2000), and length variability (Schneider and Ebert, 2004) can provide phylogenetic information. Some argue these properties make the mt-genome one of the most information-rich markers in phylogeny (Fenn et al., 2008). However these approaches have been subject to criticism (Ballard and Whitlock, 2004; Ballard and Rand, 2005; Hurst and Jiggins, 2005; Galtier et al., 2009).

Disadvantages of mtDNA.— Mitochondrial markers are not suited to every study and there are important characteristics that must be considered. First, the increased mutation rate in mtDNA decreases time to saturation (Blouin et al., 1998), limiting the phylogenetic signal at higher taxonomic levels. Second, mtDNA is subject to mitochondrial capture, meaning introgression events in the recent past can obscure true phylogenetic relationships among close relatives (Shaw, 2002; Ballard and Whitlock, 2004; Spinks and Shaffer, 2009). Third, mtDNA is highly subject to site linkage as it does not undergo recombination (Birky, 1995; Avise, 2000; Ballard and Whitlock, 2004). The final characteristic, and perhaps the most contentious, is that mtDNA markers may violate the assumption of marker neutrality: the non-recombining maternal inheritance mechanism can be prone to genetic hitchhiking, fixing new alleles faster than nDNA (Brown et al., 1979; Bazin et al., 2006; Meiklejohn et al., 2007). Additionally, several studies have indicated that mitochondria can be subject to direct and indirect selection, further confounding the assumption of neutral evolution (Ballard and Whitlock, 2004; Ballard and Rand, 2005; Hurst and Jiggins, 2005; Galtier et al., 2009). Due to the inheritance mechanism and lack of recombination, it has been argued that the mt-genome should be considered a single marker (Fenn et al., 2008). Moreover, the presence of nuclear pseudo-mitochondrial genes can confound analyses based on mt-genomes (Zhang and Hewitt, 1996). Used by themselves, mtDNA markers, even mt-genomes, can be inappropriate for studies of deeper relationships, such as those among families and infraorders.

Advantages of nDNA.— Nuclear markers can provide information on taxonomic relationships from species to order, although they are often used to resolve higher-level divergences (Baldwin et al., 1995; Friedrich and Tautz, 1995; Rokas et al., 2003; Robles et al., 2009; Chu et al., 2009). This is due to variable rates of evolution in nDNA, especially among protein-coding genes, ribosomal DNA, and introns. Protein-coding genes tend to be more conserved than other nDNA, as mutations that result in loss of protein function are subject to strong negative selection (Opperdoes, 2009). Ribosomal DNA (rDNA) tends to have highly conserved enzymatic regions and highly variable regions of expansion (Kim and Abele, 1990). Introns tend to be less conserved as they are unconstrained by protein production (Bell et al., 1998; Yeo et al., 2005; Kim and Kim, 2007).

Disadvantages of nDNA.— Aligning nDNA may be complicated by heterozygosity, multiple insertions and deletions, or by the presence of introns (Gatesy et al., 1993; Sota and Vogler, 2003; Tsang et al., 2008a; Chu et al., 2009). Also, nDNA can be more difficult to amplify, as it is typically present in fewer copies in each cell, relative to mtDNA (Zhang and Hewitt, 2003; Chu et al., 2009). This is especially true for protein-coding genes. Due to the relatively slower mutation rate characteristic of nDNA markers, nDNA is often inappropriate for studies of lower-level relationships, such as at the species- and genus-level. A final concern, which has gained appreciation over the past twenty years (Koonin, 2005), is the potential presence and effects of paralogs. Paralogous genes are versions of a gene that arose from a gene duplication event (Fitch, 1970). These copies may be under different selection pressures because they are present as more than

one copy within an individual (Kondrashov et al., 2002), although recent studies argue that this is not always the case (Studer and Robinson-Rechavi, 2009). Phylogenies are traditionally constructed using orthologous genes; that is, gene variants that arise from an ancestral gene that has undergone a speciation event (Fitch, 1970). These gene copies are believed to share important properties, such as function, that result in identical evolutionary rates (Baldauf, 2003); though this assumption is also being debated (Gabaldón and Koonin, 2013). As NGS methods have become more widely used, the ability to identify paralogs and estimate their effects is becoming increasingly important (Koonin, 2005).

Suggestions.— Because of the innate properties associated with mtDNA and nDNA, markers used to elucidate phylogenetic relationships must be chosen with the goal of the study in mind: targeted markers must be able to resolve at the taxonomic level of interest. Choice of marker can be a trade-off: low copy-number nDNA (protein-coding genes) markers may be difficult to amplify, but more easily amplified mtDNA markers are not always informative at the necessary taxonomic levels. Thus, phylogenetic studies can be strengthened by including multiple informative markers, including protein-coding genes, mtDNA, and rDNA to inform at several levels. In the decapod literature, this is implemented by Palero and Crandall (2009), Bybee et al. (2011a), Bracken-Grissom et al. (2013, 2014), and Wong et al. (2015). Currently, NGS phylogenomics methods are enabling the discovery and utilization of an unprecedented number of markers (more than 500 in a single study), informative across a range of taxonomic levels (Lemmon et al., 2012).

Species Trees vs. Gene Trees.— The goal of phylogenetic studies is a species tree. That is, a tree that reflects the evolutionary history of species. This is accomplished by reconciling the evolutionary histories of individual genetic markers to arrive at a tree that recapitulates relationships between species (Page and Charleston, 1997). Building trees with multiple, informative markers prevents the recapitulation of single-gene trees (Fig. 2), which are often inappropriate for phylogenetic studies. Individual genes can have their own unique evolutionary histories that differ from the evolutionary histories of the species and other genes (Page and Charleston, 1997). Gene trees can differ from species trees in two ways: 1) the divergence of two alleles may have occurred before the divergence of the species, and, 2) the gene tree and species tree may present different topologies (Graur and Li, 2000). Thus, analysis of a single gene recapitulates that gene's evolutionary history, and often cannot reliably inform the true species tree (Pamilo and Nei, 1988; Doyle, 1992; Page and Charleston, 1997; Degnan and Rosenberg, 2009). Indeed, a simulation study by Gadagkar et al. (2005) found that adding one gene to a single-gene analysis increases accuracy of phylogenetic inference by approximately 10%, even when the added gene is less phylogenetically informative than the first. Individually, single-gene markers are insufficient, so a variety of markers should be used to inform at the level of interest (Doyle, 1992; Pamilo and Nei, 1988; Maddison, 1997).

Insufficient Sampling and Out-group Selection

Adequate sampling is key to reliably recapitulating phylogeny (Wiens, 2003; Maddison and Knowles, 2006). Insufficient sampling can result in long-branch attraction, false results of monophyly, and incorrect outgroup rooting. All of the shortcomings associated with insufficient sampling can be curtailed by tailoring sampling effort to the purpose of the study.

Monophyly, Paraphyly, and Polyphyly.— Without adequate representation within the taxonomic level of interest, monophyly can be incorrectly inferred, resulting in subsequent discovery of paraphyly or polyphyly. This was the case for the decapod infraorder Thalassinidea, which was long perceived as monophyletic (Crandall et al., 2000; Ahyong and O’Meally, 2004; Porter et al., 2005) but only later found to be polyphyletic with additional sampling (Tsang et al., 2008a; Bracken et al., 2009a). Thalassinidea has since been divided into Axiidea and Gebiidea – relatively distant infraorders. To best ensure reliable results, every group at the level of interest should be sampled as broadly as possible. For instance, if one is inferring infraordinal relationships, multiple species within each infraorder should be represented across diverse and divergent lineages. A good example of this is Ahyong et al. (2007) which reconstructs brachyuran phylogeny, and indicates paraphyly of podotremes (also supported by Tsang et al., 2014), by thoroughly sampling sections and families within the infraorder. Frequently this is not possible due to a number of factors. If this is the case, authors

should address this in the publication and provide justification for the missing lineages (Valentine et al., 2006).

Long-Branch Attraction.— One of the most confounding results of insufficient sampling is the increased likelihood of long-branch attraction (Bergsten, 2005; Fig.3), especially in maximum parsimony analysis (Vandamme, 2009). Long-branch attraction (LBA) occurs when taxa are so divergent that mutations begin to be shared due to convergence rather than homology (Felsenstein, 1978). This convergence results in highly dissimilar taxa, which would normally be grouped on separate long branches, being “attracted” onto a single long branch. This problem should be fairly easy to identify, given some background knowledge of the lineage. Sampling more basal representatives from each clade can prevent long-branch attraction by breaking up these groups (Felsenstein, 1978; Zwickl and Hillis, 2002; Yang and Rannala, 2012).

Out-group Selection.— The final problem of insufficient sampling is improper out-group selection. This subject can, and has, occupied several papers, exclusively. We will discuss it briefly here. Without an accepted common ancestor, polarity assignment of traits is confounded (Throckmorton, 1968; Farris et al., 1970; Lundberg, 1972; de Queiroz and Gauthier, 1990; Wiley et al., 1991) and the selection of an outgroup is obscured (Wheeler, 1990). Choosing an outgroup that is too distantly related may lead to spurious rooting owing to loss of phylogenetic signal resulting from saturation. However, choosing an out-group that is too closely related can also skew analyses by aligning too closely with the taxon of interest, that is, by not serving as a “true” rooting group

(Vandamme, 2009). However, to investigate the ancient relationships within Decapoda, out-group rooting is optimized by rooting with the sister group.

In instances where the “best” out-group is difficult to identify, it is advisable to choose several: study the literature of the group of interest and find what taxa have been used in the previous studies. Since the study of decapod phylogeny began, several taxa have been proposed as the sister group: Calman (1904), Siewing (1963), Schram (1986), Wills (1998), and Schram and Hof (1998; tree unresolved) found Euphausiacea Dana, 1852 to be sister to Decapoda. Schram (1981, 1984) made a case for a polyphyletic group containing both Amphionidacea Williamson, 1973 and Euphausiacea as the sister group. And a study by Richter and Scholtz (2001) identified the subclass Hoplocarida as the sister taxon. More recently, a study by Meland and Willassen (2007) resulted in polyphyly of Decapoda, indicating several sister groups. To overcome this problem, most phylogenetic analyses must include several outgroups when rooting the resulting trees. Most molecular studies use Euphausiacea and Hoplocarida Calman, 1904 as outgroups (Bracken et al., 2009a; Qian et al., 2011; Shen et al., 2013) but to date have not included Amphionidacea due to the lack of molecular-grade tissue for this group.

Data-Recycling

One practice meant to alleviate incomplete sampling is data-recycling, which includes previously published data in a new data matrix. In phylogenetic studies, both taxa and characters are recycled to add robustness to the study. Although data-recycling can have positive impacts on the resulting tree, the pitfalls of data-recycling must be addressed.

Advantages of Recycling.— In general, researchers use previously published sequence data to circumvent the need to resample groups or to bolster taxa with few newly collected representatives. This practice can be beneficial to many phylogenetic studies by allowing them to build upon previously published datasets, which can conserve time and resources. However, using data from several sources and several authors can introduce artifacts of sampling idiosyncrasies, resulting in confounded analyses (Jenner, 2001).

Disadvantages of Recycling.— Phenotypic data matrices compiled in previous studies are reused in derivative analyses, recycling taxa and characters, potentially resulting in the dissemination of flaws in an original matrix through several subsequent studies (Jenner and Schram, 1999; Poe and Wiens, 2000; Dayrat and Tillier, 2000; Jenner, 2001).

Molecular studies can analyze the same markers that have been analyzed in previous studies, neglecting to sequence new markers. Or, new markers may be sequenced, but from previously sampled species. All of these practices can serve to reinforce prior assumptions.

Suggestions.— Phylogenetic studies that rely too heavily on recycled data typically generate the same topology, a potentially misleading result. Overall, data-recycling best serves studies when it supplements a study that generates and analyzes new characters in new representatives (Hillis et al., 2003; Bracken-Grissom et al., 2013, 2014). Also, it is a good practice to announce which data were recycled, either taxa or markers.

Inconsistent Analysis Procedures

In all phylogenetic analyses, the researcher is faced with dozens of parameter options and algorithms that could be used to estimate a phylogeny. Previous studies have shown that inputting the same dataset, but altering the model of evolution, the subsampling procedure, or the parameters can result in different trees (Buckley, 2002; Buckley and Cunningham, 2002; Lemmon and Moriarty, 2004). Careful thought must be given to these decisions. Below, we discuss four areas of concern and solutions gleaned from the literature.

Algorithm Selection.— Four algorithms commonly used in phylogenetic analysis are Neighbor Joining (NJ: Saitou and Nei, 1987), Maximum Parsimony (MP: Fitch, 1971), Maximum Likelihood (ML: Felsenstein, 1981), and Bayesian Inference (BI: Huelsenbeck and Ronquist, 2001). The robustness of results from ML and MP algorithms can be evaluated by the designation of a subsampling procedure, such as bootstrapping or jackknifing (Van de Peer, 2009). These subsampling procedures are used to generate branch support values by analyzing pseudo-replicates and calculating the percent of resulting trees containing each branch (Schmidt and von Haeseler, 2009). Bayesian Inference does not rely on subsampling, but rather calculates the posterior probability of every tree sampled from a distribution of all possible trees. Support values, then, are calculated as the percent of sampled trees that contain the nodes seen on the presented tree. For BI, branches with support values $\geq 95\%$ are considered statistically well-supported. For ML and MP, $\geq 70\%$ are considered statistically well-supported.

Nucleotide Substitution Model Selection.— One can only be as confident in a tree as one is in the model that built it (Goldman, 1993). BI, ML, and NJ require the specification of an evolutionary model. Models can be divided simply into those that assume all nucleotides occur with equal frequency (Jukes and Cantor, 1969; Kimura, 1980) and those that allow all nucleotides to occur at different frequencies (Felsenstein, 1981; Hasegawa et al., 1985; Tavaré, 1986). Some software programs, such as Random Axelerated Maximum Likelihood (RAxML: Stamatakis, 2006; Stamatakis et al., 2005, 2007, 2008), have the model set to GTR, which nests several models (Stamatakis, 2006). Programs, such as MODELTEST (Posada and Crandall, 1998) and jModelTest (Posada, 2008) are available to determine the optimal model based on the likelihood ratio and Akaike Information Criterion calculated over nested hierarchical analyses (Posada and Crandall, 1998). Currently, there is much research effort in model selection (Reid et al., 2013; Brown, 2014a,b; Lewis et al., 2014 are the most recent examples) and in determining whether current models appropriately fit the data.

Data Partitioning.— When analyzing data from multiple markers, it is often necessary to partition the data by substitution rate (Nishihara et al., 2007) or codon position (Yang, 1996). In total evidence studies, partitioning is crucial for datasets that include molecular markers and morphological characters, as seen in the phylogenetic reconstruction of lobsters and anomurans (Schnabel et al., 2011; Bracken-Grissom et al., 2013, 2014). Data that is not partitioned is subject to “mixture models,” in which each marker is analyzed under multiple substitution models and every marker is assumed to have evolved under

similar processes (Le et al., 2008). This can negatively impact tree topology (Buckley et al., 2001; Telford and Copley, 2011). Data can be partitioned on the basis of codon position, gene (e.g. 16S, 12S, COI), gene origin (nuclear vs. mitochondrial), or gene function (protein coding vs. intron). By partitioning data, researchers can group markers that are likely to have experienced similar evolutionary processes, and then analyze each group independently. This allows for the reconstruction of a phylogeny that takes into account heterogeneous evolutionary histories (Lanfear et al., 2012). As with model selection, researchers can use programs such as PartitionFinder (Lanfear et al., 2012) to statistically explore and support partitioning schemes.

Application of Coalescent Theory.— In non-coalescent approaches, genes are concatenated into a ‘supergene’ alignment and traditional tree-building algorithms are applied to generate a phylogeny in a single step (often called “concatenation phylogenies;” Gadagkar et al., 2005; Edwards, 2009). This method has been criticized for failing to resolve the evolutionary history at the species level (Edwards, 2009). Rather, non-coalescent approaches estimate the genealogical history of individuals across a multilocus dataset, which is problematic when individual gene trees are in conflict due to mechanisms such as horizontal gene transfer, gene duplication, deep coalescence, and branch length heterogeneity (Edwards, 2009; Liu et al., 2009a). It has also been criticized for over-simplifying evolution and frequently ignoring gene tree heterogeneity by including too few markers (McVay and Carstens, 2013). Coalescent approaches use genetic data to calculate population parameters in an effort to better reflect the history of a taxon (Kingman, 2000; Edwards, 2009). This allows for gene tree heterogeneity, which

enables correct species tree estimation, even in the anomaly zone where the most common gene tree does not match the species tree (Degnan and Rosenberg, 2009; Liu et al., 2009b). These analyses can be computationally demanding, and have been described as too complex, especially for long-diverged clades (McVay and Carstens, 2013). However, including variation in gene analysis has been found to be advantageous in theoretical multi-locus analyses (Kubatko and Degnan, 2007). In general, it is a good practice to analyze data using both approaches and present both trees in the publication.

PART III: A REVIEW OF HIGHER-LEVEL DECAPOD MOLECULAR PHYLOGENIES

From the first studies in the 1990s (Kim and Abele, 1990) to the next-generation studies of the 2010s (Bybee et al., 2011a,b; Qian et al., 2011; Shen et al., 2013), much progress has been made in resolving decapod phylogeny. Early studies identified informative markers, both molecular (Kim and Abele, 1990; Crandall et al., 2000; Porter et al., 2005; Tsang et al., 2008a; Chu et al., 2009) and morphological (Ahyong and O’Meally, 2004). These studies helped uncover polyphyly in *Palinura* (Ahyong and O’Meally, 2004) and *Thalassinidea* (Tsang et al., 2008a; Bracken et al., 2009a), informing phylogeneticists of which groups required more thorough and targeted sampling for phylogenetic reconstruction. The markers from these studies also served as the starting point for using NGS platforms such as targeted amplicon sequencing (Bybee et al., 2011a).

The first study by Kim and Abele (1990) sampled nine specimens spanning the suborder *Dendrobranchiata* and five infraorders: *Astacidea*, *Brachyura*, *Caridea*,

Procarididea, and Stenopodidea (though the study did not recognize the now accepted division between Procarididea and Caridea and analyzed *Palaemonetes* and *Procaris* as part of Caridea). This study sought to determine whether the 18S ribosomal subunit could and/or would infer a phylogeny that accorded with morphology-based phylogenies. The MP analysis resulted in a significantly supported tree with sufficient variation between infraorders to conclude that 18S was phylogenetically informative at the infraordinal level. The first molecular study to propose a relationship between major decapod lineages, Kim and Abele identified a marker that is frequently used in higher-level decapod phylogenetic studies today. However, interpretation of these results is limited due to the incomplete sampling at the infraordinal level and insufficient marker selection. Nonetheless, this study was based entirely on *de novo* sequences.

Crandall et al. (2000) focused on the monophyletic origins of crayfish, but sampled sufficiently to generate a tree including several decapod infraorders. Analyzing 16S mtDNA, 18S, and 28S rDNA markers, this study included species from Achelata (Palinura in the study), Anomura, Astacidea, Axiidea, Brachyura, Gebiidea, and Stenopodidea (Axiidea and Gebiidea were listed as representatives of Thalassinidea in the study). Trees were estimated using NJ, ML, and MP. The resulting tree (Fig. 1C) generated a similar topology to that of Kim and Abele (1990). Despite a lack of data partitioning, this study provided evidence that utilizing multiple gene regions allowed for resolution at several taxonomic levels.

In 2004, the first decapod total evidence study (molecular + morphology) was performed using 16S, 18S, and 28S, as well as 105 morphological characters which included spermatozoa, gill, branchiostegites, rostrum, and carapace characteristics,

among many others (Ahyong and O'Meally, 2004). Here, data-recycling was used to supplement newly generated morphological and molecular data. This study represented the most complete sampling of reptant decapod infraorders yet, including representatives from Achelata, Anomura, Astacidea, Axiidea, Brachyura, Gebiidea, Glypheidea, Polychelida, and Stenopodidea (Axiidea and Gebiidea were still recognized as Thalassinidea in this analysis). The study presented three slightly differing MP trees generated from morphological characters, molecular markers, and a combination of the two (total evidence). The total evidence tree (Fig. 1D) more closely resembled the relationships recovered in the molecular phylogeny, and all three analyses were congruent at the infraordinal level. The thorough sampling scheme helped uncover polyphyly within Palinura, resulting in its eventual division into Achelata, as the most basal of the three and sister to the fractosternalian infraorders; Polychelida, as sister to the remaining reptants; and Glypheidea, as sister to Astacidea. It should be noted that, while a partition was made between molecular and morphological data, the molecular data was unpartitioned which may have negatively impacted the resulting topology.

In 2005, Porter et al. included markers used in previous analyses (16S, 18S, 28S) but also included the histone 3 nDNA (H3) sequence for analysis. This study included representatives from Achelata, Anomura, Astacidea, Axiidea (listed as Thalassinidea), Brachyura, Caridea, Dendrobranchiata, and Stenopodidea; and was one of the first to partition data for analysis. Alignments were analyzed using ML and, for the first time in infraordinal decapod phylogenetic analysis, BI. The resulting tree unexpectedly placed Brachyura and Anomura in the middle of the tree (Fig. 1E), though these two groups traditionally fall out as more derived. Instead, Astacidea and Axiidea appeared more

derived. The authors found all sampled infraorders to be monophyletic with strong branch support, but nodal support values for the relationships between infraorders were relatively low. This may be the result of insufficient taxon sampling and/or marker selection, that is, the markers were not sufficient in resolving deep relationships.

A study published in 2008 focused solely on protein-coding markers novel to decapod phylogeny: a sodium potassium pump (NaK) and phosphoenolpyruvate carboxykinase (PEPCK), thus all sequences analyzed in the study were generated *de novo* (Tsang et al., 2008a). Despite the absence of previously generated sequence data, the study included representatives from Achelata, Anomura, Astacidea, Axiidea, Brachyura, Caridea, Dendrobranchiata, Gebiidea, Polychelida, and Stenopodidea (Axiidea and Gebiidea were included as specimens of Thalassinidea). Data was analyzed with ML, MP, and BI, resulting in strongly supported monophyly for all infraorders, except Thalassinidea, which exhibited polyphyly (Fig. 1F). The authors suggested returning to the scheme of Gurney (1938), which divided Thalassinidea into the “Homarine Group” (Axiidea) and the “Anomuran Group” (Gebiidea). In 2009, NaK and PEPCK were used again, but sequence number doubled, and an identical tree was produced (Chu et al., 2009). The protein-coding genes used by Tsang et al. (2008a) and Chu et al. (2009) supported many infraordinal to species level relationships, providing evidence that single-copy, slow-evolving, protein-coding genes are good candidates for inferring phylogenies across broad taxonomic ranges.

Toon et al. (2009) sequenced eight markers, two mitochondrial and six nuclear, for representatives of Achelata, Anomura, Astacidea, Axiidea, Brachyura, Caridea, Dendrobranchiata, and Polychelida. While many sequences were recycled from GenBank

(including 12S, 16S, 18S, 28S, and H3 for several specimens), three new nDNA markers were introduced: EF-2, EPRS, and TM9sf4. RAxML analysis of the eight markers inferred relationships that did not concur with other studies, primarily by recovering Dendrobranchiata as sister to Caridea, and Caridea as the most basal pleocyemate (Fig. 1H). However, these branches were not strongly supported. While it is not explicitly stated whether data was partitioned or not, a second analysis, which excluded the mtDNA markers, was performed but not presented.

In 2009, Bracken et al. published their work on the Decapod Tree of Life Project (Bracken et al., 2009a; Fig. 1G), combining an increased sampling effort with multiple-marker analysis. Most of the data was recycled from previous analyses (only 24 *de novo* sequences), including every currently recognized infraorder except for Procarididea. The authors used a subset of the markers used by Toon et al. (2009): 16S, 18S, 28S, and H3. Sequences were analyzed with RAxML and BI. The resulting tree provided further support for the division of Thalassinidea (Gurney, 1938; Tsang et al., 2008a,b; Robles et al., 2009). Although monophyly of all infraorders was statistically supported, there was little to no support for relationships among infraorders, due to the lack of appropriate genes to resolve deep level relationships.

Another study, aimed at investigating Procarididea evolution, also generated an infraordinal tree (Bracken et al., 2010). Based on 16S, 18S, 28S, and H3 sequence data, the findings of Bracken et al. agreed with those of Felgenhauer and Abele's (1983) comparative morphological study, establishing Procarididea as an infraorder, sister to Caridea (Fig. 1I). Dendrobranchiata was sampled, as well as every currently recognized decapod infraorder, except for Glypheidea. This study analyzed one mitochondrial

marker (16S) and three nuclear markers (18S, 28S, and H3), generating new data for taxa in Dendrobranchiata, Procarididea, and Caridea. Data for representatives from the other infraorders was recycled from GenBank. Genes were concatenated and partitioned for analysis. MODELTEST was used to identify the evolutionary model that best fit the data, and data was analyzed using RAxML (Stamatakis et al., 2005, 2007, 2008) and MrBayes (Huelsenbeck and Ronquist, 2001). To calibrate the resulting tree, thirteen fossils were included in the analysis.

Beginning in the 2010s, high-powered NGS techniques began generating huge quantities of data for phylogenetic analysis, revolutionizing molecular research. Through massively parallel, multiplexed reactions, NGS is capable of generating genomic, transcriptomic, and epigenomic data (Levin et al., 2009; McKenna et al., 2010; Metzker et al., 2010; Roukos, 2010; Ku et al., 2011; Martin and Wang, 2011; McCormack et al., 2013; Wong et al., 2015). Such sequencing efforts allow analysis of hundreds to thousands of markers across the genomes of hundreds of individuals (Gnirke et al., 2009; Mamanova et al., 2010; Lemmon and Lemmon, 2012; Lemmon et al., 2012), generating unprecedented amounts of data while using fewer resources. Applied to decapod phylogenetics relatively recently, NGS has enabled the targeting of hundreds of new markers across the order.

Targeted Amplicon Sequencing (TAS) (Bybee et al., 2011b) uses an NGS platform to sequence a high number of markers across a large number of specimens. This PCR-based approach generates amplicons optimized for NGS (Bybee et al., 2011a,b). Target genes undergo two PCRs, which barcode sequences by taxon, enabling them to be multiplexed on a NGS platform (Bybee et al., 2011a,b). The PCR amplification allows

for the use of a variety of starting materials (e.g. new specimens, alcohol-preserved tissue, museum samples). Sequencing 12S, 16S, COI, 18S, 28S, and H3 *de novo* for sixteen specimens, including a museum specimen, Bybee et al. (2011a) demonstrated the potential of TAS across Pancrustacea (including Decapoda; Fig. 1K). The study itself lacked representatives from Gebiidea, Glypheidea, and Procarididea, however the intention of this study was not to generate a robust phylogeny across Decapoda, but rather to exemplify how the method could be applied to higher-level phylogenetic inferences. The authors highlight potential problems with TAS, such as the quality of the data (reviewed by Wicker et al., 2006; Huse et al., 2007; Kunin et al., 2010), the removal of primer dimers, and biases among barcodes.

Two recent studies (Qian et al., 2011; Shen et al., 2013) have taken similar approaches to generate and analyze full mitochondrial genomes (mt-genomes) to infer decapod phylogeny. These are the first phylogenomic studies of decapods thus far. Qian et al. (2011) combined 27 previously sequenced mt-genomes with two *de novo* mt-genomes generated for the analysis. Though data was not partitioned, each of the 13 protein-coding genes were analyzed in separate alignments. The results of Qian et al. (2011) strongly support topologies from other studies (Tsang et al., 2008a; Bybee et al., 2011a; Shen et al., 2013), with Brachyura and Anomura representing derived branches and Dendrobranchiata and Caridea representing early branching groups (Fig. 1J). In addition to Dendrobranchiata, only five infraorders are sampled: Achelata, Anomura, Astacidea, Brachyura, and Caridea. Shen et al. (2013) generated two datasets: an amino acid alignment and a sequence alignment. Both were partitioned by gene. Results were similar to Qian et al., but the data showed some ambiguity as to the position of

Polychelida in relation to Achelata and Astacidea: BI of mitogenome nucleotides and ML analysis of mitogenome amino acids upheld Palinura (Polychelida + Achelata), but all other analyses, including the final tree (Fig. 1L) based on the analysis of all datasets, supported Polychelida + Astacidea. It must be noted that few analyses resulted in high support values suggesting a relationship between Polychelida + Astacidea or Polychelida + Achelata. ML analysis of mitogenome amino acids also resulted in monophyly of Thalassinida (Gebiidea + Achelata), though this result did not carry to the final tree (Fig. 1K), in which Axiidea is basal to Gebiidea. It should be noted that past results have suggested using mitochondrial genomes to infer phylogeny can be problematic, as previously discussed.

FUTURE DIRECTIONS

Arguably, one of the most promising methods for resolving the decapod tree of life has not yet been applied to decapod phylogeny: Anchored Hybrid Enrichment (AHE) is capable of targeting hundreds of loci informative at multiple taxonomic levels in a single NGS study. AHE targets many (>500) highly conserved anchored regions of the genome using probes (Lemmon et al., 2012, Lemmon and Lemmon, 2012). Each streptavidin-tagged, oligonucleotide probe targets a highly conserved sequence region flanked by more variable sequence regions. Probes can be designed to target flanking regions exhibiting different levels of variability. The result is sequence data that is phylogenetically informative at multiple taxonomic levels in a single study. By designing probes to target appropriately variable sequences, relationships can be resolved from the

deep phylogenetic level to the level of phylogeography (Carstens et al., 2012; Lemmon and Lemmon, 2012).

As NGS methods lower the cost of phylogenetic studies, allowing the discovery of unprecedented numbers of markers and inclusion of many taxa, it is important to remember the value of morphological data in phylogenetic analyses. Previous studies of decapod phylogeny have demonstrated that including morphological characters to a molecular dataset can improve the phylogeny in terms of support and sampling effort (Ahyong and O’Meally, 2004; Schnabel et al., 2011; Bracken-Grissom et al., 2013, 2014). Specifically, the inclusion of fossils in a phylogenetic study can incorporate data that cannot be generated from any other source (Novacek and Norell, 1982). Most notably, fossils can allow extinct taxa to be included in phylogenies (Beurlen and Glaessner, 1930). A rich fossil record allows researchers to estimate the age of clades (Novacek and Norell, 1982; Reid et al., 1996) and explore the origins of diversity within major lineages (Gauthier et al., 1988; Huelsenbeck, 1991; Weishampel, 1996; Bracken-Grissom et al., 2014). Using fossils to date a phylogenetic tree can add directionality to major morphological and/or behavioral transitions and uncover historical patterns in organismal biogeography (Porter et al., 2005; Bracken-Grissom et al., 2014). According to recent studies, even including just one fossil for every ten included taxa can reliably date a phylogeny (Erwin et al., 2011; Bracken-Grissom et al., 2014). In summary, as phylogenetics moves toward NGS approaches, it is important to remember the inimitable role fossils can play in recapitulating a robust, dated phylogenetic tree for Decapoda.

CONCLUSIONS

From the earliest classifications of decapods, to the super-powered molecular methods of NGS, morphological and molecular phylogenies have generated a suite of evolutionary hypotheses for higher-level relationships. From these varied hypotheses, some accord has been seen. Early studies consistently recovered three or four major lineages:

Dendrobranchiata, Caridea Dana, 1852, Stenopodidea Bate, 1888, and Reptantia, with Dendrobranchiata generally considered to be the earliest branching lineage. Reptant infraorders (Achelata, Anomura MacLeay, 1838, Astacidea, Axiidea, Brachyura Linnaeus, 1758, Gebiidea, Glypheidea Winckler, 1882, Polychelida) are typically recovered as derived lineages. Caridea and Stenopodidea frequently cluster together, either as sister groups or as close relatives. Generally, Caridea and Dendrobranchiata represent early branching lineages, while Anomura and Brachyura fall as sister clades in a more derived position on the Decapod Tree of Life. The lobster-like lineages Polychelida, Glypheidea, Achelata, and Astacidea show conflicting relationships as either a monophyletic (Tsang et al., 2008a; Chu et al., 2009; Toon et al., 2009; Bybee et al., 2011a; Qian et al., 2011) or non-monophyletic clade (Ahyong and O'Meally, 2004; Porter et al., 2005; Bracken et al., 2009a, 2010; Shen et al., 2013; Bracken-Grissom et al., 2014). The ghost shrimp infraorders, Axiidea and Gebiidea, are consistently recovered as non-monophyletic (Porter et al., 2005; Tsang et al., 2008a, Bracken et al., 2009a; Chu et al., 2009; Shen et al., 2013). Further contributing to our understanding of decapod phylogeny, many recent molecular phylogenies have focused on family-level relationships within one or more infraorders (Anomura: Ahyong et al, 2009; Tsang et al.,

2011; Bracken-Grissom et al., 2013; Axiidea/Gebiidea: Tsang et al., 2008b; Robles et al., 2009; Brachyura: Tsang et al., 2014; Caridea: Bracken et al., 2009b; Li et al., 2011; Dendrobranchiata: Ma et al., 2009; Lobster-like lineages: Bracken-Grissom et al., 2012, 2014). Past studies have undoubtedly enhanced our understanding of the Decapod Tree of Life, however several infraordinal relationships remain unclear. In pursuit of strong infraordinal-level support across Decapoda, analysis methods have become more standardized and taxon sampling has improved, while a lack of appropriate markers has remained a primary hindrance. Since the introduction of NGS, techniques have advanced and optimized to meet the challenge of deep phylogenetic questions. Excitingly, these advancements now provide researchers with hundreds to thousands of phylogenetically informative markers, enabling unprecedented insight into the evolutionary history of Decapoda.

ACKNOWLEDGEMENTS

We thank the Florida International University Presidential Fellowship for providing financial support for this review. We also thank L. E. Timm's Ph. D. committee: Dr. Eirin-Lopez, Dr. Rodriguez-Lanetty, Dr. von Wettberg, and Dr. Wensong Wu, for additional comments and suggestions. Finally, we thank Mr. Joseph Ahrens, Drs. Phil Stoddard and Brent Thoma, and the anonymous reviewers for feedback on earlier versions of this manuscript.

LITERATURE CITED

- Abele, L. G. 1991. Comparison of morphological and molecular phylogeny of the Decapoda. *Memoirs of the Queensland Museum* 31: 101-108.
- Ahyong, S. T., and D. O'Meally. 2004. Phylogeny of the Decapoda Reptantia: resolution using three molecular loci and morphology. *The Raffles Bulletin of Zoology*, 52, 673-693.
- , J. C. Lai, D. Sharkey, D. J. Colgan, and P. K. Ng. 2007. Phylogenetics of the brachyuran crabs (Crustacea: Decapoda): The status of Podotremata based on small subunit nuclear ribosomal RNA. *Molecular Phylogenetics and Evolution*, 45: 576-586.
- , K. E. Schnabel, & E. W. Maas. 2009. Anomuran phylogeny: new insights from molecular data. In J. W. Martin, K. A. Crandall, and D. L. Felder (Eds.), *Decapod Crustacean Phylogenetics [Crustacean Issues]* (pp. 399-414). Boca Raton, FL: CRC Press.
- Avise, J. C. 2000. *Phylogeography: the History and Formation of Species*. Harvard University Press.
- Baldauf, S. L. 2003. Phylogeny for the faint of heart: a tutorial. *TRENDS in Genetics* 19: 345-351.
- Baldwin, B. G., M. J. Sanderson, J. M. Porter, M. F. Wojciechowski, C. S. Campbell, and M. J. Donoghue (1995). The ITS region of nuclear ribosomal DNA: a valuable source of evidence on angiosperm phylogeny. *Annals of the Missouri Botanical Garden* 82: 247-277.
- Ballard, J. W. O., and D. M. Rand. 2005. The population biology of mitochondrial DNA and its phylogenetic implications. *Annual Review of Ecology, Evolution, and Systematics* 36: 621-642.
- , and M. C. Whitlock. 2004. The incomplete natural history of mitochondria. *Molecular Ecology* 13: 729-744.
- Bate, C. S., 1888. Report on the Crustacea Macrura collected by H.M.S. Challenger during the Years 1873–76. In: Murray, J., Zoology. Wyville Thomson, C. and J. Murray, Report on the Scientific Results of the Voyage of H.M.S. Challenger During the Years 1873–76 Under the Command of Captain George S. Nares, R.N., F.R.S. and the Late Captain Frank Tourle Thomson, R.N. Vol. 24. Edinburgh, Neill and Company. Pp. i–xc, 1–942, Plates 1–157.

- Baum, D. A., S. D. Smith, and S. S. Donovan. 2005. The tree-thinking challenge. *Science* 310: 979.
- Bazin, E., S. Glémin, and N. Galtier. 2006. Population size does not influence mitochondrial genetic diversity in animals. *Science* 312: 570-572.
- Bell, M. V., A. E. Cowper, M. P. Lefranc, J. I. Bell, and G. R. Screaton. 1998. Influence of intron length on alternative splicing of CD44. *Molecular and Cellular Biology* 18: 5930-5941.
- Bergsten, J. 2005. A review of long-branch attraction. *Cladistics* 21: 163-193.
- Beurten, K., and M. F. Glaessner. 1930. Systematik der Crustacea Decapoda auf stammesgeschichtlicher grundlage. *Zoologische Jahrbücher Abteilung Für Systematik, Ökologie Und Geographie Der Tiere* 60: 49-84.
- Birky, C. W. 1995. Uniparental inheritance of mitochondrial and chloroplast genes: mechanisms and evolution. *Proceedings of the National Academy of Sciences* 92: 11331-11338.
- . 2001. The inheritance of genes in mitochondria and chloroplasts: laws, mechanisms, and models. *Annual Review of Genetics* 35: 125-148.
- Blouin, M. S., C. A. Yowell, C. H. Courtney, and J. B. Dame. 1998. Substitution bias, rapid saturation, and the use of mtDNA for nematode systematics. *Molecular Biology and Evolution* 15: 1719-1727.
- Boas, J. E. V. 1880. Studier over Decapodernes Slægtskabsforhold. *Danske Videnskabernes Seksjeab, Copenhagen, Skrifter, Naturvidenskabelig og matematisk Afdeling* 1: 23-210.
- Boore, J. L., and W. M. Brown. 1998. Big trees from little genomes: mitochondrial gene order as a phylogenetic tool. *Current Opinion in Genetics and Development* 8: 668-674.
- Borradaile, L. A. 1907. On the classification of the decapod crustaceans. *Annals and Magazine of Natural History* 19: 457-486.
- Boyko, C. B., and J. D. Williams. 2009. Crustacean parasites as phylogenetic indicators in decapod evolution. In J. W. Martin, K. A. Crandall and D. L. Felder (Eds.), *Decapod Crustacean Phylogenetics [Crustacean Issues]* (pp. 197-220). Boca Raton, FL: CRC Press.

- Bracken, H. D., A. Toon, D. L. Felder, J. W. Martin, M. Finley, J. Rasmussen, F. Palero, and K. A. Crandall. 2009a. The decapod tree of life: compiling the data and moving toward a consensus of decapod evolution. *Arthropod Systematics and Phylogeny* 67: 99-116.
- , S. De Grave, & D. L. Felder. 2009b. Phylogeny of the infraorder Caridea based on mitochondrial and nuclear genes (Crustacea: Decapoda). In J. W. Martin, K. A. Crandall, and D. L. Felder (Eds.), *Decapod Crustacean Phylogenetics [Crustacean Issues]* (pp. 281-305). Boca Raton, FL: CRC Press.
- , ———, A. Toon, D. L. Felder, and K. A. Crandall. 2010. Phylogenetic position, systematic status, and divergence time of the Procarididea (Crustacea: Decapoda). *Zoologica Scripta*, 39: 198-212.
- Bracken-Grissom, H. D., S. T. Ah Yong, R. D. Wilkinson, R. M. Feldmann, C. E. Schweitzer, J. W. Breinholt, M. Bendall, F. Palero, T.-Y. Chan, D. L. Felder, R. Robles, K.-H. Chu, L.-M. Tsang, D. Kim, J. W. Martin, and K. A. Crandall. 2014. The emergence of the lobsters: phylogenetic relationships, morphological evolution and divergence time comparisons of an ancient group (Decapoda: Achelata, Glypheidea, Polychelida). *Systematic Biology* 63: 457-479.
- , M. E. Cannon, P. Cabezas, R. M. Feldmann, C. E. Schweitzer, S. T. Ah Yong, D. L. Felder, R. Lemaitre, and K. A. Crandall. 2013. A comprehensive and integrative reconstruction of evolutionary history for Anomura (Crustacea: Decapoda). *BMC Evolutionary Biology* 13: 1-128.
- , C. H. Yang, D. Kim, K. A. Crandall, & T. Y. Chan. 2012. Phylogenetic relationships, character evolution, and taxonomic implications within the slipper lobsters (Crustacea: Decapoda: Scyllaridae). *Molecular Phylogenetics and Evolution* 62: 237-250.
- Brown, J. M. 2014a. Predictive approaches to assessing the fit of evolutionary models. *Systematic Biology* 63: 289-292.
- . 2014b. Detection of implausible phylogenetic inferences using posterior predictive assessment of model fit. *Systematic Biology* 63: 334-348.
- Brown, W. M., M. George, and A. C. Wilson. 1979. Rapid evolution of animal mitochondrial DNA. *Proceedings of the National Academy of Sciences* 76: 1967-1971.
- Buckley, T. R., and C. W. Cunningham. 2002. The effects of nucleotide substitution model assumptions on estimates of nonparametric bootstrap support. *Molecular Biology and Evolution* 19: 394-405.

- , Simon, C., and G. K. Chambers. 2001. Exploring among-site rate variation models in a maximum likelihood framework using empirical data: effects of model assumptions on estimates of topology, branch lengths, and bootstrap support. *Systematic Biology* 50: 67-86.
- . 2002. Model misspecification and probabilistic tests of topology: evidence from empirical data sets. *Systematic Biology* 51: 509-523.
- Burkenroad, M. D. 1963. The evolution of the Eucarida, (Crustacea, Eumalacostraca), in the relation of the fossil record. *Tulane Studies in Geology* 2: 1-17.
- Bybee, S. M., H. D. Bracken-Grissom, B. D. Haynes, R. A. Hermansen, R. L. Byers, M. J. Clement, J. A. Udall, E. R. Wilcox, and K. A. Crandall. 2011b. Targeted amplicon sequencing (TAS): a scalable next-gen approach to multilocus, multitaxa phylogenetics. *Genome Biology and Evolution* 3: 1312-1323.
- , ———, R. A. Hermansen, M. J. Clement, K. A. Crandall, and D. L. Felder. (2011a). Directed next generation sequencing for phylogenetics: An example using Decapoda (Crustacea). *Zoologischer Anzeiger* 250: 497-506.
- Calman, W. D. 1904. On the classification of the Crustacea Malacostraca. *Annals and Magazine of Natural History* 13: 144-158.
- Carstens, B., A. R. Lemmon, and E. M. Lemmon. 2012. The promises and pitfalls of next-generation sequencing data in phylogeography. *Systematic Biology* 61: 713-715.
- Chu, K. H., L.-M. Tsang, K. Y. Ma, T.-Y. Chan, and P. K. L. Ng. 2009. Decapod phylogeny: What can protein-coding genes tell us?. In J. W. Martin, K. A. Crandall, and D. L. Felder (Eds.), *Decapod Crustacean Phylogenetics [Crustacean Issues]* (pp. 89-99). Boca Raton, FL: CRC Press.
- Clark, P. F. 2009. The bearing of larval morphology on brachyuran phylogeny. In J. W. Martin, K. A. Crandall, and D. L. Felder (Eds.), *Decapod Crustacean Phylogenetics [Crustacean Issues]* (pp. 221-241). Boca Raton, FL: CRC Press.
- Claus, C. 1872. *Gründzuge der Zoologie. Zum gebrauch an Universitäten und Höheren Lehranstalten sowie zum Selbststudium (zweite vermehrte Auflage)*. Marburg und Leipzig: N.G. Elwert'sche Universitäts-Buchshandlung.
- Crandall, K. A., D. J. Harris, and J. W. Fetzner. 2000. The monophyletic origin of freshwater crayfish estimated from nuclear and mitochondrial DNA sequences. *Proceedings of the Royal Society of London* 267B: 1679-1686.

- Dana, J. D. 1852. Crustacea. Part I. United States Exploring Expedition. During the years 1838, 1839, 1840, 1841, 1842. Under the command of Charles Wilkes, U.S.N. Vol. 13. Philadelphia, C. Sherman. 685 pp.
- Darwin, C. 1859. The Origin of Species by Means of Natural Selection. London: Murray.
- Dayrat, B., and S. Tillier. 2002. Evolutionary relationships of euthyneuran gastropods (Mollusca): a cladistic re-evaluation of morphological characters. *Zoological Journal of the Linnean Society* 135: 403-470.
- De Grave, S., N. D. Pentcheff, S. T. Ahyong, T.-Y. Chan, K. A. Crandall, P. C. Dworschak, D. L. Felder, R. M. Feldmann, C. H. J. M. Fransen, L. Y. D. Goulding, R. Lemaitre, M. E. Y. Low, J. W. Martin, P. K. L. Ng, C. E. Schweitzer, S. H. Tan, D. Tshudy, and R. Wetzer. 2009. A classification of living and fossil genera of decapod crustaceans. *Raffles Bulletin of Zoology* 21: 1-109.
- Degnan, J. H., and N. A. Rosenberg. 2009. Gene tree discordance, phylogenetic inference and the multispecies coalescent. *Trends in Ecology and Evolution* 24: 332-340.
- Dixon, C. J., S. T. Ahyong, and F. R. Schram. 2003. A new hypothesis of decapod phylogeny. *Crustaceana* 76: 935-975.
- Doyle, J. J. 1992. Gene trees and species trees: molecular systematics as one-character taxonomy. *Systematic Botany* 17: 144-163.
- Edwards, S. V. 2009. Is a new and general theory of molecular systematics emerging? *Evolution* 63: 1-19.
- Elson, J. L., and R. N. Lightowlers. 2006. Mitochondrial DNA clonality in the dock: can surveillance swing the case? *Trends in Genetics* 22: 603-607.
- Erwin, D. H., M. Laflamme, S. M. Tweedt, E. A. Sperling, D. Pisani, and K. J. Peterson. 2011. The Cambrian conundrum: early divergence and later ecological success in the early history of animals. *Science* 334: 1091-1097.
- Farris, J. S., A. G. Kluge, and M. J. Eckardt. 1970. A numerical approach to phylogenetic systematics. *Systematic Biology* 19: 172-189.
- Felgenhauer, B.E. and L.G. Abele. 1983. Phylogenetic relationships among shrimp-like decapods. In F. R. Schram Ed. *Crustacean Phylogeny [Crustacean Issues]* (pp. 291-311). Rotterdam: A. A. Balkema.
- Felsenstein, J. 1978. Cases in which parsimony or compatibility methods will be positively misleading. *Systematic Zoology* 27: 401-410.

- . 1981. Evolutionary trees from DNA sequences: a maximum likelihood approach. *Journal of Molecular Evolution* 17: 368-376.
- Fenn, J. D., H. Song, S. L. Cameron, and M. F. Whiting. 2008. A preliminary mitochondrial genome phylogeny of Orthoptera (Insecta) and approaches to maximizing phylogenetic signal found within mitochondrial genome data. *Molecular Phylogenetics and Evolution* 49: 59-68.
- Fitch, W. M. 1970. Distinguishing homologous from analogous proteins. *Systematic Biology* 19: 99-113.
- . 1971. Toward defining the course of evolution: minimum change for a specific tree topology. *Systematic Biology* 20: 406-416.
- Forterre, P., and H. Philippe. 1999. Where is the root of the universal tree of life?. *Bioessays* 21: 871-879.
- Friedrich, M., and D. Tautz. 1995. Ribosomal DNA phylogeny of the major extant arthropod classes and the evolution of myriapods. *Nature* 376: 165-167.
- Gabaldón, T. and E. V. Koonin. 2013. Functional and evolutionary implications of gene orthology. *Nature Reviews Genetics* 14: 360-366.
- Gadagkar, S. R., M. S. Rosenberg, and S. Kumar. 2005. Inferring species phylogenies from multiple genes: concatenated sequence tree versus consensus gene tree. *Journal of Experimental Zoology Part B: Molecular and Developmental Evolution* 304: 64-74.
- Galtier, N., B. Nabholz, S. Glémin, and G. D. D. Hurst. 2009. Mitochondrial DNA as a marker of molecular diversity: a reappraisal. *Molecular Ecology* 18: 4541-4550.
- Gatesy, J., R. DeSalle, and W. Wheeler. 1993. Alignment-ambiguous nucleotide sites and the exclusion of systematic data. *Molecular Phylogenetics and Evolution* 2: 152-157.
- Gauthier, J., A. G. Kluge and T. Rowe. 1988. Amniote phylogeny and the importance of fossils. *Cladistics* 4: 105-209.
- Gnirke, A., A. Melnikov, J. Maguire, P. Rogov, E. M. LeProust, W. Brockman, T. Fennell, G. Giannoukos, S. Fisher, C. Russ, S. Gabriel, D. B. Jaffe, E. S. Lander, and C. Nusbaum. 2009. Solution hybrid selection with ultra-long oligonucleotides for massively parallel targeted sequencing. *Nature Biotechnology* 27: 182-189.
- Goldman, N. 1993. Simple diagnostic statistical tests of models for DNA substitution. *Journal of Molecular Evolution* 37: 650-661.

- Graur, D., and W. H. Li. 2000. *Fundamentals of Molecular Evolution*, 2nd edition. Sunderland, MA: Sinauer Associates.
- Gurney, R. 1938. Larvae of the decapod Crustacea. V. Nephropsidea and Thalassinidea. *Discovery Reports* 17: 291-344.
- Hall, B. G. 2004. *Phylogenetic Trees Made Easy: a how-to Manual* Vol. 547. Sunderland: Sinauer Associates.
- Hasegawa, M., H. Kishino, and T. A. Yano. 1985. Dating of the human-ape splitting by a molecular clock of mitochondrial DNA. *Journal of Molecular Evolution* 22: 160-174.
- Hillis, D. M., D. D. Pollock, J. A. McGuire, and D. J. Zwickl. 2003. Is sparse taxon sampling a problem for phylogenetic inference?. *Systematic Biology* 52: 124.
- Huelsenbeck, J. P. 1991. When are fossils better than extant taxa in phylogenetic analysis?. *Systematic Biology* 40: 458-469.
- , and F. Ronquist. 2001. MRBAYES: Bayesian inference of phylogenetic trees. *Bioinformatics* 17: 754-755.
- Hurst, G. D., and F. M. Jiggins. 2005. Problems with mitochondrial DNA as a marker in population, phylogeographic and phylogenetic studies: the effects of inherited symbionts. *Proceedings of the Royal Society B: Biological Sciences* 272: 1525-1534.
- Huse, S. M., J. A. Huber, H. G. Morrison, M. L. Sogin, and D. M. Welch. 2007. Accuracy and quality of massively parallel DNA pyrosequencing. *Genome Biology and Evolution* 8: R143.
- Huxley, T. H. 1878. On the classification and the distribution of the crayfishes. *Proceedings of the Zoological Society of London* 1878: 752-788.
- Jenner, R. A. 2001. Bilaterian phylogeny and uncritical recycling of morphological data sets. *Systematic Biology* 50: 730-742.
- , and F. R. Schram. 1999. The grand game of metazoan phylogeny: rules and strategies. *Biological Reviews* 74: 121-142.
- Jukes, T. H., and C. R. Cantor. 1969 Evolution of protein molecules. In Munro ed., *Mammalian Protein Metabolism* (pp. 21-132). New York, NY: Academic Press.

- Kim, W., and L. G. Abele. 1990. Molecular phylogeny of selected decapod crustaceans based on 18S rRNA nucleotide sequences. *Journal of Crustacean Biology* 10: 1-13.
- Kim, Y. K., and V. N. Kim. 2007. Processing of intronic microRNAs. *The EMBO Journal* 26: 775-783.
- Kimura, M. 1980. A simple method for estimating evolutionary rates of base substitutions through comparative studies of nucleotide sequences. *Journal of Molecular Evolution* 16: 111-120.
- Kingman, J. F. 2000. Origins of the coalescent: 1974-1982. *Genetics* 156: 1461-1463.
- Kondrashov, F. A., I. B. Rogozin, Y. I. Wolf, & E. V. Koonin. 2002. Selection in the evolution of gene duplications. *Genome Biology* 3: 8-1.
- Koonin, E. V. 2005. Orthologs, paralogs, and evolutionary genomics. *Annual Review of Genetics* 39: 309-338.
- Krell, F. T., and P. S. Cranston, P. S. 2004. Which side of the tree is more basal?. *Systematic Entomology* 29: 279-281.
- Ku, C. S., N. Naidoo, M. Wu, and R. Soong. 2011. Studying the epigenome using next generation sequencing. *Journal of Medical Genetics* 48: 721-730.
- Kubatko, L. S., and J. H. Degnan. 2007. Inconsistency of phylogenetic estimates from concatenated data under coalescence. *Systematic Biology* 56: 17-24.
- Kunin, V., A. Engelbrektson, H. Ochman, and P. Hugenholtz. 2010. Wrinkles in the rare biosphere: Pyrosequencing errors can lead to artificial inflations of diversity estimates. *Environmental Microbiology* 12: 118-123.
- Lanfear, R., B. Calcott, S. Y. Ho, and S. Guindon. 2012. PartitionFinder: combined selection of partitioning schemes and substitution models for phylogenetic analyses. *Molecular Biology and Evolution* 29: 1695-1701.
- Latreille, P. A. 1802. *Histoire naturelle, générale et particulière des Crustacés et des Insectes*. Ouvrage faisant suite à l'histoire naturelle générale et particulière, composée par Leclerc de Buffon, et rédigée par C.S. Sonnini, membre de plusieurs sociétés savantes. Familles naturelles des genres. Vol. 3. Paris, F. DuFart. 467 pp.
- . 1817. *Nouveau dictionnaire d'histoire naturelle, appliquée aux arts, à l'agriculture, à l'économie rurale et domestique, à la médecine, etc.* Vol. 10. Paris: Déterville.

- . 1831. *Cours d'Entomologie, ou de l'Histoire Naturelle des Crustacés, des Arachnides, des Myriapodes et des Insectes; a l'Usage des Élèves de l'École du Muséum d'Histoire Naturelle*. Paris: Librairie Encyclopédique de Roret.
- Le, S. Q., N. Lartillot, and O. Gascuel. 2008. Phylogenetic mixture models for proteins. *Philosophical Transactions of the Royal Society B: Biological Sciences* 363: 3965-3976.
- Lemmon, A. R., S. A. Emme, and E. M. Lemmon. 2012. Anchored hybrid enrichment for massively high-throughput phylogenomics. *Systematic Biology* 61: 727-744.
- and E. M. Lemmon. 2012. High-throughput identification of informative nuclear loci for shallow-scale phylogenetics and phylogeography. *Systematic Biology* 61: 745-761.
- , and E. C. Moriarty. 2004. The importance of proper model assumption in Bayesian phylogenetics. *Systematic Biology* 53: 265-277.
- Levin, J. Z., M. F. Berger, X. Adiconis, P. Rogov, A. Melnikov, T. Fennell, C. Nussbaum, L. A. Garraway, and A. Gnirke. 2009. Targeted next-generation sequencing of a cancer transcriptome enhances detection of sequence variants and novel fusion transcripts. *Genome Biology* 10: R115.
- Lewis, P. O., W. Xie, M. H. Chen, Y. Fan, and L. Kuo. 2014. Posterior predictive Bayesian phylogenetic model selection. *Systematic Biology* 63: 309-321.
- Li, C. P., S. De Grave, T. Y. Chan, H. C. Lei, & K. H. Chu. 2011. Molecular systematics of caridean shrimps based on five nuclear genes: implications for superfamily classification. *Zoologischer Anzeiger* 250: 270-279.
- Linnaeus, C., 1758. *Systema Naturae per Regna Tria Naturae, Secundum Classes, Ordines, Genera, Species, cum Characteribus, Differentiis, Synonymis, Locis*. Vol. 1. Holmiae, Laurentii Salvii. iii, 824 pp.
- Liu, L., L. Yu, L. Kubatko, D. K. Pearl, and S. V. Edwards. 2009b. Coalescent methods for estimating phylogenetic trees. *Molecular Phylogenetics and Evolution* 53: 320-328.
- , ———, D. K. Pearl, and S. V. Edwards. 2009a. Estimating species phylogenies using coalescence times among sequences. *Systematic Biology* 58: 468-477.
- Lundberg, J. G. 1972. Wagner networks and ancestors. *Systematic Biology* 21: 398-413.

- Ma, K. Y., T. Y. Chan, & K. H. Chu. 2009. Phylogeny of penaeoid shrimps (Decapoda: Penaeoidea) inferred from nuclear protein-coding genes. *Molecular Phylogenetics and Evolution* 53: 45-55.
- MacLeay, W. S. 1838. On the brachyurous decapod Crustacea brought from the Cape by Dr. Smith. In: Smith, A., *Illustrations of the Annulosa of South Africa; being a portion of the objects of natural history chiefly collected during an expedition into the interior of South Africa, under the direction of Dr. Andrew Smith, in the years 1834, 1835, and 1836; fitted out by "The Cape of Good Hope Association for Exploring Central Africa"*. London, Smith, Elder, and Co. Pp. 53–71, 2 plates.
- Maddison, W. P. 1997. Gene trees in species trees. *Systematic Biology* 46: 523-536.
- , and L. L. Knowles. 2006. Inferring phylogeny despite incomplete lineage sorting. *Systematic Biology* 55: 21-30.
- Mamanova, L., A. J. Coffey, C. E. Scott, I. Kozarewa, E. H. Turner, A. Kumar, E. Howard, J. Shendure, and D. J. Turner. 2010. Target-enrichment strategies for next-generation sequencing. *Nature Methods* 7: 111-118.
- Martin, J. A., and Z. Wang. 2011. Next-generation transcriptome assembly. *Nature Reviews Genetics* 12: 671-682.
- Martin, J. W., and G. E. Davis. 2001. An updated classification of the recent Crustacea. *Natural History Museum of Los Angeles County Science Series* 39: 1-124.
- McCormack, J. E., S. M. Hird, A. J. Zellmer, B. C. Carstens, and R. T. Brumfield. 2013. Applications of next-generation sequencing to phylogeography and phylogenetics. *Molecular Phylogenetics and Evolution* 66: 526-538.
- McKenna, A., M. Hanna, E. Banks, A. Sivachenko, K. Cibulskis, A. Kernytsky, K. Garimella, D. Altshuler, S. Gabriel, M. Daly, and M. A. DePristo. 2010. The Genome Analysis Toolkit: a MapReduce framework for analyzing next-generation DNA sequencing data. *Genome research* 20: 1297-1303.
- McVay, J. D., and B. C. Carstens. 2013. Phylogenetic model choice: justifying a species tree or concatenation analysis. *Journal of Phylogenetics and Evolutionary Biology* 1: 1, 1-8.
- Meiklejohn, C. D., K. L. Montooth, and D. M. Rand. 2007. Positive and negative selection on the mitochondrial genome. *Trends in Genetics* 23: 259-263.
- Meland, K., and E. Willassen. 2007. The disunity of "Mysidacea" Crustacea. *Molecular Phylogenetics and Evolution* 44: 1083-1104.

- Metzker, M. L. 2010. Sequencing technologies—the next generation. *Nature Reviews Genetics* 11: 31-46.
- Milne Edwards, H. 1834. Histoire naturelle des Crustacés, comprenant l'anatomie, la physiologie et la classification de ces animaux. Librairie Encyclopédique de Roret. Vol. 1–3. Paris: Roret. 1468, 2532, 3638 pp, Atlas 1–32, Plates I–XLII.
- Monod, T., and L. Laubier. 1996. Les Crustacés dans la Biosphère. In *Traité de Zoologie, Anatomie, Systematique, Biologie. Crustacés. Tome VII. Fascicule II. Generalités suite et Systematique*, ed. J. Forest, 91-166. Paris: Masson, 1002 pp.
- Moore, W. S. 1995. Inferring phylogenies from mtDNA variation: mitochondrial-gene trees versus nuclear-gene trees. *Evolution* 49: 718-726.
- Nishihara, H., N. Okada, and M. Hasegawa. 2007. Rooting the eutherian tree: the power and pitfalls of phylogenomics. *Genome Biology* 8: R199.
- Novacek, M. J., and M. A. Norell. 1982. Fossils, phylogeny, and taxonomic rates of evolution. *Systematic Biology* 31: 366-375.
- Opperdoes, F. R. 2009. Phylogenetic analysis using protein sequences. In P. Lemey, M. Salemi, and A-M. Vandamme Eds., *The Phylogenetic Handbook: a Practical Approach to Phylogenetic Analysis and Hypothesis Testing* (pp. 313-331). Cambridge, MA: Cambridge University Press.
- Page, R. D., and M. A. Charleston. 1997. From gene to organismal phylogeny: reconciled trees and the gene tree/species tree problem. *Molecular Phylogenetics and Evolution* 7: 231-240.
- Palero, F., and K. A. Crandall. 2009. Phylogenetic inference using molecular data, pp. 67-88. In, J. W. Martin, K. A. Crandall, and D. L. Felder (eds.), *Decapod Crustacean Phylogenetics. Crustacean Issues 18*. CRC Press, Boca Raton.
- Pamilo, P., and M. Nei. 1988. Relationships between gene trees and species trees. *Molecular Biology and Evolution* 5: 568-583.
- Poe, S., and J. J. Wiens. 2000. Character selection and the methodology of morphological phylogenetics. In J. J. Wiens Ed., *Phylogenetic Analysis of Morphological Data* (pp. 20-36). Washington, D.C.: Smithsonian Institution Press.
- Porter, M. L., and T. W. Cronin. 2009. A shrimp's eye view of evolution: How useful are visual characters in decapod phylogenetics? pp. 183-195. In, J. W. Martin, K. A. Crandall and D. L. Felder (eds.), *Decapod Crustacean Phylogenetics. Crustacean Issues 18*. CRC Press, Boca Raton.

- , M. Perez-Losada, and K. A. Crandall. 2005. Model-based multi-locus estimation of decapod phylogeny and divergence times. *Molecular Phylogenetics and Evolution* 37: 355-369.
- Posada, D. 2008. jModelTest: phylogenetic model averaging. *Molecular Biology and Evolution* 25: 1253-1256.
- , and K. A. Crandall. 1998. Modeltest: testing the model of DNA substitution. *Bioinformatics* 14: 817-818.
- Qian, G., Q. Zhao, A. Wang, L. Zhu, K. Zhou, and H. Sun. 2011. Two new decapod Crustacea: Malacostraca complete mitochondrial genomes: Bearings on the phylogenetic relationships within the Decapoda. *Zoological Journal of the Linnean Society* 162: 471-481.
- de Queiroz, K., and J. Gauthier. 1990. Phylogeny as a central principle in taxonomy: phylogenetic definitions of taxon names. *Systematic Zoology* 39: 307-322.
- Rafinesque, C. S. 1815. *Analyse de la Nature, ou Tableau de l'Univers et des Corps Organisés*. Palermo: L'Imprimerie de Jean Barravecchia.
- Reid, D. G., E. Rumbak, and R. H. Thomas. 1996. DNA, morphology and fossils: phylogeny and evolutionary rates of the gastropod genus *Littorina*. *Philosophical Transactions of the Royal Society B: Biological Sciences* 351: 877-895.
- Reid, N. M., S. M. Hird, J.M. Brown, T. A. Pelletier, J. D. McVay, J. D. Satler, and B. C. Carstens. 2013. Poor fit to the multispecies coalescent is widely detectable in empirical data. *Systematic Biology* 63: 322-333.
- Richter, S., and G. Scholtz. 2001. Phylogenetic analysis of the Malacostraca Crustacea. *Journal of Zoological Systematics and Evolutionary Research* 39: 113-136.
- Robles, R., C. Tudge, P. C. Dworschak, G. C. B. Poore, and D. L. Felder. 2009. Molecular phylogeny of the Thalassinidea based on nuclear and mitochondrial genes, pp. 309-326. In, J. W. Martin, K. A. Crandall and D. L. Felder (eds.), *Decapod Crustacean Phylogenetics*. Crustacean Issues 18. CRC Press, Boca Raton.
- Rokas, A., and P. W. Holland. 2000. Rare genomic changes as a tool for phylogenetics. *Trends in Ecology and Evolution* 15: 454-459.
- , Williams, B. L., King, N., and S. B. Carroll. 2003. Genome-scale approaches to resolving incongruence in molecular phylogenies. *Nature* 425: 798-804.

- Roukos, D. H. 2010. Next-generation sequencing and epigenome technologies: potential medical applications. *Expert Review of Medical Devices* 7: 723-726.
- de Saint Laurent, M., 1979. Vers une nouvelle classification des Crustacés Décapodes Reptantia. *Bulletin de l'Office National des Pêches République Tunisienne, Ministère de l'Agriculture*, 3: 15–31.
- Saitou, N., and M. Nei. 1987. The neighbor-joining method: a new method for reconstructing phylogenetic trees. *Molecular Biology and Evolution* 4: 406-425.
- Schmidt, H. A., and A. von Haeseler. 2009. Phylogenetic inference using maximum likelihood methods. In P. Lemey, M. Salemi, and A-M. Vandamme Eds., *The Phylogenetic Handbook: a Practical Approach to Phylogenetic Analysis and Hypothesis Testing* (pp. 181-198). Cambridge, MA: Cambridge University Press.
- Schnabel, K. E., S. T. Ahyong, and E. W. Maas. 2011. Galatheaidea are not monophyletic—molecular and morphological phylogeny of the squat lobsters (Decapoda: Anomura) with recognition of a new superfamily. *Molecular Phylogenetics and Evolution*, 58: 157-168.
- Schneider, A., and D. Ebert. 2004. Covariation of mitochondrial genome size with gene lengths: evidence for gene length reduction during mitochondrial evolution. *Journal of Molecular Evolution* 59: 90-96.
- Scholtz, G., and S. Richter. 1995. Phylogenetic systematics of the reptantian Decapoda Crustacea, Malacostraca. *Zoological Journal of the Linnean Society* 113: 289-328.
- Schram, F. R. 1981. On the classification of the Eumalacostraca. *Journal of Crustacean Biology* 1: 1-10.
- . 1984. Relationships within eumalacostracan crustaceans. *Transactions of the San Diego Society of Natural History* 20: 301-312.
- . 1986. *Crustacea*. New York: Oxford University Press.
- . 2001. Phylogeny of decapods: Moving towards a consensus. *Hydrobiologia* 449: 1-20.
- , and C. H. J. Hof. 1998. Fossil taxa and the relationships of major crustacean groups. In G. Edgecombe Ed., *Arthropod Fossils and Phylogeny* (pp. 273-302). New York: Columbia University Press.
- Shaw, K. L. 2002. Conflict between nuclear and mitochondrial DNA phylogenies of a recent species radiation: what mtDNA reveals and conceals about modes of

- speciation in Hawaiian crickets. *Proceedings of the National Academy of Sciences* 99: 16122-16127.
- Shen, H., A. Braband, and G. Scholtz. 2013 Mitogenomic analysis of decapod crustacean phylogeny corroborates traditional views on their relationships. *Molecular Phylogenetics and Evolution* 66: 776–789.
- Siewing, R. 1963. Studies in malacostracan morphology: Results and problems. In H. B. Whittington, and W. D. I. Rolfe Eds., *Phylogeny and Evolution of Crustacea* (pp. 85-103). Cambridge, MA: Museum of Comparative Zoology.
- Simon, C., F. Frati, A. Beckenbach, B. Crespi, H. Liu, and P. Flook. 1994. Evolution, weighting, and phylogenetic utility of mitochondrial gene sequences and a compilation of conserved polymerase chain reaction primers. *Annals of the Entomological Society of America* 87: 651-701.
- Sota, T., and A. P. Vogler. 2003. Reconstructing species phylogeny of the carabid beetles *Ohomopterus* using multiple nuclear DNA sequences: heterogeneous information content and the performance of simultaneous analyses. *Molecular Phylogenetics and Evolution* 26: 139-154.
- Spinks, P. Q., and H. B. Shaffer. 2009. Conflicting mitochondrial and nuclear phylogenies for the widely disjunct *Emys* Testudines: Emydidae species complex, and what they tell us about biogeography and hybridization. *Systematic Biology* 58: 1-20.
- Stamatakis, A. 2006. RAxML-VI-HPC: maximum likelihood-based phylogenetic analyses with thousands of taxa and mixed models. *Bioinformatics* 22: 2688-2690.
- , F. Blagojevic, D. S. Nikolopoulos, and C. D. Antonopoulos. 2007. Exploring new search algorithms and hardware for phylogenetics: RAxML meets the IBM cell. *The Journal of VLSI Signal Processing Systems for Signal, Image, and Video Technology* 48: 271-286.
- , P. Hoover, and J. Rougemont. 2008. A rapid bootstrap algorithm for the RAxML web servers. *Systematic Biology* 57: 758-771.
- , T. Ludwig, and H. Meier. 2005. RAxML-III: a fast program for maximum likelihood-based inference of large phylogenetic trees. *Bioinformatics* 21: 456-463.
- Studer, R. A., and M. Robinson-Rechavi. 2009. How confident can we be that orthologs are similar, but paralogs differ?. *Trends in Genetics* 25: 210-216.

- Talavera, G., and R. Vila. 2011. What is the phylogenetic signal limit from mitogenomes? The reconciliation between mitochondrial and nuclear data in the Insecta class phylogeny. *BMC Evolutionary Biology* 11: 315-329.
- Tavaré, S. 1986. Some probabilistic and statistical problems in the analysis of DNA sequences. *Lectures on Mathematics in the Life Sciences* 17: 57-86.
- Telford, M. J., and R. R. Copley. 2011. Improving animal phylogenies with genomic data. *Trends in Genetics* 27: 186-195.
- Throckmorton, L. H. 1968. Concordance and discordance of taxonomic characters in *Drosophila* classification. *Systematic Biology* 17: 355-387.
- Toon, A., M. Finley, J. Staples, and K. A. Crandall. 2009. Decapod phylogenetics and molecular evolution, pp. 15-29. In, J. W. Martin, K. A. Crandall and D. L. Felder (eds.), *Decapod Crustacean Phylogenetics*. *Crustacean Issues* 18. CRC Press, Boca Raton.
- Tsang, L.-M., T. Y. Chan, S. T. Ahyong, and K. H. Chu. 2011. Hermit to king, or hermit to all: multiple transitions to crab-like forms from hermit crab ancestors. *Systematic Biology*, 60: 616-629.
- , F.-J. Lin, K. H. Chu, and T.-Y. Chan. 2008b. Phylogeny of Thalassinidea Crustacea, Decapoda inferred from three rDNA sequences: implications for morphological evolution and superfamily classification. *Journal of Zoological Systematics and Evolutionary Research* 46: 216-223.
- , K. Y. Ma, S. T. Ahyong, T.-Y. Chan, and K. H. Chu. 2008a. Phylogeny of Decapoda using two nuclear protein-coding genes: Origin and evolution of the Reptantia. *Molecular Phylogenetics and Evolution* 48: 359-368.
- Valentine, J. W., D. Jablonski, S. Kidwell, and K. Roy. 2006. Assessing the fidelity of the fossil record by using marine bivalves. *Proceedings of the National Academy of Sciences*, 103: 6599-6604.
- Van de Peer, Y. 2009. Phylogenetic inference based on distance methods. In P. Lemey, M. Salemi, and A-M. Vandamme Eds., *The Phylogenetic Handbook: a Practical Approach to Phylogenetic Analysis and Hypothesis Testing* (pp. 142-160). Cambridge, MA: Cambridge University Press.
- Vandamme, A.-M. 2009. Basic concepts of molecular evolution. In P. Lemey, M. Salemi, and A-M. Vandamme Eds., *The Phylogenetic Handbook: a Practical Approach to Phylogenetic Analysis and Hypothesis Testing* (pp. 3-29). Cambridge, MA: Cambridge University Press.

- Weishampel, D. B. 1996. Fossils, phylogeny, and discovery: a cladistic study of the history of tree topologies and ghost lineage durations. *Journal of Vertebrate Paleontology* 16: 191-197.
- Wheeler, W. C. 1990. Nucleic acid sequence phylogeny and random out-groups. *Cladistics* 6: 363-367.
- Wicker, T., E. Schlagenhauf, A. Graner, T. J. Close, B. Keller, and S. Nils. 2006. 454 sequencing put to the test using the complex genome barley. *BMC Genomics* 7: 275.
- Wiens, J. J. 2003. Missing data, incomplete taxa, and phylogenetic accuracy. *Systematic Biology* 52: 528-538.
- Wiley, E. O., D. Siegel-Causey, D. R. Brooks, and V. A. Funk. 1991. *The Compleat Cladist: A Primer of Phylogenetic Procedures*. Kansas: The University of Kansas Museum of Natural History.
- Williamson, D. I. 1973. *Amphionides, reynaudii* (H. Milne Edwards) representative of a proposed new order of eucaridan Malacostraca. *Crustaceana* 25: 35-50.
- Wills, M. 1998. A phylogeny of the recent and fossil Crustacea derives from morphological characters, pp. 189-209. In, R. A. Fortey, and R. H. Thomas (eds.), *Arthropod Relationships*. Chapman and Hall, London.
- Winckler, T. C., 1882. Carcinological investigation on the genera *Pemphix*, *Glyphea* and *Araeosternus*. *Annals and Magazine of Natural History* (5)10: 133-149, 306-317.
- Wong, J. M., J. L. Perez-Moreno, T.-Y. Chan, T. M. Frank, and H. D. Bracken-Grissom. 2015. Phylogenetic and transcriptomic analyses reveal the evolution of bioluminescence and light detection in marine deep-sea shrimps of the family Oplophoridae (Crustacea: Decapoda). *Molecular Phylogenetics and Evolution* 83: 278-292.
- Yang, Z. 1996. Among-site rate variation and its impact on phylogenetic analyses. *Trends in Ecology and Evolution* 11: 367-372.
- , and B. Rannala. 2012. Molecular phylogenetics: principles and practice. *Nature Reviews Genetics* 13: 303-314.
- Yeo, G. W., E. Van Nostrand, D. Holste, T. Poggio, and C. B. Burge. 2005. Identification and analysis of alternative splicing events conserved in human and mouse. *Proceedings of the National Academy of Sciences of the United States of America* 102: 2850-2855.

Zhang, D. X., and G. M. Hewitt. 1996. Nuclear integrations: challenges for mitochondrial DNA markers. *Trends in Ecology and Evolution* 11: 247-251.

———, and ———. 2003. Nuclear DNA analyses in genetic studies of populations: practice, problems and prospects. *Molecular Ecology* 12: 563-584.

Zwickl, D. J., and D. M. Hillis. 2002. Increased taxon sampling greatly reduces phylogenetic error. *Systematic Biology* 51: 588-598.

Tables

Table 1. The gene markers and out-group(s) used in higher-level (Infraorder) decapod phylogeny studies to date.

Publication	Genes Used	Gene Origin	Gene Function	Infraorders Not Included
Kim and Abele, 1990	18S	nDNA	ribosomal subunit	Achelata, Anomura, Axiidea, Gebiidea, Glypheidea, Polychelida
Crandall et al., 2000	16S	mtDNA	ribosomal subunit	Caridea, Glypheidea, Polychelida, Procarididea
	18S	nDNA	ribosomal subunit	
	28S	nDNA	ribosomal subunit	
Ahyong & O'Meally, 2004	16S	mtDNA	ribosomal subunit	Caridea, Procarididea
	18S	nDNA	ribosomal subunit	
	28S	nDNA	ribosomal subunit	
Porter et al. 2005	16S	mtDNA	ribosomal subunit	Gebiidea, Glypheidea, Polychelida, Procarididea

	18S	nDNA	ribosomal subunit	
	28S	nDNA	ribosomal subunit	
	H3	nDNA	protein-coding	
Tsang et al. 2008a	PEPCK	nDNA	protein-coding	Glypheidea, Procarididea
	NaK	nDNA	protein-coding	
Chu et al. 2009	PEPCK	nDNA	protein-coding	Glypheidea, Procarididea
	NaK	nDNA	protein-coding	
Toon et al. 2009	12S	mtDNA	ribosomal subunit	Gebiidea, Glypheidea, Procarididea, Stenopodidea
	16S	mtDNA	ribosomal subunit	
	18S	nDNA	ribosomal subunit	
	28S	nDNA	ribosomal subunit	

	H3	nDNA	protein-coding	
	EF-2	nDNA	protein-coding	
	EPRS	nDNA	protein-coding	
	TM9sf4	nDNA	protein-coding	
Bracken et al. 2009	16S	mtDNA	ribosomal subunit	Procarididea
	18S	nDNA	ribosomal subunit	
	28S	nDNA	ribosomal subunit	
	H3	nDNA	protein-coding	
Bracken et al. 2010	16S	mtDNA	ribosomal subunit	Glypheidea
	18S	nDNA	ribosomal subunit	
	28S	nDNA	ribosomal subunit	

	H3	nDNA	protein-coding	
Bybee et al. 2011a	12S	mtDNA	ribosomal subunit	Gebiidea, Glypheidea, Procarididea
	16S	mtDNA	ribosomal subunit	
	18S	nDNA	ribosomal subunit	
	28S	nDNA	ribosomal subunit	
	H3	nDNA	protein-coding	
	COI	mtDNA	protein-coding	
Qian et al. 2011 (whole mt genome)	cox1	mtDNA	protein-coding	Axiidea, Gebiidea, Glypheidea, Polychelida, Procarididea, Stenopodidea
	cox2	mtDNA	protein-coding	
	cox3	mtDNA	protein-coding	
	nad1	mtDNA	protein-coding	

	nad2	mtDNA	protein-coding	
	nad3	mtDNA	protein-coding	
	nad4	mtDNA	protein-coding	
	nad4L	mtDNA	protein-coding	
	nad5	mtDNA	protein-coding	
	nad6	mtDNA	protein-coding	
	atp6	mtDNA	protein-coding	
	atp8	mtDNA	protein-coding	
	cob	mtDNA	protein-coding	
	rrnS	mtDNA	ribosomal subunit	
	rrnL	mtDNA	ribosomal subunit	

	A	mtDNA	tRNA	
	R	mtDNA	tRNA	
	N	mtDNA	tRNA	
	D	mtDNA	tRNA	
	C	mtDNA	tRNA	
	E	mtDNA	tRNA	
	Q	mtDNA	tRNA	
	G	mtDNA	tRNA	
	H	mtDNA	tRNA	
	I	mtDNA	tRNA	
	L1	mtDNA	tRNA	

	L2	mtDNA	tRNA	
	K	mtDNA	tRNA	
	M	mtDNA	tRNA	
	F	mtDNA	tRNA	
	P	mtDNA	tRNA	
	S1	mtDNA	tRNA	
	S2	mtDNA	tRNA	
	T	mtDNA	tRNA	
	Y	mtDNA	tRNA	
	W	mtDNA	tRNA	
	V	mtDNA	tRNA	

	nCR	mtDNA	intron	
Shen et al., 2013 (whole mt genome)	cox1	mtDNA	protein- coding	Glypheidea, Procarididea
	cox2	mtDNA	protein- coding	
	cox3	mtDNA	protein- coding	
	nad1	mtDNA	protein- coding	
	nad2	mtDNA	protein- coding	
	nad3	mtDNA	protein- coding	
	nad4	mtDNA	protein- coding	
	nad4L	mtDNA	protein- coding	
	nad5	mtDNA	protein- coding	
	nad6	mtDNA	protein- coding	

	atp6	mtDNA	protein-coding	
	atp8	mtDNA	protein-coding	
	cob	mtDNA	protein-coding	
	rrnS	mtDNA	ribosomal subunit	
	rrnL	mtDNA	ribosomal subunit	
	A	mtDNA	tRNA	
	R	mtDNA	tRNA	
	N	mtDNA	tRNA	
	D	mtDNA	tRNA	
	C	mtDNA	tRNA	
	E	mtDNA	tRNA	

	Q	mtDNA	tRNA	
	G	mtDNA	tRNA	
	H	mtDNA	tRNA	
	I	mtDNA	tRNA	
	L1	mtDNA	tRNA	
	L2	mtDNA	tRNA	
	K	mtDNA	tRNA	
	M	mtDNA	tRNA	
	F	mtDNA	tRNA	
	P	mtDNA	tRNA	
	S1	mtDNA	tRNA	

	S2	mtDNA	tRNA	
	T	mtDNA	tRNA	
	Y	mtDNA	tRNA	
	W	mtDNA	tRNA	
	V	mtDNA	tRNA	
	nCR	mtDNA	intron	

Figure Captions

Figure 1. Phylogenetic trees of infraordinal decapod phylogeny including: A, Dixon et al. (2003) morphological analysis; B, Scholtz and Richter (1995) meta-analysis. Major molecular studies include: C, Crandall et al. (2003) analysis of 18S; D, Ahyong and O'Meally (2004) analysis of 16S, 18S, 28S, and morphological characters; E, Porter et al. (2005) analysis of 16S, 18S, 28S, and H3; F, Tsang et al. (2008a) analysis of PEPCK and NAK; G, Bracken et al. (2009a) analysis of 16S, 18S, 28S, and H3; H, Toon et al. (2009) analysis of 12S, 16S, 18S, 28S, H3, EF-2, EPRS, and TM9sf4; I, Bracken et al. (2010) analysis of 16S, 18S, 28S, and H3; J, Qian et al. (2011) analysis of whole mt-genome; K, Bybee et al. (2011a) analysis of 12S, 16S, 18S, 28S, H3, and COI; L, Shen et al. (2013) analysis of whole mt-genome.

Figure 2. An illustration of a species tree (depicted with double-lines) compared to four arbitrary single-gene trees. While the true species tree is always the same, the gene trees recapitulate different relationships when samples from the same species groups.

Figure 3. An illustration of long-branch attraction (LBA), in which distantly related taxa have accrued so many differences that they cluster together. In this figure, species A and D are truly distantly-related (left tree), but cluster together due to LBA (right tree). Figure adapted from Forterre and Philippe (1999).

Figures

Figure 1

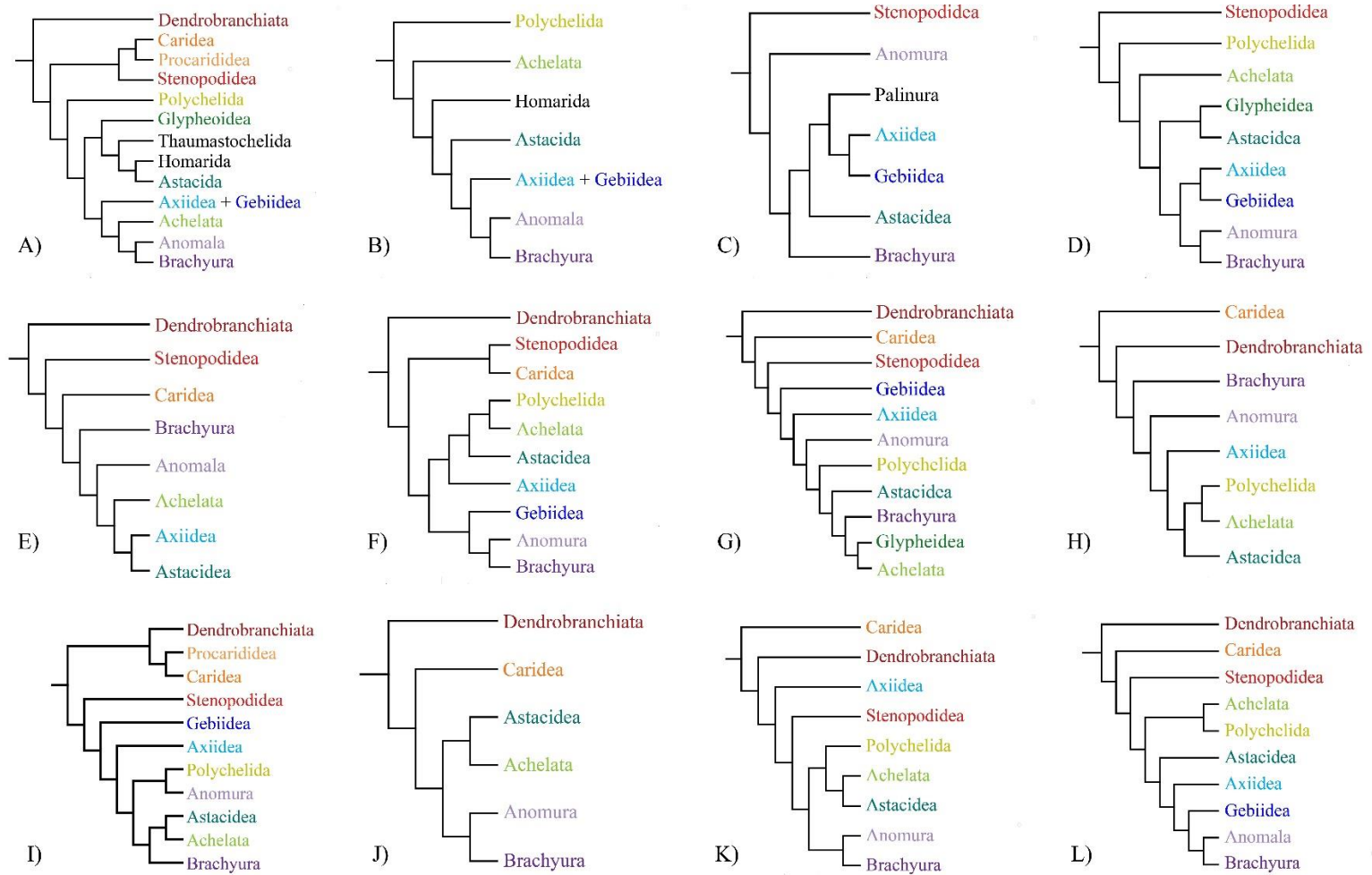


Figure 2

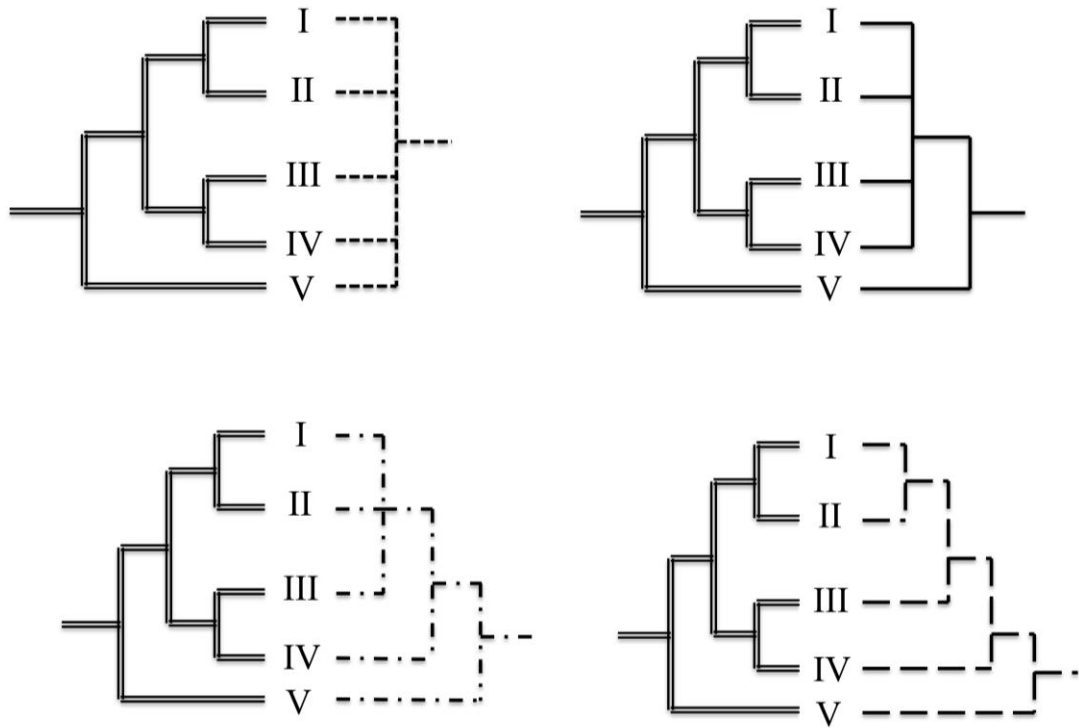
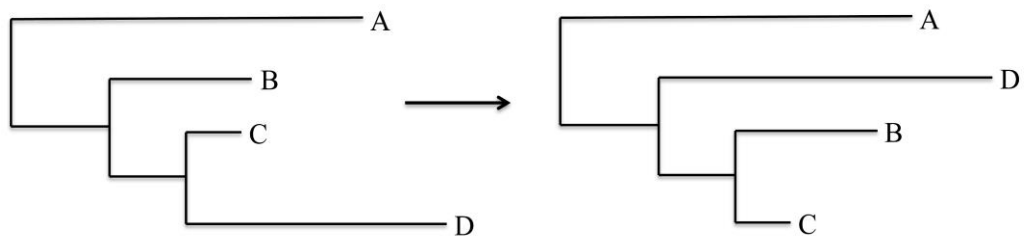


Figure 3



Appendices Captions

Appendix 1: A list of taxon names mentioned in this paper, 'Accepted' status indicates whether the name is currently accepted and is listed according to De Grave et al., 2009.

Appendices

Appendix 1

Taxon	Accepted	Taxonomic Rank	Includes	Authority
Achelata	Yes	Infraorder	Palinura, sans the infraorder Polychelida	Scholtz and Richter, 1995
Amphionidacea	Yes	Order	<i>Amphionides reynaudii</i> as sole representative	Williamson, 1973
Anomala	No	Infraorder	Anomura, sans the thalassinoids	Latreille, 1817
Anomura	Yes	Infraorder	Anomala, plus the thalassinoids	MacLeay, 1838
Astacida	No	Superfamily	Monophyletic clade of freshwater crayfish	Dixon et al., 2003
Astacidea	Yes	Infraorder	---	Latreille, 1802

Astacura	No	Infraorder	---	Borradaile, 1907
Axiidea	Yes	Infraorder	Some representatives of the unaccepted Infraorder Thalassinidea	de Saint Laurent, 1979
Brachyura	Yes	Infraorder	---	Latreille, 1802
Caridea	Yes	Infraorder	---	Dana, 1852
Decapoda	Yes	Suborder	Achelata, Anomura, Astacidea, Axiidea, Brachyura, Caridea, Dendrobranchiata, Gebiidea, Glypheidea, Polychelida, Procarididea, Stenopodidea	Latreille, 1802
Dendrobranchiata	Yes	Suborder	Penaeoidea, Sergestoidea	Bate, 1888
Eucarida	Yes	Superorder	Amphionidacea, Decapoda, Euphausiacea	Calman, 1904
Euphausiacea	Yes	Order	Bentheuphausiidae, Euphausiidae	Dana, 1852

Eurysternalia	No	Unranked	Achelata, Anomura, Brachyura	Dixon et al., 2003
Gebiidea	Yes	Infraorder	Some representatives of the unaccepted Infraorder Thalassinidea	de Saint Laurent, 1979
Glypheidea	Yes	Infraorder	---	Winckler, 1882
Glypheoidea	Yes	Superfamily	---	Winckler, 1882
Heterochelida	No	Suborder	Caridea, Thalassinidea	Beurlen and Glaessner, 1930
Homarida	No	Infraorder	---	Huxley, 1878
Lineata	Yes	Unranked	Anomura, Brachyura, Thalassinidea	Ahyong and O'Meally, 2004
Meiura	Yes	Unranked	Anomura, Brachyura	Dixon et al., 2003

Natantia	No	Suborder	Caridea, Penaeoidea, Stenopodidea	Boas, 1880
Paguroidea	Yes	Superfamily	---	Latreille, 1802
Palinura	No	Infraorder	Achelata, Polychelida	Latreille, 1802
Penaeidae	Yes	Family	---	Burkenroad, 1963
Penaeoidea	Yes	Superfamily	---	Rafinesque, 1815
Pleocyemata	Yes	Suborder	Achelata, Anomura, Astacidea, Axiidea, Brachyura, Caridea, Gebiidea, Glypheidea, Polychelida, Procarididea, Stenopodidea	Burkenroad, 1963
Polychelida	Yes	Infraorder	---	Scholtz and Richter, 1995
Procarididea	Yes	Infraorder	---	Felgenhauer and Abele, 1983

Reptantia	No	Unranked	Achelata, Anomura, Astacidea, Axiidea, Brachyura, Gebiidea, Glypheidea, Polychelida	Boas, 1880
Stenopodidea	Yes	Infraorder	---	Claus, 1872
Sterropoda	No	Infraorder	Eurysternalia, Thalassinida	Dixon et al., 2003
Thalassinida	No	Infraorder	Axiidea, Gebiidea	Dixon et al., 2003
Thalassinidea	No	Infraorder	Axiidea, Gebiidea	Latreille, 1831
Thaumastochelelida	No	Infraorder	---	Bate, 1888

CHAPTER III

A TREE MONEY GROWS ON: THE FIRST INCLUSIVE MOLECULAR
PHYLOGENY OF THE ECONOMICALLY IMPORTANT PINK SHRIMP
(DECAPODA, *FARFANTEPENAEUS*) REVEALS CRYPTIC DIVERSITY

ABSTRACT

Species of *Farfantepenaeus* support economically important shrimp fisheries throughout the Western Hemisphere, necessitating proper fisheries management of these species. To be effective, species management should be informed of the potential presence of cryptic species and of the evolutionary forces driving biodiversity, which is best accomplished through a robust phylogenetic framework. The present study represents the first comprehensive molecular phylogeny of shrimps belonging to the genus *Farfantepenaeus*. Targeting three mitochondrial genes (12S, 16S, and COI), gene trees and a phylogeny for the genus were inferred using maximum likelihood and Bayesian inference. In general, the phylogenetic relationships inferred here largely agree with those recovered from morphological data, including the most recent designation of *F. isabellae* as sister to *F. subtilis*. Molecular divergence was found between northern and southern populations of *F. brasiliensis*, suggesting the existence of unrecognized subspecies. However, previous recognition of *F. duorarum* and *F. notialis* as two species was not supported by this study. The phylogeny inferred here also uncovers phylogeographic signal of latitudinal speciation in the genus. The phylogeny we present here provides valuable insight into the evolutionary history of *Farfantepenaeus*, improving our ability to effectively manage these economically important species.

Keywords: pink shrimp, penaeid, phylogeny, cryptic diversity, genetics, fisheries management

INTRODUCTION

In 2015, almost 59,000 metric tons of penaeid shrimp in the genus *Farfantepenaeus* (Burukovsky, 1972, 1997), representing \$213.5 million in ex-vessel value, were fished from the Gulf of Mexico and Atlantic Ocean off the southern U.S. (compiled NMFS Landings query, 2/28/2018). The *Farfantepenaeus* spp. landings represented 59% of total U.S. penaeid shrimp landings in the combined Gulf of Mexico and Atlantic Ocean that year. With the occurrence of *Farfantepenaeus* spp. admixtures on various fishing grounds (e.g., Sheridan et al. 1987; Arreguín-Sanchez et al 1999, 2008; Charuau and Die 2000; Shepard and Die 2000), effective fishery management is dependent on an understanding of the evolutionary forces driving biodiversity (Bernatchez 1995), which is greatly facilitated by a robust, comprehensive phylogenetic framework. Phylogenies can be critical to identifying evolutionarily significant units (ESUs) and determining whether certain units require unique management considerations (Ryder 1986). Much focus has been placed on identifying ESUs determined by reproductive isolation (Waples 1991), however it has been argued that this over-emphasis negatively impacts maintenance of adaptive diversity (Crandall et al. 2000), which is critical to the evolutionary success of a species (Frankel 1974; Lande and Shannon 1996; Moritz 2002). In this, phylogenies are crucial: while distinct, historically isolated populations of a species may exist, they may not be reciprocally monophyletic. This means these populations are the result of evolutionary processes *within* the ESU and the goal of management should be to maintain these processes (Crandall et al. 2000).

Proper classification, informed by an understanding of evolutionary relationships within the taxon of interest, is crucial to species conservation and management. Species

divisions within *Farfantepenaeus* are determined largely by morphology of external sexual structures (Figure 1) (Pérez-Farfante 1967, 1969, 1970a, 1970b, 1970c, 1988; Pérez-Farfante and Kensley 1997) and/or biogeography (Burukovsky 1972). When established, the subgenus *Farfantepenaeus* included six species: *F. duorarum* (Burkenroad 1939), *F. brasiliensis* (Latreille 1817), *F. aztecus* (Ives 1891), *F. californiensis* (Holmes 1900), *F. brevirostris* (Kingsley 1878), and *F. paulensis* (Pérez-Farfante 1967). *Farfantepenaeus subtilis* (Pérez-Farfante 1967) and *F. notialis* (Pérez-Farfante 1967) were included as subspecies of *F. aztecus* and *F. duorarum*, respectively (Pérez-Farfante 1967). *Farfantepenaeus* was named as a subgenus of *Penaeus* in 1972 (Burukovsky, 1972) and *F. brasiliensis* was designated the type species in a brief note in 1997 (Burukovsky 1997). In the same year, Pérez-Farfante and Kensley (1997) produced a seminal monograph that elevated several penaeid sub-genera, including *Farfantepenaeus*, to the level of genus. In the same work, the subspecies *F. notialis* and *F. subtilis* were considered valid species (Pérez-Farfante and Kensley, 1997). Since then, confusion has arisen concerning the taxonomic rank and placement of two morphotypes of *F. subtilis* described from the western Atlantic. This is discussed in greater detail in the Methods section, *Morphological Identification of Specimens*. Morphotype II has since been described as sister to/subclade of either *F. paulensis* or *F. subtilis* MI (D’Incao et al. 1998; Gusmão et al. 2000; D. Maggioni 1996; R. Maggioni et al. 2001). Most recently, MII has been named *F. subtilis* sensu stricto and *F. subtilis* MI has been formally described as *F. isabelae* (Tavares and Gusmão 2016). While phylogenetic relationships have been inferred between several species of *Farfantepenaeus* (Baldwin et al. 1998; Gusmão et al. 2000; Lavery et al. 2004; R. Maggioni et al. 2001; Tavares and Gusmão

2016; Voloch et al. 2005), these studies did not include all species within the genus, and frequently included, at most, two mitochondrial genes. Given the economic value of this group and the concomitant fishing pressures, a clear understanding of biodiversity and evolutionary relatedness is needed.

Previous studies have identified the existence of cryptic species within *Farfantepenaeus*, uncertainty of monophyly at the genus- and species-levels (Gusmão et al. 2000; R. Maggioni et al. 2001), and population genetic structure within *F. notialis* (García-Machado et al. 2001, 2018; Robainas-Barcia et al. 2008). Specifically, the use of external sexual morphology to define species has proved convoluted because, although fully developed in adults, they are often absent or underdeveloped in juveniles and thus their utility for species identification is subjective and can be inconsistent (Ditty and Alvarado Bremer 2011; Teodoro et al. 2016). Over the past three decades, population genetics studies of a wide variety of marine fauna occurring along the southeastern coast of the United States have indicated significant genetic diversity between the Gulf of Mexico and the non-Gulf Atlantic (see review by Avise 1992 and Young et al. 2002 for a decapod-specific example). This suggests that species of *Farfantepenaeus* with large distributional ranges throughout the Gulf and into the Atlantic should be investigated for potential cryptic species (see Figure 3 for species ranges). *Farfantepenaeus brasiliensis*, whose range extends from North Carolina, USA to the coasts of Brazil (including an extension into the Gulf of Mexico along the Yucatan coast), and *F. duorarum*, with a range from Chesapeake Bay, Virginia, USA to the Yucatan, Mexico, seem likely candidates for cryptic diversity.

The present study represents the first comprehensive phylogeny of the economically important shrimp genus *Farfantepenaeus*, with the inclusion of all nine currently recognized species of *Farfantepenaeus*. Phylogenetic relationships within *Farfantepenaeus* were recapitulated and the phylogeographic structure of mitochondrial haplotypes was examined to address three primary objectives: 1) examine evolutionary relationships within the genus and characterize it in a biogeographical framework and 2) investigate cryptic diversification within the genus. Both objectives are needed to properly manage and conserve species within this heavily fished genus.

METHODS

Specimen Collection

In total, 171 postlarval, juvenile, and adult shrimp were collected for inclusion in the study. Most specimens were directly collected by the authors while others were donated by colleagues. Specimens were either collected aboard shrimp vessels and preserved on the ship or by field biologists and returned to the laboratory. Collected specimens were frozen at -20°C or directly stored in 70% ethanol. Every extant species of *Farfantepenaeus* was included, either as a collected specimen or through sequence data acquired from GenBank (Table 1 and Table S1). *Litopenaeus vannamei* (Boone 1931), *L. stylirostris* (Stimpson 1874), and *L. setiferus* (Linnaeus 1767) were included as outgroups. Some individuals had morphological characters that matched *F. notialis*, despite having been collected from outside of the described range of the species. These individuals were labeled “*F. nr. notialis*” to distinguish them from specimens of the species collected from within-range. This study also included representatives from both

F. subtilis morphotypes: morphotype I (MI) and morphotype II (MII) were initially divided based on the adrostral sulcus, rostral shape, 6th pleonite keel to sulcus (K/S) ratio, petasma, and thelycum (Pérez-Farfante 1969). For the purposes of clarity, in this paper individuals identified as *F. subtilis* MI will be designated as such, though they have now been re-classified as *F. isabellae*, and *Farfantepenaeus subtilis* s. str. will be referred to as “*F. subtilis* MII”.

Morphological Identification of Specimens

Collected specimens were identified taxonomically in the Ecological Investigations Laboratory at the Southeast Fisheries Science Center in Miami, Florida (Pérez-Farfante 1967, 1969, 1970a, 1970b, 1970c, 1988; Pérez-Farfante and Kensley, 1997) or identified by colleagues. Four morphological traits are especially useful in identifying species within the genus *Farfantepenaeus*: 1) adrostral sulcus, 2) keel height to sulcus width ratio (K/S) of the 6th pleonite (i.e., abdominal somite), and characteristics of 3) petasma and 4) thelycum, the external genitalia of males and females, respectively (Figure 2). The adrostral sulcus (groove) and carina (ridge) flank the rostrum and postrostral crest. Adrostral sulci and carina that extend posteriorly beyond the epigastric tooth and usually to the dorsal posterior carapace margin are defining characteristics of the genus *Farfantepenaeus*, known as the “grooved shrimp” (Pérez-Farfante and Kensley 1997). Differences in adrostral sulci length and width may distinguish *Farfantepenaeus* species. The ratio of keel height to sulcus width refers to the dorsomedian keel and the dorsolateral sulcus of the 6th pleonite (abdominal segment). This ratio, measured at ~1/3 the somite length from the posterior margin of the 6th pleonite, may be useful to separate

certain species in this genus, even in juvenile stages, which either exhibit incompletely-developed external reproductive structures or lack them all together.

In individuals whose carapace length exceeds 8-10mm, reproductive external structures are sufficiently developed to assist with species identification (Pérez-Farfante 1970b, 1970c). Reproductive structure morphology is especially useful for identifying sub-adults and adults to species (Pérez-Farfante 1969, 1970a, 1970b, 1970c, 1988). In males, diagnostically useful specific features associated with the petasma include the shape of the ventral costa terminus on the ventrolateral lobule, the presence and pattern of distomarginal spines along the lateral lobe, and the shape of the distomedian projection of the median lobe. In practice, we also compare the shape and size of the proxomedian projection of the median lobe. In females, specific features of the thelycum that are diagnostically useful include the shape and curvature of the anteriomedian corners and median margins of lateral plates, which shield the seminal receptacle, as well as the shape and/or relative dimensions of the anterior process, posterior process, and median carina of the median protuberance.

DNA extraction, PCR, and sequencing

Abdominal muscle tissue was plucked from individuals and DNA was extracted using the Qiagen DNeasy Blood and Tissue Kit, following the manufacturer's instructions. After DNA extraction, three mitochondrial genes common to phylogenetic analysis (Cunningham et al. 1992; Gusmão et al. 2000; Lavery et al. 2004; Voloch et al. 2005) were sequenced in 170 specimens and several GenBank sequences were downloaded for inclusion in our dataset. Cytochrome oxidase subunit I (COI) and the two

ribosomal structural genes, 12S and 16S, were targeted to infer interspecific relationships (as utilized in Schubart et al. 2000; Stillman and Reeb 2001). Primer combinations and annealing temperatures for each gene are included in Table 2.

PCR amplification reactions were performed in 26.75 μL volumes containing 2 μL of DNA template, 6.45 μL of sterile non-DEPC treated water, 5 μL of 5x combinatorial PCR enhancer solution (CES), 3 μL of 2mM deoxyribonucleotide triphosphate mix (dNTPs), 2.5 μL of 10x PCR Buffer, 2.3 μL of 5M betaine, 2 μL of each 10 μM forward and reverse primer, and 1.5 μL of 0.1g/mL bovine serum albumin (BSA). Unpurified PCR products were sent to Beckman Coulter Genomics (Danvers, MA, USA) for purification and sequencing on an Applied Biosystems PRISM 3730xl DNA Analyzer.

Phylogenetic Analyses

Sequences were assembled into contigs and cleaned in Sequencher 5.0.1 (GeneCodes, Ann Arbor, MI, USA). To prevent the inclusion of pseudogenes, COI sequences were visually inspected for indels and stop codons. After experts in shrimp taxonomy confirmed morphological identifications, sequences were queried against the GenBank (NCBI) database as a secondary means of identification. This assisted in diagnosing contamination and tentative mis-identifications, both of which were removed from analysis. Using Geneious 8.1.3, sequences were cleaned and primers were removed. Cleaned sequences were aligned using MAFFT (Kato and Standley 2013) and missing data were designated with a “?” for any incomplete sequences. Some species lacked data at a locus entirely (such as *F. paulensis*, which could only be represented with COI data).

For this reason, as well as for the purpose of including as much data for as many taxa as possible, phylogenetic analyses were carried out on the single-gene alignments in addition to the concatenated dataset (12S+16S+COI). All sequences were uploaded to GenBank (Table S1).

To determine models of evolution for each gene and partitioning across the concatenated data matrix, PartitionFinder v1.1.1 (Lanfear et al. 2012) was utilized. Single-gene trees and the concatenated tree were constructed in RAxML v7.4.2 (Stamatakis 2006) and the RAxML bootstopping action was selected. Each tree had 1000 bootstrap replicates. This was completed on the CIPRES Science Gateway v3.1 (Miller et al. 2010). Bootstrap values were mapped onto the resulting topology using FigTree v1.4.2 (Rambaut 2012). Single-gene trees were inspected for potentially contaminated sequences and conflicting topologies. When contamination was found, these sequences were removed from the single-gene alignment(s) and the concatenated dataset and new maximum likelihood trees were obtained.

Bayesian inference was conducted in MrBayes v3.2.6 (Huelsenbeck and Ronquist 2001; Ronquist and Huelsenbeck 2003) for each gene and for the concatenated dataset of all genes. By analyzing individual gene trees, as well as a concatenated tree, more representatives could be included across all species. Across datasets, the analysis was run with two simultaneous chains for 10,000,000 generations, or until the average standard deviation of split frequencies fell below 0.005, sampling every 1000 generations. The first 25% of trees were discarded as burn-in and a consensus tree was built from the remaining trees.

Genetic Distance

Genetic distances were calculated for each single-gene alignment in MEGA6 (Tamura et al. 2013) using maximum composite likelihood. Rates among sites were assumed to have a gamma distribution, and variance was estimated with 100 bootstrap replicates.

RESULTS

Across all species and all genes, 253 sequences were included in the analyses, including 193 *de novo* sequences. These *de novo* sequences have been uploaded to GenBank (MG000981-MG001172; see Table S1). Twenty of the *de novo* sequences were removed after preliminary trees indicated individuals were misidentified or DNA template was contaminated. To investigate cryptic speciation within *Farfantepenaues brasiliensis* and *F. duorarum*, 143 sequences and 73 sequences were included of each species, respectively. Overall, four major clades were recovered (Fig 3): Clade 1 contains *Farfantepenaues brevirostris*, sister to all the remaining *Farfantepenaues* species; Clade 2 consists of *F. duorarum*, *F. notialis*/*F. nr. notialis*; Clade 3 consists of *F. paulensis*, *F. aztecus*, *F. isabelae*/*F. subtilis* MI, and *F. subtilis* MII; and Clade 4 is comprised of *F. californiensis* and *F. brasiliensis*.

Concatenated Analysis (12S + 16S + COI)

The concatenated data matrix included 70 individuals. In total, 189 new sequences were generated, including 66 new 12S sequences (369 bps), 62 new 16S sequences (501 bps), and 61 new COI sequences (659 bps). Every species was

represented in the concatenated analyses (“Concatenated” in Table 1 and Table S1). The results from PartitionFinder partitioned 12S+16S together under the Hasegawa-Kishino-Yano model with invariable sites and gamma distribution (HKY+I+G). Cytochrome oxidase subunit I (COI) was partitioned by codon: position 1 was best fit by the Felsenstein 81 model (F81); position 2 by Tamura-Nei with invariable sites (TrN+I); and position 3 by Tamura-Nei with equal base frequencies and invariable sites (TrNef+I).

With the exception of *Farfantepenaeus notialis*, all currently recognized species have high nodal support (>0.99 posterior probability and >94 bootstrap support; Figure 3). Individuals of *F. brasiliensis* fall out into two highly supported subclades associated with collection locality.

Clade 1, containing *F. brevirostris*, is confidently recovered as sister to the remaining *Farfantepenaeus* spp. (1.0/100). Clade 2 consists of a polytomy including representatives of *F. notialis*/*F. nr. notialis* and *F. duorarum* (1.0/100). *Farfantepenaeus isabellae*/*F. subtilis* MI (1.0/94) is recovered as sister to *F. subtilis* MII and this clade exists as a polytomy with *F. aztecus* and *F. paulensis* in Clade 3. Nodal support for the polytomy is high (0.99/100). Clade 4 reveals strong population structure within *F. brasiliensis*: individuals fall into two strongly supported subclades divided by collection locality, *F. brasiliensis* N collected from the Gulf of Mexico and Florida Peninsula (1.0/77) and *F. brasiliensis* S collected off the east coast of Central and South America (from Nicaragua to Brazil) (1.0/99). The *F. brasiliensis* clade is confidently recovered as sister to *F. californiensis* (1.0/100).

Single Gene Trees (12S, 16S, COI)

Results from PartitionFinder specified the Jukes-Cantor (JC69) model for the 12S and 16S datasets. Cytochrome oxidase subunit I (COI) was partitioned by codon position: all three were best approximated by Tamura-Nei, position 3 was best fit by additionally including fixed equal base frequencies and gamma distribution across sites (1: TrN, 2: TrN, 3: TrNef+G).

The 12S RAxML and Bayesian trees (Figure 4) differ slightly from the concatenated tree. *Farfantepenaeus brasiliensis* does not fall as two distinct clades in the 12S tree, instead forming a polytomy of *F. brasiliensis* N, *F. brasiliensis* S, and two representatives of *F. brasiliensis* N. *Farfantepenaeus paulensis* is not included in the 12S alignment, so the branch containing sisters *F. isabellae/F. subtilis* MI and *F. subtilis* MII falls as sister to all other species except *F. brevisrostris*. Clade 3 is fractured resulting in *F. aztecus* falling as sister to Clade 4 (0.96). In this tree, *F. duorarum* and *F. notialis/F. nr. notialis* fall out in a polytomy.

The 16S RAxML and Bayesian trees (Figure 4) are very similar to the concatenated tree, however in the 16S trees, Clade 2 falls as sister to Clade 3 (0.51/46) instead of being sister to Clades 3 and 4 (0.99/93) as seen in the concatenated tree. The relationships within Clade 3 differ due to a lack of *F. paulensis* sequences in the 16S alignment. In the 16S trees, *F. isabellae/F. subtilis* MI and *F. subtilis* MII form a highly supported clade (1.0/86), sister to *F. aztecus* (1.0/92).

Cytochrome oxidase subunit I (COI) sequences were included for *F. paulensis*, but no COI sequence data were obtained for *F. brevisrostris*. Because of this, only Clades 2-4 were recovered (Figure 4). The COI trees differ from the concatenated tree in two

respects only: first, *F. brasiliensis* forms a single clade with *F. brasiliensis* N falling out as a highly supported subclade alongside the comb-like terminal nodes of *F. brasiliensis* S; second, the relationships within Clade 3 are very different. In the RAxML tree, *F. isabellae/F. subtilis* MI and *F. subtilis* MII form a poorly supported clade (37), sister to *F. aztecus*. This clade, which also lacks strong support (24), is recovered as sister to *F. paulensis* (96). The Bayesian tree recovers a well-supported clade containing *F. aztecus* and *F. paulensis* (0.95), sister to *F. subtilis* MII (0.79). *F. isabellae/F. subtilis* MI is strongly supported as sister to this clade (1.0). In this tree, *F. duorarum* and *F. notialis/F. nr. notialis* form two reciprocally monophyletic clades.

Genetic Distances between Species

Genetic distances were measured between all species pairs in MEGA by grouping individuals by species identification (unidentified individuals were not included) and performing between-group calculations. Two analyses were run: a “lumped” analysis on species and a “split” analysis in which designation was made between *F. brasiliensis* N (North; collected from the Gulf of Mexico and the Florida Peninsula) and *F. brasiliensis* S (South; collected off the east coast of Central and South America). Similar results were seen across each single-gene analysis, but here only the COI values are discussed because this is the only marker for which data were available for all *Farfantepenaeus* species (Table 3). Genetic distances measured between species were >3% with two exceptions: in both analyses, the genetic distance between *F. notialis/F. nr. notialis* and *F. duorarum* was only 1.2%; in the split analysis, the genetic distance between the northern and southern *F. brasiliensis* was 2.3%. Excluding these values, distances ranged from 3.3%

(between *F. isabellae*/*F. subtilis* MI and *F. subtilis* MII) to 21.5% (between *F. aztecus* and the outgroup *Litopenaeus vannamei*).

DISCUSSION

This study represents the first comprehensive phylogeny of the genus *Farfantepenaeus* and utilizes more molecular markers than any previous study. Though previous studies lacked representatives of *F. brevirostris* and typically did not include representatives of both *F. isabellae*/*F. subtilis* MI and *F. subtilis* MII, the phylogenetic relationships recovered through concatenated data analysis recover the same three clades (Clades 2-4) as previous molecular studies (Lavery et al. 2004; Voloch et al. 2005). However, in investigating cryptic speciation, our results uncovered evidence for previously undescribed population structure in *F. brasiliensis*, lack of evidence for species status of *F. notialis*, and strong molecular support for *F. isabellae*, previously described as *F. subtilis* morphotype I, as sister to *F. subtilis* morphotype II.

Phylogenetic Relationships and Morphological Considerations

The concatenated tree recovers *F. brevirostris*, previously not included in molecular phylogenies, as sister to the remaining species. *Farfantepenaeus brevirostris* and *F. californiensis* are both Pacific species, but are differentiated by the detailed structure of the gastrofrontal carina (anteriorly indistinct or well-defined, respectively), gastro-orbital carina (short or long, respectively), adrostral sulcus (mesially directed toward posterior or almost straight, respectively), distomedian projection of the petasma (short and apically blunt with 1-4 teeth or long and apically pointed with teeth absent,

respectively), and the auricle (absent or present and relatively large, respectively) (Pérez-Farfante 1988). Interestingly, *F. brevirostris* is distantly related to *F. californiensis*, despite both being the only two Pacific species in the genus *Farfantepenaeus*.

The concatenated tree recovers a clade containing *F. notialis* and *F. nr. notialis* nested within *F. duorarum*, and only a small genetic distance was recovered between these taxa (0.012). This differs from previous molecular phylogenies which confidently separate *F. duorarum* and *F. notialis* (Lavery et al. 2004; Voloch et al. 2005), including molecular analyses with low resolution at deeper nodes (Maggioni et al. 2001). Previous topologies may be a result of data recycling since both Lavery et al. and Voloch et al. include *F. notialis* as a single GenBank sequence collected from Cuba (X84350; García-Machado et al. 1999). The analysis presented here also included this sequence, as well as five sequences of *F. nr. notialis* (collected from multiple sites within Biscayne Bay on the southeast coast of Florida, USA). The specimens that were identified as *F. nr. notialis* were all collected outside the current distributional range, but grouped with the *F. notialis* GenBank sequence from within the described range (Cuba). Nodal support for this clade was low (0.65/28). However, as we have only included mitochondrial sequence data in this study, the lack of resolution between *F. duorarum* and *F. notialis* may be the result of incomplete lineage sorting at the mitochondrial level, rather than a lack of reciprocal monophyly between these species.

Morphologically, there is little to differentiate between *F. duorarum* and *F. notialis*. The primary distinguishing characteristic for adults is difference in K/S (<3 or >3, respectively) (Pérez-Farfante 1988). The initial separation of *F. subtilis* as a subspecies of *F. aztecus* was also by means of difference in K/S (Pérez-Farfante 1967),

but the morphological difference here may have been more pronounced: modal K/S ratio was 3.5 for *F. subtilis* vs. 1.25 for *F. aztecus*. At the time, Pérez-Farfante (1967) suggested this difference in K/S she observed between populations of *F. subtilis* could have been due to environmental factors. The variability Pérez-Farfante viewed may have been due to looking at *F. subtilis* intermingled with what later was described as *F. isabellae*, as suggested by Tavares and Gusmão (2016) in the description of *F. isabellae*. Teodoro et al. (2016) reported difficulty in discriminating between *Farfantepenaeus* species using morphological features: only 38% of taxonomically identified *F. paulensis* and *F. brasiliensis* juveniles had identity confirmed with molecular methods. Our results suggest that another morphologic characteristic commonly used in *Farfantepenaeus* taxonomy, adrostral sulci condition, may not be diagnostic. Additional molecular data, especially the inclusion of nuclear genes, are needed to resolve the relationship between *F. notialis* and *F. duorarum*.

Farfantepenaeus aztecus, *F. paulensis*, *F. isabellae/F. subtilis* MI, and *F. subtilis* MII form a clade. In previous studies, wherein *F. subtilis* is only included as MI, all three possible arrangements have been recovered (Lavery et al. 2004; R. Maggioni et al. 2001; Voloch et al. 2005). The analysis conducted here recovered a clade of *F. isabellae/F. subtilis* MI and *F. subtilis* MII sister to *F. aztecus* and *F. paulensis* in an unresolved polytomy. These four taxa are differentiated morphologically by the adrostral sulcus (long in *F. aztecus* and *F. paulensis*; short, shallow, and posteriorly narrow in *F. isabellae/F. subtilis* MI; and short and of equal width along its entire length in *F. subtilis* MII), median sulcus (long and deep in *F. aztecus*; short, shallow, and rarely continuous in *F. paulensis*), dorsolateral sulcus (broad in *F. aztecus*, narrow in *F. paulensis*), and K/S

(less than 3 in *F. aztecus*, greater than 3 in *F. paulensis*). Additionally, reproductive morphology can be used to distinguish between these four taxa, specifically: the distal part of the ventral costa of the petasma (tapered to a point and armed with a patch of tightly grouped small teeth in *F. aztecus*, blunt and straight with irregular teeth around the border in *F. paulensis*, or unarmed with a narrow patch of small teeth irregularly occurring around the border in *F. subtilis* MI and MII) and thelycum processes (both broad in *F. aztecus*, both narrow in *F. paulensis*, anterior process sharply pointed and posterior process diamond-shaped in *F. isabelae/F. subtilis* MI, or anterior process rounded and posterior process foliaceous in *F. subtilis* MII) (Pérez-Farfante 1988). Our results support the species status of *F. isabelae*, specifically as *F. subtilis* MI, and find relatively large genetic distance between *F. isabelae/F. subtilis* MI and its sister, *F. subtilis* MII. Despite the polytomy at the deeper node, the reciprocally monophyletic sister relationship between *F. isabelae/F. subtilis* MI and *F. subtilis* MII, when considered alongside the genetic distances and branch lengths separating the species in this clade, suggests that *F. subtilis* MII does not represent the northernmost population of *F. paulensis*, as has been posited in previous research (D’Incao et al. 1998).

Farfantepenaeus brasiliensis and *F. californiensis* are consistently recovered as a clade, in agreement with previous molecular studies analyzing 16S and COI data (Lavery et al. 2004; Voloch et al. 2005). Both species bear a long distomedian petasma projection which folds distally to form a large, inwardly protruding auricle (Pérez-Farfante 1988). The two species differ in their distributions: as their names suggest, *F. brasiliensis* occurs in the Atlantic and *F. californiensis* occupies a Pacific range. Additionally, *F. brasiliensis* is typically distinguished from other species of *Farfantepenaeus* by the dark red spot

which occurs at the juncture of the 3rd and 4th abdominal segments, though this is also present in *F. duorarum* and *F. notialis* (Pérez-Farfante 1988), albeit less consistently.

The presence of polytomies within the phylogenetic tree indicates a need for additional molecular data. The addition of nuclear genes would likely clarify these relationships and may resolve the tree. Unfortunately, we were unable to include these in this study, largely due to a lack of voucher specimens. *Farfantepenaeus notialis* and *F. paulensis* are only included here as GenBank Accessions as we were unable to obtain samples from these species. Without taxonomically identified samples in hand, we are unable to confidently or responsibly include additional loci for *F. notialis* or *F. paulensis*. As such, we interpret our results cautiously, aware of the limitations of this study.

Phylogeographic Patterns

Interpreting the phylogeny as a whole, an intriguing phylogeographic signal is revealed: latitudinal speciation supporting a biogeographic break between the coasts of North America and Central/South America. Clade 1 contains the Pacific species *F. brevisrostris* and is recovered as sister to the rest of the *Farfantepenaeus* species. This agrees with previous work suggesting the genus originated in the Indo-Pacific (Baldwin et al. 1998; Dall et al. 1990; Lavery et al. 2004). The relationships between the remaining species exhibit a latitudinal trend within each clade.

Farfantepenaeus duorarum, *F. notialis*/*F. nr. notialis* form Clade 2. These species currently have described ranges that reflect this biogeographic break: *F. duorarum* has been reported along the east coast of the U.S. and along the Gulf coast through Mexico and *F. notialis* is found in the Caribbean, along the coast of Brazil (FAO 1983; Heemstra

and Randall 1993), and in the southern Gulf of Mexico in Mexican estuaries (May-Kú and Ordóñez-López 2006; Pérez-Castañeda and Defeo 2000). However, the molecular results suggest this may not be a true break: low genetic distance and intermixed terminal nodes of *F. notialis*/*F. nr. notialis* and *F. duorarum* bring the validity of *F. notialis* as a species into question. The genetic homogeneity seen between *F. duorarum* and *F. notialis* could be attributed to oceanographic currents, especially the Gulf Loop Current, which would mix individuals of *F. duorarum* and *F. notialis* near the limits of their respective southern and northern ranges in the Gulf of Mexico. Indeed, *F. duorarum* and *F. notialis*, along with *F. brasiliensis*, have been reported as co-occurring in estuaries in the southern Gulf of Mexico (May-Kú and Ordóñez-López, 2006; Pérez-Castañeda and Defeo, 2000).

All species within Clade 3, *F. aztecus*, *F. isabellae*/*F. subtilis* MI, *F. paulensis*, and *F. subtilis* MII, occur along the western Atlantic at slightly overlapping latitudes: *F. aztecus* occupies the northern shores, along the east coast of the U. S. and in the Gulf of Mexico (FAO 1983; Heemstra and Randall 1993); *F. isabellae*/*F. subtilis* MI has a described range in the Caribbean, ranging from Cuba to northern Brazil, which entirely overlaps with the range of its sister *F. subtilis* MII (FAO 1983; Heemstra and Randall 1993; Tavares and Gusmão 2016). The range of *F. paulensis* also overlaps *F. subtilis* MII to a large degree, with a described range from northern Brazil to Rio de La Plata (Heemstra and Randall 1993), *F. paulensis* co-occurs with *F. subtilis* MII from northern Brazil to Rio de Janeiro. In general, it appears that *F. aztecus* occupies territory north of the Equator, *F. isabellae*/*F. subtilis* MI and *F. subtilis* MII are distributed across the Equator, and *F. paulensis* occurs south of the Equator. Such phylogeographic structure

has been associated with historical low sea levels (Dall et al. 1990): hypothetically, populations of a species could have become separated and formed new species when low sea levels geographically isolated basins.

Clade 4 is comprised of *F. californiensis* and *F. brasiliensis*, a Pacific and Atlantic species, respectively. Expanding from an Indo-Pacific origin, *Farfantepenaeus* is hypothesized to have migrated eastward and westward (Baldwin et al. 1998; Dall et al. 1990; Lavery et al. 2004). The eastward expansion, combined with oscillating sea levels beginning in the Pliocene, would have allowed trans-isthmus migration into the Atlantic Ocean and subsequently impeded back-migration (Baldwin et al. 1998; Lavery et al. 2004). Clade 4 does not exhibit the latitudinal speciation pattern seen in Clade 3, as *F. brasiliensis* extends along the coast of North and South America (FAO 1983; Heemstra and Randall 1993). However, the strongly supported northern and southern subclades of *F. brasiliensis* do lend support to the biogeographic break between the coasts of North America and those of Central/South America (Avice 1992; Young et al. 2002, Cowen et al. 2006).

The phylogeographic patterns indicated in our results are intriguing, providing tentative evidence of the biogeographic role of oceanographic currents in the evolutionary history of species of *Farfantepenaeus*. Our results prompt further inquiry into the effects of the major current systems of the Western North Atlantic, Caribbean, and Gulf of Mexico as source and succor of speciation in the genus.

Investigation of Cryptic Diversification within Pink Shrimp and Economic Implications

Early allozyme studies of genetic diversity within the genus indicated very small genetic distances between species (Mulley and Latter 1980; Nelson and Hedgecock 1980; Redfield et al. 1980; Salini 1987; Sunden and Davis 1991; Tam and Chu 1993), causing researchers to posit that these shrimps were very slow-evolving (Dall et al. 1990). More recent studies of diversity within the species of *Farfantepenaeus* found 8%-24% distance in COI alone (Baldwin et al. 1998). The results of the present study agree with these recent studies: except for *F. notialis*/*F. nr. notialis*-*F. duorarum*, all interspecific distances were >3% (3.3%-21.5%). Genetic distance between *F. notialis*/*F. nr. notialis* and *F. duorarum* was 1.2%, which is more than 50% higher than the previous measure of 0.7% (Gusmao et al. 2000). This may be a consequence of the collection of *F. notialis* from outside the described species range. The results indicate substantial genetic distance between the northern and southern representatives of *F. brasiliensis* (2.3%), perhaps even representing distinct ESUs.

Pérez-Farfante (1967) established *notialis* as a subspecies of *duorarum*, even before the genus *Farfantepenaeus* was established. The two taxa were primarily distinguished by variation in adrostral sulcus condition. Described petasmas and thelycums were very similar between these two species (Pérez-Farfante 1970a, 1970c). In molecular phylogenies, *F. notialis* is treated, and supported, as the sister species to *F. duorarum*. However, the phylogenetic trees and calculated genetic distances presented here do not support *F. notialis* as a species distinct from *F. duorarum*. Indeed, the small genetic distance between the two is less than half the traditional minimum distance for indicating a species (3.0%). Due to the limited sampling from within the currently

recognized distributional range of *F. notialis*, the findings should be interpreted critically, however *F. duorarum* and *F. notialis* do not appear to represent separate ESUs. While this may be the case, the phylogenetic analyses indicate *F. notialis* adds structure within the clade, which is otherwise fairly homogeneous. The genetic diversity represented by this structure must be preserved, so in this respect, treating the two as distinct ESUs may be beneficial to prevent over-harvesting of *F. notialis*, whose larger distribution makes it an economic target for a greater number of nations. Future phylogenies need to include representatives of *F. duorarum* and *F. notialis* throughout their currently described distributional ranges, nuclear data, and, ideally, the holotypes in order to validate or refute the results we present here.

Individuals of *Farfantepenaeus brasiliensis* fall into two subclades, strongly suggesting two distinct ESUs. Indeed, Pérez-Farfante noted two geographically separated populations of *F. brasiliensis*, differing in K/S (Pérez-Farfante 1970c: Fig. 5, pg 168; Pérez-Farfante 1988: Fig. 13, pg 10 and reproduced here in Figure 2D and D'). Although the northern (Barbuda and Saint Augustine, Florida, USA: Pérez-Farfante 1970a and 1998, respectively) and southern (Camocin, Brazil and Rio de Janeiro, Brazil: Pérez-Farfante 1970c and 1988, respectively) populations described by Pérez-Farfante do not align with the northern and southern geography we find, a latitudinal pattern is supported. While genetic distance alone is not enough to warrant new species status, revealing population structure across the distributional range has importance to fishery management. Varying fishing pressure may be experienced across the distribution of this species. In the southern part of its range, *F. brasiliensis* is one of two species that constitute the over 57,000-ton Brazilian “pink shrimp” fishery (IBAMA 2011), whereas

in the north *F. brasiliensis* may be a lesser, and generally unrecognized, component of commercial *Farfantepenaeus* landings. Given the immense importance of genetic diversity to species health, such uneven fishing pressure may be threatening diversity unique to *F. brasiliensis* S while unintentionally applying positive selection pressure to *F. brasiliensis* N. A summary of evidence for and against separating *F. notialis* from *F. duorarum* and *F. brasiliensis* N from *F. brasiliensis* S is presented in Table S2.

CONCLUSIONS

The work we present here agrees well with previous molecular work in many respects, while also furthering our understanding of taxonomy and evolutionary relationships within *Farfantepenaeus*. In including *F. brevirostris* for the first time, we identify it as sister to the remaining species in the genus. Additionally, we provide evidence establishing *F. subtilis* MII as sister to *F. isabellae*/*F. subtilis* MI, contradicting a previous hypothesis that *F. subtilis* MII represented a population of *F. paulensis*. However, our results call into question whether accepted diagnostic characters (K/S and adrostral sulci condition) are taxonomically informative. Our concatenated phylogeny does not separate *F. notialis* and *F. duorarum* into separate species, though this may be an artefact of the sequence data used, rather than a true lack of speciation. We also uncovered structure within *F. brasiliensis*, indicating the existence of two populations. Our study also uncovers a previously undescribed phylogeographic signal of latitudinal speciation in the genus. Overall, this work provides an inclusive, robust phylogeny that contributes to our knowledge of *Farfantepenaeus*.

FUTURE WORK

Future efforts should focus on increasing the number and genetic source of molecular markers (e.g. nuclear, as per Timm and Bracken-Grissom, 2015), as well as on the discovery and inclusion of diagnostic morphological characters. A total evidence approach would further clarify evolutionary relationships within *Farfantepenaeus* and may allow for time calibration of the phylogeny. Additionally, more thorough sampling along species' ranges would better elucidate the biogeographic factors facilitating speciation in the genus (Ayre et al. 2009). The population structure we find is unexpected and may inform us about the role of oceanographic features in marine speciation processes. To investigate population structure in more species of *Farfantepenaeus*, a population genetics/genomics level study should be completed, focusing on the species along the described distribution. Research efforts in the realm of *Farfantepenaeus* evolution should focus on contextualizing phylogeographic patterns in terms of environmental factors (e.g. currents, juvenile and adult habitats, and geological events) and economic pressures (e.g. fishing pressures and active species management efforts).

ACKNOWLEDGEMENTS

Logistic support for this project was provided by the Protected Resources and Biodiversity Division of the Southeast Fisheries Science Center, National Marine Fisheries Service, Miami, Florida. This research was made possible in part by a grant from The Gulf of Mexico Research Initiative, and in part by a Division of Environmental Biology National Science Foundation (NSF) grant awarded to HBG (DEB#1556059), as well as the FIU Presidential Fellowship and the FIU Doctoral Evidence Acquisition

Fellowship. Data are publicly available through the Gulf of Mexico Research Initiative Information and Data Cooperative (GRIIDC) at <https://data.gulfresearchinitiative.org> (doi:<doi identifier>). The authors would like to specially thank Robin Cascioli and Michelle Harangody for their assistance in collecting and identifying specimens. The authors extend huge thanks to Dr. Fernando Mantelatto and Dr. Darryl Felder who both donated specimens or tissues for inclusion into the study. They also thank L. E. Timm's PhD committee: Dr. Eirin-Lopez, Dr. Rodriguez-Lanetty, Dr. von Wettberg, and Dr. Wensong Wu, for additional comments and suggestions. Finally, they thank the anonymous reviewers for feedback on earlier versions of this manuscript. This is contribution #xx from the Marine Education and Research Center in the Institute of Water and Environment at Florida International University.

LITERATURE CITED

- Avise, J. C. (1992). Molecular population structure and the biogeographic history of a regional fauna : a case history with lessons for conservation biology. *Oikos* **63**, 62–76.
- Ayre, D. J., Minchinton, T. E., and Perrin, C. (2009). Does life history predict past and current connectivity for rocky intertidal invertebrates across a marine biogeographic barrier? *Molecular Ecology* **18**, 1887–1903.
- Baldwin, J. D., Bass, A. L., Bowen, B. W., and Clark, W. H. (1998). Molecular phylogeny and biogeography of the marine shrimp *Penaeus*. *Molecular Phylogenetics and Evolution* **10**, 399–407.
- Bernatchez, L. (1995). A role for molecular systematics in defining evolutionarily significant units in fishes. In *American Fisheries Society Symposium*.
- Burukovsky, R. N. (1972). Nekotorye voprosy sistematiki i rasprostraneniya krevetok roda *Penaeus*. In T. AtlantNIRO (Ed.), *Rybokhozyaistvennyyeissledovaniya v Atlanticheskoy okeane* (Vol. 2, pp. 3–21). Kalingrad.

- Burukovsky, R. N. (1997). Selection of a type species for *Farfantepenaeus* Burukovsky (Crustacea: Decapoda: Penaeidae). *Proceedings of the Biological Society of Washington* **110**, 154.
- Cowen, R.K., Paris, C.B., Srinivasan, A. (2006) Scaling of connectivity in marine populations. *Science* **311**, 522-527.
- Crandall, K. A., Bininda-Emonds, O. R. R., Mace, G. M., and Wayne, R. K. (2000). Considering evolutionary processes in conservation biology. *Trends in Ecology and Evolution* **15**, 290–295.
- Cunningham, C. W., Blackstone, N. W., and Buss, L. W. (1992). Evolution of king crabs from hermit crab ancestors. *Nature* **355**, 539–542.
- D’Incao, F., Delevedove, G., Maggioni, D., and Maggioni, R. (1998). Evidência genética da presença de *Farfantepenaeus paulensis* (Pérez Farfante, 1967) no litoral nordeste do Brasil (Decapoda: Penaeidae). *Nauplius* **6**, 129–137.
- Dall, W., Hill, B. J., Rothlisberg, P. C., and Staples, D. J. (1990). The Biology of Penaeidae. In *Advances in Marine Biology*.
- Ditty, J. G., and Alvarado Bremer, J. R. (2011). Species discrimination of postlarvae and early juvenile brown shrimp (*Farfantepenaeus aztecus*) and pink shrimp (*F. duorarum*) (Decapoda: Penaeidae): coupling molecular genetics and comparative morphology to identify earlylife stages. *Journal of Crustacean Biology* **31**, 126–137.
- FAO. (1983). *Penaeidae*.
- Frankel, O. H. (1974). Genetic conservation: our evolutionary responsibility. *Genetics* **78**, 53–65.
- García-Machado, E., Pempera, M., Dennebouy, N., Oliva-Suarez, M., Mounolou, J. C., and Monnerot, M. (1999). Mitochondrial genes collectively suggest the paraphyly of Crustacea with respect to Insecta. *Journal of Molecular Evolution* **49**, 142–149.
- García-Machado, E., Robainas, A., Espinosa, G., Oliva, M., Páez, J., Verdecia, N., and Monnerot, M. (2001). Allozyme and mitochondrial DNA variation in Cuban populations of the shrimp *Farfantepenaeus notialis* (Crustacea: Decapoda). *Marine Biology* **138**, 701–707.
- García-Machado, E., Ulmo-Díaz, G., Castellanos-Gell, J., and Casane, D. (2018). Patterns of population connectivity in marine organisms of Cuba. *Bulletin of Marine Science* **94**, 1–20.

- Gusmão, J., Lazoski, C., and Sole-Cava, A. M. (2000). A new species of *Penaeus* (Crustacea: Penaeidae) revealed by allozyme and cytochrome oxidase I analyses. *Marine Biology* **137**, 435–446.
- Heemstra, P. C., and Randall, J. E. (1993). *FAO Species Catalogue* (Vol. 16).
- Huelsenbeck, J. P., and Ronquist, F. (2001). MrBayes: Bayesian inference of phylogenetic trees. *Bioinformatics* **17**, 754–755.
- IBAMA. (2011). *Instituto Brasileiro do Meio Ambiente e dos Recursos Naturais Renováveis*.
- Katoh, K., and Standley, D. M. (2013). MAFFT multiple sequence alignment software version 7: Improvements in performance and usability. *Molecular Biology and Evolution* **30**, 772–780.
- Lande, R., and Shannon, S. (1996). The role of genetic variation in adaptation and population persistence in a changing environment. *Evolution* **50**, 434–437.
- Lanfear, R., Calcott, B., Ho, S. Y. W., and Guindon, S. (2012). PartitionFinder: Combined selection of partitioning schemes and substitution models for phylogenetic analyses. *Molecular Biology and Evolution* **29**, 1695–1701.
- Lavery, S., Chan, T. Y., Tam, Y. K., and Chu, K. H. (2004). Phylogenetic relationships and evolutionary history of the shrimp genus *Penaeus* s.l. derived from mitochondrial DNA. *Molecular Phylogenetics and Evolution* **31**, 39–49.
- Maggioni, D. (1996). Caracterização de algumas espécies do gênero *Penaeus* do litoral brasileiro através de eletroenfonque. *Nauplius* **4**, 129–137.
- Maggioni, R., Rogers, A. D., Maclean, N., and D’Incao, F. (2001). Molecular phylogeny of western Atlantic *Farfantepenaeus* and *Litopenaeus* shrimp based on mitochondrial 16S partial sequences. *Molecular Phylogenetics and Evolution* **18**, 66–73.
- May-Kú, M. A., and Ordóñez-López, U. (2006). Spatial patterns of density and size structure of penaeid shrimps *Farfantepenaeus brasiliensis* and *Farfantepenaeus notialis* in a hypersaline lagoon in the Yucatán Peninsula, Mexico. *Bulletin of Marine Science* **79**, 259–271.
- Miller, M. A., Pfeiffer, W., and Schwartz, T. (2010). Creating the CIPRES Science Gateway for inference of large phylogenetic trees. In *2010 Gateway Computing Environments Workshop*, GCE 2010.
- Moritz, C. (2002). Strategies to protect biological diversity and the evolutionary processes that sustain it. *Systematic Biology* **51**, 238–254.

- Mulley, J. C., and Latter, B. D. H. (1980). Genetic variation and evolutionary relationships within a group of thirteen species of penaeid prawns. *Evolution* **34**, 904–916.
- Nelson, K., and Hedgecock, D. (1980). Enzyme polymorphism and adaptive strategy in the decapod Crustacea. *The American Naturalist* **116**, 238–280.
- Pérez-Castañeda, R., and Defeo, O. (2000). Population structure of the penaeid shrimp *Farfantepenaeus notialis* in its new range. *Bulletin of Marine Science* **67**, 1069–1074.
- Pérez-Farfante, I. (1967). A new species and two new subspecies of shrimp of the genus *Penaeus* from western Atlantic. *Proceedings of the Biological Society of Washington* **80**, 83–100.
- Pérez-Farfante, I. (1969). Western Atlantic shrimps of the genus *Penaeus*. *U.S. Fish and Wildlife Service Fishery Bulletin*, 461–591.
- Pérez-Farfante, I. (1970a). Características diagnósticas de los juveniles de *Penaeus aztecus subtilis*, *P. duorarum notialis* y *P. brasiliensis* (Crustacea, Decapoda, Penaeidae). *Separatas Memorias Sociedad de Ciencias Naturales La Salle* **30**, 159–182.
- Pérez-Farfante, I. (1970b). Claves ilustradas para la identificación de los camarones comerciales de la América Latina. *No. Folleto 1605*.
- Pérez-Farfante, I. (1970c). Diagnostic characters of juveniles of the shrimps *Penaeus aztecus aztecus*, *P. duorarum duorarum*, and *P. brasiliensis* (Crustacea, Decapoda, Penaeidae). *U.S. Fish and Wildlife Service Special Scientific Report—Fisheries* **599**, 1–26.
- Pérez-Farfante, I. (1988). Illustrated key to the penaeoid shrimps of commerce in the Americas. *NOAA Technical Report* **64**, 32.
- Pérez-Farfante, I., and Kensley, B. F. (1997). Penaeoid and Sergestoid shrimps and prawns of the world: Keys and diagnoses for the families and genera. *Memoires Du Museum National d'Histoire Naturelle* **175**, 1–233.
- Rambaut, A. (2012). *FigTree v1.4*. Edinburgh, UK: University of Edinburgh.
- Redfield, J. A., Hedgecock, D., Nelson, K., and Salini, J. P. (1980). Low heterozygosity in tropical marine crustaceans of Australia and the trophic stability hypothesis. *Marine Biology Letters*.
- Robainas-Barcia, A., Blanco, G., Sánchez, J. A., Monnerot, M., Solignac, M., and García-Machado, E. (2008). Spatiotemporal genetic differentiation of Cuban

- natural populations of the pink shrimp *Farfantepenaeus notialis*. *Genetica* **133**, 283–294.
- Ronquist, F., and Huelsenbeck, J. P. (2003). MrBayes 3: Bayesian phylogenetic inference under mixed models. *Bioinformatics* **19**, 1572–1574.
- Ryder, O. A. (1986). Species conservation and systematics: the dilemma of subspecies. *Trends in Ecology and Evolution* **1**, 9–10.
- Salini, J. (1987). Genetic variation and population subdivision in the greentail prawn *Metapenaeus bennettiae* (Racek and Dall). *Marine and Freshwater Research* **38**, 339–349.
- Schubart, C. D., Cuesta, J. A., Diesel, R., and Felder, D. L. (2000). Molecular phylogeny, taxonomy, and evolution of nonmarine lineages within the American grapsoid crabs (Crustacea: Brachyura). *Molecular Phylogenetics and Evolution* **15**, 179–190.
- Stamatakis, A. (2006). RAxML-VI-HPC: Maximum likelihood-based phylogenetic analyses with thousands of taxa and mixed models. *Bioinformatics* **22**, 2688–2690.
- Stillman, J. H., and Reeb, C. A. (2001). Molecular phylogeny of eastern Pacific porcelain crabs, genera *Petrolisthes* and *Pachycheles*, based on the mtDNA 16S rDNA sequence: phylogeographic and systematic implications. *Molecular Phylogenetics and Evolution* **19**(2), 236–245.
- Sunden, S. L. F., and Davis, S. K. (1991). Evaluation of genetic variation in a domestic population of *Penaeus vannamei* (Boone): a comparison with three natural populations. *Aquaculture* **97**, 131–142.
- Tam, Y. K., and Chu, K. H. (1993). Electrophoretic study on the phylogenetic relationships of some species of *Penaeus* and *Metapenaeus* (Decapoda: Penaeidae) from the South China Sea. *Journal of Coastal Research* **13**, 697–705.
- Tamura, K., Stecher, G., Peterson, D., Filipski, A., and Kumar, S. (2013). MEGA6: Molecular Evolutionary Genetics Analysis version 6.0. *Molecular Biology and Evolution* **30**, 2725–2729.
- Tavares, C., and Gusmão, J. (2016). Description of a new Penaeidae (Decapoda: Dendrobranchiata) species, *Farfantepenaeus isabelae* sp. nov. *Zootaxa* **4171**, 505–516.
- Teodoro, S. S. A., Terossi, M., Mantelatto, F. L., and Costa, R. C. (2016). Discordance in the identification of juvenile pink shrimp (*Farfantepenaeus brasiliensis* and *F. paulensis*: Family Penaeidae): An integrative approach using morphology, morphometry and barcoding. *Fisheries Research* **183**, 244–253.

- Timm, L., and Bracken-Grissom, H. D. (2015). The forest for the trees: evaluating molecular phylogenies with an emphasis on higher-level Decapoda. *Journal of Crustacean Biology* **35**, 577–592.
- Voloch, C. M., Freire, P. R., and Russo, C. A. M. (2005). Molecular phylogeny of penaeid shrimps inferred from two mitochondrial markers. *Genetics and Molecular Research* **4**, 668–674.
- Waples, R. S. (1991). Pacific Salmon, *Oncorhynchus* spp., and the definition of “species” under the Endangered Species Act. *Marine Fisheries Review* **53**, 11–22.
- Young, A. M., Torres, C., Mack, J. E., and Cunningham, C. W. (2002). Morphological and genetic evidence for vicariance and refugium in Atlantic and Gulf of Mexico populations of the hermit crab *Pagurus longicarpus*. *Marine Biology* **140**, 1059–1066.

Tables

Table 1. Number of individuals included in the study, including the total number and the number of *de novo* sequences generated (reported in parentheses).

Species	12S total(new)	16S total(new)	COI total(new)	Concatenated
<i>F. aztecus</i>	4 (3)	11 (1)	1 (1)	4
<i>F. brasiliensis</i> N	20 (20)	21 (21)	21 (21)	21
<i>F. brasiliensis</i> S	6 (6)	10 (6)	71 (6)	6
<i>F. brevirostris</i>	3 (3)	3 (3)	0 (0)	3
<i>F. californiensis</i>	4 (2)	4 (2)	2 (2)	4
<i>F. duorarum</i>	22 (22)	30 (21)	21 (21)	21
<i>F. isabelae</i>	2 (2)	1 (1)	2 (2)	2
<i>F. notialis</i>	1 (0)	1 (0)	1 (0)	2
<i>F. nr. notialis</i>	5 (5)	5 (5)	5 (5)	5
<i>F. paulensis</i>	0 (0)	0 (0)	46 (0)	5
<i>F. subtilis</i> MI	1 (1)	9 (0)	1 (1)	9
<i>F. subtilis</i> MII	2 (2)	10 (2)	2 (2)	10
Total	70 (66)	105 (62)	173 (61)	92

Table 2. The primer pairs and annealing temperatures associated with PCR amplification of three mitochondrial genes used in this study.

Targeted Gene	Forward Primer	Reverse Primer	Anneal Temp
12S	12Sf 5'-GAAACCAGGATTAGATACCC-3' (Mokady et al. 1994)	12S1r 5'-AGCGACGGGCGATATGTAC-3' (Buhay et al. 2007)	50°C
16S	16SH 5'-CCGGTCTGAACTCAGATCACGT-3' (Palumbi et al. 2002)	16SL 5'-CGCCTGTTTAACAAAAACAT-3' (Palumbi et al. 2002)	46°C
16S	16S-fcray 5'-GACCGTGCKAAGGTAGCATAATC-3' (K. A. Crandall & Fitzpatrick, 1996)	16S-rcray 5'-CCGGTYTGAACCAAATCATGTAAA-3' Developed in Crandall Lab	52°C-58°C
16S	16S-L2/L9 5'-TGCCTGTTTATCAAAAAACAT-3' 5'-CGCCTGTTTATCAAAAAACAT-3' (Palumbi et al. 2002)	16S-1472 5'-AGATAGAAACCAACCTGG-3' (Crandall & Fitzpatrick 1996)	40°C
COI	LCOI-1472 5'-GGTCAACAAATCATAAAGATATTG-3' (Folmer et al. 1994)	HCOI-2198 5'-TAAACTCAGGGTGACCAAAAAATCA-3' (Folmer et al. 1994)	40°C

Table 3. Genetic distances between species are presented for a “lumped” analysis (below the diagonal), in which *F. brasiliensis* is analyzed as a single species, and a “split” analysis (above the diagonal), in which *F. brasiliensis* is divided into the two subclades suggested by the concatenated phylogram. Values are from COI data. Values below 0.03 are indicated with *.

	<i>1</i>	<i>2</i>	<i>3</i>	<i>4</i>	<i>5</i>	<i>6</i>	<i>7</i>	<i>8</i>	<i>9</i>	<i>10</i>
1. <i>F. aztecus</i>		0.118	0.110	0.134	0.146	0.090	0.153	0.119	0.100	0.215
2. <i>F. brasiliensis</i> N			0.023*	0.051	0.136	0.091	0.136	0.112	0.100	0.211
3. <i>F. brasiliensis</i> S	0.112			0.042	0.126	0.083	0.126	0.109	0.099	0.200
4. <i>F. californiensis</i>	0.134	0.044			0.127	0.103	0.126	0.125	0.110	0.199
5. <i>F. duorarum</i>	0.146	0.129	0.127			0.110	0.012*	0.143	0.110	0.178
6. <i>F. isabellae/F. subtilis</i> MI	0.090	0.085	0.103	0.110			0.115	0.078	0.033	0.176
7. <i>F. notialis/F. nr. notialis</i>	0.153	0.128	0.126	0.012*	0.115			0.149	0.114	0.182
8. <i>F. paulensis</i>	0.119	0.110	0.125	0.143	0.078	0.149			0.090	0.202
9. <i>F. subtilis</i> MII	0.100	0.099	0.110	0.110	0.033	0.114	0.090			0.178
10. Outgroup	0.215	0.203	0.199	0.178	0.176	0.182	0.202	0.178		

Figure Captions

Figure 1. For each species, the thelycum (left) and petasma (right) are shown. Species' name colors correspond to colors used on gene trees, distribution maps, and the phylogeny. Illustrations are adapted from the FAO key (FAO 1983) and Tavares & Gusmão (2017).

Figure 2. Bayesian phylogram based on concatenated molecular data (12S+16S+COI). Vertical colored bars represent species and the black vertical bar denotes outgroups. Clades are designated by gray brackets which connect to color-coded distribution maps. Support values (Bayesian posterior probabilities/maximum likelihood bootstrap) are noted above each branch.

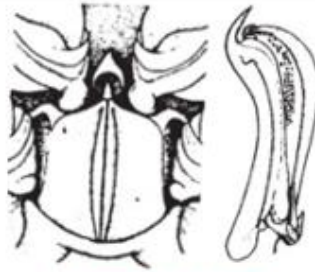
Figure 3. From left to right: Single-gene phylograms for 12S, 16S, and COI, including an expanded view of the *Farfantepenaeus brasiliensis* N and S clades from the COI tree. Nodes supported by Bayesian posterior probabilities >0.9 and bootstrap support >70 are denoted with * above each branch.

Figures

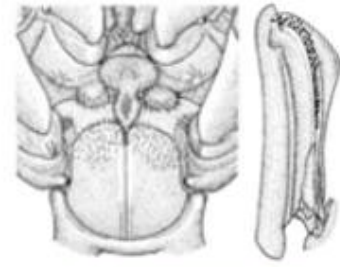
Figure 1



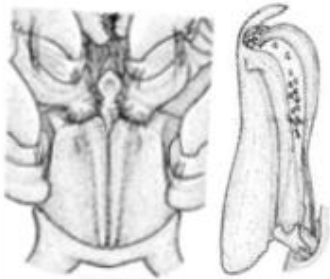
F. aztecus



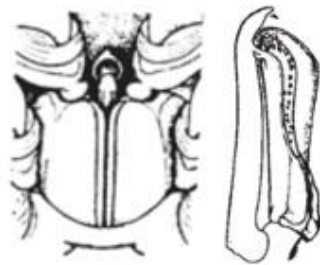
F. brasiliensis



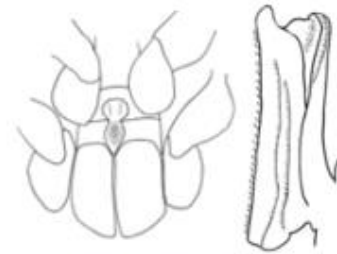
F. brevirostris



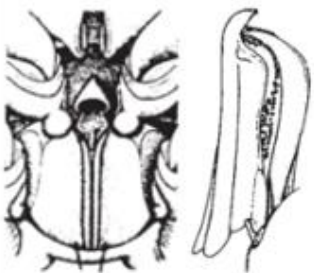
F. californiensis



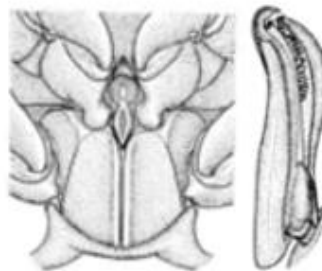
F. duorarum



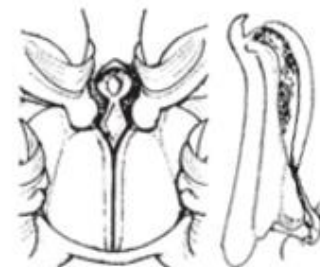
F. isabelae



F. notialis



F. paulensis



F. subtilis

Figure 2

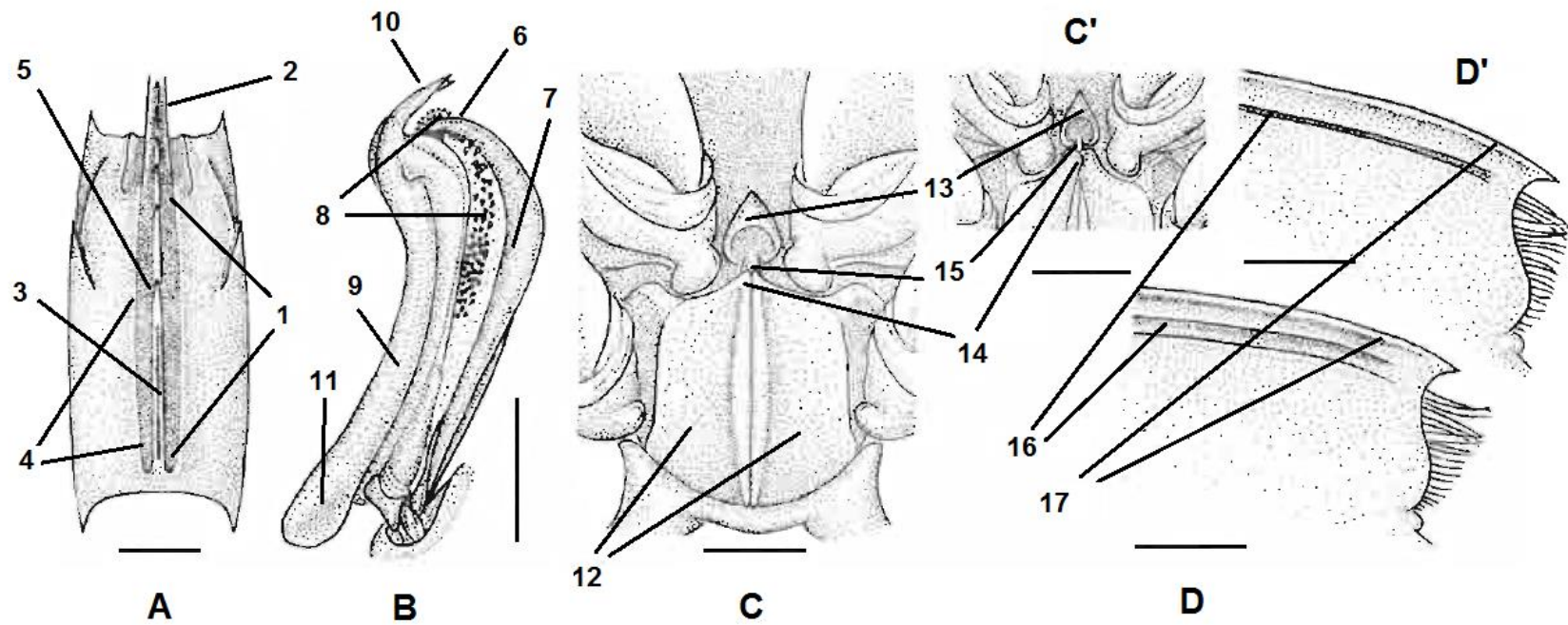


Figure 3

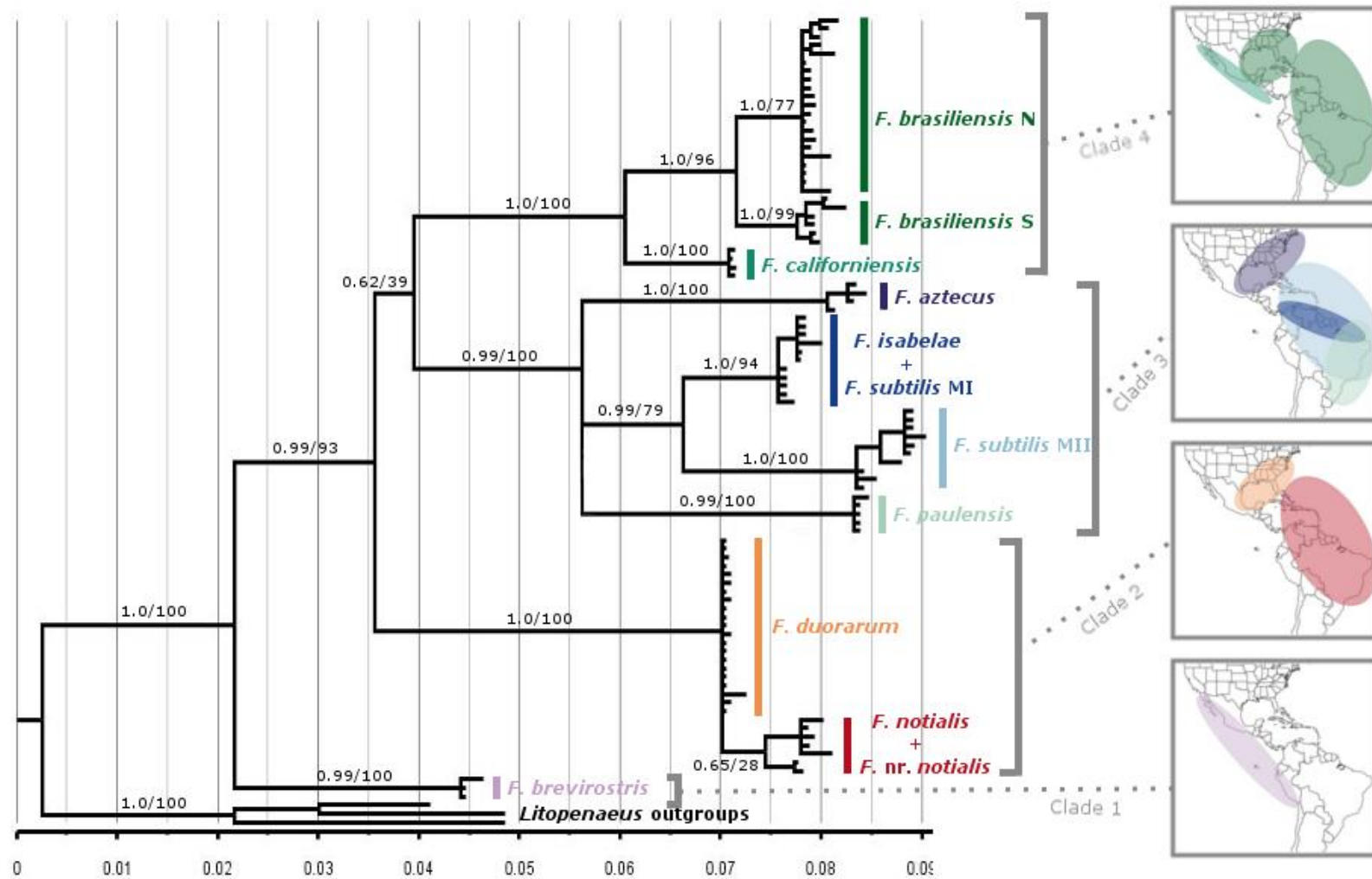
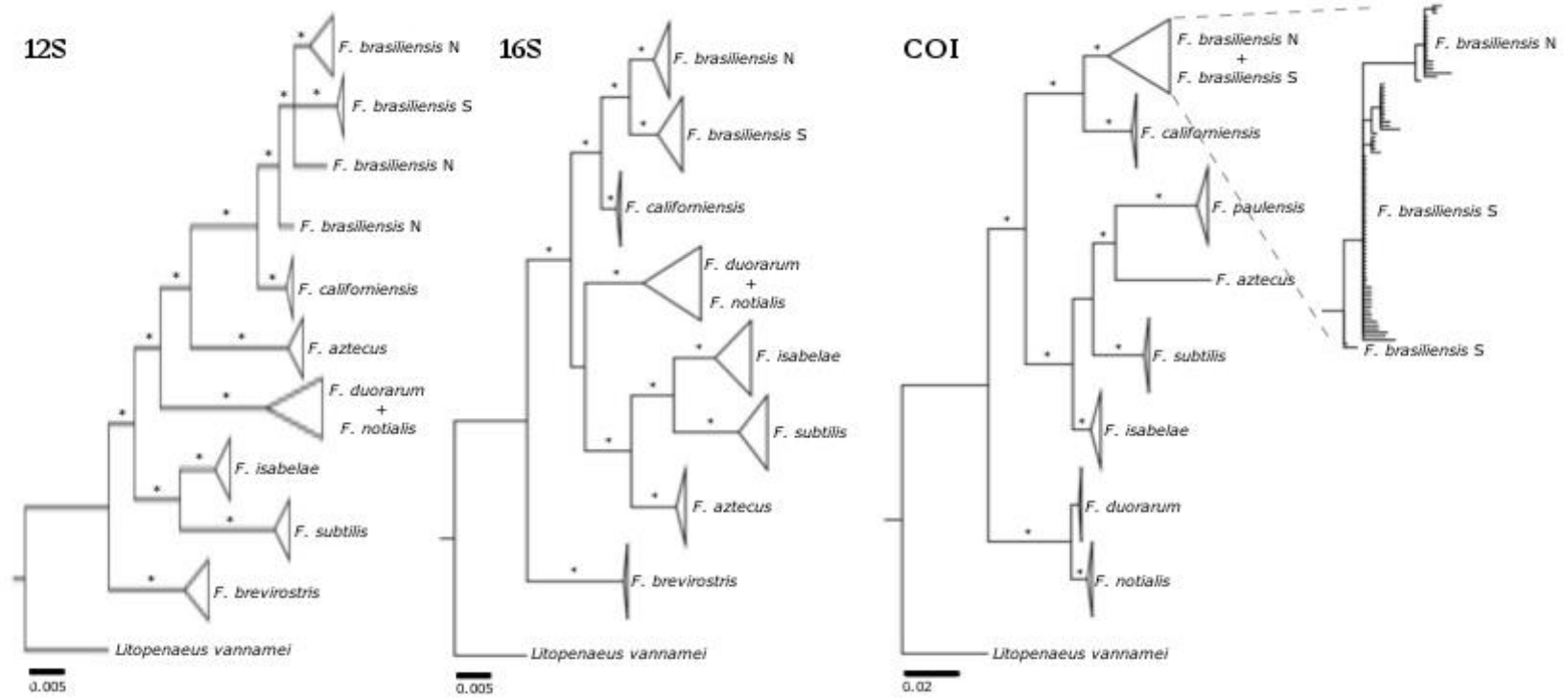


Figure 4



Appendices Captions

Appendix 1. Species identifications, GenBank accession numbers, and collection localities for all individuals included in each alignment: 12S, 16S, COI, and concatenated (12S+16S+COI).

Appendices

Species	HBG	Collection Locale	12S	16S	COI	CONCATENATED
<i>Farfantepenaeus aztecus</i>	N/A	Caribbean and/or South America		AF192051- AF192052		AF192051
<i>Farfantepenaeus aztecus</i>	N/A	Galveston Bay, TX		HM014401		
<i>Farfantepenaeus aztecus</i>	N/A	Greece		KF953960- KF953963, KF983532		
<i>Farfantepenaeus aztecus</i>	N/A	Gulf Breeze, FL		HQ214010		
<i>Farfantepenaeus aztecus</i>	HBG3688	Gulf of Mexico	MG001012	MG001048		MG001012, MG001048
<i>Farfantepenaeus aztecus</i>	HBG3696	Gulf of Mexico	MG001014			
<i>Farfantepenaeus aztecus</i>	N/A	Gulf of Mexico	JF899779	AF279811		AF279811, JF899779
<i>Farfantepenaeus aztecus</i>	HBG3694	Sabine Lake, TX	MG001013		MG001171	MG001013, MG001171
<i>Farfantepenaeus brasiliensis</i> N	HBG1137	Biscayne Bay	MG000983	MG001060	MG001137	MG000983, MG001060, MG001137
<i>Farfantepenaeus brasiliensis</i> N	HBG1139	Biscayne Bay	MG000995	MG001074	MG001138	MG000995, MG001074, MG001138
<i>Farfantepenaeus brasiliensis</i> N	HBG1140	Biscayne Bay	MG000984	MG001075	MG001139	MG000984, MG001075, MG001139
<i>Farfantepenaeus brasiliensis</i> N	HBG1145	Biscayne Bay	MG000985	MG001076	MG001140	MG000985, MG001076, MG001140

<i>Farfantepenaeus brasiliensis</i> N	HBG1146	Biscayne Bay	MG001002	MG001061	MG001149	MG001002, MG001061, MG001149
<i>Farfantepenaeus brasiliensis</i> N	HBG1147	Biscayne Bay	MG000997	MG001062	MG001146	MG000997, MG001062, MG001146
<i>Farfantepenaeus brasiliensis</i> N	HBG1191	Biscayne Bay	MG000986	MG001063	MG001157	MG000986, MG001063, MG001157
<i>Farfantepenaeus brasiliensis</i> N	HBG1197	Biscayne Bay	MG000998	MG001070	MG001147	MG000998, MG001063, MG001147
<i>Farfantepenaeus brasiliensis</i> N	HBG1200	Biscayne Bay	MG000992	MG001064	MG001153	MG000992, MG001064, MG001153
<i>Farfantepenaeus brasiliensis</i> N	HBG1619	Biscayne Bay	MG000987	MG001077	MG001141	MG000987, MG001077, MG001141
<i>Farfantepenaeus brasiliensis</i> N	HBG1620	Biscayne Bay	MG000988	MG001065	MG001142	MG000988, MG001065, MG001142
<i>Farfantepenaeus brasiliensis</i> N	HBG1624	Biscayne Bay		MG001066	MG001150	MG001066, MG001150
<i>Farfantepenaeus brasiliensis</i> N	HBG1636	Biscayne Bay	MG000999	MG001071	MG001148	MG000999, MG001071, MG001148
<i>Farfantepenaeus brasiliensis</i> N	HBG1649	Biscayne Bay	MG000993	MG001078	MG001151	MG000993, MG001078, MG001151
<i>Farfantepenaeus brasiliensis</i> N	HBG1664	Biscayne Bay	MG000990	MG001068	MG001144	MG000990, MG001068, MG001144
<i>Farfantepenaeus brasiliensis</i> N	HBG1667	Biscayne Bay	MG001001	MG001069	MG001154	MG001001, MG001069, MG001154

<i>Farfantepenaeus brasiliensis</i> N	HBG1669	Biscayne Bay	MG000996	MG001079	MG001155	MG000996, MG001079, MG001155
<i>Farfantepenaeus brasiliensis</i> N	HBG1670	Biscayne Bay	MG000991	MG001073	MG001145	MG000991, MG001073, MG001145
<i>Farfantepenaeus brasiliensis</i> N	HBG1652	Everglades	MG000994	MG001080	MG001152	MG000994, MG001080, MG001152
<i>Farfantepenaeus brasiliensis</i> N	HBG1655	Everglades	MG000989	MG001067	MG001143	MG000989, MG001067, MG001143
<i>Farfantepenaeus brasiliensis</i> N	HBG3697	Gulf of Mexico	MG001000	MG001072	MG001156	MG001000, MG001072, MG001156
<i>Farfantepenaeus brasiliensis</i> S	HBG7603	Brazil	MG001007	MG001053	MG001163	MG001007, MG001053, MG001163
<i>Farfantepenaeus brasiliensis</i> S	HBG7604	Brazil	MG001008	MG001052	MG001161	MG001008, MG001052, MG001161
<i>Farfantepenaeus brasiliensis</i> S	N/A	Cananea, Sao Paulo			KF783862, KF989378- KF989414	
<i>Farfantepenaeus brasiliensis</i> S	N/A	Caribbean and/or South America		AF192054		
<i>Farfantepenaeus brasiliensis</i> S	HBG3689	Nicaragua	MG001003	MG001054	MG001158	MG001003, MG001054, MG001158
<i>Farfantepenaeus brasiliensis</i> S	HBG3693	Nicaragua	MG001005	MG001055	MG001159	MG001005, MG001055, MG001159
<i>Farfantepenaeus brasiliensis</i> S	N/A	Santos, Sao Paulo			KF989415- KF989423	

<i>Farfantepenaeus brasiliensis</i> S	HBG3690	Ubatuba, Sao Paulo	MG001004	MG001057	MG001160	MG001004, MG001057, MG001160
<i>Farfantepenaeus brasiliensis</i> S	HBG3698	Ubatuba, Sao Paulo	MG001006	MG001056	MG001162	MG001006, MG001056, MG001162
<i>Farfantepenaeus brasiliensis</i> S	N/A	Ubatuba, Sao Paulo			KF989360- KF989377	
<i>Farfantepenaeus brasiliensis</i> S	N/A	US Virgin Islands		HM014402, HM014403, HM014405		
<i>Farfantepenaeus brevirostris</i>	HBG3695	Costa Rica	MG001017	MG001109		MG001017, MG001109
<i>Farfantepenaeus brevirostris</i>	HBG3687	Panama	MG001015	MG001107		MG001015, MG001107
<i>Farfantepenaeus brevirostris</i> S	HBG3692	Panama	MG001016	MG001108		MG001016, MG001108
<i>Farfantepenaeus californiensis</i>	HBG3685	Baja, Mexico	MG000981	MG001058	MG001164	MG000981, MG001058, MG001164
<i>Farfantepenaeus californiensis</i>	N/A	Northwest of Mexico	EU497054, NC012738	EU497054, NC012738		EU497054, NC012738
<i>Farfantepenaeus californiensis</i>	HBG3703	Panama	MG000982	MG001059	MG001165	MG000982, MG001059, MG001165
<i>Farfantepenaeus duorarum</i>	HBG1621	Biscayne Bay	MG001025	MG001086	MG001130	MG001025, MG001086, MG001130

<i>Farfantepenaeus duorarum</i>	HBG1661	Biscayne Bay	MG001026	MG001087	MG001117	MG001026, MG001087, MG001117
<i>Farfantepenaeus duorarum</i>	N/A	Caribbean and/or South America		AF192055- AF192056		
<i>Farfantepenaeus duorarum</i>	HBG1076	Everglades	MG001020	MG001081	MG001111	MG001020, MG001081, MG001111
<i>Farfantepenaeus duorarum</i>	HBG1077	Everglades	MG001040	MG001082	MG001112	MG001040, MG001082, MG001112
<i>Farfantepenaeus duorarum</i>	HBG1078	Everglades	MG001021	MG001103	MG001113	MG001021, MG001103, MG001113
<i>Farfantepenaeus duorarum</i>	HBG1102	Everglades	MG001022	MG001083	MG001114	MG001022, MG001083, MG001114
<i>Farfantepenaeus duorarum</i>	HBG1103	Everglades	MG001023	MG001084	MG001115	MG001023, MG001084, MG001115
<i>Farfantepenaeus duorarum</i>	HBG1105	Everglades	MG001024	MG001085	MG001116	MG001024, MG001085, MG001116
<i>Farfantepenaeus duorarum</i>	N/A	Gulf Breeze, FL		HQ214007		
<i>Farfantepenaeus duorarum</i>	HBG3702	Gulf of Mexico	MG001041	MG001100	MG001129	MG001041, MG001100, MG001129
<i>Farfantepenaeus duorarum</i>	N/A	Gulf of Mexico		AF279812		
<i>Farfantepenaeus duorarum</i>	N/A	Key Largo, FL		HQ214013		
<i>Farfantepenaeus duorarum</i>	N/A	Mexico		JF899810		
<i>Farfantepenaeus duorarum</i>	HBG1672	North of Everglades	MG001027	MG001091	MG001118	MG001027, MG001091, MG001118

<i>Farfantepenaeus duorarum</i>	HBG1676	North of Everglades	MG001028	MG001101	MG001119	MG001028, MG001101, MG001119
<i>Farfantepenaeus duorarum</i>	HBG1680	North of Everglades	MG001029	MG001092	MG001120	MG001029, MG001092, MG001120
<i>Farfantepenaeus duorarum</i>	HBG2437	North of Everglades	MG001030	MG001093	MG001121	MG001030, MG001093, MG001121
<i>Farfantepenaeus duorarum</i>	HBG2438	North of Everglades	MG001036	MG001094	MG001122	MG001036, MG001094, MG001122
<i>Farfantepenaeus duorarum</i>	HBG2439	North of Everglades	MG001039	MG001095	MG001123	MG001039, MG001095, MG001123
<i>Farfantepenaeus duorarum</i>	HBG2471	North of Everglades	MG001033	MG001097	MG001126	MG001033, MG001097, MG001126
<i>Farfantepenaeus duorarum</i>	HBG2472	North of Everglades	MG001034	MG001098	MG001127	MG001034, MG001098, MG001127
<i>Farfantepenaeus duorarum</i>	HBG2474	North of Everglades	MG001037	MG001106	MG001131	MG001037, MG001106, MG001131
<i>Farfantepenaeus duorarum</i>	HBG2478	North of Everglades	MG001035			
<i>Farfantepenaeus duorarum</i>	N/A	Panacea, FL		HQ214006		
<i>Farfantepenaeus duorarum</i>	HBG3701	Perdido Key	MG001038	MG001099	MG001128	MG001038, MG001099, MG001128
<i>Farfantepenaeus duorarum</i>	N/A	Saint Joseph Bay, FL		HQ214011		
<i>Farfantepenaeus duorarum</i>	HBG2460	South of Biscayne Bay	MG001031	MG001096	MG001124	MG001031, MG001096, MG001124
<i>Farfantepenaeus duorarum</i>	HBG2464	South of Biscayne Bay	MG001032	MG001102	MG001125	MG001032, MG001102, MG001125

<i>Farfantepenaeus duorarum</i>	N/A	Unknown		AY601732		
<i>Farfantepenaeus isabellae</i>	HBG7601	Brazil	MG001010		MG001167	MG001010, MG001167
<i>Farfantepenaeus isabellae</i>	HBG7602	Brazil	MG001011	MG001049	MG001168	MG001011, MG001049, MG001168
<i>Farfantepenaeus notialis</i>	HBG1138	Biscayne Bay	MG001042	MG001104	MG001132	MG001042, MG001104, MG001132
<i>Farfantepenaeus notialis</i>	HBG1188	Biscayne Bay	MG001043	MG001088	MG001133	MG001043, MG001088, MG001133
<i>Farfantepenaeus notialis</i>	HBG1617	Biscayne Bay	MG001046	MG001089	MG001134	MG001046, MG001089, MG001134
<i>Farfantepenaeus notialis</i>	HBG1654	Biscayne Bay	MG001044	MG001090	MG001135	MG001044, MG001090, MG001135
<i>Farfantepenaeus notialis</i>	N/A	Cuba	X84350	AJ133054	X84350	AJ133054, X84350
<i>Farfantepenaeus notialis</i>	HBG2455	South of Biscayne Bay	MG001045	MG001105	MG001136	MG001045, MG001105, MG001136
<i>Farfantepenaeus paulensis</i>	N/A	Cananea, Sao Paulo			KF783861, KF989432- KF989448	KF783861, KF989432
<i>Farfantepenaeus paulensis</i>	N/A	Rio de Janeiro			KM065406, KM065409, KM065413	
<i>Farfantepenaeus paulensis</i>	N/A	Rio Grande do Sul			KM065407, KM065410- KM065412	

<i>Farfantepenaeus paulensis</i>	N/A	RS, Brazil			KF989458- KF989461	KF989458
<i>Farfantepenaeus paulensis</i>	N/A	Santos, Sao Paulo			KF989449- KF989457	KF989449
<i>Farfantepenaeus paulensis</i>	N/A	Ubatuba, Sao Paulo			KF989424- KF989431	KF989424
<i>Farfantepenaeus subtilisMI</i>	HBG1662	Biscayne Bay	MG001009	MG001050	MG001166	MG001009, MG001050, MG001166
<i>Farfantepenaeus subtilisMI</i>	N/A	Caribbean and/or South America		AF192061- AF192068		AF192061- AF192068
<i>Farfantepenaeus subtilisMI</i>	N/A	Unknown		AY344193		
<i>Farfantepenaeus subtilisMII</i>	HBG7599	Brazil	MG001018		MG001169	MG001018, MG001169
<i>Farfantepenaeus subtilisMII</i>	HBG7600	Brazil	MG001019	MG001051	MG001170	MG001019, MG001051, MG001170
<i>Farfantepenaeus subtilisMII</i>	N/A	Caribbean and/or South America		AF192069- AF192076		AF192069- AF192076
<i>Litopenaeus vannamei</i>	HBG1607	Washington, DC	MG001047	MG001110	MG001172	MG001047, MG001110, MG001172
<i>Litopenaeus setiferous</i>	N/A	Gulf of Mexico	AF279841	AF279819		AF279841, AF279819
<i>Litopenaeus stylirostris</i>	N/A	Western Atlantic		AF255057		AF255057

CHAPTER IV

BATHYNOMUS GIGANTEUS (ISOPODA: CIROLANIDAE) AND THE CANYON: A POPULATION GENETICS ASSESSMENT OF DE SOTO CANYON AS A GLACIAL REFUGIUM FOR THE GIANT DEEP-SEA ISOPOD

ABSTRACT

Population genetics has gained popularity as a method to discover glacial refugia in terrestrial species, but has only recently been applied to the marine realm. The last glacial maxima occurred 20,000ya, decreasing sea levels by 120m and exposing much of the continental shelf in the northern Gulf of Mexico, with the exception of De Soto Canyon (2100m depth). The goal of this study was to determine whether population dynamics of the giant deep-sea isopod, *Bathynomus giganteus*, were better explained by habitat diversity or by the past presence of a marine glacial refugium in De Soto Canyon. To accomplish this we 1) measured genetic diversity in De Soto Canyon and adjacent regions, 2) characterized gene flow and connectivity between these regions, and 3) investigated historical changes to population size. We sequenced three mitochondrial loci (12S, 16S, and COI) from 212 individuals and also performed a next-generation sequencing pilot study using double digest Restriction site-Associated DNA sequencing. We found high genetic diversity and connectivity throughout the study regions, migration between all three regions, low population differentiation, and evidence of population expansion. This study suggests habitat heterogeneity, rather than the presence of a glacial refugium, has had an historical effect on the population dynamics of *B. giganteus*.

KEYWORDS: population genetics/genomics; ddRADseq; *Bathynomus giganteus*; glacial refugia; deep-sea; De Soto Canyon; habitat diversity

INTRODUCTION

In the last three million years, there have been 11 major glaciation events (Richmond & Fullerton, 1986), with the most recent reducing sea levels by 120-125m 20,000 years ago. Many studies have focused on the impact on terrestrial species and habitats (reviewed in Avise, 1992; Hewitt, 2004; Provan & Bennett, 2008; Taberlet, 1998; Taberlet et al., 1998), including plants (Petit, 2003; Lewis & Crawford, 1995; Beck et al., 2008), fish (Bernatchez & Dodson, 1991; Bernatchez & Wilson, 1998; Nesbø et al., 1999), and insects (Hewitt, 1996; Knowles, 2001; Trewick & Wallis, 2001). Recently, research focus has turned to the identification and impacts of glaciation on population structure and demography of marine species (Campo et al., 2009; Dömel et al., 2015; García-Merchán et al., 2012; Kearse et al., 2012; Maggs et al., 2008; Mäkinen & Merilä, 2008; Médail & Diadema, 2009; Palero et al., 2008; Provan & Bennett, 2008; Provan et al., 2005; Thatje et al., 2005; Zemplak et al., 2008). These studies frequently uncovered evolutionary impacts of glacial refugia on populations, such as the establishment and reintroduction of unique lineages (Mäkinen & Merilä, 2008; Zemplak et al., 2008), which is similar to terrestrial studies. But many studies also concluded that the marine environment imposes unique ecological considerations, such as physical oceanographic characteristics that determine the location and suitability of a refugium (Dömel et al., 2015; Médail & Diadema, 2009; Thatje et al., 2005).

The northern Gulf of Mexico was impacted by the last Pleistocene glaciation as sea levels fell 120-125m. This left the majority of the Mississippi-Alabama shelf exposed and substantially decreased depth over the continental slopes (Sager et al., 1992). De Soto Canyon sits just off of the Mississippi-Alabama shelf and served as the northernmost

intrusion of marine abyss during this period. While the canyon has a measured depth and maximum width of 2100m and 5000m, respectively, it is better defined as an embayment as it lacks steep walls – sloping gently to depth with a network of smaller, more traditional canyons branching off of it (Coleman et al., 2014). The role of this canyon as a potential extension of the deeper, central marine refugium in the Gulf of Mexico has not been investigated, though today the minimum depth of the canyon is 100-150m (Nguyen, 2014). However, if De Soto Canyon maintained a benthic community in the northernmost Gulf of Mexico during the last glaciation, it would have served as a vital source of biodiversity during re-colonization and expansion as sea levels rose to interglacial levels.

The Gulf of Mexico is a highly heterogeneous basin in terms of geology and physical geography. The west Florida slope exhibits some complex topographical features and is primarily comprised of carbonate from ancient coral reefs. Moving north, De Soto Canyon is described as a boundary to this slope. West of De Soto Canyon, the Texas/Louisiana shelf is extremely intricate, containing intermittent banks, four canyon systems, and a number of substrates, including carbonate, clay, silt, and mud from the Mississippi River. Input from the Mississippi River can disperse as far as the west Florida slope before giving way to the carbonate substrate. The Texas/Louisiana shelf/slope region is considered one of the most geologically and geographically complex in the world (Brooke & Schroeder, 2007). Given this high complexity, and the established relationship between deep-sea habitat heterogeneity and high genetic diversity (Levin et al., 2001; Vanreusel et al., 2010), it is also possible that population dynamics in the Gulf of Mexico may be more heavily influenced by the density of microhabitats in regions of the northern Gulf than by the presence of a glacial refugium. However, it is also

important to recognize that regions serve as glacial refugia because they are ecologically and historically suited to do so (Médail & Diadema, 2009). Therefore, a region with many environmental factors that promote or maintain genetic diversity may also predispose it to be a successful glacial refugium. Because of the number of variables that can influence genetic diversity (drift, mutation, selection, effective population size, migration, demographic stability over time, etc.) it can be difficult to find patterns through the noise (Taylor & Roterman, 2017), but is still possible with careful attention and proper analyses (Maggs et al., 2008).

Bathynomus giganteus A. Milne-Edwards, 1879 is a deep-sea isopod that can reach lengths of over 36cm with a described range that includes the Atlantic Ocean and Pacific Ocean at depths ranging from 100-2100m (Poore & Bruce, 2012). This benthic crustacean is primarily a detritivore, though stomach content analysis has indicated facultative carnivory (Chamberlain et al., 1986; Barradas-Ortiz et al., 2003). Reproduction occurs seasonally, primarily in the winter and spring, and development is direct: an adult female develops a pouch where her offspring brood until they emerge as tiny adults (Briones-Fourzan & Lozano-Alvarez, 1991; Barradas-Ortiz et al., 2003). In the marine environment, populations are usually demographically connected by the exchange of planktonic larvae (Grosberg & Cunningham, 2001; Gaines et al., 2007). Phylogeographic and biogeographic barriers to pelagic larval dispersal tend to be centered on regions where currents no longer provide reliable larval transport along the geographic range (Briggs, 1974), however the adult life stage of marine invertebrates has been found to contribute substantially to gene flow, especially when the adult is pelagic (Cowen & Sponaugle, 2009; Havermans et al., 2013) but also in benthic species (Leese et

al., 2010). In this, *B. giganteus* may have an advantage over the majority of other deep-sea isopod species: while deep-sea isopods are primarily (if not exclusively) benthic, swimming behavior has been documented in *B. giganteus* (Chamberlain et al., 1986) and personally witnessed by the authors.

While much attention has been paid to the role of surface production (Campbell & Aarup, 1992), particle flux (Sibuet et al., 1989), and benthic biomass (Rowe, 1983) in determining diversity of abyssal marine invertebrates, the historical effects of a glacial refugium or habitat heterogeneity on population dynamics in the northern Gulf of Mexico requires further investigation. The objective of this study is to determine whether population dynamics are better explained by habitat diversity or by the past presence of a marine glacial refugium in De Soto Canyon. We accomplished this using three mitochondrial loci (12S, 16S, and cytochrome oxidase subunit I) and over 2000 SNPs discovered through double digest Restriction site-Associated DNA sequencing (ddRADseq; see Online Resource ddRADseq Supplement). Specifically, we 1) quantified genetic diversity in the De Soto Canyon, as well as a region to the east, near the Mississippi River Delta, and a region to the west along the Florida Slope, 2) characterized gene flow and connectivity between these three regions, and 3) investigated historical changes to population size and tested migration models to elucidate population demography over time. If De Soto Canyon served as a glacial refugium, we expect to see high diversity in the canyon and evidence of population expansion in the east and west. If habitat diversity is a primary driver of population dynamics, we expect to see highest diversity west of De Soto Canyon, near the Mississippi River Delta, as this region is one of the most habitat-heterogeneous in the world (Brooke & Schroeder, 2007). Given the

wide dispersal of Mississippi River sediment, managing to make it as far as the west Florida slope, we expect to see a similar west-to-east pattern of decreasing diversity if habitat heterogeneity is driving diversity dynamics. Because the sample distribution is relatively small, and even a migration rate of a few individuals per generation is enough to prevent differentiation (Hartl & Clark, 1997; Taylor & Roterman, 2017), we do not expect to see population divergence between regions.

METHODS

Samples were collected by long-line, in which hooks are baited on-ship and let out to lie on the ocean floor. With this method, we collected over 200 samples (Online Resource Table S1) from the northeastern Gulf of Mexico (Figure 1) over the course of three Deep-C research cruises carried out on the University of South Florida R/V Weatherbird II in April 2011, August 2011, and August 2012. After collection, specimens were frozen and kept at -20°C on deck, returned to lab and stored at -20°C. Tissue samples were collected in August 2014 and stored at -20°C in 70% ethanol. Upon returning to lab they were recorded in the HBG database and archived in the Florida International Crustacean Collection (FICC).

DNA was extracted using the Qiagen DNeasy Blood and Tissue kit following the provided protocol. To increase DNA yield, 40ul of DL-Dithiothreitol (DTT) was added to the tissue during the initial lysis step and AE buffer was heated to 56° prior to elution. The quality of every DNA extraction was ascertained by running a 2% agarose gel and through Qubit assay (Life Technologies).

Traditional Sanger Sequencing Three mitochondrial genes were sequenced for all samples: the 12S and 16S mitochondrial ribosomal subunits and cytochrome c oxidase subunit I (COI). Genes were amplified in 25ul PCR reactions. The 12S subunit was amplified using the 12SF (5'-GAAACCAGGATTAGATACCC-3'; Mokady et al., 1994) and 12S1R (5'-AGCGACGGGCGATATGTAC-3'; Buhay et al., 2007) primers with an annealing temperature of 52°C. The 16S subunit was amplified using a dual forward primer containing L2 (5'-TGCCTGTTTATCAAAAACAT-3'; Palumbi et al., 2002) and L9 (5'-CGCCTGTTTATCAAAAACAT-3'; Palumbi et al., 2002) and the reverse primer 1472 (5'-AGATAGAAACCAACCTGG-3'; Crandall & Fitzpatrick, 1996), with an annealing temperature of 46°C. COI was amplified using LCOI-1490 (5'-GGTCAACAAATCATAAAGATATTG-3'; Folmer et al., 1994) and HCOI-2198 (5'-TAAACTTCAGGGTGACCAAAAATCA-3'; Folmer et al., 1994), with an annealing temperature of 38°C. Sequences were analyzed by Beckman-Coulter Genomics Services single-pass PCR sequencing, cleaned in Geneious v.8.0.5 (Kearse et al., 2012), and aligned with MAFFT (Katoh & Standley, 2013). Sequences were divided into three regions based on collection locality: west of De Soto Canyon (wDC), De Soto Canyon (DC), and east of De Soto Canyon (eDC).

Next-Generation Sequencing Of the individuals included in the Sanger dataset, 16 were found to have high molecular weight DNA in suitable quantities to be included in the ddRADseq pilot study. Following the double digest RADseq method (Peterson et al., 2012), DNA from 16 individuals was digested with EcoRI and SphI (New England Biolabs). Custom-made, sample-specific barcoded adapters (Table 1), based on those utilized by Peterson et al. (2012), were annealed onto the resulting fragments, allowing

for pooling of individuals into sublibraries. Sublibraries were size selected for 275bp on a PippinPrep (Sage Science). The size-selected sublibraries were then amplified via PCR with Phusion Hi-Fidelity Polymerase (Thermo Scientific). During this step, indices and Illumina adapters were incorporated into the fragments. Sublibraries were subsequently pooled into the final library. The final library was quality-checked on an Agilent BioAnalyzer 2100 (Agilent Technologies). The library was sequenced on an Illumina HiSeq2500 at the University of Texas at Austin's Genome Sequencing and Analysis Facility.

Raw sequence files were quality-filtered, aligned, and assembled with the STACKS v1.45 (Catchen et al., 2013) on the FIU High Performance Computing Cluster (HPCC). Reads were demultiplexed, cleaned (-c), and quality-filtered (-q) with the process_radtags program. Identical reads were aligned within each individual in ustacks, and consensus reads were catalogued in cstacks. All putative loci were matched against the catalog with sstacks before individual genotype calls were corrected according to accumulated population data in rxstacks. Finally, the populations tool was used to generate a file of aligned SNPs. For a SNP to be called, it had to meet a minimum read depth (-m=5) and it had to be present in 25% of the individuals of a population (-r=0.25) to be called for that population. A SNP had to be present in all three populations (wDC, DC, and eDC) to be retained. Only one SNP was called per locus to generate a final alignment of unlinked SNPs. We applied a missing data filter to this alignment which allowed 15% missing data per locus and 10% missing data per individual. Loci under selection were identified by testing whether each was in Hardy-Weinberg equilibrium

(HWE) using Nei G_{IS} in GenoDive v2.0b23 (Meirmans & Van Tienderen, 2004). Loci found to be under selection were removed.

Analysis of Sanger Data

Across loci, nucleotide diversity (π), haplotype diversity (h), and the selection coefficient Tajima's D (Tajima, 1983) were calculated for each region (wDC: West De Soto, DC: De Soto, and eDC: East De Soto) in DNAsp v5 (Librado & Rozas, 2009) and significant differences in diversity and selection between regions were tested with ANOVA. To measure population differentiation and connectivity, we performed hierarchical Analyses of Molecular Variance (AMOVAs) for each dataset in GenAlEx v6.501 (Peakall & Smouse, 2006; Peakall & Smouse, 2012) with 999 permutations to assess statistical significance. Due to the haploid nature of the mitochondrial sequence data, as well as the potential differences between ribosomal sequence data (12S and 16S) vs. protein-coding data (COI), Φ_{PT} was calculated instead of the more traditional Φ_{ST} .

To test for population structure, multi-dimensional scaling (MDS) plots were rendered for each locus using the R package MASS (Venables & Ripley, 2002). Multi-dimensional scaling is very similar to Principle Component Analysis (PCA), with the exception that PCA preserves covariance within the data while MDS preserves distance between points. As genetic distance between individuals is of primary interest in addressing the role of De Soto Canyon during the last glacial maximum, MDS were chosen to better display distances between individuals.

Extended Bayesian Skyline Plot (EBSP) analyses were executed in BEAST2 (Bouckaert et al., 2014) for the purpose of estimating historical changes in population

size for each region (wDC, DC, and eDC), as well as the complete data set (wDC+DC+eDC). Single-locus alignments were loaded individually (12S, 16S, and COI) into BEAUTi2 to set parameters. The COI alignment was divided by codon position (1+2+3) and site model parameters were set according to the results of PartitionFinder. For all data sets, the clock rate was set by 12S with a clock rate of 0.5 and the clock rates for the 16S and COI alignments were estimated in relation to the 12S alignment. In the absence of estimates of clock rates for 16S and COI, rates were set to 0.005. All additional parameters were set according to the manual, with the exception of the MCMC parameters: 200,000,000 generations were run, logged every 5,000th.

Additionally, Bayesian inference as implemented in MIGRATE-N (Beerli & Palczewski, 2010) was used to test models of population demography and determine the most likely migration patterns between regions. As per the manual, default settings were used, then the data was re-analyzed using the resultant estimates of θ for each population and migration rates between populations to inform parameters to ensure default parameters were appropriate for the data set. The number of recorded steps was increased from the default (5,000) to 20,000 and static heating was used across four chains, swapping every tenth step. To confirm results and ensure 20,000 steps was adequate, analyses were rerun with 1,000,000 steps and results compared between runs.

Analysis of ddRADseq Data

Nucleotide diversity (π) was calculated for each population (wDC, DC, and eDC) in DNAsp v5 (Librado & Rozas, 2009) and was included in the ANOVA testing for regional effects on diversity and selection. As the ddRADseq data set consisted entirely

of unique haplotypes, haplotype diversity was not calculated. Also, given small sample sizes (wDC N=2, DC N=3, eDC N=5), Tajima's D could not be calculated.

Genetic distances due to population differentiation (F_{ST}) were calculated in GenoDive v2.0b23 (Meirmans & Van Tienderen, 2004) with 999 permutations to assess significance. A hierarchical Analysis of Molecular Variance (AMOVA) was calculated using the Infinite Allele Model with 999 permutations to assess significance. Missing data were replaced with randomly drawn alleles determined by overall allele frequencies.

To test for population structure, K -means clustering was conducted in the Bayesian program STRUCTURE v2.3.4 (Pritchard et al., 2000). $K=1-7$ were each tested 10 times under the admixture model with 200,000 Markov Chain Monte Carlo generations following a burn-in of 20,000 generations. STRUCTURE results were collated in STRUCTURE HARVESTER v0.6.94 (Earl & VonHoldt, 2012) wherein *ad hoc* posterior probability models (Pritchard et al., 2000) and the Evanno method (Evanno et al. 2005) were used to infer the optimal K value. The final distrupt plot was generated and edited using STRUCTURE PLOT v2.0 (Ramasamy et al., 2014). To facilitate comparison between data sets (Sanger vs ddRADseq), a MDS plot was rendered for the ddRADseq data set as well.

RESULTS

A total of 570 *de novo* sequences were generated across three markers, including 205 12S sequences, 205 16S sequences, and 160 COI sequences. Sequence data is archived under GenBank Accession numbers MG229070-MG229274 (12S), MG229275-MG229479 (16S), and MG229480-MG229639 (COI); and are publicly available in the

Gulf of Mexico Research Initiative's Information and Data Cooperative (GRIIDC) under doi: 10.7266/N7VX0F19. The final concatenated alignment contained 1450bp of sequence data for all three loci across 147 individuals. Across these three loci, 75 SNPs and 78 haplotypes were identified for analysis (Table 2). Individuals missing data at a locus were not included in the concatenated data set.

Raw fastq files are publicly available in the Gulf of Mexico Research Initiative's Information and Data Cooperative (GRIIDC) under doi: 10.7266/N7VX0F19. The STACKS populations tool was used to generate a file of 4487 aligned, unlinked SNPs from the ddRADseq dataset. Two individuals failed to assemble in STACKS. Application of the missing data filter resulted in 2681 retained loci across 10 individuals. Allele frequencies were found to differ significantly from Hardy-Weinberg Equilibrium in 301 SNPs, resulting in 2380 SNPs in the final dataset. Given the low representation of each region in the dataset (wDC N=2, DC N=3, and eDC N=5), results of this pilot study should be interpreted cautiously.

Population Differentiation and Connectivity Results of AMOVA indicate very high gene flow between regions, with among population variance ranging from 0%-1.5% across loci (Table 3). The majority of variance (98.5%-100%) is due to differences between individuals, regardless of the region from which they were sampled. Across data sets hierarchical AMOVAs yielded p -values greater than 0.05 (0.081-0.548), with the exception of the ddRADseq dataset (0.001). Calculations of population differentiation (Φ_{PT} for 12S, 16S, and COI; F_{ST} for ddRADseq) indicate nearly nonexistent population differentiation (Table 4). In the Sanger data, values ranged from -0.002 to 0.016, suggesting virtually every allele is found in every region included in analysis. Analysis of

ddRADseq data yielded the highest F_{ST} value (0.143) between De Soto Canyon and the region to the west, however the result is not statistically significant. These results provide strong evidence that the De Soto Canyon in no way impedes gene flow in *Bathynomus giganteus* and suggests historical connectivity between the canyon and the continental slope.

Multidimensional scaling plots for each data set do not indicate individuals clustering into groups (Figure 2). If individuals from each region were more genetically similar (smaller genetic distances) three clusters would be rendered. However, in every plot, the majority of individuals cluster together with one or two outliers. The STRUCTURE results however, give clear indication of three groups and admixture between all three (Figure 3). The first group consists of five individuals from wDC, DC, and eDC. The second contains three individuals from wDC and eDC. The third group only contains individuals from DC.

Genetic Diversity and Endemicity The genetic diversity metrics π and h were calculated across loci and regions (Table 5) and were found to be relatively high compared to similar studies of deep-sea invertebrates (Etter et al., 2005). Across all analyses, nucleotide diversity (π) was highest west of De Soto Canyon (12S: 1.162, 16S: 2.36, COI: 3.148, ddRADseq: 0.262) compared to DC (12S: 0.574, 16S: 1.502, COI: 2.879, ddRADseq: 0.171) and eDC (12S: 0.780, 16S: 0.836, COI: 2.797, ddRADseq: 0.261) were very similar. This is especially notable in the ddRADseq data, in which wDC had the lowest sample size (N=2). The lowest π values were calculated from ddRADseq data, though this is likely due to small sample sizes (N=2-5). Haplotype diversity (h) differed from the trend seen in π : De Soto consistently yielded the lowest diversity (12S:

0.476, 16S: 0.418, COI: 0.838) compared to wDC (12S: 0.490, 16S: 0.436, COI: 0.909) and eDC (12S: 0.523, 16S: 0.507, COI: 0.866).

Though diversity was hypothesized to be significantly higher in the canyon, ANOVA results did not indicate significant differences in diversity in any region for either metric (for π , $p=0.79$; for h , $p=0.96$). An analysis of the percent of unique endemic haplotypes (number of unique endemic haplotypes/total number of unique haplotypes) within each region found De Soto Canyon had the highest overall (12S+16S+COI) percent of unique endemic haplotypes (21.1%), followed by eDC (18.4%) and wDC (16.7%) (Figure 4).

Selection and Historical Demography Tajima's D was estimated for each region across all Sanger datasets. All values were negative, between -2.182 and -0.945, and most were significant (after 1000 simulations, only 12S in DC, 12S in wDC, and COI in wDC exhibited $D_{sim} < D_{obs}$ in more than 500). Negative Tajima's D values indicate a deficiency of rare alleles. Typically, this deficiency is associated with recovery following a population bottleneck. Analysis of Variance testing of Tajima's D values across loci by region indicate that selection is not significantly different between regions ($p=0.96$). These results were confirmed by modeling changes in population sizes with EBSPs. Overall, the rate of population expansion was highest when the entire data set was analyzed as a whole (increasing by a factor of ~40 in the last 15,000 years). By population, eDC had the highest growth rate (increasing by a factor of ~17 in the last 18,000 years), followed by DC (increasing by a factor of ~11 over the last 20,000 years), and finally wDC (increasing by a factor of ~8 in the last 30,000 years). The fact that all three regions experienced statistically similar selection pressures, combined with high

connectivity and resultant low population differentiation, suggests migration of *Bathynomus giganteus* between the tested regions in northern Gulf of Mexico.

The concatenated Sanger data set was analyzed in MIGRATE-N, and the posterior probabilities of 18 models were estimated using Bayesian inference. The parameters and thermodynamically integrated log marginal likelihood of each model are presented in Table 6. The 18 models ranged from a single panmictic population, to three, entirely separate populations. All models were tested with 20,000 and 1,000,000 steps, but the results did not change substantially between runs, so the results from the 20,000 step analyses are reported (Table 6). The model indicated to be most likely given the data (highest log marginal likelihood) supported three populations (wDC, DC, and eDC) and bi-directional migration between all three.

DISCUSSION

Previous studies have established four metrics as evidence for a region to be classified as a glacial refugium: connectivity, diversity, endemism, and population expansion. First, connectivity must exist between the hypothetical/purported refugium population and nearby populations (Petit, 2003; Bernatchez & Dodson, 1991; Trewick & Wallis, 2001). Second, diversity is typically higher within the refugium population, though in species with limited/low dispersal, highest diversity tends to be found in populations between refugia (Lewis & Crawford, 1995; Beck et al., 2008; Petit, 2003; Provan & Bennett, 2008; Thatje et al., 2005). Third, and relatedly, the refugium population is likely to contain the highest number of unique, endemic haplotypes (haplotypes which occur in one population but are not present in any others) (Provan &

Bennett, 2008; Knowles, 2001). The final line of evidence comes from analysis of historical selection: all populations should exhibit a signal of expansion following a bottleneck (Campo et al., 2009; Maggs et al., 2008; Provan et al., 2005). Glaciation events cause dramatic and quick range changes (GRIP Project Members, 1993), which many species are unable to cope with in real time (Atkinson et al., 1987). Such range contractions cause high mortality along distribution margins, but also allow for population expansion as range increases during interglacial periods (Nesbø et al., 1999; Knowles, 2001). The role of habitat heterogeneity in shaping population dynamics is deduced through associations of genetic diversity and habitat diversity (Levin et al., 2001; Vanreusel et al., 2010), where we expect the highest genetic diversity to be associated with the most complex habitat. However, it is important to note that these two drivers, the hypothesized presence of a glacial refugium and habitat diversity, may themselves be interrelated (Médail & Diadema, 2009).

Across regions and data types, we find 1) low differentiation and high population connectivity, indicating strong gene flow between regions; 2) relatively high genetic diversity across regions; 3) slightly elevated levels of endemism in East De Soto Canyon compared to adjacent regions; and 4) evidence that a bottleneck was experienced and recovery is underway across all regions in the northern Gulf of Mexico, which may correlate to the last glaciation event of the Pleistocene. In light of these findings, we will discuss the potential impact of habitat heterogeneity and/or the presence of a glacial refugium on the current and historical population dynamics of the deep-sea isopod *Bathynomus giganteus* in the northern Gulf.

Population Differentiation and Connectivity

Across the De Soto Canyon, *Bathynomus giganteus* exhibits similar genetic diversity values, regardless of geographic location. It seems that this high diversity and low population differentiation is sustained through high population connectivity. However, it is also possible that low divergence and F_{ST} values are evidence for recent population expansion (Stamatis et al, 2004) out of the putative De Soto Canyon refugium or recent re-acquaintance of separated populations (Taylor & Roterman, 2017). Given the small geographic distance between sites and the low migration rate required to prevent genetic divergence, we are inclined to interpret these results as evidence of moderate, historical gene flow.

Bathynomus giganteus lacks a pelagic larval phase, which could potentially impede migration (see Marko, 2004 for a more thorough investigation of this often-incorrect inference). Our results indicate that not only are individuals capable of traversing the canyon, but they apparently do so quite freely. This is not too surprising considering *Bathynomus giganteus* are known to be quite efficient swimmers (per observation). No unique genetic signature was found on either side of the canyon, nor within the canyon itself. Moreover, multi-dimensional scaling does not cluster individuals by collection location to any appreciable extent.

Our analyses of population differentiation suggests high connectivity contributes to the even distribution of diversity in the northern Gulf of Mexico. This was somewhat unexpected as many studies in the Atlantic deep-sea have found strong differentiation corresponding to depth in motile taxa (Doyle, 1972; France & Kocher, 1996; Siebenaller, 1978; Taylor & Roterman, 2017; Wilson, 1983), though the swimming ability of *B.*

giganteus may help explain high connectivity between regions. Additionally, a study of the bathyal gastropod *Bathybembix bairdii* indicated low population differentiation as well (Siebenaller, 1978) and more recent studies of gastropods and bivalves found population-level differences in diversity decreased with depth, as factors associated with population differentiation, such as environmental heterogeneity and topographical complexity, also tend to decrease along a depth gradient (Etter et al., 2005; Etter & Rex, 1990; Rex et al., 1993).

In characterizing connectivity between regions, we find there are functionally no barriers to gene flow between regions in the northern Gulf of Mexico. This suggests that, if De Soto Canyon served as a glacial refugium during the last Pleistocene glaciation event, individuals of *B. giganteus* migrated out of the canyon into adjacent regions as sea-levels rose. However, lack of population differentiation also suggests that differences in habitat do not impede gene flow between regions.

Genetic Diversity and Endemicity

Previous population genetics studies of deep-sea invertebrates provide context for our findings of relatively high genetic diversity (Doyle, 1972; Etter & Rex, 1990; Etter et al., 2005; France & Kocher, 1996; Raupach et al., 2007; Siebenaller, 1978; Zardus et al., 2006). Studies of deep-sea mollusk population genetics found similar haplotype diversity values, however our analyses indicate much higher diversity in *B. giganteus* than in mollusks targeted in previous studies (Etter et al., 2005; Zardus et al., 2006), despite larger sample sizes (see Table 5 for comparison with previous studies of diversity in marine bivalves). This difference may be due in part to the loci analyzed: in the Etter et

al. study, 16S was sequenced (225bps); our study sequenced a larger portion of 16S (527bps) in addition to 12S (336bps), and COI (596bps).

The high haplotype diversity may be explained by the species' dispersal ability: while it lacks a pelagic larval stage, individuals migrate great distances over the course of their lives, perhaps even into adjacent oceanic basins. This may be facilitated by strong swimming behavior. High diversity within *Bathynomus giganteus* is likely maintained through the unique habitat conditions of the northern Gulf of Mexico, as suggested by previous studies of genetic diversity in the marine benthos (Campbell & Aarup, 1992; Levin et al., 2001; Rex, 1983; Sibuet et al., 1989; Vanreusel et al., 2010).

Analyses of molecular diversity revealed non-De Soto sites (wDC and eDC) had very similar haplotype diversity values, slightly higher than values measured for De Soto Canyon. This seems to support the habitat diversity hypothesis, instead of the De Soto Canyon refugium: if the canyon had served as a refugium, we would expect diversity values to be substantially higher within it and for it to contain the highest proportion of endemic haplotypes (see Introduction). Instead, we find eDC contains the highest proportion of endemic haplotypes. Moreover, every haplotype sampled can be found in eDC. Differences in diversity between regions may be better explained by habitat diversity: the high degree and variety of organic particulate influx from the Mississippi River contributes to habitat heterogeneity, a crucial feature for the sustenance of diversity in the deep-sea benthos (Grassle & Maciolek, 1992; Etter & Grassle, 1992). This riverine input flows directly over the wDC sites and is known to disperse as far as the west Florida slope (Brooke & Schroeder, 2007), from which the eDC samples were collected.

De Soto Canyon, by contrast, is hard-bottomed, high relief, and primarily the result of erosion (Brooke & Schroeder, 2007; Gore, 1992; Nowlin, 1971).

Selection and Historical Demography

Our results indicate a bottleneck was experienced across regions in the northern Gulf of Mexico, but populations are expanding. This may be indicative of sea level rise, range expansion, and concomitant population growth. Given the relative dearth of information available on major disruptions in the benthic deep-sea, it is difficult to definitively deduce the cause of this bottleneck. However, the last glaciation is indicated for three reasons: first, sea levels were 120-125m lower causing dramatic range contraction in the northern Gulf of Mexico, which includes the distributional range of *B. giganteus*; second, periods of glaciation are also associated with decreased precipitation, which in turn depress the input of organic particulate matter into the deep Gulf of Mexico and could increase microhabitat homogeneity and decrease diversity through mortality (Grassle & Maciolek, 1992; Etter & Grassle, 1992); third the timing of population expansion indicated by EBSPs suggest expansion began approximately 15,000-30,000 years ago. This correlates well with the retreat of the last glacial maximum, with the exception of the population west of De Soto Canyon. The last glacial maximum of the Pleistocene occurred approximately 20,000 years ago, alongside the estimated beginning of expansion for the De Soto Canyon population and that east of the canyon. However, the population west of De Soto appears to have begun increasing 30,000 years ago. Not only does the wDC population expand at a much lower rate, but the Tajima's D values associated with this region ($D=-1.585$) was the lowest measured in this study and was not

statistically significant. This provides justification for an intriguing inference: the population west of De Soto seems to have been relatively unimpacted by the last glacial maximum, suggesting the population is relatively stable. In non-marine environments, long-term stability of a population can be a predictor of higher genetic diversity (Carnaval et al., 2009). Thus, regional stability in the wDC, combined with the bi-directional gene flow indicated by migration analysis and lack of population differentiation, may contribute to high genetic diversity for the entire northern Gulf.

Selection coefficient values and rates of population expansion exhibited an increasing trend from east to west, away from the Mississippi River Delta, the most geologically, topographically, and geographically diverse region included in the study. Rather than supporting De Soto Canyon as a glacial refugium, for which we would expect the coefficient to be highest and the expansion rate lowest for the region, we instead find those characteristics in the region west of De Soto. This provides evidence for the influence of habitat diversity on population demography in the northern Gulf of Mexico.

CONCLUSIONS

Our investigation into the historical role of De Soto Canyon and habitat diversity in the northern Gulf of Mexico illuminates population dynamics of a charismatic deep-sea invertebrate in the region and increases our understanding of an often over-looked environment. Despite low population differentiation, high connectivity, and a strong signal of population expansion, we find diversity to be lowest in the canyon. Our results lend support to the intriguing hypothesis that population dynamics have historically been

influenced by the unique habitat diversity found in the northern Gulf, rather than by the presence of a putative glacial refugium. To more confidently evaluate the role of the De Soto Canyon in past glaciation events, a more inclusive ddRADseq study should be undertaken to include samples from a broader geographic range.

ACKNOWLEDGEMENTS

This research was made possible in part by a grant from The Gulf of Mexico Research Initiative through the Florida Institute of Oceanography, a grant to the Deep-C Consortium, and a grant to the Deep Pelagic Nekton Dynamics of the Gulf of Mexico (DEEPEND) Consortium. Funding was also provided by the Florida International University (FIU) Presidential Fellowship and the FIU Doctoral Evidence Acquisition Fellowship. All data are publicly available through the Gulf of Mexico Research Initiative Information & Data Cooperative (GRIIDC) at <https://data.gulfresearchinitiative.org> (doi: 10.7266/N7VX0F19). We would like to specially thank Dr. Mike Heithaus and Dr. Dean Grubbs for their support in sample collection. We also thank L. E. Timm's PhD committee: Dr. José Eirin-Lopez, Dr. Mauricio Rodriguez-Lanetty, Dr. Eric von Wettberg, and Dr. Wensong Wu; as well as Ms. Emily Warschefsky, Mr. Joseph Ahrens, and Dr. Danielle DeLeo for additional comments and suggestions. Finally, we thank the anonymous reviewers for feedback on earlier versions of this manuscript. This is contribution #84 from the Center for Coastal Oceans Research in the Institute of Water and Environment at Florida International University.

LITERATURE CITED

- Allendorf, F. W. & G. Luikart, 2009. Conservation and the Genetics of Populations. John Wiley & Sons.
- Atkinson, T., K. Briffa & G. Coope, 1987. Seasonal temperatures in Britain during the past 22,000 years, reconstructed using beetle remains. *Nature* 325: 587–592.
- Awise, J. C., 1992. Molecular population structure and the biogeographic history of a regional fauna : a case history with lessons for conservation biology. *Oikos* 63: 62–76.
- Barradas-Ortiz, C., P. Briones-Fourzán & E. Lozano-Álvarez, 2003. Seasonal reproduction and feeding ecology of giant isopods *Bathynomus giganteus* from the continental slope of the Yucatán peninsula. *Deep Sea Research Part I: Oceanographic Research Papers* 50: 495–513.
- Beck, J. B., H. Schmuths & B. A. Schaal, 2008. Native range genetic variation in *Arabidopsis thaliana* is strongly geographically structured and reflects Pleistocene glacial dynamics. *Molecular Ecology* 17: 902–915.
- Beerli, P. & M. Palczewski, 2010. Unified framework to evaluate panmixia and migration direction among multiple sampling locations. *Genetics* 185: 313–326.
- Bernatchez, L. & J. J. Dodson, 1991. Phylogeographic structure in mitochondrial DNA of the Lake Whitefish (*Coregonus clupeaformis*) and its relation to Pleistocene glaciations. *Evolution* 45: 1016–1035.
- Bernatchez, L. & C. C. Wilson, 1998. Comparative phylogeography of Nearctic and Palearctic fishes. *Molecular Ecology* 7: 431–452.
- Bouckaert, R., J. Heled, D. Kühnert, T. Vaughan, C. H. Wu, D. Xie, M. Suchard, A. Rambaut & A. J. Drummond, 2014. BEAST 2: a software platform for Bayesian evolutionary analysis. *PLoS Computational Biology* 10: 1–6.
- Briggs, J. C., 1974. *Marine Zoogeography*. New York: McGraw-Hill.
- Briones-Fourzan, P. & E. Lozano-Alvarez, 1991. Aspects of the biology of the giant isopod *Bathynomus giganteus* A. Milne Edwards, 1879 (Flabellifera: Cirolanidae), off the Yucatan Peninsula. *Journal of Crustacean Biology* 11: 375–385.
- Brooke, S. & W. W. Schroeder, 2007. State of deep coral ecosystems in the Gulf of Mexico region: Texas to the Florida Straits. *The State of Deep Coral Ecosystems of the United States: 2007*.

- Buhay, J. E., G. Moni, N. Mann & K. A. Crandall, 2007. Molecular taxonomy in the dark: Evolutionary history, phylogeography, and diversity of cave crayfish in the subgenus *Aviticambarus*, genus *Cambarus*. *Molecular Phylogenetics and Evolution* 42: 435–448.
- Campbell, J. W. & T. Aarup, 1992. New production in the North Atlantic derived from seasonal patterns of surface chlorophyll. *Deep Sea Research Part A. Oceanographic Research Papers* 39: 1669–1694.
- Campo, D., J. Molares, L. Garcia, P. Fernandez-Rueda, C. Garcia-Gonzalez & E. Garcia-Vazquez, 2009. Phylogeography of the European stalked barnacle (*Pollicipes pollicipes*): Identification of glacial refugia. *Marine Biology* 157: 147–156.
- Carnaval, A. C., M. J. Hickerson, C. F. B. Haddad, M. T. Rodrigues & C. Moritz, 2009. Stability predicts genetic diversity in the Brazilian Atlantic forest hotspot. *Science* 323: 785–789.
- Chamberlain, S. C., V. B. Meyer-Rochow & W. P. Dossert, 1986. Morphology of the compound eye of the giant deep-sea isopod *Bathynomus giganteus*. *Journal of Morphology* 189: 145–56.
- Coleman, F. C., J. P. Chanton & E. P. Chassinger, 2014. Ecological connectivity in northeastern Gulf of Mexico - The Deep-C Initiative. *International Oil Spill Conference Proceedings 2014*: 1972–1984.
- Cowen, R. K. & S. Sponaugle, 2009. Larval dispersal and marine population connectivity. *Annual Review of Marine Science* 1: 443–466.
- Crandall, K. A. & J. F. Fitzpatrick, 1996. Crayfish molecular systematics: using a combination of procedures to estimate phylogeny. *Systematic Biology* 45: 1–26.
- Dömel, J. S., P. Convey & F. Leese, 2015. Genetic data support independent glacial refugia and open ocean barriers to dispersal for the Southern Ocean sea spider *Austropallene cornigera* (Möbius, 1902). *Journal of Crustacean Biology* 35: 480–490.
- Doyle, R. W., 1972. Genetic variation in *Ophiomusium lymani* (Echinodermata) populations in the deep sea. *Deep Sea Research and Oceanographic Abstracts* 19: 661–664.
- Etter, R. J. & F. Grassle, 1992. Patterns of species diversity in the deep sea as a function of sediment particle size diversity. *Nature* 360: 576–578.

- Etter, R. J. & M. A. Rex, 1990. Population differentiation decreases with depth in deep-sea gastropods. *Deep Sea Research Part A. Oceanographic Research Papers* 37: 1251–1261.
- Etter, R. J., M. A. Rex, M. R. Chase & J. M. Quattro, 2005. Population differentiation decreases with depth in deep-sea bivalves. *Evolution* 59: 1479–1491.
- Excoffier, L. & H. E. L. Lischer, 2010. Arlequin suite ver 3.5: A new series of programs to perform population genetics analyses under Linux and Windows. *Molecular Ecology Resources* 10: 564–567.
- Folmer, O., W. R. Hoeh, M. B. Black, & R. C. Vrijenhoek, 1994. Conserved primers for PCR amplification of mitochondrial DNA from different invertebrate phyla. *Molecular Marine Biology and Biotechnology* 3: 294–299.
- France, S. C. & T. D. Kocher, 1996. Geographic and bathymetric patterns of mitochondrial 16S rRNA sequence divergence among deep-sea amphipods, *Eurythenes gryllus*. *Marine Biology* 126: 633–643.
- Gaines, S., B. Gaylord, L. Gerber, A. Hastings & B. Kinlan, 2007. Connecting places: the ecological consequences of dispersal in the sea. *Oceanography* 20: 90–99.
- García-Merchán, V. H., A. Robainas-Barcia, P. Abelló, E. Macpherson, F. Palero, M. García-Rodríguez, L. G. de Sola & M. Pascual, 2012. Phylogeographic patterns of decapod crustaceans at the Atlantic-Mediterranean transition. *Molecular Phylogenetics and Evolution* 62: 664–672.
- Goodall-Copestake, W. P., G. A. Tarling & E. J. Murphy, 2012. On the comparison of population-level estimates of haplotype and nucleotide diversity: A case study using the gene *cox1* in animals. *Heredity* 109: 50–56.
- Gore, R. H., 1992. *The Gulf of Mexico*. Sarasota, FL: Pineapple Press Inc.
- Grassle, J. F. & N. J. Maciolek, 1992. Deep-sea species richness: regional and local diversity estimates from quantitative bottom samples. *The American Naturalist* 139: 313–341.
- GRIP Project Members, 1993. Climate instability during the last inter-glacial period recorded in the GRIP ice core. *Nature* 364: 203–207.
- Grosberg, R. & C. W. Cunningham, 2001. Genetic structure in the sea: from populations to communities. *Marine Community Ecology* 2001: 61–84.
- Hartl, D. L. & A. G. Clark, 1997. *Principles of Population Genetics*. Sunderland: Sinauer Associates.

- Havermans, C., G. Sonet, C. d'Udekem d'Acoz, Z. T. Nagy, P. Martin, S. Brix, T. Riehl, S. Agrawal & C. Held, 2013. Genetic and morphological divergences in the cosmopolitan deep-sea amphipod *Eurythenes gryllus* reveal a diverse abyss and a bipolar species. *PLoS ONE* 8: e74218.
- Hewitt, G. M., 1996. Some genetic consequences of ice ages, and their role in divergence and speciation. *Biological Journal of the Linnean Society* 58: 247–276.
- Hewitt, G. M., 2004. Genetic consequences of climatic oscillations in the Quaternary. *Philosophical Transactions of the Royal Society of London. Series B, Biological Sciences* 359: 183–195.
- Katoh, K. & D. M. Standley, 2013. MAFFT multiple sequence alignment software version 7: Improvements in performance and usability. *Molecular Biology and Evolution* 30: 772–780.
- Kearse, M., R. Moir, A. Wilson, S. Stones-Havas, M. Cheung, S. Sturrock, S. Buxton, A. Cooper, S. Markowitz, C. Duran, T. Thierer, B. Ashton, P. Mantjies & A. Drummond, 2012. Geneious Basic: an integrated and extendable desktop software platform for the organization and analysis of sequence data. *Bioinformatics* 28: 1647–1649.
- Knowles, L., 2001. Did the Pleistocene glaciations promote divergence? Tests of explicit refugial models in montane grasshoppers. *Molecular Ecology* 10: 691–701.
- Leese, F., S. Agrawal & C. Held, 2010. Long-distance island hopping without dispersal stages: Transportation across major zoogeographic barriers in a Southern Ocean isopod. *Naturwissenschaften* 97: 583–594.
- Levin, L. A., R. J. Etter, M. A. Rex, A. J. Gooday, C. R. Smith, J. Pineda, C. T. Stuart, R. R. Hessler & D. Pawson, 2001. Environmental influences on regional deep-sea species diversity. *Annual Review of Ecology and Systematics* 32: 51–93.
- Lewis, P. O. & D. J. Crawford, 1995. Pleistocene refugium endemics exhibit greater allozymic diversity than widespread congeners in the genus *Polygonella* (Polygonaceae). *American Journal of Botany* 82: 141–149.
- Librado, P. & J. Rozas, 2009. DnaSP v5: a software for comprehensive analysis of DNA polymorphism data. *Bioinformatics* 25: 1451–1452.
- Maggs, C. A., R. Castilho, D. Foltz, C. Henzler, M. T. Jolly, J. Kelly, J. Olsen, K. E. Perez, W. Stam, R. Väinölä, F. Viard & J. Wares, 2008. Evaluating signatures of glacial refugia for North Atlantic benthic marine taxa. *Ecology* 89: S108–S122.

- Mäkinen, H. S. & J. Merilä, 2008. Mitochondrial DNA phylogeography of the three-spined stickleback (*Gasterosteus aculeatus*) in Europe - Evidence for multiple glacial refugia. *Molecular Phylogenetics and Evolution* 46: 167–182.
- Marko, P. B., 2004. “What’s larvae got to do with it?” Disparate patterns of post-glacial population structure in two benthic marine gastropods with identical dispersal potential. *Molecular Ecology* 13: 597–611.
- Médail, F. & K. Diadema, 2009. Glacial refugia influence plant diversity patterns in the Mediterranean Basin. *Journal of Biogeography* 36: 1333–1345.
- Mokady, O., S. Rozenblatt, D. Graur & Y. Loya, 1994. Coral-host specificity of Red Sea Lithophaga bivalves: interspecific and intraspecific variation in 12S mitochondrial ribosomal RNA. *Molecular Marine Biology & Biotechnology* 3: 158–164.
- Nei, M., 1987. *Molecular Evolutionary Genetics*. Columbia University Press.
- Nei, M. & W.-H. Li, 1979. Mathematical model for studying genetic variation in terms of restriction endonucleases. *Proceedings of the National Academy of Sciences of the United States of America* 76: 5269–5273.
- Nesbø, C. L., T. Fossheim, L. A. Vøllestad & K. S. Jakobsen, 1999. Genetic divergence and phylogeographic relationships among European perch (*Perca fluviatilis*) populations reflect glacial refugia and postglacial colonization. *Molecular Ecology* 8: 1387–1404.
- Nguyen, T. T., 2014. Variability of cross-slope flow in the De Soto Canyon region. Florida State University.
- Nowlin, W. D., 1971. Water masses and general circulation of the Gulf of Mexico. *Oceanology* 6: 28–33.
- Palero, F., P. Abelló, E. Macpherson, M. Gristina & M. Pascual, 2008. Phylogeography of the European spiny lobster (*Palinurus elephas*): Influence of current oceanographical features and historical processes. *Molecular Phylogenetics and Evolution* 48: 708–717.
- Palumbi, S. R., A. Martin, S. Romano, W. O. McMillan, L. Stice & G. Grabowski, 2002. *The simple fool’s guide to PCR version 2*. Honolulu: University of Hawaii.
- Peterson, B. K., J. N. Weber, E. H. Kay, H. S. Fisher & H. E. Hoekstra, 2012. Double digest RADseq: an inexpensive method for de novo SNP discovery and genotyping in model and non-model species. *PloS One* 7: e37135.

- Petit, R. J., 2003. Glacial refugia: hot spots but not melting pots of genetic diversity. *Science* 300: 1563–1565.
- Poore, G. C. B. & N. L. Bruce, 2012. Global diversity of marine isopods (except Asellota and crustacean symbionts). *PLoS ONE* 7: e43529.
- Provan, J. & K. D. Bennett, 2008. Phylogeographic insights into cryptic glacial refugia. *Trends in Ecology and Evolution* 23: 564–571.
- Provan, J., R. A. Wattier & C. A. Maggs, 2005. Phylogeographic analysis of the red seaweed *Palmaria palmata* reveals a Pleistocene marine glacial refugium in the English Channel. *Molecular Ecology* 14: 793–803.
- Raupach, M. J., M. Malyutina, A. Brandt & J. W. Wägele, 2007. Molecular data reveal a highly diverse species flock within the munnopsoid deep-sea isopod *Betamorpha fusiformis* (Barnard, 1920) (Crustacea: Isopoda: Asellota) in the Southern Ocean. *Deep-Sea Research Part II: Topical Studies in Oceanography* 54: 1820–1830.
- Rex, M. A., 1983. Geographic Patterns of Species Diversity in Deep-Sea Benthos. In G. T. Rowe (Ed.), *Deep-Sea Biology* (pp. 453–472). New York, NY: John Wiley & Sons, Inc.
- Rex, M. A., C. T. Stuart, R. R. Hessler, J. A. Allen, H. L. Sanders & G. D. F. Wilson, 1993. Global-scale latitudinal patterns of species diversity in the deep-sea benthos. *Nature* 365: 636–639.
- Richmond, G. M. & D. S. Fullerton, 1986. Summation of Quaternary glaciations in the United States of America. *Quaternary Science Reviews* 5: 183–196.
- Rowe, G. T., 1983. Biomass and Production of the Deep-Sea Macrobenthos. In G. T. Rowe (Ed.), *Deep-Sea Biology* (pp. 97–121). New York, NY: John Wiley & Sons, Inc.
- Sager, W. W., W. W. Schroeder, J. S. Laswell, K. S. Davis, R. Rezak & S. R. Gittings, 1992. Mississippi-Alabama outer continental shelf topographic features formed during the late Pleistocene-Holocene transgression. *Geo-Marine Letters* 12: 41–48.
- Sibuet, M., C. E. Lambert, R. Chesselet & L. Laubier, 1989. Density of the major size groups of benthic fauna and trophic input in deep basins of the Atlantic Ocean. *Journal of Marine Research* 47: 851–867.
- Siebenaller, J. F., 1978. Genetic variation in deep-sea invertebrate populations: The bathyal gastropod *Bathybembix bairdii*. *Marine Biology* 47: 265–275.

- Stamatis, C., A. Triantafyllidis, K. A. Moutou & Z. Mamuris, 2004. Mitochondrial DNA variation in Northeast Atlantic and Mediterranean populations of Norway lobster, *Nephrops norvegicus*. *Molecular Ecology* 13: 1377–1390.
- Taberlet, P., 1998. Biodiversity at the intraspecific level: The comparative phylogeographic approach. *Journal of Biotechnology* 64: 91–100.
- Taberlet, P., L. Fumagalli, A.-G. Wust-Saucy & J.-F. Cossons, 1998. Comparative phylogeography and postglacial colonization. *Molecular Ecology* 7: 453–464.
- Tajima, F., 1983. Evolutionary relationship of DNA sequences in finite populations. *Genetics* 105: 437–460.
- Taylor, M. L. & C. N. Roterman, 2017. Invertebrate population genetics across Earth's largest habitat: The deep-sea floor. *Molecular Ecology* 26: 4872–4896.
- Thatje, S., C.-D. Hillenbrand & R. Larter, 2005. On the origin of Antarctic marine benthic community structure. *Trends in Ecology & Evolution* 20: 534–540.
- Trewick, S. A. & G. P. Wallis, 2001. Bridging the “beech-gap”: New Zealand invertebrate phylogeography implicates Pleistocene glaciation and Pliocene isolation. *Evolution* 55: 2170–2180.
- Vanreusel, A., G. Fonseca, R. Danovaro, M. C. Da Silva, A. M. Esteves, T. Ferrero, G. Gad, V. Galtsova, C. Gambi, V. Da Fonsêca Genevois, J. Ingels, B. Ingole, N. Lampadariou, B. Merckx, D. Miljutin, M. Miljutina, M. Raes, A. Tchesunov, J. Vanaverbeke, S. Van Gaeve, V. Venekey, T. N. Bezerra, H. Flint, J. Copley, E. Pape, D. Zeppilli, P. A. Martinez & J. Galeron, 2010. The contribution of deep-sea macrohabitat heterogeneity to global nematode diversity. *Marine Ecology* 31: 6–20.
- Venables, W. N. & B. D. Ripley, 2002. *Modern Applied Statistics with S (Fourth)*. New York: Springer.
- Wilson, G. D. F., 1983. Variation in the deep-sea isopod *Eurycope iphthima* (Asellota, Eurycopidae): depth related clines in rostral morphology and in population. *Journal of Crustacean Biology* 3: 127–140.
- Zardus, J. D., R. J. Etter, M. R. Chase, M. A. Rex & E. E. Boyle, 2006. Bathymetric and geographic population structure in the pan-Atlantic deep-sea bivalve *Deminucula atacellana* (Schenck, 1939). *Molecular Ecology* 15: 639–651.

Zemlak, T. S., E. M. Habit, S. J. Walde, M. A. Battini, E. D. M. Adams & D. E. Ruzzante, 2008. Across the southern Andes on fin: glacial refugia, drainage reversals and a secondary contact zone revealed by the phylogeographical signal of *Galaxias platei* in Patagonia. *Molecular Ecology* 17: 5049–5061.

Tables

Table 1. Custom-made, sample-specific barcoded adapters used in the study. The first column lists the two individual specimens associated with each barcode, differentiated by Illumina i7 internal index. Both strands of each adapter are given (1.1 and 1.2) in the 5' to 3' direction. These strands are annealed prior to ligation to the ddRADseq fragments. The barcode section of the adapter is underlined.

<i>Individuals associated with barcode and (i7)</i>	<i>Adapter</i>	<i>Strand</i>	<i>Sequence (5' to 3')</i>
<i>HBG2483 (Idx37)</i>	<i>adapt1</i>	1.1	ACACTCTTTCCCTACACGACGCTCTTCCGATCT <u>CCAGAGTGCATG</u>
<i>HBG2616 (Idx42)</i>		1.2	<u>ACACTCTGGAGATCGGAAGAGCGTCGTGTAGGGAAAGAGTGT</u>
<i>HBG2517 (Idx37)</i>	<i>adapt2</i>	1.1	ACACTCTTTCCCTACACGACGCTCTTCCGATCT <u>TGAGCGACTCATG</u>
<i>HBG2618 (Idx42)</i>		1.2	<u>AGTCGCTCAAGATCGGAAGAGCGTCGTGTAGGGAAAGAGTGT</u>
<i>HBG2536 (Idx37)</i>	<i>adapt3</i>	1.1	ACACTCTTTCCCTACACGACGCTCTTCCGATCT <u>TGGTCTCTGCATG</u>
<i>HBG2619 (Idx42)</i>		1.2	<u>CAGAGACCAAGATCGGAAGAGCGTCGTGTAGGGAAAGAGTGT</u>
<i>HBG2555 (Idx37)</i>	<i>adapt4</i>	1.1	ACACTCTTTCCCTACACGACGCTCTTCCGATCT <u>GTAATCCAGCATG</u>
<i>HBG2637 (Idx42)</i>		1.2	<u>CTGGATTACAGATCGGAAGAGCGTCGTGTAGGGAAAGAGTGT</u>
<i>HBG2569 (Idx37)</i>	<i>adapt5</i>	1.1	ACACTCTTTCCCTACACGACGCTCTTCCGATCT <u>GAATGCGTCCATG</u>
<i>HBG2655 (Idx42)</i>		1.2	<u>GACGCATTCAGATCGGAAGAGCGTCGTGTAGGGAAAGAGTGT</u>
<i>HBG2588 (Idx37)</i>	<i>adapt6</i>	1.1	ACACTCTTTCCCTACACGACGCTCTTCCGATCT <u>ATCAGTGACCATG</u>
<i>HBG2664 (Idx42)</i>		1.2	<u>GTCACTGATAGATCGGAAGAGCGTCGTGTAGGGAAAGAGTGT</u>
<i>HBG2590 (Idx37)</i>	<i>adapt7</i>	1.1	ACACTCTTTCCCTACACGACGCTCTTCCGATCT <u>CACCGACTACATG</u>
<i>HBG2679 (Idx42)</i>		1.2	<u>TAGTCGGTGAGATCGGAAGAGCGTCGTGTAGGGAAAGAGTGT</u>
<i>HBG2604 (Idx37)</i>	<i>adapt8</i>	1.1	ACACTCTTTCCCTACACGACGCTCTTCCGATCT <u>GACGCGTGACATG</u>
<i>HBG2693 (Idx42)</i>		1.2	<u>TCACGCGTCAGATCGGAAGAGCGTCGTGTAGGGAAAGAGTGT</u>

Table 2. Sampling effort for each data type and region. The number of individuals (N), number of single nucleotide polymorphisms (SNPs), and haplotypes are given for De Soto Canyon (DC) and the regions lying east and west of the canyon (eDC and wDC, respectively).

	Concatenated Sanger				ddRADseq			
	eDC	DC	wDC	All	eDC	DC	wDC	All
N	62	58	27	147	5	3	2	10
SNPs	52	47	32	75	1891	570	588	2681
Haplotypes	44	35	18	78	5	3	2	10

Table 3. Results of the hierarchical AMOVAs conducted to characterize genetic variation among individuals ($F_{IT} = 98.5\%$), among individuals within populations ($F_{IS} = 0\%$), and among populations ($F_{ST} = 1.5\%$). The Infinite Allele Model was used with 999 permutations to assess statistical significance. Any missing data was replaced with randomly drawn alleles determined by the overall allele frequencies of the data set. The Concatenated Sanger AMOVA yielded statistically significant results ($p = 0.048$). AMOVA results indicate the vast majority of variance is due to differences between individuals (F_{IT}), regardless of the region from which they were sampled. * indicates p -value < 0.05 .

	F_{ST}	F_{IS}	F_{IT}
Concatenated Sanger*	1.5%	0.0%	98.5%
ddRADseq*	1.5%	0.0%	98.5%

Table 4. Inter-population genetic distances between the De Soto Canyon (DC), and the regions lying east and west of the canyon (eDC and wDC, respectively) are reported below the diagonal. *P*-values are reported above the diagonal.

	Concatenated Sanger			ddRADseq		
	eDC	DC	wDC	eDC	DC	wDC
eDC	---	0.459	0.394	---	0.257	1.000
DC	-0.003	---	0.457	0.068	---	0.208
wDC	-0.001	-0.001	---	0.000	0.143	---

Table 5. Diversity metrics, nucleotide diversity (π) and haplotype diversity (h), and Tajima's D and significance value for each population in each dataset. * indicates p -values <0.05 ; ** indicates p -values < 0.01 ($D_{sim} < D_{obs}$, 1000 simulations). Diversity values from previous studies of molecular diversity in marine invertebrates, specifically bivalves, are also reported. For these previous studies, the sample size (N) is given in place of "region".

	Concatenated Sanger				ddRADseq				Etter et al., 2005	Zardus et al., 2006
	eDC	DC	wDC	All	eDC	DC	wDC	All	N = 268	N = 130
π	0.003	0.003	0.003	0.003	0.261	0.171	0.262	0.234	0.0029-0.0175	0.0217
h	0.942	0.880	0.929	0.901					0.277-0.783	0.731
D	-2.122*	-1.976*	-1.585	-2.210**						

Table 6. Models tested in MIGRATE-N and their associated thermodynamically integrated log marginal likelihood (lmL). Results presented here are from the 20,000-step runs analyzing the Sanger data set. Populations are put in parentheses and the symbols between them indicate the direction of migration (<, >, or <>) or its absence (x). The direction listed before (wDC) indicates direction between eDC and wDC. When two populations are listed within the same set of parentheses, e.g. (wDC+DC), it means that individuals collected from these two regions are treated as a single population. Models are listed in order of decreasing lmL.

Model	Description	lmL
8	<> (wDC) <> (DC) <> (eDC)	-3163.25
6	> (wDC) x (DC) < (eDC)	-3168.97
7	x (wDC) <> (DC) <> (eDC)	-3171.19
5	x (wDC) < (DC) > (eDC)	-3178.6
16	(wDC+eDC) > (DC)	-3709.45
15	(wDC+eDC) < (DC)	-3709.88
13	(wDC) > (DC+eDC)	-3711.17
9	(wDC+DC) < (eDC)	-3713.53
12	(wDC) < (DC+eDC)	-3715.95
4	< (wDC) > (DC) x (eDC)	-3721.9
14	(wDC) <> (DC+eDC)	-3726.54
10	(wDC+DC) > (eDC)	-3726.97
3	x (wDC) < (DC) < (eDC)	-3727.37
17	(wDC+eDC) <> (DC)	-3732.62
2	x (wDC) > (DC) > (eDC)	-3733.77
11	(wDC+DC) <> (eDC)	-3735.55
18	(wDC+DC+eDC) panmictic	-3739.52
1	x (wDC) x (DC) x (eDC)	-4157.71

Figure Captions

Figure 1. A bathymetric map of sampling sites. Warmer colors denote shallower depths. Collection sites are marked with white points and circles indicate grouping of collection sites across three geographic areas: western De Soto, De Soto Canyon, and eastern De Soto. This map was derived from the “Bathymetry of the Gulf of Mexico and Adjacent Areas of the Caribbean Sea and Atlantic Ocean in Shaded Relief” figure within the International Bathymetric Chart of the Caribbean Sea and Gulf of Mexico (IBCCA) map set, under the National Oceanic and Atmospheric Administration’s National Geophysical Data Center (NOAA NGDC).

Figure 2. Multi-dimensional scaling plots as heat maps built from MAFFT-aligned concatenated Sanger data (left); as well as the plot rendered from 2380 SNPs identified with ddRADseq (right). In the heat maps, higher density of individuals is denoted with warmer colors. In both plots, individuals are clustered based on genetic distance. Note the difference in scale between plots. Across plots, we do not see evidence of genetic differentiation.

Figure 3. Percent of shared haplotypes (found across regions) and endemic haplotypes (number of unique endemic haplotypes/total number of haplotypes) found within the study area, from analysis of the concatenated Sanger data set, are presented in the bar chart on the left. Note that East De Soto Canyon contains the highest percent of endemic haplotypes across loci.

Shared haplotypes are further divided in the pie chart to the right. The 13 shared haplotypes found in the data are expressed as percentages shared between: all regions (wDC-DC-eDC = 6), West De Soto Canyon and De Soto Canyon (wDC-DC = 0), De Soto Canyon and East De Soto Canyon (DC-eDC = 6), and West De Soto Canyon and East De Soto Canyon (wDC-eDC = 1).

Figure 4. On the left are Tajima's D values for each species following analysis of the concatenated Sanger data set. * indicates $p < 0.05$. ** indicates $p < 0.01$. All values indicate population growth and, with the exception of wDC, all are statistically significant. To the right of the Tajima's D graph are four Extended Bayesian Skyline Plots (EBSPs) generated in BEAST. Top to bottom: West De Soto Canyon + De Soto Canyon + East De Soto Canyon, West De Soto Canyon, De Soto Canyon, and East De Soto Canyon. The horizontal axis describes time (in thousands of years) and the vertical axis measures population size. In these visual representations of the EBSP posterior samples for each analysis: the solid lines define the 95% central posterior density (CPD) and the dotted line traces the median value over time. Note that all regions experienced population growth, individually and overall (in agreement with the Tajima's D values). Population growth was most dramatic in the analysis of all samples (ALL, top), which was expected. By region, population growth was fastest in the east (EDC, bottom) and slowest in the west (WDC, second from the top).

Figures

Figure 1

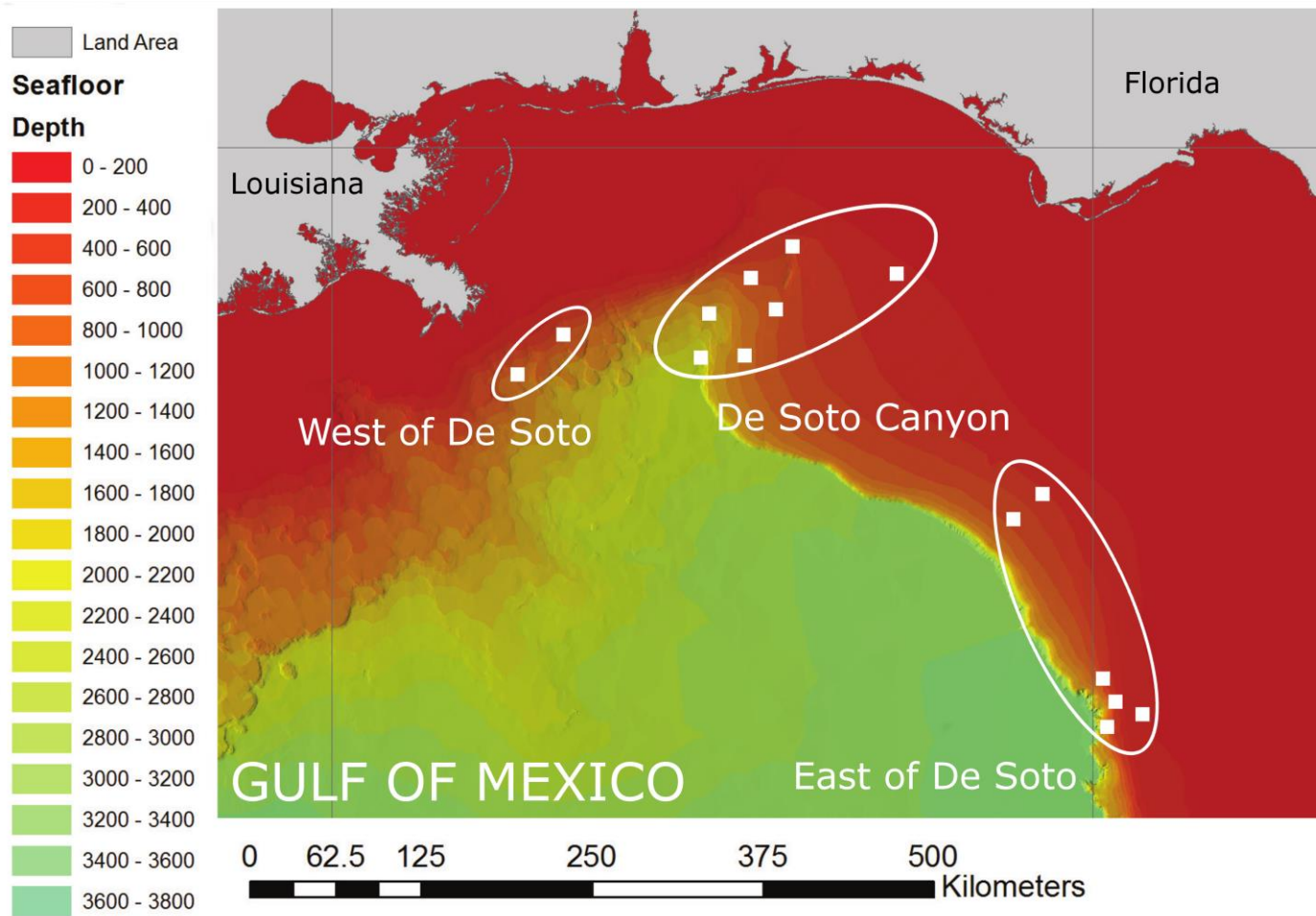


Figure 2

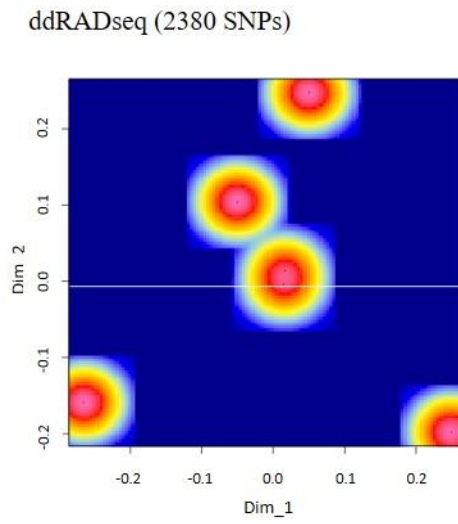
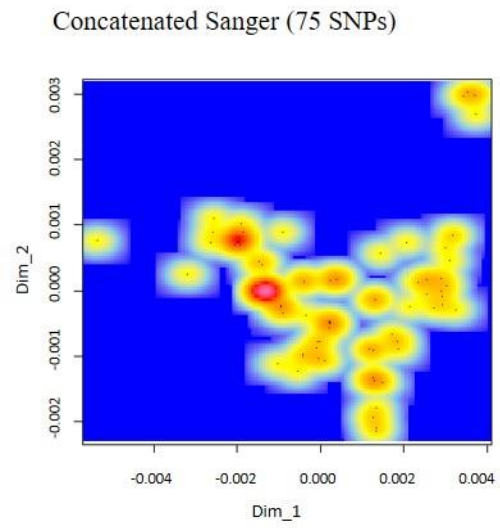


Figure 3

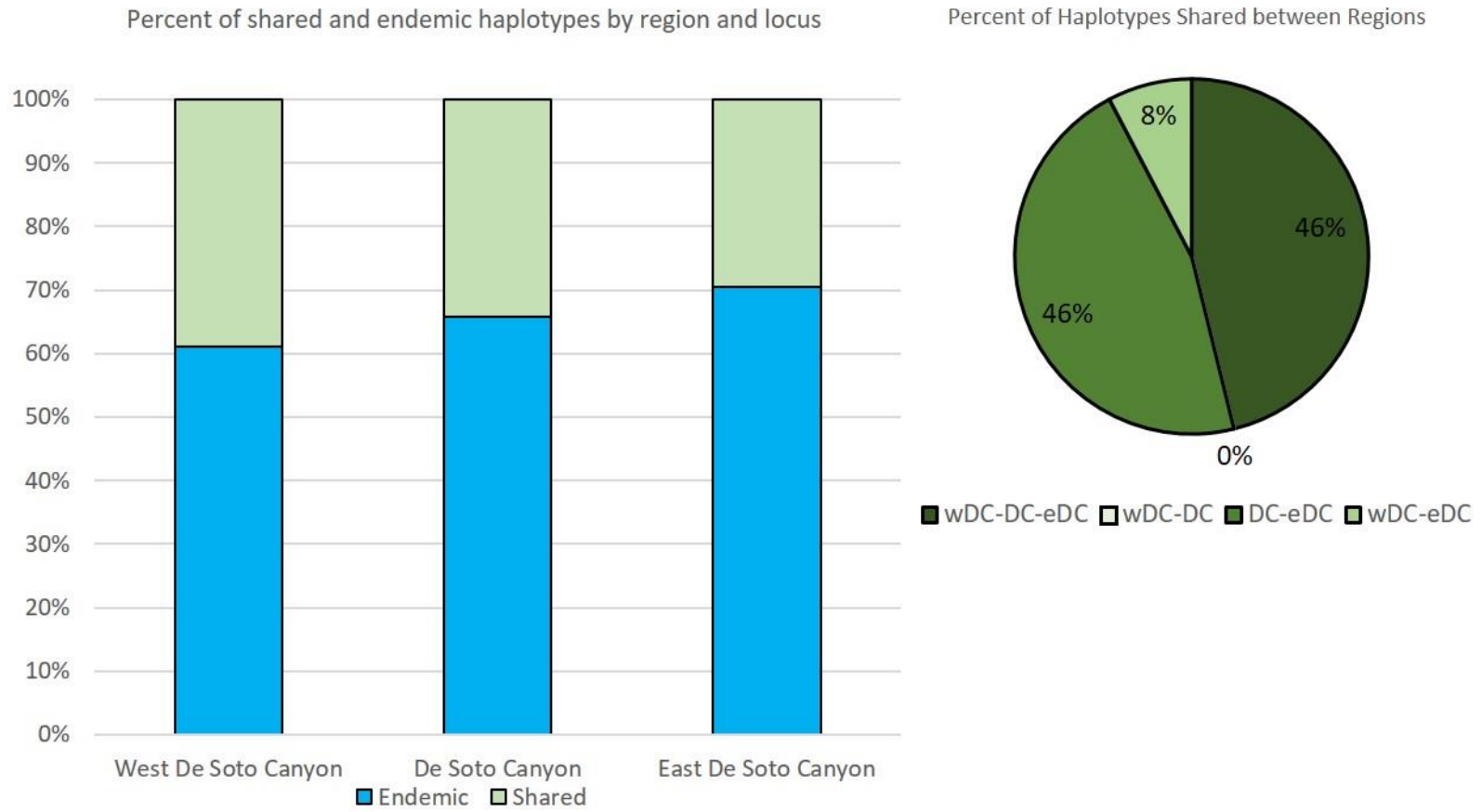
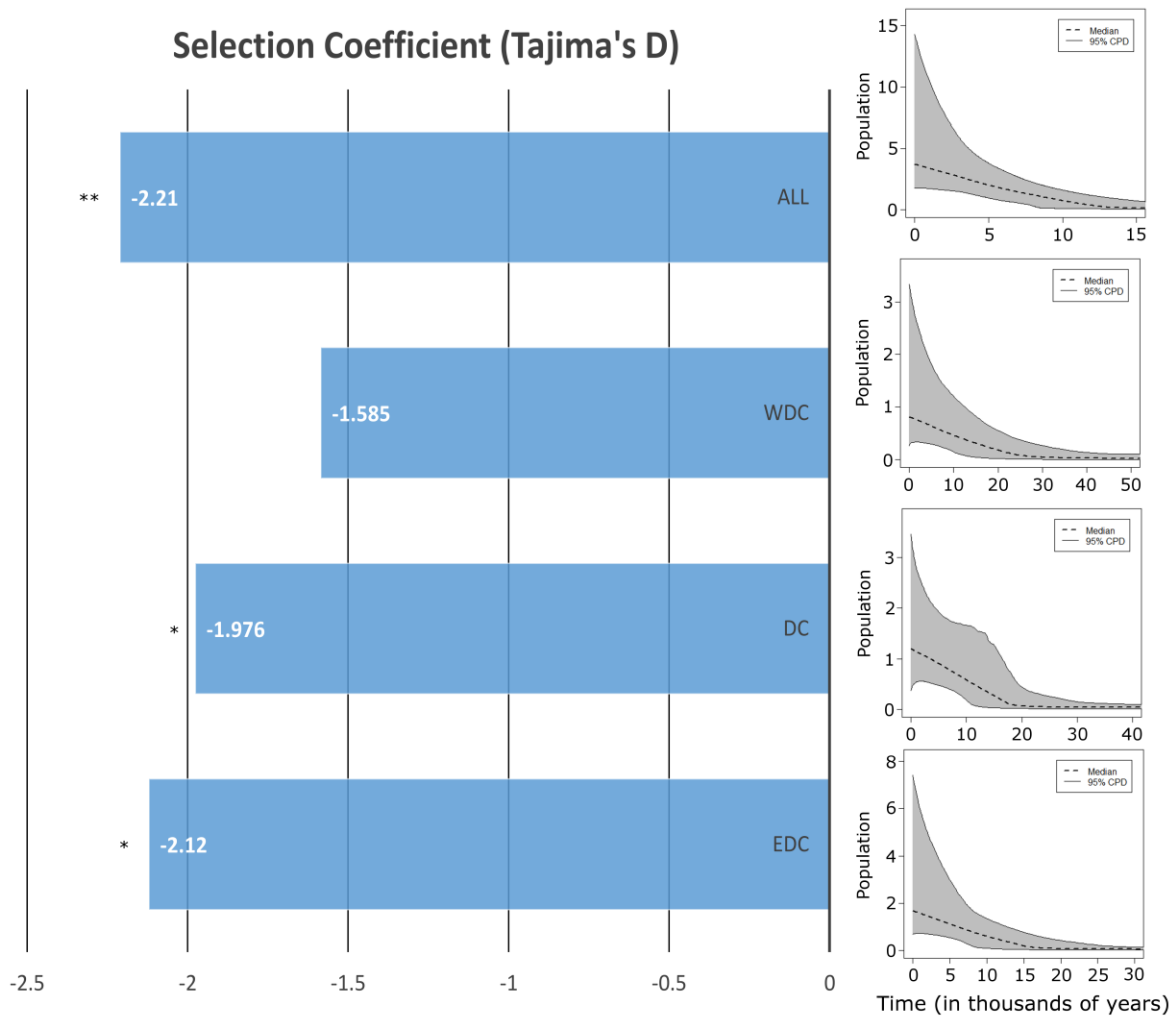


Figure 4



Appendices Captions

Appendix 1. All samples included in the study, including: HBG number, GenBank accession numbers for each de novo sequence, and collection data such as date, site location, assigned region, and site coordinates. Samples targeted for ddRADseq are indicated in **bold**.

Appendices

Appendix 1

HBG #	Species	Date	Region	Location	Site	Latitude	Longitude	12S Accession	16S Accession	COI Accession
HBG2482	<i>B. giganteus</i>	4-Apr-2012	DC	East wall of De Soto Canyon	DA3_12-025	29.139°N	-87.008°W	---	MG229272	MG229480
HBG2483	<i>B. giganteus</i>	10-Apr-2011	eDC	NW Florida Slope	MFSA1_11-015	27.911°N	-85.540°W	MG229070	MG229273	MG229481
HBG2486	<i>B. giganteus</i>	5-Apr-2012	DC	East wall of De Soto Canyon	DB5_12-020	29.308°N	-86.678°W	MG229071	MG229274	MG229482
HBG2492	<i>B. giganteus</i>	2-Apr-2012	eDC	West Florida Slope	WFSE3_12-014	26.923°N	-84.922°W	MG229072	MG229272	MG229483
HBG2497	<i>B. giganteus</i>	2-Apr-2012	eDC	West Florida Slope	WFSE3_12-014	26.923°N	-84.922°W	MG229073	---	MG229484
HBG2498	<i>B. giganteus</i>	2-Apr-2012	eDC	West Florida Slope	WFSE3_12-014	26.923°N	-84.922°W	MG229074	MG229279	MG229485
HBG2499	<i>B. giganteus</i>	2-Apr-2012	eDC	West Florida Slope	WFSE3_12-014	26.923°N	-84.922°W	MG229075	MG229280	---
HBG2500	<i>B. giganteus</i>	2-Apr-2012	eDC	West Florida Slope	WFSE3_12-014	26.923°N	-84.922°W	MG229076	MG229281	MG229486
HBG2501	<i>B. giganteus</i>	2-Apr-2012	eDC	West Florida Slope	WFSE3_12-014	26.923°N	-84.922°W	MG229077	MG229282	MG229487
HBG2502	<i>B. giganteus</i>	2-Apr-2012	eDC	West Florida Slope	WFSE3_12-014	26.923°N	-84.922°W	MG229078	MG229283	MG229488
HBG2503	<i>B. giganteus</i>	2-Apr-2012	eDC	West Florida Slope	WFSE3_12-014	26.923°N	-84.922°W	MG229079	MG229284	MG229489
HBG2504	<i>B. giganteus</i>	2-Apr-2012	eDC	West Florida Slope	WFSE3_12-014	26.923°N	-84.922°W	MG229080	MG229285	MG229490
HBG2505	<i>B. giganteus</i>	4-Apr-2012	DC	East wall of De Soto Canyon	DA3_12-025	29.139°N	-87.008°W	MG229081	MG229286	MG229491
HBG2506	<i>B. giganteus</i>	4-Apr-2012	DC	East wall of De Soto Canyon	DA3_12-025	29.139°N	-87.008°W	MG229082	MG229287	MG229492
HBG2507	<i>B. giganteus</i>	4-Apr-2012	DC	East wall of De Soto Canyon	DA3_12-025	29.139°N	-87.008°W	MG229083	MG229288	---
HBG2508	<i>B. giganteus</i>	4-Apr-2012	DC	East wall of De Soto Canyon	DA3_12-025	29.139°N	-87.008°W	MG229084	MG229289	---
HBG2509	<i>B. giganteus</i>	4-Apr-2012	DC	East wall of De Soto Canyon	DA3_12-025	29.139°N	-87.008°W	MG229085	MG229290	MG229493
HBG2510	<i>B. giganteus</i>	4-Apr-2012	DC	East wall of De Soto Canyon	DA3_12-025	29.139°N	-87.008°W	MG229086	MG229291	MG229494
HBG2511	<i>B. giganteus</i>	4-Apr-2012	DC	East wall of De Soto Canyon	DA3_12-025	29.139°N	-87.008°W	MG229087	MG229292	MG229495
HBG2512	<i>B. giganteus</i>	4-Apr-2012	DC	East wall of De Soto Canyon	DA3_12-025	29.139°N	-87.008°W	MG229088	MG229293	MG229496
HBG2513	<i>B. giganteus</i>	4-Apr-2012	DC	East wall of De Soto Canyon	DA3_12-025	29.139°N	-87.008°W	MG229089	MG229294	MG229497
HBG2514	<i>B. giganteus</i>	4-Apr-2012	DC	East wall of De Soto Canyon	DA3_12-025	29.139°N	-87.008°W	MG229090	MG229295	MG229498
HBG2515	<i>B. giganteus</i>	4-Apr-2012	DC	East wall of De Soto Canyon	DA3_12-025	29.139°N	-87.008°W	MG229091	MG229296	MG229499

HBG2516	<i>B. giganteus</i>	4-Apr-2012	DC	East wall of De Soto Canyon	DA3_12-025	29.139°N	-87.008°W	MG229092	MG229297	MG229500
HBG2517	<i>B. giganteus</i>	4-Apr-2012	DC	East wall of De Soto Canyon	DA3_12-025	29.139°N	-87.008°W	MG229093	MG229298	MG229501
HBG2518	<i>B. giganteus</i>	4-Apr-2012	DC	East wall of De Soto Canyon	DA3_12-025	29.139°N	-87.008°W	MG229094	MG229299	MG229502
HBG2519	<i>B. giganteus</i>	4-Apr-2012	DC	East wall of De Soto Canyon	DA3_12-025	29.139°N	-87.008°W	MG229095	MG229300	MG229503
HBG2520	<i>B. giganteus</i>	4-Apr-2012	DC	East wall of De Soto Canyon	DA3_12-025	29.139°N	-87.008°W	MG229096	MG229301	MG229504
HBG2521	<i>B. giganteus</i>	4-Apr-2012	DC	East wall of De Soto Canyon	DA3_12-025	29.139°N	-87.008°W	MG229097	MG229302	MG229505
HBG2522	<i>B. giganteus</i>	4-Apr-2012	DC	East wall of De Soto Canyon	DA3_12-025	29.139°N	-87.008°W	MG229098	MG229303	MG229506
HBG2523	<i>B. giganteus</i>	4-Apr-2012	DC	East wall of De Soto Canyon	DA3_12-025	29.139°N	-87.008°W	MG229099	MG229304	MG229507
HBG2524	<i>B. giganteus</i>	4-Apr-2012	DC	East wall of De Soto Canyon	DA3_12-025	29.139°N	-87.008°W	MG229100	MG229305	MG229508
HBG2525	<i>B. giganteus</i>	6-Apr-2012	DC	De Soto Canyon Groove	DC3_12-036	29.454°N	-86.895°W	MG229101	MG229306	MG229509
HBG2526	<i>B. giganteus</i>	6-Apr-2012	DC	De Soto Canyon Groove	DC3_12-036	29.454°N	-86.895°W	MG229102	MG229307	MG229510
HBG2527	<i>B. giganteus</i>	6-Apr-2012	DC	De Soto Canyon Groove	DC3_12-036	29.454°N	-86.895°W	MG229103	MG229308	MG229511
HBG2528	<i>B. giganteus</i>	6-Apr-2012	DC	De Soto Canyon Groove	DC3_12-036	29.454°N	-86.895°W	MG229104	MG229309	MG229512
HBG2529	<i>B. giganteus</i>	10-Apr-2012	DC	East wall of De Soto Canyon	DF2_12-038	29.029°N	-87.295°W	MG229105	MG229310	MG229513
HBG2530	<i>B. giganteus</i>	6-Apr-2012	DC	West wall of De Soto Canyon	DD3_12-033	29.492°N	-87.109°W	MG229106	MG229311	MG229514
HBG2531	<i>B. giganteus</i>	6-Apr-2012	DC	West wall of De Soto Canyon	DD3_12-033	29.492°N	-87.109°W	MG229107	MG229312	MG229515
HBG2532	<i>B. giganteus</i>	6-Apr-2012	DC	West wall of De Soto Canyon	DD3_12-033	29.492°N	-87.109°W	MG229108	MG229313	MG229516
HBG2533	<i>B. giganteus</i>	6-Apr-2012	DC	West wall of De Soto Canyon	DD3_12-033	29.492°N	-87.109°W	MG229109	MG229314	MG229517
HBG2534	<i>B. giganteus</i>	4-Apr-2012	DC	East wall of De Soto Canyon	DA1_12-024	29.143°N	-86.808°W	MG229110	MG229315	---
HBG2535	<i>B. giganteus</i>	4-Apr-2012	DC	East wall of De Soto Canyon	DA1_12-024	29.143°N	-86.808°W	MG229111	MG229316	MG229518
HBG2536	<i>B. giganteus</i>	4-Apr-2012	DC	East wall of De Soto Canyon	DA1_12-024	29.143°N	-86.808°W	MG229112	MG229317	---
HBG2537	<i>B. giganteus</i>	6-Apr-2012	DC	De Soto Canyon Groove	DC1_12-035	29.449°N	-87.951°W	---	MG229318	MG229519
HBG2538	<i>B. giganteus</i>	6-Apr-2012	DC	De Soto Canyon Groove	DC1_12-035	29.449°N	-87.951°W	MG229113	MG229319	MG229520
HBG2539	<i>B. giganteus</i>	6-Apr-2012	DC	De Soto Canyon Groove	DC1_12-035	29.449°N	-87.951°W	MG229114	MG229320	MG229521
HBG2540	<i>B. giganteus</i>	6-Apr-2012	DC	De Soto Canyon Groove	DC1_12-035	29.449°N	-87.951°W	MG229115	MG229321	MG229522
HBG2541	<i>B. giganteus</i>	6-Apr-2012	DC	De Soto Canyon Groove	DC1_12-035	29.449°N	-87.951°W	MG229116	MG229322	---
HBG2542	<i>B. giganteus</i>	6-Apr-2012	DC	De Soto Canyon Groove	DC1_12-035	29.449°N	-87.951°W	MG229117	MG229323	MG229523
HBG2543	<i>B. giganteus</i>	6-Apr-2012	DC	De Soto Canyon Groove	DC1_12-035	29.449°N	-87.951°W	MG229118	MG229324	MG229524

HBG2544	<i>B. giganteus</i>	6-Apr-2012	DC	De Soto Canyon Groove	DC1_12-035	29.449°N	-87.951°W	MG229119	MG229325	MG229525
HBG2545	<i>B. giganteus</i>	6-Apr-2012	DC	De Soto Canyon Groove	DC1_12-035	29.449°N	-87.951°W	MG229120	MG229326	MG229526
HBG2546	<i>B. giganteus</i>	5-Apr-2012	DC	West wall of De Soto Canyon	DE5_12-029	29.189°N	-87.403°W	---	MG229327	MG229527
HBG2547	<i>B. giganteus</i>	5-Apr-2012	DC	West wall of De Soto Canyon	DE3_12-030	29.301°N	-87.330°W	MG229121	MG229328	MG229528
HBG2548	<i>B. giganteus</i>	5-Apr-2012	DC	West wall of De Soto Canyon	DE3_12-030	29.301°N	-87.330°W	MG229122	MG229329	---
HBG2549	<i>B. giganteus</i>	5-Apr-2012	DC	West wall of De Soto Canyon	DE3_12-030	29.301°N	-87.330°W	MG229123	MG229330	---
HBG2550	<i>B. giganteus</i>	5-Apr-2012	DC	West wall of De Soto Canyon	DE3_12-030	29.301°N	-87.330°W	MG229124	MG229331	---
HBG2551	<i>B. giganteus</i>	5-Apr-2012	DC	West wall of De Soto Canyon	DE3_12-030	29.301°N	-87.330°W	MG229125	MG229332	---
HBG2552	<i>B. giganteus</i>	5-Apr-2012	DC	West wall of De Soto Canyon	DE3_12-030	29.301°N	-87.330°W	MG229126	MG229333	---
HBG2553	<i>B. giganteus</i>	5-Apr-2012	DC	West wall of De Soto Canyon	DE3_12-030	29.301°N	-87.330°W	MG229127	MG229334	---
HBG2554	<i>B. giganteus</i>	5-Apr-2012	DC	West wall of De Soto Canyon	DE3_12-030	29.301°N	-87.330°W	MG229128	MG229335	---
HBG2555	<i>B. giganteus</i>	5-Apr-2012	DC	West wall of De Soto Canyon	DE3_12-030	29.301°N	-87.330°W	MG229129	MG229336	---
HBG2556	<i>B. giganteus</i>	5-Apr-2012	DC	West wall of De Soto Canyon	DE3_12-030	29.301°N	-87.330°W	MG229130	MG229337	---
HBG2557	<i>B. giganteus</i>	5-Apr-2012	DC	West wall of De Soto Canyon	DE3_12-030	29.301°N	-87.330°W	MG229131	MG229338	---
HBG2558	<i>B. giganteus</i>	5-Apr-2012	DC	West wall of De Soto Canyon	DE3_12-030	29.301°N	-87.330°W	MG229132	MG229339	---
HBG2559	<i>B. giganteus</i>	5-Apr-2012	DC	West wall of De Soto Canyon	DE3_12-030	29.301°N	-87.330°W	MG229133	MG229340	---
HBG2560	<i>B. giganteus</i>	5-Apr-2012	DC	West wall of De Soto Canyon	DE3_12-030	29.301°N	-87.330°W	MG229134	MG229341	---
HBG2561	<i>B. giganteus</i>	5-Apr-2012	DC	West wall of De Soto Canyon	DE3_12-030	29.301°N	-87.330°W	MG229135	MG229342	MG229529
HBG2562	<i>B. giganteus</i>	5-Apr-2012	DC	West wall of De Soto Canyon	DE3_12-030	29.301°N	-87.330°W	MG229136	MG229343	---
HBG2563	<i>B. giganteus</i>	5-Apr-2012	DC	West wall of De Soto Canyon	DE3_12-030	29.301°N	-87.330°W	MG229137	MG229344	---
HBG2564	<i>B. giganteus</i>	5-Apr-2012	DC	West wall of De Soto Canyon	DE3_12-030	29.301°N	-87.330°W	MG229138	MG229345	---
HBG2565	<i>B. giganteus</i>	5-Apr-2012	DC	West wall of De Soto Canyon	DE3_12-030	29.301°N	-87.330°W	MG229139	MG229346	---
HBG2566	<i>B. giganteus</i>	5-Apr-2012	DC	West wall of De Soto Canyon	DE3_12-030	29.301°N	-87.330°W	MG229140	MG229347	---
HBG2567	<i>B. giganteus</i>	5-Apr-2012	DC	West wall of De Soto Canyon	DE3_12-030	29.301°N	-87.330°W	MG229141	MG229348	---
HBG2568	<i>B. giganteus</i>	5-Apr-2012	DC	East wall of De Soto Canyon	DA5_12-026	29.162°N	-87.124°W	MG229142	MG229349	MG229530
HBG2569	<i>B. giganteus</i>	5-Apr-2012	DC	East wall of De Soto Canyon	DA5_12-026	29.162°N	-87.124°W	MG229143	MG229350	MG229531
HBG2570	<i>B. giganteus</i>	13-Apr-2012	wDC	Western Desoto	WDC1_12-053	28.750°N	-88.593°W	MG229144	MG229279	MG229532
HBG2571	<i>B. giganteus</i>	13-Apr-2012	wDC	Western Desoto	WDC2_12-054	28.750°N	-88.593°W	MG229145	---	MG229533

HBG2572	<i>B. giganteus</i>	12-Apr-2012	wDC	Western Desoto	WDA3_12-052	28.824°N	-88.840°W	MG229146	MG229351	MG229534
HBG2573	<i>B. giganteus</i>	12-Apr-2012	wDC	Western Desoto	WDA3_12-052	28.824°N	-88.840°W	MG229147	MG229352	---
HBG2574	<i>B. giganteus</i>	12-Apr-2012	wDC	Western Desoto	WDA3_12-052	28.824°N	-88.840°W	MG229148	MG229353	---
HBG2575	<i>B. giganteus</i>	12-Apr-2012	wDC	Western Desoto	WDA3_12-052	28.824°N	-88.840°W	MG229149	MG229354	---
HBG2576	<i>B. giganteus</i>	12-Apr-2012	wDC	Western Desoto	WDA3_12-052	28.824°N	-88.840°W	MG229150	MG229355	---
HBG2577	<i>B. giganteus</i>	12-Apr-2012	wDC	Western Desoto	WDA3_12-052	28.824°N	-88.840°W	MG229151	MG229356	---
HBG2578	<i>B. giganteus</i>	12-Apr-2012	wDC	Western Desoto	WDA3_12-052	28.824°N	-88.840°W	MG229152	MG229357	---
HBG2579	<i>B. giganteus</i>	12-Apr-2012	wDC	Western Desoto	WDA3_12-052	28.824°N	-88.840°W	MG229153	MG229358	---
HBG2580	<i>B. giganteus</i>	12-Apr-2012	wDC	Western Desoto	WDA3_12-052	28.824°N	-88.840°W	MG229154	MG229359	---
HBG2581	<i>B. giganteus</i>	12-Apr-2012	wDC	Western Desoto	WDA3_12-052	28.824°N	-88.840°W	MG229155	MG229360	---
HBG2582	<i>B. giganteus</i>	12-Apr-2012	wDC	Western Desoto	WDA3_12-052	28.824°N	-88.840°W	MG229156	MG229361	---
HBG2583	<i>B. giganteus</i>	12-Apr-2012	wDC	Western Desoto	WDA3_12-052	28.824°N	-88.840°W	MG229157	MG229362	---
HBG2584	<i>B. giganteus</i>	12-Apr-2012	wDC	Western Desoto	WDA3_12-052	28.824°N	-88.840°W	MG229158	MG229363	---
HBG2585	<i>B. giganteus</i>	12-Apr-2012	wDC	Western Desoto	WDA3_12-052	28.824°N	-88.840°W	MG229159	MG229364	---
HBG2586	<i>B. giganteus</i>	12-Apr-2012	wDC	Western Desoto	WDA3_12-052	28.824°N	-88.840°W	MG229160	MG229365	---
HBG2587	<i>B. giganteus</i>	12-Apr-2012	wDC	Western Desoto	WDA3_12-052	28.824°N	-88.840°W	MG229161	MG229366	---
HBG2588	<i>B. giganteus</i>	12-Apr-2012	wDC	Western Desoto	WDA3_12-052	28.824°N	-88.840°W	MG229162	MG229367	---
HBG2589	<i>B. giganteus</i>	12-Apr-2012	wDC	Western Desoto	WDA3_12-052	28.824°N	-88.840°W	MG229163	MG229368	MG229535
HBG2590	<i>B. giganteus</i>	12-Apr-2012	wDC	Western Desoto	WDA3_12-052	28.824°N	-88.840°W	MG229164	MG229369	MG229536
HBG2591	<i>B. giganteus</i>	12-Apr-2012	wDC	Western Desoto	WDB3_12-047	28.924°N	-88.516°W	MG229165	MG229370	---
HBG2592	<i>B. giganteus</i>	12-Apr-2012	wDC	Western Desoto	WDB3_12-047	28.924°N	-88.516°W	MG229166	MG229371	---
HBG2593	<i>B. giganteus</i>	12-Apr-2012	wDC	Western Desoto	WDB3_12-047	28.924°N	-88.516°W	MG229167	MG229372	---
HBG2594	<i>B. giganteus</i>	12-Apr-2012	wDC	Western Desoto	WDB3_12-047	28.924°N	-88.516°W	MG229168	MG229373	---
HBG2595	<i>B. giganteus</i>	12-Apr-2012	wDC	Western Desoto	WDB3_12-047	28.924°N	-88.516°W	MG229169	MG229374	MG229537
HBG2596	<i>B. giganteus</i>	12-Apr-2012	wDC	Western Desoto	WDB3_12-047	28.924°N	-88.516°W	MG229170	MG229375	MG229538
HBG2597	<i>B. giganteus</i>	12-Apr-2012	wDC	Western Desoto	WDB3_12-047	28.924°N	-88.516°W	MG229171	MG229376	MG229539
HBG2598	<i>B. giganteus</i>	12-Apr-2012	wDC	Western Desoto	WDB3_12-047	28.924°N	-88.516°W	MG229172	MG229377	MG229540
HBG2599	<i>B. giganteus</i>	12-Apr-2012	wDC	Western Desoto	WDB3_12-047	28.924°N	-88.516°W	MG229173	MG229378	MG229541

HBG2600	<i>B. giganteus</i>	12-Apr-2012	wDC	Western Desoto	WDB3_12-047	28.924°N	-88.516°W	MG229174	MG229379	MG229542
HBG2601	<i>B. giganteus</i>	12-Apr-2012	wDC	Western Desoto	WDB3_12-047	28.924°N	-88.516°W	MG229175	MG229380	MG229543
HBG2602	<i>B. giganteus</i>	12-Apr-2012	wDC	Western Desoto	WDB3_12-047	28.924°N	-88.516°W	MG229176	MG229381	MG229544
HBG2603	<i>B. giganteus</i>	10-Apr-2011	eDC	NW Florida Slope	MFSA1_11-015	27.911°N	-85.540°W	MG229177	MG229382	MG229545
HBG2604	<i>B. giganteus</i>	10-Apr-2011	eDC	NW Florida Slope	MFSA1_11-015	27.911°N	-85.540°W	MG229178	MG229383	MG229546
HBG2605	<i>B. giganteus</i>	10-Apr-2011	eDC	NW Florida Slope	MFSA1_11-015	27.911°N	-85.540°W	MG229179	MG229384	MG229547
HBG2606	<i>B. giganteus</i>	10-Apr-2011	eDC	NW Florida Slope	MFSA1_11-015	27.911°N	-85.540°W	MG229180	MG229385	MG229548
HBG2607	<i>B. giganteus</i>	10-Apr-2011	eDC	NW Florida Slope	MFSA1_11-015	27.911°N	-85.540°W	MG229181	MG229386	MG229549
HBG2608	<i>B. giganteus</i>	10-Apr-2011	eDC	NW Florida Slope	MFSA1_11-015	27.911°N	-85.540°W	MG229182	MG229387	MG229550
HBG2609	<i>B. giganteus</i>	10-Apr-2011	eDC	NW Florida Slope	MFSA1_11-015	27.911°N	-85.540°W	MG229183	MG229388	MG229551
HBG2610	<i>B. giganteus</i>	10-Apr-2011	eDC	NW Florida Slope	MFSA1_11-015	27.911°N	-85.540°W	MG229184	MG229389	MG229552
HBG2611	<i>B. giganteus</i>	10-Apr-2011	eDC	NW Florida Slope	MFSA1_11-015	27.911°N	-85.540°W	MG229185	MG229390	MG229553
HBG2612	<i>B. giganteus</i>	10-Apr-2011	eDC	NW Florida Slope	MFSA1_11-015	27.911°N	-85.540°W	MG229186	MG229391	MG229554
HBG2613	<i>B. giganteus</i>	10-Apr-2011	eDC	NW Florida Slope	MFSA1_11-015	27.911°N	-85.540°W	MG229187	MG229392	MG229555
HBG2614	<i>B. giganteus</i>	10-Apr-2011	eDC	NW Florida Slope	MFSA1_11-015	27.911°N	-85.540°W	MG229188	MG229393	MG229556
HBG2615	<i>B. giganteus</i>	10-Apr-2011	eDC	NW Florida Slope	MFSA1_11-015	27.911°N	-85.540°W	MG229189	MG229394	MG229557
HBG2616	<i>B. giganteus</i>	10-Apr-2011	eDC	NW Florida Slope	MFSA1_11-015	27.911°N	-85.540°W	MG229190	---	MG229558
HBG2617	<i>B. giganteus</i>	10-Apr-2011	eDC	NW Florida Slope	MFSA1_11-015	27.911°N	-85.540°W	MG229191	MG229395	MG229559
HBG2618	<i>B. giganteus</i>	10-Apr-2011	eDC	NW Florida Slope	MFSA1_11-015	27.911°N	-85.540°W	MG229192	MG229396	MG229560
HBG2619	<i>B. giganteus</i>	10-Apr-2011	eDC	NW Florida Slope	MFSA1_11-015	27.911°N	-85.540°W	MG229193	MG229397	MG229561
HBG2620	<i>B. giganteus</i>	10-Apr-2011	eDC	NW Florida Slope	MFSA1_11-015	27.911°N	-85.540°W	MG229194	MG229398	MG229562
HBG2621	<i>B. giganteus</i>	10-Apr-2011	eDC	NW Florida Slope	MFSA1_11-015	27.911°N	-85.540°W	MG229195	MG229399	MG229563
HBG2623	<i>B. giganteus</i>	8-Apr-2011	eDC	West Florida Slope	WFSF2_11-010	26.940°N	-85.024°W	MG229196	MG229400	---
HBG2624	<i>B. giganteus</i>	8-Apr-2011	eDC	West Florida Slope	WFSF2_11-010	26.940°N	-85.024°W	MG229197	MG229401	---
HBG2625	<i>B. giganteus</i>	8-Apr-2011	eDC	West Florida Slope	WFSF2_11-010	26.940°N	-85.024°W	MG229198	MG229402	MG229564
HBG2626	<i>B. giganteus</i>	8-Apr-2011	eDC	West Florida Slope	WFSF2_11-010	26.940°N	-85.024°W	MG229199	MG229403	---
HBG2627	<i>B. giganteus</i>	8-Apr-2011	eDC	West Florida Slope	WFSF2_11-010	26.940°N	-85.024°W	MG229200	MG229404	MG229565
HBG2628	<i>B. giganteus</i>	8-Apr-2011	eDC	West Florida Slope	WFSF2_11-010	26.940°N	-85.024°W	MG229201	MG229405	MG229566

HBG2629	<i>B. giganteus</i>	8-Apr-2011	eDC	West Florida Slope	WFSF2_11-010	26.940°N	-85.024°W	MG229202	MG229406	---
HBG2630	<i>B. giganteus</i>	8-Apr-2011	eDC	West Florida Slope	WFSF2_11-010	26.940°N	-85.024°W	MG229203	MG229407	MG229567
HBG2631	<i>B. giganteus</i>	8-Apr-2011	eDC	West Florida Slope	WFSF2_11-010	26.940°N	-85.024°W	MG229204	MG229408	MG229568
HBG2632	<i>B. giganteus</i>	8-Apr-2011	eDC	West Florida Slope	WFSF2_11-010	26.940°N	-85.024°W	MG229205	MG229409	MG229569
HBG2633	<i>B. giganteus</i>	8-Apr-2011	eDC	West Florida Slope	WFSF2_11-010	26.940°N	-85.024°W	MG229206	MG229410	MG229570
HBG2634	<i>B. giganteus</i>	8-Apr-2011	eDC	West Florida Slope	WFSF2_11-010	26.940°N	-85.024°W	MG229207	MG229411	MG229571
HBG2635	<i>B. giganteus</i>	8-Apr-2011	eDC	West Florida Slope	WFSF2_11-010	26.940°N	-85.024°W	MG229208	MG229412	MG229572
HBG2636	<i>B. giganteus</i>	8-Apr-2011	eDC	West Florida Slope	WFSF2_11-010	26.940°N	-85.024°W	MG229209	MG229413	MG229573
HBG2637	<i>B. giganteus</i>	8-Apr-2011	eDC	West Florida Slope	WFSF2_11-010	26.940°N	-85.024°W	MG229210	MG229414	MG229574
HBG2638	<i>B. giganteus</i>	8-Apr-2011	eDC	West Florida Slope	WFSF2_11-010	26.940°N	-85.024°W	MG229211	MG229415	MG229575
HBG2639	<i>B. giganteus</i>	8-Apr-2011	eDC	West Florida Slope	WFSF2_11-010	26.940°N	-85.024°W	MG229212	MG229416	MG229576
HBG2640	<i>B. giganteus</i>	8-Apr-2011	eDC	West Florida Slope	WFSF2_11-010	26.940°N	-85.024°W	MG229213	MG229417	MG229577
HBG2641	<i>B. giganteus</i>	8-Apr-2011	eDC	West Florida Slope	WFSF2_11-010	26.940°N	-85.024°W	MG229214	MG229418	MG229578
HBG2644	<i>B. giganteus</i>	7-Apr-2011	eDC	West Florida Slope	WFSA3_11-003	26.719°N	-84.907°W	MG229215	MG229419	MG229579
HBG2645	<i>B. giganteus</i>	7-Apr-2011	eDC	West Florida Slope	WFSA3_11-003	26.719°N	-84.907°W	MG229216	MG229420	MG229580
HBG2646	<i>B. giganteus</i>	7-Apr-2011	eDC	West Florida Slope	WFSA3_11-003	26.719°N	-84.907°W	MG229217	MG229421	MG229581
HBG2647	<i>B. giganteus</i>	7-Apr-2011	eDC	West Florida Slope	WFSA3_11-003	26.719°N	-84.907°W	MG229218	MG229422	MG229582
HBG2648	<i>B. giganteus</i>	7-Apr-2011	eDC	West Florida Slope	WFSA3_11-003	26.719°N	-84.907°W	MG229219	MG229423	MG229583
HBG2649	<i>B. giganteus</i>	7-Apr-2011	eDC	West Florida Slope	WFSA3_11-003	26.719°N	-84.907°W	MG229220	MG229424	MG229584
HBG2650	<i>B. giganteus</i>	7-Apr-2011	eDC	West Florida Slope	WFSA3_11-003	26.719°N	-84.907°W	MG229221	MG229425	MG229585
HBG2651	<i>B. giganteus</i>	7-Apr-2011	eDC	West Florida Slope	WFSA3_11-003	26.719°N	-84.907°W	MG229222	MG229426	MG229586
HBG2652	<i>B. giganteus</i>	7-Apr-2011	eDC	West Florida Slope	WFSA3_11-003	26.719°N	-84.907°W	MG229223	MG229427	MG229587
HBG2653	<i>B. giganteus</i>	7-Apr-2011	eDC	West Florida Slope	WFSA3_11-003	26.719°N	-84.907°W	MG229224	MG229428	MG229588
HBG2654	<i>B. giganteus</i>	7-Apr-2011	eDC	West Florida Slope	WFSA3_11-003	26.719°N	-84.907°W	MG229225	MG229429	MG229589
HBG2655	<i>B. giganteus</i>	7-Apr-2011	eDC	West Florida Slope	WFSA3_11-003	26.719°N	-84.907°W	MG229226	MG229430	MG229590
HBG2656	<i>B. giganteus</i>	7-Apr-2011	eDC	West Florida Slope	WFSA3_11-003	26.719°N	-84.907°W	MG229227	MG229431	MG229591
HBG2657	<i>B. giganteus</i>	7-Apr-2011	eDC	West Florida Slope	WFSA3_11-003	26.719°N	-84.907°W	MG229228	MG229432	---
HBG2658	<i>B. giganteus</i>	7-Apr-2011	eDC	West Florida Slope	WFSA3_11-003	26.719°N	-84.907°W	MG229229	MG229433	MG229592

HBG2659	<i>B. giganteus</i>	7-Apr-2011	eDC	West Florida Slope	WFSA3_11-003	26.719°N	-84.907°W	MG229230	MG229434	MG229593
HBG2660	<i>B. giganteus</i>	7-Apr-2011	eDC	West Florida Slope	WFSA3_11-003	26.719°N	-84.907°W	MG229231	MG229435	MG229594
HBG2661	<i>B. giganteus</i>	7-Apr-2011	eDC	West Florida Slope	WFSA3_11-003	26.719°N	-84.907°W	MG229232	MG229436	MG229595
HBG2662	<i>B. giganteus</i>	7-Apr-2011	eDC	West Florida Slope	WFSA3_11-003	26.719°N	-84.907°W	MG229233	MG229437	MG229596
HBG2663	<i>B. giganteus</i>	7-Apr-2011	eDC	West Florida Slope	WFSA3_11-003	26.719°N	-84.907°W	MG229234	MG229438	MG229597
HBG2664	<i>B. giganteus</i>	8-Apr-2011	eDC	West Florida Slope	WFSC2_11-008	26.822°N	-84.816°W	MG229235	MG229439	MG229598
HBG2665	<i>B. giganteus</i>	8-Apr-2011	eDC	West Florida Slope	WFSC2_11-008	26.822°N	-84.816°W	MG229236	MG229440	MG229599
HBG2666	<i>B. giganteus</i>	8-Apr-2011	eDC	West Florida Slope	WFSC2_11-008	26.822°N	-84.816°W	MG229237	MG229441	MG229600
HBG2667	<i>B. giganteus</i>	8-Apr-2011	eDC	West Florida Slope	WFSC2_11-008	26.822°N	-84.816°W	MG229238	---	MG229601
HBG2668	<i>B. giganteus</i>	8-Apr-2011	eDC	West Florida Slope	WFSC2_11-008	26.822°N	-84.816°W	MG229239	MG229442	MG229602
HBG2669	<i>B. giganteus</i>	14-Apr-2011	DC	West wall of De Soto Canyon	DE3_11-031	29.182°N	-87.215°W	MG229240	MG229443	MG229603
HBG2670	<i>B. giganteus</i>	14-Apr-2011	DC	West wall of De Soto Canyon	DE3_11-031	29.182°N	-87.215°W	MG229241	MG229444	MG229604
HBG2671	<i>B. giganteus</i>	14-Apr-2011	DC	West wall of De Soto Canyon	DE3_11-031	29.182°N	-87.215°W	MG229242	MG229445	MG229605
HBG2672	<i>B. giganteus</i>	14-Apr-2011	DC	West wall of De Soto Canyon	DE3_11-031	29.182°N	-87.215°W	MG229243	MG229446	MG229606
HBG2673	<i>B. giganteus</i>	14-Apr-2011	DC	West wall of De Soto Canyon	DE3_11-031	29.182°N	-87.215°W	MG229244	MG229447	MG229607
HBG2674	<i>B. giganteus</i>	14-Apr-2011	DC	West wall of De Soto Canyon	DE3_11-031	29.182°N	-87.215°W	MG229245	MG229448	MG229608
HBG2675	<i>B. giganteus</i>	14-Apr-2011	DC	West wall of De Soto Canyon	DE3_11-031	29.182°N	-87.215°W	MG229246	MG229449	MG229609
HBG2676	<i>B. giganteus</i>	29-Aug-2011	wDC	Western Desoto	WDA3_11-063	28.848°N	-88.831°W	---	MG229450	MG229610
HBG2677	<i>B. giganteus</i>	29-Aug-2011	wDC	Western Desoto	WDA3_11-063	28.848°N	-88.831°W	MG229247	MG229451	MG229611
HBG2678	<i>B. giganteus</i>	29-Aug-2011	wDC	Western Desoto	WDA3_11-063	28.848°N	-88.831°W	MG229248	MG229452	MG229612
HBG2679	<i>B. giganteus</i>	28-Aug-2011	wDC	Western Desoto	WDB3_11-058	28.927°N	-83.507°W	MG229249	MG229453	MG229613
HBG2680	<i>B. giganteus</i>	28-Aug-2011	wDC	Western Desoto	WDB3_11-058	28.927°N	-83.507°W	MG229250	MG229454	MG229614
HBG2681	<i>B. giganteus</i>	28-Aug-2011	wDC	Western Desoto	WDB3_11-058	28.927°N	-83.507°W	MG229251	MG229455	MG229615
HBG2682	<i>B. giganteus</i>	28-Aug-2011	wDC	Western Desoto	WDB3_11-058	28.927°N	-83.507°W	MG229252	MG229456	MG229616
HBG2683	<i>B. giganteus</i>	28-Aug-2011	wDC	Western Desoto	WDB3_11-058	28.927°N	-83.507°W	MG229253	MG229457	MG229617
HBG2684	<i>B. giganteus</i>	28-Aug-2011	wDC	Western Desoto	WDB3_11-058	28.927°N	-83.507°W	MG229254	MG229458	MG229618
HBG2685	<i>B. giganteus</i>	28-Aug-2011	wDC	Western Desoto	WDB3_11-058	28.927°N	-83.507°W	MG229255	MG229459	MG229619
HBG2686	<i>B. giganteus</i>	28-Aug-2011	wDC	Western Desoto	WDB3_11-058	28.927°N	-83.507°W	MG229256	MG229460	MG229620

HBG2687	<i>B. giganteus</i>	28-Aug-2011	wDC	Western Desoto	WDB3_11-058	28.927°N	-83.507°W	MG229257	MG229461	MG229621
HBG2688	<i>B. giganteus</i>	28-Aug-2011	wDC	Western Desoto	WDB3_11-058	28.927°N	-83.507°W	MG229258	MG229462	MG229622
HBG2689	<i>B. giganteus</i>	28-Aug-2011	wDC	Western Desoto	WDB3_11-058	28.927°N	-83.507°W	MG229259	MG229463	MG229623
HBG2690	<i>B. giganteus</i>	28-Aug-2011	wDC	Western Desoto	WDB3_11-058	28.927°N	-83.507°W	MG229260	MG229464	MG229624
HBG2691	<i>B. giganteus</i>	28-Aug-2011	wDC	Western Desoto	WDB3_11-058	28.927°N	-83.507°W	MG229261	---	---
HBG2692	<i>B. giganteus</i>	27-Aug-2011	DC	West wall of De Soto Canyon	DE5_11-056	29.186°N	-87.427°W	MG229262	MG229465	MG229625
HBG2693	<i>B. giganteus</i>	25-Aug-11	eDC	North Slope	NA1_11-045	29.136°N	-85.957°W	MG229263	MG229466	MG229626
HBG2694	<i>B. giganteus</i>	27-Aug-2011	DC	West wall of De Soto Canyon	DF2_11-057	29.020°N	-87.308°W	MG229264	MG229467	MG229627
HBG2695	<i>B. giganteus</i>	27-Aug-2011	DC	West wall of De Soto Canyon	DF2_11-057	29.020°N	-87.308°W	MG229265	MG229468	MG229628
HBG2696	<i>B. giganteus</i>	23-Aug-2011	DC	West wall of De Soto Canyon	DD3_11-053	29.374°N	-87.060°W	MG229266	MG229469	MG229629
HBG2697	<i>B. giganteus</i>	23-Aug-2011	DC	West wall of De Soto Canyon	DD3_11-053	29.374°N	-87.060°W	MG229267	MG229470	MG229630
HBG2698	<i>B. giganteus</i>	23-Aug-2011	DC	West wall of De Soto Canyon	DD3_11-053	29.374°N	-87.060°W	MG229268	MG229471	MG229631
HBG2699	<i>B. giganteus</i>	23-Aug-2011	DC	West wall of De Soto Canyon	DD3_11-053	29.374°N	-87.060°W	MG229269	MG229472	MG229632
HBG2700	<i>B. giganteus</i>	23-Aug-2011	DC	West wall of De Soto Canyon	DD3_11-053	29.374°N	-87.060°W	MG229270	MG229473	MG229633
HBG2701	<i>B. giganteus</i>	23-Aug-2011	DC	West wall of De Soto Canyon	DD3_11-053	29.374°N	-87.060°W	---	MG229474	MG229634
HBG2702	<i>B. giganteus</i>	12-Apr-2012	wDC	Western Desoto	WDA3_12-052	28.824°N	-88.840°W	MG229271	MG229475	MG229635
HBG2703	<i>B. giganteus</i>	23-Aug-2011	DC	West wall of De Soto Canyon	DD3_11-053	29.374°N	-87.060°W	---	MG229476	MG229636
HBG2704	<i>B. giganteus</i>	23-Aug-2011	DC	West wall of De Soto Canyon	DD3_11-053	29.374°N	-87.060°W	MG229272	MG229477	MG229637
HBG2705	<i>B. giganteus</i>	23-Aug-2011	DC	West wall of De Soto Canyon	DD3_11-053	29.374°N	-87.060°W	MG229273	MG229478	MG229638
HBG2706	<i>B. giganteus</i>	23-Aug-2011	DC	West wall of De Soto Canyon	DD3_11-053	29.374°N	-87.060°W	MG229274	MG229479	MG229639

CHAPTER V
EFFECTS OF DIEL VERTICAL MIGRATION AND THE GULF LOOP CURRENT
ON POPULATION DYNAMICS OF MESOPELAGIC SHRIMPS IN THE GULF OF
MEXICO

ABSTRACT

The Gulf of Mexico experiences frequent perturbations, both natural and anthropogenic. To better understand the impacts of these events, we must inventory natural variability within the ecosystem, communities, species, and populations. This daunting task can begin with population genomics studies of species common to the Gulf. Genetic diversity and population connectivity serve as informative metrics for species health and resilience, respectively. Specifically, this focus aims to establish biological baselines for three species of mesopelagic shrimp (*Acantheephyra purpurea*, *Systellaspis debilis*, and *Robustosergia robusta*) that are common within the Gulf and the greater Atlantic. Additionally, we seek to contextualize our results in terms of the major oceanographic mixing feature in the region, the Gulf Loop Current. Generally, we find lower genetic diversity and population differentiation between basins in the oplophorid species (*A. purpurea* and *S. debilis*), which brood their young and exhibit strong diel vertical migratory behavior, compared to the sergestid (*R. robusta*), which exhibits broadcast spawning and distinctly weaker diel vertical migration, however we also find evidence that all three species undergo some amount of inbreeding. Here, we present evidence of a negative correlation between surface abundance and genetic diversity. We hypothesize that this correlation may be due to the relationships between surface abundance and access to the fastest moving waters of the Gulf Loop Current.

INTRODUCTION

The Gulf of Mexico is a region with a relatively high rate of environmental perturbations. In the past decade alone, the region has been struck to two major

hurricanes, Hurricane Ike in 2008 and Hurricane Harvey in 2017, and two major oil spills: the Deepwater Horizon Oil Spill in 2010 and the Shell Spill in 2016. However, the Gulf of Mexico also hosts a hyper-diverse mesopelagic zone (Sutton et al., 2017) and is described as a unique biogeographic ecoregion, distinct from the Caribbean Sea, Sargasso Sea, and greater Atlantic Ocean (Backus et al., 1977; Gartner, 1988). The frequent perturbations, both natural and anthropogenic, may have a drastic impact on the Gulf mesopelagic given its unique biological importance. Because of this threat, we must begin establishing biological baselines for common midwater species, preferably species with key functions in the trophic web. Additionally, research efforts must focus on diagnosing Gulf health, contextualizing health in relation to the Gulf's relationship to the greater Atlantic, and understanding the role(s) of major oceanographic features on inter-basin population connectivity.

In the cases of enigmatic species, which are both difficult to directly observe and require specialized collection techniques, population genomic studies can frequently be the only realistic avenues to infer life history and species' ecology. Genetic diversity and genetic connectivity, common metrics targeted in population genomics, provide especially valuable information about the species as a whole and are established proxies for species health and resilience, respectively (Cowen & Sponaugle, 2009; Danovaro et al., 2008; Hellberg et al., 2002; Hughes & Stachowicz, 2004). Genetic diversity is measured as the number of alleles present within a population or species. A population's or species' ability to adapt to new or changing environments are closely tied to higher genetic diversity (Cowen & Sponaugle, 2009; Danovaro et al., 2008; Hughes & Stachowicz, 2004). Thus, local adaptation can be crucial to a population's maintained

health in the face of environmental perturbations. The movement and distribution of genetic diversity within or between systems is described by population connectivity. Population connectivity can be characterized as inter-population gene flow or migration or the historical demography of populations, such as recent separation or re-mixing of distinct populations and/or changes to population size. Ecologically, all of this is crucial to species resilience: following a localized perturbation event, migration between geographically separated populations can provide a functional genetic reservoir outside the disturbed area (Cowen & Sponaugle, 2009; Hellberg et al., 2002).

This study focuses on population genomics of three mesopelagic crustacean species common to the Gulf of Mexico and Atlantic, specifically in relation to the Gulf Loop Current, the principal mixing feature in the eastern Gulf of Mexico (Figure 1). Generally, it is described as flowing anticyclonically (clockwise) occupying the surface to 800-1200m of the water column (Hamilton et al., 2015; Oey et al., 2005). It is characterized by relatively warm, fast-moving water with speeds as fast as 1.7 m s^{-1} (Forristall et al., 1992) in the top 100m of the water column (Hamilton et al., 2015), decreasing to a maximum speed of 0.4 m s^{-1} between 100m to 200m depth, and continuing to slow with depth. Below 1000m depth, water movement is generally considered to be independent of the Gulf Loop Current (Hamilton et al., 2015; Oey et al., 2005). Additionally, the Gulf Loop Current releases cyclonic (counterclockwise) rings, with diameters ranging from 200km to 300km across, which travel west toward Mexico and Texas (Oey et al., 2005). These features are likely to have real, biologically significant impacts on diversity within the Gulf (Milligan et al., in prep).

The role of the Gulf Loop Current as inter-basin biological conveyor belt makes it the interface between individual organismal behavior and ecosystem properties: many midwater animals exhibit diel vertical migratory behavior, occupying deeper water during the day and moving into epipelagic/surface water at night (Brierley, 2014; Loose & Dawidowicz, 1994), giving them greater access to the fastest moving waters of the Gulf Loop Current. This behavior results in a number of “midwater” species having substantial increases in surface abundance over a diel cycle. It also results in three general regimes in terms of surface abundance: surficial non-migrators with consistently high surface abundance (that is, the majority of individuals are located in surface waters regardless of solar cycle), diel vertical migrators with mid-to-high surface abundance at night, and deep non-migrators with consistently low-to-no surface abundance. Recently, a population genetics/genomics study of three species of cephalopod, one species representing each of these regimes (Figure 2), found a pattern between surface abundance and inter-basin population dynamics in the Gulf of Mexico and the Atlantic Ocean (Timm & Judkins et al., in prep). The surficial non-migrator had low diversity and high connectivity. The deep non-migrator exhibited significantly higher diversity and significant population differentiation. The migrating species had intermediate diversity values and evidence of significant, but low, population differentiation. Timm & Judkins et al. (in prep) posit that this putative relationship between surface abundance and inter-basin population dynamics is due to the division of these regimes into concomitant “tiers” of access to the Gulf Loop Current: surficial non-migrators have greatest access to the fastest-flowing layer of the current; migrators have temporally defined access to this

layer; and deep non-migrators lack access to this layer, but may be able to take some advantage of slower, deeper layers.

Here, we seek to investigate whether this trend holds for three species of crustaceans: two diel vertical migrators, *Acantheephyra purpurea* A. Milne-Edwards, 1888 and *Systellaspis debilis* (A. Milne-Edwards, 1888), and a weak migrator, *Robustosergia robusta* (Smith, 1882) (Fig 3). To date, the relationship between surface abundance and inter-basin population dynamics has not been explored in a weak migrator, which represents a new regime with a different tire of access: a fraction of the population has access to the fastest-flowing layer at night, as opposed to strong migrators who have the majority of the population moving into this layer at night. Also of importance are differences between species in terms of life history, specifically in brooding behavior and generation time.

Acantheephyra purpurea and *S. debilis* both brood their eggs, meaning migrating adults may also be ferrying their offspring between basins. *Robustosergia robusta* is a broadcast spawner, meaning the Gulf Loop Current-facilitated inter-basin transport of individuals, already compromised by weak diel vertical migration, may be further inhibited by highly dangerous, high-mortality transfer of young between basins. Moreover, surveys have indicated that *R. robusta* diel vertical migratory behavior differs geographically, though individuals consistently stay below the seasonal thermocline (Donaldson, 1975; Foxton, 1970; Frogliia & Giannini, 1982; Frogliia & Gramitto, 2000), indicating individuals may be primarily “tracking” water temperature, regardless of the depth at which these temperatures occur. This is particularly important in terms of the Gulf Loop Current, which displaces the water column downward and generally increases

the average water temperature across depths, with effects measurable to below 1500m (Milligan et al., in prep). Additionally, there is evidence of an ontological shift in diel vertical migration behavior in *R. robusta* and several other sergestid species: larvae migrate into shallower waters than juveniles, which in turn migrate into shallower waters than adults (Flock & Hopkins, 1992). These insights into diel vertical migration makes discrete depth abundance plots necessary to analyze this behavior in the Gulf.

This study seeks fine-scale resolution to identify differences in diversity and connectivity across relatively small geographic distances. Additionally, we hope to gain a genome-wide perspective without assuming the costs of whole-genome sequencing which, given the hypothesized genome sizes of *A. purpurea* and *S. debilis* (~9 Gb), is itself unrealistic. To address our objectives with the greatest power realistically available, we utilized a powerful next-generation sequencing (NGS) method, double digest Restriction site Associated DNA sequencing (ddRADseq, as described by Peterson et al., 2012). This approach allowed us to query a theoretically representative, reproducible fraction of the genome and generated orders of magnitude more data with greater statistical power than traditional population genetics studies have done.

Our study represents a comparative, NGS investigation into the role of behavior and oceanography on population dynamics in three species of crustacean ubiquitous to the mesopelagic Gulf. The overall goal of this study is to diagnose species and ecosystem health and resilience in the Gulf. To accomplish this goal we 1) quantify genetic diversity in each species and compare between the Gulf and the Atlantic; 2) characterize population connectivity between the Gulf and Atlantic; 3) correlate surface abundance with these metrics; and 4) improve our understanding of crustacean health and resilience

in the region, specifically in the context of species- and/or population-specific diel vertical migratory behavior and the major oceanographic feature of the region, the Gulf Loop Current.

METHODS

Specimens of *Acanthephyra purpurea*, *Systellaspis debilis*, and *Robustosergia robusta* were collected from the northern Gulf of Mexico during the wet (August) and dry (May) seasons of 2015 and 2016 as part of the Gulf of Mexico Research Initiative (GOMRI)-funded Deep Pelagic Nekton Dynamics of the Gulf of Mexico (DEEPEND) project on the R/V Point Sur (Figure 4). In 2016, samples of *A. purpurea* and *S. debilis* were also collected from the Florida Straits aboard the R/V Walton Smith. All three species were collected from Bear Seamount in the Atlantic in 2014 during exploratory trawling on the NOAA Ship Pisces.

Gulf samples were collected with a Multiple Opening/Closing Net and Environmental Sensing System (MOC-10) rigged with six 3-mm mesh nets, allowing for discrete depth sampling. Samples were collected from Bear Seamount with a modified Irish herring trawl. Finally, a tucker trawl was used to collect samples from the Florida Straits.

All samples were identified to species and collected as whole-specimens, either in 70% EtOH or a RNA-stabilizing buffer, and stored at -20°C onboard the vessel before being transferred to a -80°C freezer in the CRUSTOMICS lab at Florida International University. Collected samples were then given a unique voucher ID in the CRUSTOMICS lab database, including all relevant collection data. Muscle tissue was

plucked for each specimen and stored in 70% EtOH or a RNA-stabilizing buffer, in accordance with how the whole-specimen was originally collected, and stored in a -80°C freezer. Voucher specimens were preserved in 70% EtOH and deposited in the Florida International Crustacean Collection. In total, 247 samples of *A. purpurea* were collected, 218 samples of *S. debilis*, and 95 samples of *R. robusta*. For each species, a subset of individuals was selected to provide adequate ($n > 10$) representation for each basin (Atlantic and Gulf). These subsets and general information about each species included in this study are detailed in Supplementary Table 1.

DNA Extraction and Sample Barcoding

DNA was extracted with the DNeasy Blood and Tissue Kit (Qiagen), following the protocol provided by the manufacturer. Due to the high quality of DNA necessary for robust ddRADseq data, several quality control measures were taken. First, the amount of DNA was ascertained with the Qubit dsDNA High Sensitivity Assay (Thermo Fisher). Next, DNA extractions were visualized on a 2% agarose gel with GelRed (Biotium) run for 90min at 100V to ensure the presence of exclusively high molecular weight DNA. Samples with <500ng DNA and/or a preponderance of degraded DNA were excluded from library prep.

Finally, to confirm species identification, every individual eligible for ddRADseq library prep was DNA barcoded using the mitochondrial genes 16S ribosomal subunit, 16S (*A. purpurea* and *S. debilis*) or cytochrome oxidase subunit I, COI (*R. robusta*). Polymerase Chain Reaction (PCR) occurred in 25- μ l volumes: 12.5 μ l GoTaq DNA Polymerase (Promega), 1 μ l of each primer, 6.5 μ l of sterile distilled water, and 2 μ l of

template DNA. The primer combinations, sequences, and references, as well as annealing temperatures and amplicon length (in base pairs) are presented in Table 1. All PCR products were visualized on a 1% agarose gel in the same manner as the DNA extractions.

Amplicons were cleaned and sequenced at the Genewiz sequencing facility in Newark, NJ, USA. Quality filtering of raw reads, contig assembly, ambiguity determination, primer removal, and alignment with MAFFT (Katoh & Standley, 2013) occurred in Geneious v.9.3 (Kearse et al., 2012). The alignment was visually inspected for errors in MEGA7 (Kumar, Stecher, & Tamura, 2016) before determining the reading frame and codon position of COI.

Cleaned, aligned sequences were queried against the NCBI GenBank database using the Basic Local Alignment Search Tool (BLAST) for standard nucleotide. Before querying, we confirmed that all three species were present in the database for the locus we sequenced (16S or COI). A barcode was considered a match when the percent identity of the match was $\geq 99\%$. Only individuals whose taxonomic identification was confirmed by BLAST results were included in ddRADseq library prep.

NGS with ddRADseq

Library Preparation ddRADseq libraries were successfully prepared for 89 individuals of *A. purpurea*, 82 individuals of *S. debilis*, and 87 individuals of *R. robusta*. Reduced representation libraries were prepared according to the double digest RADseq (ddRADseq) method (Peterson et al., 2012). Generally, enzyme trials were completed to determine the appropriate enzyme combinations and size selection windows. DNA was

digested with a combination of two enzymes (New England Biolabs) and custom barcoded adapters were synthesized and ligated to the fragments resulting from double digest. Once barcoded, samples could be pooled into sublibraries, which were size selected on a PippinPrep (Sage Science). Specific enzyme combinations, custom barcoded adapter sequences, and size selection schemes are reported in Table 2. Size selected fragments were then amplified via PCR with Phusion Hi-Fidelity Polymerase (Thermo Scientific), which also incorporated indices (i7) and Illumina adapters into the fragments and allowed for pooling of sublibraries into the final libraries; twelve sublibraries per library and one library per species. The final libraries were quality checked on an Agilent BioAnalyzer 2100 (Agilent Technologies) before the library was sent for sequencing on an Illumina NextSeq, SE75 high output, at the Georgia Genomics Facility at the University of Georgia.

Quality Filtering and Data Assembly Raw sequence files were processed with the STACKS v1.45 (Catchen et al., 2013) pipeline on the FIU High Performance Computing Cluster (HPCC). In `process_radtags`, reads were demultiplexed, cleaned (-c), and quality-filtered (-q). The `ustacks` program aligned identical reads within each individual, then these consensus reads were catalogued in `cstacks`. All putative loci were queried against this catalog with `sstacks` before `rxstacks` corrected individual genotype calls according to the accumulated population data. Finally, the `populations` program output a file of aligned, putatively unlinked single-nucleotide polymorphisms (SNPs). Two requirements had to be met for a given SNP to be called: first, the minimum read depth (-m=5) had to be met; second, the SNP needed to be found in 25% of the individuals of a population (-r=0.25) for the SNP to be called for that population. After SNPs were called according to

these parameters, two additional requirements needed to be met for a given SNP to be retained: the SNP had to be present in all populations (Atlantic and Gulf or anticyclonic region, mixed water/loop boundary, and common water) and, to increase the likelihood of excluding linked loci, only one random SNP was called per locus (--write_random_snp).

Each file of aligned SNPs then underwent an iterative missing data filter. Loci with >95% missing data were removed, followed by individuals with >95% missing data. This was repeated with 90% missing data, then 85%, and so on. This was repeated until only 10% missing data was allowed by locus and individual or until ~500 loci remained. This “500 SNP” rule was necessary in the case of the oplophorids *A. purpurea* and *S. debilis*, as strict filtering resulted in data sets reduced to unusably small sizes. This is likely the result of very large genome sizes: the amount of data returned from the Illumina NextSeq is relatively fixed, therefore larger genomes will yield smaller amounts of consistently reproducible reads across individuals. Finally, we used BayeScan v2.1 (Foll & Gaggiotti, 2008) to identify F_{ST} outliers within each filtered data set. Any loci identified as outliers were removed.

Data Analysis

Several genetic diversity indices were calculated in GENODIVE v2.0b23 (Meirmans & Van Tienderen, 2004), including: observed heterozygosity (H_o), the inbreeding coefficient (G_{is}), and expected heterozygosity (H_e , which was calculated from the H_o and G_{is} values). Jackknifing over loci was used to calculate standard deviation.

GENODIVE was also used to measure population differentiation (F_{ST}) and calculate hierarchical Analyses of Molecular Variance (AMOVAs) with the Infinite

Allele Model. Both analyses were run under 999 permutations to assess significance. For the AMOVAs, missing data were replaced with randomly drawn alleles determined by overall allele frequencies.

We employed the Bayesian program STRUCTURE v2.3.4 (Pritchard et al., 2000) to test for population structure within the data. Seven K -values were tested ($K=1-7$) 10 times each under the admixture model. Following a burn-in of 20,000 generations, 200,000 Markov Chain Monte Carlo generations ran. In STRUCTURE HARVESTER v0.6.94 (Earl & VonHoldt, 2012), STRUCTURE results were collated and *ad hoc* posterior probability models (Pritchard et al., 2000) and the Evanno method (Evanno et al., 2005) were used to infer the optimal K value. STRUCTURE HARVESTER also generated CLUster Matching and Permutation Program (CLUMPP) files for individuals and populations. These files were input into CLUMPP v1.1.2 (Jakobsson & Rosenberg, 2007), resulting in input files compatible with *distruct* v1.1 (Rosenberg, 2004) and facilitating the visualization of estimated membership coefficients.

Two additional, non-model based methods were also employed for inferring and visualizing population structure: multi-dimensional scaling (MDS) plots and Principle Component Analyses (PCAs) were rendered for each data set using the R packages MASS (Venables & Ripley, 2002) and *ade4* (Jombart & Ahmed, 2011), respectively. These methods are very similar, however MDS preserves distance/dissimilarity between data points while PCA preserves covariance within the data.

Testing for Correlation

To test for correlation between surface abundance and genetic diversity indices, we began by defining “surface abundance” as the percent of total abundance found above 600m. We plotted each diversity index (observed and expected heterozygosity and the inbreeding coefficient) against surface abundance for each species. Data from Timm & Judkins et al. (in prep) (Timm et al., 2018a) was also included to increase sample size and robustness. A trendline was fit to each index and R^2 was used to determine goodness-of-fit. To statistically test for correlation, we calculated Kendall’s τ and Spearman’s rank. We did not calculate Pearson’s index because the data was not normally distributed.

RESULTS

Of the 268 prepared libraries (89 individuals of *A. purpurea*, 84 individuals of *S. debilis*, and 95 individuals of *R. robusta*), 262 could be aligned and assembled within STACKS (89 of *A. purpurea*, 84 of *S. debilis*, and 89 of *R. robusta*). The initial data sets included: 596 SNPs (*A. purpurea*), 652 SNPs (*S. debilis*), and 4196 SNPs (*R. robusta*). After applying the missing data filter, the *A. purpurea* data set included 522 SNPs across 87 individuals, the *S. debilis* data set included 525 SNPs across 91 individuals, and the *R. robusta* data set included 1066 SNPs across 37 individuals. Across all data sets, only the *R. robusta* set was found to contain F_{ST} outliers: three SNPs were identified by BAYESCAN and removed from the final data set. This information is summarized in Supplementary Table 1 and raw fastq reads have been uploaded and are publicly available through the Gulf of Mexico Research Initiative’s Information & Data Cooperative (Timm et al., 2018b).

Diversity

Values across species were very similar (Ho: 0.057-0.089; He: 0.094-0.122) with exception of the inbreeding coefficient which was highest in *A. purpurea* (0.534), slightly lower in *S. debilis* (0.425), and lowest in *R. robusta* (0.146) (Figure 5). As the inbreeding coefficient reflects the relationship between Ho and He ($[\text{He}-\text{Ho}]/\text{He}$), it ranges from -1 to 1, with positive values indicating inbreeding or a recent decrease in population size. These results are reported in Table 3.

Observed heterozygosity is the actual, measured amount of heterozygosity found in a population and can be impacted by an excess of homozygosity. Expected heterozygosity, however, describes the theoretical amount of heterozygosity present assuming the population of interest is in Hardy-Weinberg Equilibrium. It considers the number of alleles as well as their abundance, regardless of homozygosity. These two metrics, observed and expected heterozygosity, are compared using the inbreeding coefficient, as described in the Methods section. In all species and basins studied here, expected heterozygosity was found to be higher than observed heterozygosity, with the largest difference in *A. purpurea*, followed by *S. debilis*, then *R. robusta*. Generally, inbreeding coefficients approaching 1 indicate decreases in population size or local purifying selection, suggesting that the oplophorids have experienced population decreases or uneven selection pressures that *R. robusta* has not faced.

When diversity was compared by basin (Gulf vs. Atlantic), the Atlantic was typically found to have higher diversity, though this difference was greatest in the oplophorids: *A. purpurea* (Atlantic = 0.058 [Ho], 0.116 [He]; Gulf = 0.044 [Ho], 0.114

[He]) and *S. debilis* (Atlantic = 0.070 [Ho]; Gulf = 0.048 [Ho]), though measures of He in *S. debilis* broke trend (Atlantic = 0.080; Gulf = 0.098). The difference in diversity between basins for *R. robusta* was very small (Atlantic = 0.090 [Ho], 0.105 [He]; Gulf = 0.089 [Ho], 0.104 [He]). In this species, the inbreeding coefficient was found to be slightly lower in the Gulf than the Atlantic (Atlantic = 0.148; Gulf = 0.143), while the oplophorids had significantly higher G_{is} in the Gulf compared to the Atlantic (*A. purpurea*: Atlantic = 0.500; Gulf = 0.614; *S. debilis*: Atlantic = 0.126; Gulf = 0.510). This is illustrated in Figure 6.

Population Differentiation and Structure

AMOVA results, reported in Figure 7, indicate a lack of population differentiation between basins in the oplophorids: FIT ranged from 80.6% in *S. debilis* to 83.9% in *A. purpurea* and the rest of molecular variance was accounted for by FIS (19.4% in *S. debilis* and 16.1% in *A. purpurea*). The majority of variance in *R. robusta* was from FIT (71.9%), however the remainder was comprised of FIS (11.9%) and FST (16.2%), indicating statistically significant genetic differentiation between the Gulf and the Atlantic.

STRUCTURE results strongly support and aptly illustrate the AMOVA results for each species (Figure 8). For the oplophorids, optimal k was determined to be 2; for *R. robusta*, k=3 was deemed optimal. In the oplophorids, the admixture of ancestral populations within each individual is nearly identical between basins, while there is some variation within each basin. *Robustosergia robusta*, however, exhibits a dramatic difference in admixture proportion by basin. While admixture from all three ancestral

populations is present in every individual, the individuals from the Atlantic consist of nearly equal admixture from populations 1 and 2, with the majority from population 3, while individuals from the Gulf have a very small proportion of admixture from population 3, nearly identical proportions of admixture from population 1 as seen in the Atlantic, and the vast majority of admixture from population 2.

The PCAs and MDSs present these results another way: both oplophorid species have all individuals fall into a single cluster (further supported by affinity propagation identifying one cluster within each data set), regardless of the basin from which they were collected. Conversely, the population differentiation seen in the AMOVA results for *R. robusta*, as well as the STRUCTURE analysis, is made further evident in the PCA and MDS: both plots show two distinct clusters, one containing individuals from the Atlantic and the other containing Gulf specimens. Results from PCA and MDS are depicted in Figure 8).

Testing for Correlation

Generally, a negative correlation between surface abundance and genetic diversity was statistically supported (Figure 9). Across analyses, correlation was strongest between surface abundance and observed heterozygosity ($R^2 = 0.868$, Pearson = -0.932, $r_s = -0.942$, τ statistically significant; Table 4). Correlation between surface abundance and expected heterozygosity was weaker ($R^2 = 0.494$, Pearson = -0.703, $r_s = -0.543$, τ not statistically significant; Table 4). Inbreeding coefficient was not found to be correlated to surface abundance ($R^2 = 0.073$, Pearson = 0.27, $r_s = -0.543$, τ not statistically significant; Table 4).

DISCUSSION

This study aimed to increase our understanding of health and resilience of midwater crustaceans in the Gulf of Mexico. Our results describe the state and flux of genetic variation in three species of mesopelagic shrimp and illuminate the potential for recovery in a perturbation-prone Gulf. Generally, our results exhibited fairly clear distinctions between two taxonomic groups: the oplophorids *A. purpurea* and *S. debilis*, and the sergestid *R. robusta*.

Health and Diversity

Generally, we find observed heterozygosity to be lower than expected heterozygosity, resulting in substantial inbreeding coefficients. However, diversity was highest, and inbreeding lowest, in *R. robusta*. Diversity values were similar between the oplophorids, *A. purpurea* and *S. debilis*, however, the inbreeding coefficient was much higher in *A. purpurea*. The oplophorids also differed from *R. robusta* in analyses of population connectivity and structure: *Robustosergia robusta* had significant population differentiation between basins, with each basin exhibiting a different pattern of admixture from three ancestral populations. Oplophorids, however, exhibit no differentiation between basins and all individuals within a species exhibit the same pattern of admixture from two ancestral populations, regardless of source basin (Gulf vs. Atlantic).

With this new information, we investigated how diversity is organized between the Gulf of Mexico and the Atlantic. Between basins, expected and observed heterozygosity paralleled each other well within each species, with the exception of *S.*

debilis in the Atlantic, wherein the two were nearly equal, greatly decreasing the inbreeding coefficient. In the oplophorids, inbreeding was lower in the Atlantic compared to the Gulf, with the Florida Straits being nearly equal to the Atlantic (in the case of *A. purpurea*) or significantly higher than the Gulf (in the case of *S. debilis*). This may be indicative of Gulf-localized perturbation or purifying selection affecting the oplophorids. However, the low inbreeding coefficient, high diversity, and small inter-basin diversity differences seen in *R. robusta* suggest quite different dynamics compared to the oplophorids.

Connectivity and Resilience

To better understand the processes that maintain these population dynamics, we investigated how this inter-basin organization is maintained through population structure and connectivity. Here again, we found a notable difference between the oplophorids and *R. robusta*. The oplophorids exhibited high population connectivity, indicating historical and current gene flow. Results of population structure analyses indicate each oplophorid species consists of a single population spanning the Gulf and the Atlantic. Individuals from these populations are comprised of admixture from two ancestral populations of each species. *Robustosergia robusta*, however, exhibits significant population differentiation between basins. Analyses of population structure indicate this is coupled with different patterns of admixture from three ancestral populations, forming two distinct genetic signatures.

Our improved understanding of population structure and connectivity helps explain how diversity is organized and how population dynamics are maintained. High

connectivity and little population structure in oplophorids, evinced by high F_{IT} , low F_{ST} , and results of structure analyses, may constrain genetic diversity through purifying selection. Because the single population must contend with two very different basins and environments (Backus et al., 1977; Gartner, 1988; Sutton et al., 2017). Any potential local or basin-specific adaptations must also be fit for the other basin and vice versa. Additionally, in the case of *S. debilis*, it seems the entire inter-basin population is impacted by local perturbations, such as a decrease in numbers of individuals in the Gulf. *Robustosergia robusta*, however, exhibits the highest diversity and lowest inbreeding of species included in this study. This may be attributable to a larger number of ancestral populations (three, instead of two in the oplophorids) or potentially local adaptation to the Gulf of Mexico and the Atlantic Ocean, relatively independently. Relatively high, statistically significant F_{ST} , indicating population differentiation between basins, could suggest local adaptation following the recent separation and isolation of two distinct subspecies. However to fully address this, more work is needed, specifically a comprehensive phylogeny of sergestids.

This study particularly focused on diel vertical migration of adults, resultant surface/epipelagic abundance, and population dynamics. Including data from Timm & Judkins (in prep) (Timm et al., 2018a), we find a trend of high surface abundance associated with low (if not 0) F_{ST} . However, this relationship appears to be binary. Perhaps there is some critical surface abundance that maintains migration and prevents population differentiation. But this requires much more stringent, statistical testing to properly investigate. Genetic diversity shows much higher variability, allowing for statistical testing of correlation. Generally, an indirect/negative correlation was found,

with higher surface abundance associated with lower genetic diversity. This relationship was clearest in observed heterozygosity, though still present in expected heterozygosity. It was nearly absent in the inbreeding coefficient.

Overall, our results suggest that the oplophorid species are more likely to exhibit resilience in the face of ecological perturbations, compared to *Robustosergia robusta*: low differentiation in the oplophorids suggests gene flow, either through larval dispersal or migration of adults; while significant population differentiation in the sergestid shrimp indicates the existence of a Gulf population, distinct from the Atlantic population, which may be more susceptible to Gulf-localized perturbations.

Considering Life History and Behavior

The two taxa investigated here, Oplophoridae and Sergestidae, differ in many ways, including brooding behavior and strength of diel vertical migration. Brooding behavior, exhibited by the oplophorids, may contribute greatly to connectivity between basins by facilitating inter-basin migration: while fecundity may differ by reproductive strategy (Ramirez Llodra, 2002), brooded young tend to have a better chance of survivorship (MacIntosh et al., 2014). Moreover, a survey of the broadcast-spawning *R. robusta* from 1992 describes an ontological shift in diel vertical migration strength, with juvenile shrimp exhibiting stronger migration behavior than adults (Flock & Hopkins, 1992). As such, though larvae of *R. robusta* may have better access to the fastest moving waters of the Gulf Loop Current, they may also be less likely to survive and contribute to the effective population. The authors have noted this anecdotally: on research cruises to the Florida Straits, adults of *A. purpurea*, *S. debilis*, and sergestids with diel vertical

migration described in the literature as strong (Flock & Hopkins, 1992) were quite abundant, but adults of *R. robusta* were functionally absent. Larvae of these species, even when confidently identified and taxonomically linked to the adult stage, were neither noted nor collected. However, as mentioned, this is purely anecdotal. Statistical analysis of size distributions along the depth gradient is called for to clarify the role of larvae as migrants connecting the Gulf and Atlantic. While larvae can be critical for population connectivity in marine species (Cowen & Sponaugle, 2009; Gaines et al., 2007; Palumbi, 2003), there is also strong evidence that potential dispersal is often not correlated with realized dispersal (Shanks, 2009).

Population Dynamics and the Gulf Loop Current

In many ways, this study only scratches the surface as far as uncovering the mechanisms driving and maintaining natural variability in the Gulf of Mexico. The establishment of baselines for genetic diversity and connectivity is crucial to understanding the Gulf and for future appraisal of damages following disturbance events. Here, we present evidence of a correlation between surface abundance and population dynamics, specifically genetic diversity. We hypothesize that this may be best explained by the Gulf Loop Current: populations with higher abundance in the surface or epipelagic have greater access to the fastest moving waters of the Gulf Loop Current in the Gulf of Mexico. It can be logically reasoned that this access would facilitate bi-directional transport (either passive movement or active migration) between the Gulf of Mexico and the greater Atlantic Ocean. This would also maintain, and thus explain, a single

population spanning the Gulf and Atlantic, homogenizing if not functionally preventing local adaptation and population differentiation.

However in this study, as well as the cephalopod study (Timm & Judkins et al., 2018), sample sizes of species with low surface abundance (namely the deep non-migrator *Vampyroteuthis infernalis* and the weak migrator *Robustosergia robusta*) were small enough to bring the results into some question and require cautious interpretation. First, more individuals of these species must be included. Additionally, before attempts to model this surface abundance-genetic diversity correlation are undertaken, the correlation should be tested in more species, specifically fishes. When or if model testing begins, pervasive depth-dependent environmental variables (i.e. salinity, temperature, dissolved oxygen concentration, and chlorophyll concentration) should be considered as well as physical oceanographic parameters, such as water velocity and direction in relation to the Florida Straits.

Diagnosis for the Gulf

The results presented here, contextualized in terms of environment (the Gulf Loop Current) and life history (reproductive strategy and diel vertical migratory behavior), serve as the first glimpse of the natural variability present in the Gulf midwater and begin to describe potential drivers of this variability. We set out to better understand population dynamics of mesopelagic crustaceans in the Gulf of Mexico through a comparative population genomics approach and the insight we have gained provides perspective as we attempt to diagnose health and resilience in the Gulf. First, we find that the oplophorids included in this study, *A. purpurea* and *S. debilis*, each form a single population spanning

the eastern Gulf of Mexico and the northwest Atlantic. While this is associated with lower diversity, suggesting a lack of natural variability within each population and raising some concern over these species' health, it also indicates unimpeded gene flow between basins. This is a good prognosis for resilience in the Gulf. *Robustosergia robusta*, however, shows an opposite trend: high diversity, indicative of natural variability and species health, and population differentiation between basins suggests lower potential for resilience. The unique genetic signatures of each basin mean that, despite gene flow between basins, diversity lost within one basin could not be replenished by migration from the other basin.

CONCLUSIONS

Perhaps most critically, our results indicate separate “stories”, separate population dynamics, for each species included here. This suggests the importance of understanding the differences between the life histories and behaviors of each species. Comparatively, our results bespeak the importance of access to a major oceanographic feature of the region, the Gulf Loop Current, for determining population dynamics. However, individual organisms, populations, and species are likely far from passive particles in this process, but rather control their movement into and out of the current through diel vertical migratory behavior.

ACKNOWLEDGEMENTS

This research was made possible in part by a grant from The Gulf of Mexico Research Initiative through the Florida Institute of Oceanography to the Deep Pelagic

Nekton Dynamics of the Gulf of Mexico (DEEPEND) Consortium, as well as a Division of Environmental Biology National Science Foundation (NSF) grant awarded to HBG (DEB#1556059). Collection of samples from Bear Seamount in the North Atlantic was made possible through NOAA's National Systematics Laboratory exploratory trawling program. Funding was also provided by the Florida International University (FIU) Presidential Fellowship, the FIU Doctoral Evidence Acquisition Fellowship, and the FIU Dissertation Year Fellowship. All data are publicly available through the Gulf of Mexico Research Initiative Information & Data Cooperative (GRIIDC) at <https://data.gulfresearchinitiative.org>. We would like to specially thank Dr. Tammy Frank, Dr. Rosanna Milligan, Ms. Devan Nichols, and Mr. Richard Hartland for their support in sample collection, t-plot generation, and statistical analysis. We also thank L. E. Timm's PhD committee: Dr. José Eirin-Lopez, Dr. Mauricio Rodriguez-Lanetty, Dr. Eric von Wettberg, and Dr. Wensong Wu. We especially thank Dr. Emily Warschefsky, Dr. Shannon O'Leary, Mr. Joseph Ahrens, and Mr. Jordon Rahaman for advice and feedback on ddRADseq library prep and data assembly. Finally, we thank the anonymous reviewers for feedback on earlier versions of this manuscript. This is contribution #xx from the Center for Coastal Oceans Research in the Institute of Water and Environment at Florida International University.

LITERATURE CITED

Backus, R. H., Craddock, J. E., Haedrich, R. L., & Robison, B. H. (1977). Atlantic mesopelagic zoogeography. In *Memoirs of the Sear Foundation for Marine Research*, 266-286.

- Brierley, A. S. (2014). Diel vertical migration. *Current Biology*, 24, R1074–R1076.
- Catchen, J., Hohenlohe, P. A., Bassham, S., Amores, A., & Cresko, W. A. (2013). Stacks: An analysis tool set for population genomics. *Molecular Ecology*, 22, 3124–3140.
- Crandall, K. A., & Fitzpatrick, J. (1996). Crayfish molecular systematics: using a combination of procedures to estimate phylogeny. *Systematic Biology*, 45, 1–26.
- Cowen, R. K., & Sponaugle, S. (2009). Larval dispersal and marine population connectivity. *Annual Review of Marine Science*, 1, 443–466.
- Danovaro, R., Gambi, C., Dell’Anno, A., Corinaldesi, C., Fraschetti, S., Vanreusel, A., ... Gooday, A. J. (2008). Exponential decline of deep-sea ecosystem functioning linked to benthic biodiversity loss. *Current Biology*, 18, 1–8.
- Donaldson, H. A. (1975). Vertical distribution and feeding of sergestid shrimps (Decapoda: Natantia) collected near Bermuda. *Marine Biology*, 31, 37–50.
- Earl, D. A., & VonHoldt, B. M. (2012). STRUCTURE HARVESTER: A website and program for visualizing STRUCTURE output and implementing the Evanno method. *Conservation Genetics Resources*, 4, 359–361.
- Evanno, G., Regnaut, S., & Goudet, J. (2005). Detecting the number of clusters of individuals using the software STRUCTURE: a simulation study. *Molecular Ecology*, 14, 2611–2620.
- Flock, M. E., & Hopkins, T. L. (1992). Species composition, vertical distribution, and food habits of the sergestid shrimp. *Journal of Crustacean Biology*, 12, 210–223.
- Foll, M., & Gaggiotti, O. (2008). A genome-scan method to identify selected loci appropriate for both dominant and codominant markers: A Bayesian perspective. *Genetics*, 180, 977–993.
- Folmer, O., Hoeh, W., Black, M., & Vrijenhoek, R. C. (1994). Conserved primers for PCR amplification of mitochondrial DNA from different invertebrate phyla. *Molecular Marine Biology and Biotechnology*, 3, 294–299.
- Forristall, G. Z., Schaudt, K. J., & Cooper, C. K. (1992). Evolution and kinematics of a loop current eddy in the Gulf of Mexico during 1985. *Journal of Geophysical Research*, 97, 2173–2184.
- Foxton, P. (1970). The vertical distribution of pelagic decapods [Crustacea: Natantia] collected on the Sond Cruise 1965 II. The Penaeidea and general discussion.

Journal of the Marine Biological Association of the United Kingdom, 50, 961–1000.

- Frogliani, C., & Giannini, S. (1982). Osservazioni sugli spostamenti verticali nictemerali di *Sergestes arcticus* Kroyer e *Sergia robusta* (Smith) (Crustacea, Decapoda, Sergestidae) nel Mediterraneo Occidentale. *Atti Del Convegno Delle Unità Operative Afferenti Ai Sottoprogetti Risorse Biologiche E Inquinamento Marino*, 1, 311–319.
- Frogliani, C., & Gramitto, M. E. (2000). A new pelagic shrimp of the genus *Sergia* (Decapoda, Sergestidae) from the Atlantic Ocean. *Journal of Crustacean Biology*, 20, 71–77.
- Gaines, S., Gaylord, B., Gerber, L., Hastings, A., & Kinlan, B. (2007). Connecting places: the ecological consequences of dispersal in the sea. *Oceanography*, 20, 90–99.
- Gartner, J. V. (1988). The lanternfishes (Pisces: myctophidae) of the eastern Gulf of Mexico. *Fishery Bulletin*, 85, 81–98.
- Hamilton, P., Donohue, K., Hall, C., Leben, R., Quian, H., Sheinbaum, J., & Watts, R. (2015). *Observations and Dynamics of the Loop Current*. New Orleans, LA: U. S. Department of the Interior, Bureau of Ocean Energy Management (BOEM).
- Hellberg, M. E., Burton, R. S., Neigel, J. E., & Palumbi, S. R. (2002). Genetic assessment of connectivity among marine populations. *Bulletin of Marine Science*, 70, 273–290.
- Hughes, A. R., & Stachowicz, J. J. (2004). Genetic diversity enhances the resistance of a seagrass ecosystem to disturbance. *Proceedings of the National Academy of Sciences of the United States of America*, 101, 8998–9002.
- Jakobsson, M., & Rosenberg, N. A. (2007). CLUMPP: A cluster matching and permutation program for dealing with label switching and multimodality in analysis of population structure. *Bioinformatics*, 23, 1801–1806.
- Jombart, T., & Ahmed, I. (2011). adegenet 1.3-1: New tools for the analysis of genome-wide SNP data. *Bioinformatics*, 27, 3070–3071.
- Katoh, K., & Standley, D. M. (2013). MAFFT multiple sequence alignment software version 7: Improvements in performance and usability. *Molecular Biology and Evolution*, 30, 772–780.
- Kearse, M., Moir, R., Wilson, A., Stones-Havas, S., Cheung, M., Sturrock, S., ... Drummond, A. (2012). Geneious Basic: an integrated and extendable desktop

- software platform for the organization and analysis of sequence data. *Bioinformatics*, 28, 1647–1649.
- Kumar, S., Stecher, G., & Tamura, K. (2016). MEGA7: Molecular Evolutionary Genetics Analysis version 7.0 for bigger datasets. *Molecular Biology and Evolution*, 33, 1870–1874.
- Loose, C. J., & Dawidowicz, P. (1994). Trade-offs in diel vertical migration by zooplankton: the costs of predator avoidance. *Ecology*, 75, 2255–2263.
- MacIntosh, H., de Nys, R., & Whalan, S. (2014). Contrasting life histories in shipworms: Growth, reproductive development and fecundity. *Journal of Experimental Marine Biology and Ecology*, 459, 80–86.
- Meirmans, P. G., & Van Tienderen, P. H. (2004). GENOTYPE and GENODIVE: two programs for the analysis of genetic diversity of asexual organisms. *Molecular Ecology Notes*, 4, 792–794.
- Milligan, R., Cook, A., Johnston, M., & Sutton, T. (in prep). The impact of warm core eddies on the structure of deep-pelagic fish fauna in the Gulf of Mexico.
- Oey, L.-Y., Ezer, T., & Lee, H.-C. (2005). Loop Current, Rings, and Related Circulation in the Gulf of Mexico: A Review of Numerical Models and Future Challenges. In W. Sturges & A. Lugo-Fernandez (Eds.), *Circulation in the Gulf of Mexico: Observations and Models* (Vol. 161, pp. 31–56). Washington, DC: American Geophysical Union.
- Palumbi, S. R. (2003). Population genetics, demographic connectivity, and the design of marine reserves. *Ecological Applications*, 13, S146–S158.
- Palumbi, S., Martin, A., Romano, S., McMillan, W. O., Stice, L., & Grabowski, G. (2002). *The Simple Fool's Guide to PCR, version 2*. Honolulu: University of Hawaii.
- Peterson, B. K., Weber, J. N., Kay, E. H., Fisher, H. S., & Hoekstra, H. E. (2012). Double digest RADseq: an inexpensive method for de novo SNP discovery and genotyping in model and non-model species. *PloS One*, 7, e37135.
- Pritchard, J. K., Stephens, M., & Donnelly, P. (2000). Inference of population structure using multilocus genotype data. *Genetics*, 155, 945–959.
- Ramirez Llodra, E. (2002). Fecundity and life-history strategies in marine invertebrates. *Advances in Marine Biology*, 43, 87–170.

- Rosenberg, N. A. (2004). DISTRUCT: A program for the graphical display of population structure. *Molecular Ecology Notes*, 4, 137–138.
- Shanks, A. L. (2009). Pelagic larval duration and dispersal distance revisited. *The Biological Bulletin*, 216, 373–385.
- Sutton, T. T., Clark, M. R., Dunn, D. C., Halpin, P. N., Rogers, A. D., Guinotte, J., ... Heino, M. (2017). A global biogeographic classification of the mesopelagic zone. *Deep-Sea Research Part I: Oceanographic Research Papers*, 126, 85–102.
- Timm, L. E.*, Judkins, H.*, Sosnowski, A., Breitbart, M., Vecchione, M., & Bracken-Grissom, H. D. (in prep). *Evolutionary Bioinformatics*. Invited manuscript. *co-first authors.
- Timm, L. E., Sosnowski, A., Judkins, H., & Bracken-Grissom H. D. (2018a). DEEPEND: raw ddRADseq data, in fastq format, for population genomic analysis of the cephalopod species *Cranchia scabra*, *Pyroteuthis margaritifera*, and *Vampyroteuthis infernalis*. Distributed by: Gulf of Mexico Research Initiative nad Data Cooperative (GRIIDC), Harte Research Institute, Texas A&M University – Corpus Christi.
- Timm, L. E., Isma, L., & Bracken-Grissom H. D. (2018b). DEEPEND: raw ddRADseq data, in fastq format, for comparative population genomic analysis of the mesopelagic shrimp species *Acantheephyra purpurea*, *Systellaspis debilis*, and *Sergia robusta*; as well as single-locus barcode sequences (16S ribosomal subunit and cytochrome c oxidase subunit I) for every individual included in the ddRADseq data set.. Distributed by: Gulf of Mexico Research Initiative nad Data Cooperative (GRIIDC), Harte Research Institute, Texas A&M University – Corpus Christi.
- Venables, W. N., & Ripley, B. D. (2002). *Modern Applied Statistics with S* (Fourth). New York: Springer.

Tables

Table 1. The primer pairs and annealing temperatures associated with PCR amplification of two mitochondrial genes targeted for DNA barcoding of samples included in the ddRADseq library preparations.

Targeted Gene	Forward Primer (5' to 3')	Reverse Primer (5' to 3')	Anneal Temp
16S	16S-L2/L9 TGCCTGTTTATCAAAAACAT CGCCTGTTTATCAAAAACAT (Palumbi et al., 2002)	16S-1472 AGATAGAAACCAACCTGG (Crandall & Fitzpatrick, 1996)	58.9°C (<i>A. purpurea</i>) 46.0°C (<i>S. debilis</i>)
COI	LCOI-1472 GGTCAACAAATCACAAAGATATTG (Folmer et al., 1994)	HCOI-2198 TAAACTTCAGGGTGACCAAAAATCA (Folmer et al., 1994)	40.0°C – 41.5°C

Table 2. Details of ddRADseq protocol for each species, including enzymes, custom-made barcoded-adapter sequences, and size selection schemes. Both strands of each adapter are given (1.1 and 1.2) in the 5' to 3' direction. These strands are annealed prior to ligation to the ddRADseq fragments. The barcode section of the adapter is underlined. Note that the overhang in the 1.1 strands differs between the “oplo” and the “flex” adapters. Illumina i7 adapters were also used, specifically index 1, 3, 7, 12, 13, 16, 21, 24, 29, 37, 42, and 43.

Species	Enzyme 1	Enzyme 2	Adapter	Strand	Sequence (5' to 3')	Targeted Size
<i>Acanthephyra purpurea</i>	SbfI	NotI	oplo1	1.1	ACACTCTTTCCTACACGACGCTCTTCCGATCTCCAGAGTGTGGCC	Tight 475
				1.2	<u>ACACTCTGGAGATCGGAAGAGCGTCGTGTAGGGAAAGAGTGT</u>	
			oplo2	1.1	ACACTCTTTCCTACACGACGCTCTTCCGATCTTGAGCGACTGGCC	
				1.2	<u>AGTCGCTCAAGATCGGAAGAGCGTCGTGTAGGGAAAGAGTGT</u>	
			oplo3	1.1	ACACTCTTTCCTACACGACGCTCTTCCGATCTGGTCTCTGGGCC	
				1.2	<u>CAGAGACCAAGATCGGAAGAGCGTCGTGTAGGGAAAGAGTGT</u>	
			oplo4	1.1	ACACTCTTTCCTACACGACGCTCTTCCGATCTGTAATCCAGGGCC	
				1.2	<u>CTGGATTACAGATCGGAAGAGCGTCGTGTAGGGAAAGAGTGT</u>	
<i>Systellaspis debilis</i>	SbfI	NotI	oplo5	1.1	ACACTCTTTCCTACACGACGCTCTTCCGATCTGAATGCGTCGGCC	Tight 275
				1.2	<u>GACGCATTCAAGATCGGAAGAGCGTCGTGTAGGGAAAGAGTGT</u>	
			oplo6	1.1	ACACTCTTTCCTACACGACGCTCTTCCGATCTATCAGTGACGGCC	
				1.2	<u>GTCACTGATAGATCGGAAGAGCGTCGTGTAGGGAAAGAGTGT</u>	
			oplo7	1.1	ACACTCTTTCCTACACGACGCTCTTCCGATCTCACCGACTAGGCC	
				1.2	<u>TAGTCGGTGAGATCGGAAGAGCGTCGTGTAGGGAAAGAGTGT</u>	

			oplo8	1.1	ACACTCTTTCCCTACACGACGCTCTTCCGATCTGACGCGTGAGGCC	
				1.2	TCACGCGTCAGATCGGAAGAGCGTCGTGTAGGGAAAGAGTGT	
<i>Robustosergia robusta</i>	EcoRI	NlaIII	flex1	1.1	ACACTCTTTCCCTACACGACGCTCTTCCGATCTCCAGAGTGCATG	Tight 475
				1.2	ACACTCTGGAGATCGGAAGAGCGTCGTGTAGGGAAAGAGTGT	
			flex2	1.1	ACACTCTTTCCCTACACGACGCTCTTCCGATCTGAGCGACTCATG	
				1.2	AGTCGCTCAAGATCGGAAGAGCGTCGTGTAGGGAAAGAGTGT	
			flex3	1.1	ACACTCTTTCCCTACACGACGCTCTTCCGATCTGGTCTCTGCATG	
				1.2	CAGAGACCAAGATCGGAAGAGCGTCGTGTAGGGAAAGAGTGT	
			flex4	1.1	ACACTCTTTCCCTACACGACGCTCTTCCGATCTGTAATCCAGCATG	
				1.2	CTGGATTACAGATCGGAAGAGCGTCGTGTAGGGAAAGAGTGT	
			flex5	1.1	ACACTCTTTCCCTACACGACGCTCTTCCGATCTGAATGCGTCCATG	
				1.2	GACGCATTGAGATCGGAAGAGCGTCGTGTAGGGAAAGAGTGT	
			flex6	1.1	ACACTCTTTCCCTACACGACGCTCTTCCGATCTATCAGTGACCATG	
				1.2	GTCACTGATAGATCGGAAGAGCGTCGTGTAGGGAAAGAGTGT	
			flex7	1.1	ACACTCTTTCCCTACACGACGCTCTTCCGATCTACCCGACTACATG	
				1.2	TAGTCGGTGAGATCGGAAGAGCGTCGTGTAGGGAAAGAGTGT	
			flex8	1.1	ACACTCTTTCCCTACACGACGCTCTTCCGATCTGACGCGTGACATG	
				1.2	TCACGCGTCAGATCGGAAGAGCGTCGTGTAGGGAAAGAGTGT	

Table 3. Diversity indices, including the inbreeding coefficient (Gis), observed heterozygosity (Ho), and expected heterozygosity (He), for the three targeted species: *Acanthephyra purpurea*, *Systellaspis debilis*, and *Robustosergia robusta*.

	Gis				Ho				He			
	Overall	Atlantic	FL Straits	Gulf	Overall	Atlantic	FL Straits	Gulf	Overall	Atlantic	FL Straits	Gulf
<i>A. purpurea</i>	0.534	0.500	0.502	0.614	0.057	0.058	0.063	0.044	0.122	0.116	0.127	0.114
<i>S. debilis</i>	0.425	0.126	0.582	0.510	0.054	0.070	0.039	0.048	0.094	0.080	0.093	0.098
<i>R. robusta</i>	0.146	0.148	---	0.143	0.089	0.090	---	0.089	0.104	0.105	---	0.104

Table 4. Results of testing for correlation between surface/epipelagic abundance (“SA”, here defined as above 600m) and three diversity metrics: inbreeding coefficient (Gis), expected heterozygosity (He), and observed heterozygosity (Ho). R^2 is taken from the trendline and has been discussed in a previous figure. Pearson’s index ranges from -1 (strong negative/indirect correlation) to 1 (strong positive/direct correlation) with values closer to 0 indicating weak correlation. However, Pearson is a parametric test. As our data are not normally distributed, Spearman’s r_s and Kendall’s τ (non-parametric tests) were also carried out. Spearman’s r_s is interpreted in the same way as Pearson’s index, but when $|r_s| > 0.5$, the correlation is considered strong. Here, this is indicated with *. Kendall’s τ is compared to a critical value. When $|\tau| >$ critical value, correlation is not significant (“Not sig”, in table). When $|\tau| \leq$ critical value, correlation is significant (“Sig”).

	R^2	Pearson	Spearman	Kendall
SA x Gis	0.073	0.27	-0.543*	Not sig
SA x He	0.494	-0.703	-0.543*	Not sig
SA x Ho	0.868	-0.932	-0.942*	Sig

Figure Captions

Figure 1. The general route of the Gulf Loop Current in the Gulf of Mexico. Image taken from NASA's Earth Observatory/U.S. Naval Research Laboratory. Arrows indicate direction of flow and colors represent speed with warmer colors denoting faster speeds (see legend).

Figure 2. Results taken from Timm & Judkins et al., 2018. TOP: the targeted species, from left-to-right, *Cranchia scabra* Leach, 1817, *Pyroteuthis margaritifera* (Rüppell, 1884), and *Vampyroteuthis infernalis* Chun, 1903 (Photo credit: Dr. Danté Fenolio). MIDDLE: relative abundance, indicated by bar length, is plotted by depth (in meters) and solar cycle ("Day" is represented by gray or white bars to the left; "Night" is represented by black bars to the right). BOTTOM: results of Principal Component Analyses are presented for each species. For the species with high surface abundance (*C. scabra* and *P. margaritifera*), individuals form a single cluster within the PCA. However, *V. infernalis*, which has low surface abundance forms two non-basin-specific clusters.

Figure 3. TOP: from left-to-right, three species of mesopelagic shrimp targeted in this study, including the oplophorids *Acanthephyra purpurea* A. Milne-Edwards, 1888 and *Systellaspis debilis* (A. Milne-Edwards, 1888), and the sergestid *Robustosergia robusta* (Smith, 1882) (Photo credit: Dr. Danté Fenolio). BOTTOM: relative abundance, indicated by bar length, is plotted by depth (in meters) and solar cycle ("Day" is represented by gray or white bars to the left; "Night" is represented by black bars to the right).

Figure 4. A map of sites sampled over the course of four Deep Pelagic Nekton Dynamics of the Gulf of Mexico (DEEPEND) cruises which took place in 2015 and 2016.

Figure 5. This graph depicts the different diversity indices (observed heterozygosity in blue, expected heterozygosity in green, and inbreeding coefficient in grey) for *Acanthephyra purpurea*, *Systellaspis debilis*, and *Robustosergia robusta*.

Figure 6. Across the top, diversity (reported as expected heterozygosity) is compared between basins (Atlantic in grey, Florida Straits in blue, and Gulf of Mexico in pink) for *Acanthephyra purpurea*, *Systellaspis debilis*, and *Robustosergia robusta*. Below, three diversity indices (observed heterozygosity, expected heterozygosity, and inbreeding coefficient) are given for each basin. The red-themed graph depicts interbasin diversity for *A. purpurea*, blue-themed for *S. debilis*, and purple-themed for *R. robusta*.

Figure 7. Results of the hierarchical AMOVAs conducted to characterize genetic variation among individuals ($F_{IT} = 71.9\% - 83.9\%$), among individuals within populations ($F_{IS} = 11.9\% - 19.4\%$), and among populations ($F_{ST} = 0\% - 16.2\%$). The Infinite Allele Model was used with 999 permutations to assess statistical significance, which is reported in parentheses. Any missing data was replaced with randomly drawn alleles determined by the overall allele frequencies of the data set. AMOVA results indicate the vast majority of variance is due to differences between individuals (F_{IT}), regardless of the region from which they were sampled. * indicates $p\text{-value} < 0.05$.

Figure 8. DISTRUCT plots, Principal Component Analyses (PCAs), and multidimensional scaling (MDS) heat maps for *Acanthephyra purpurea*, *Systellaspis debilis*, and *Robustosergia robusta*.

TOP: Population membership plots built on k-means clustering analyses of (from left to right) *A. purpurea*, *S. debilis*, and *R. robusta*. The *A. purpurea* and *S. debilis* plots are divided into samples collected from the Atlantic, Florida Straits, and Gulf of Mexico. The *R. robusta* plot does not include any individuals from the Florida Straits. Using STRUCTURE, $k = 1-7$ were tested ten times each, with 20,000 generations of burn-in and an additional 200,000 MCMC generations. After analysis, the optimal k was chosen using Evanno and deltaK in STRUCTURE HARVESTER. The optimal k value is reported alongside the DISTRUCT plot.

MIDDLE: PCAs plotted in R using the adegenet package. Here, we see individuals of *A. purpurea* and *S. debilis* each form a single cluster. Individuals of *R. robusta* form two basin-specific clusters: a cluster of individuals from the Atlantic and a cluster from the Gulf of Mexico.

BOTTOM: MDS plots built on genetic distance between individuals of (from left to right) *A. purpurea*, *S. debilis*, and *R. robusta*. Plots are colored with heat maps, in which similarity is colored with warmer colors and distance is colored with colder colors. These heat maps strongly agree with the PCAs: individuals of *A. purpurea* and *S. debilis* are assigned to large single-clusters while individuals of *R. robusta* are arranged in two clusters.

Figure 9. TOP: species included in testing for correlation in increasing order of surface/epipelagic abundance. From left to right: *Vampyroteuthis infernalis*, *Robustosergia robusta*, *Pyroteuthis margaritifera*, *Cranchia scabra*, *Acantheephyra purpurea*, and *Systellaspis debilis*.

UPPER MIDDLE: T-plots of discrete depth abundances for each species, divided by solar cycle (day to the left and night to the right). LOWER MIDDLE: Principal Component Analyses for each species. BOTTOM: graph relating genetic diversity (inbreeding coefficient [Gis] in blue, expected heterozygosity [He] in red, and observed heterozygosity [Ho] in purple) to abundance in the surface/epipelagic (here, we define this as above 600m). We find an indirect relationship, with diversity decreasing as the percent of individuals found in the surface/epipelagic increases. This correlation is strongest in Ho ($R^2=0.87$) compared to He ($R^2=0.49$) and Gis ($R^2=0.073$).

Figures

Figure 1

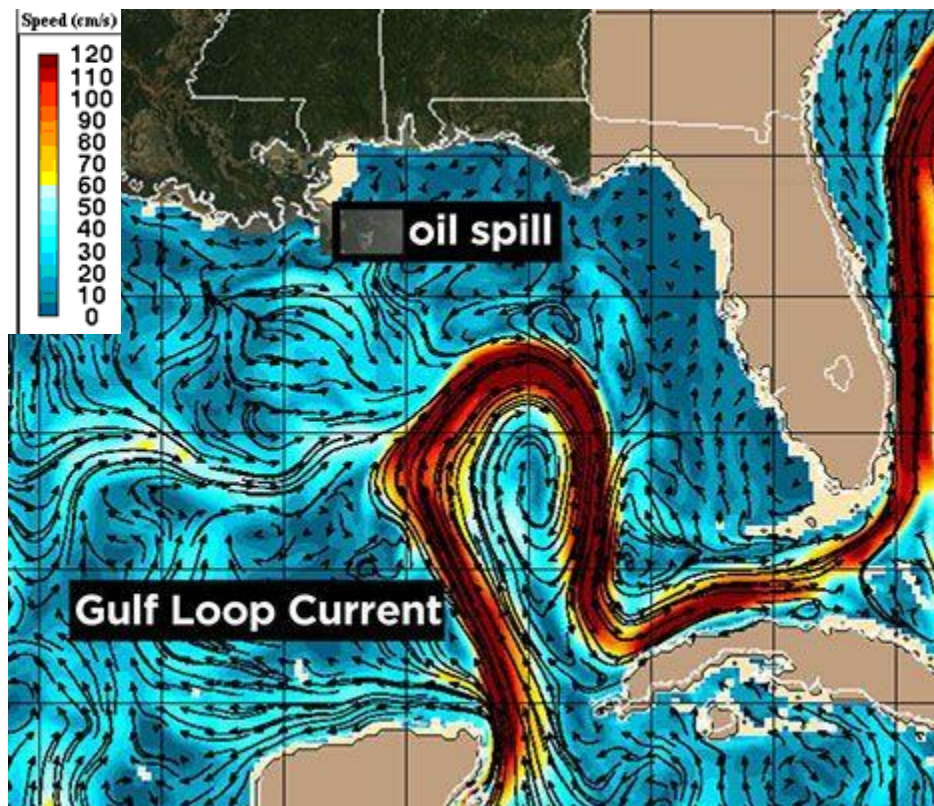


Figure 2

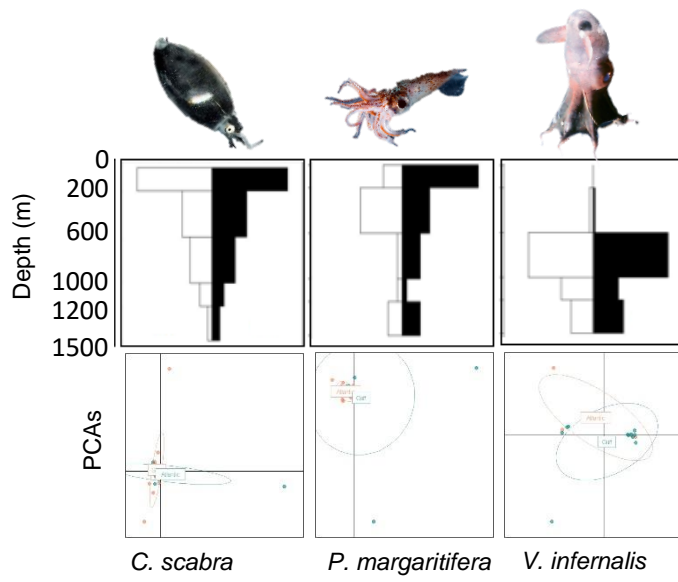


Figure 3

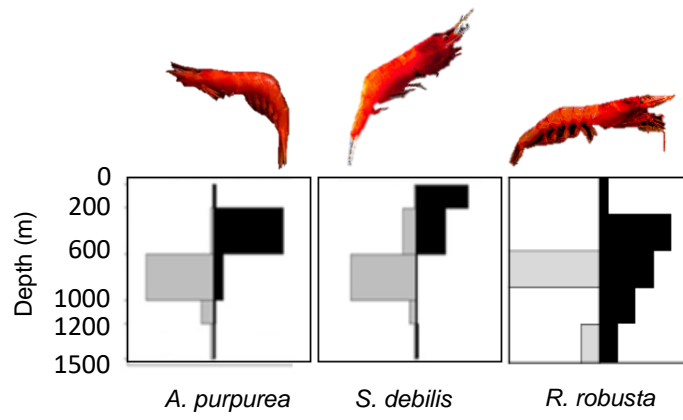


Figure 4

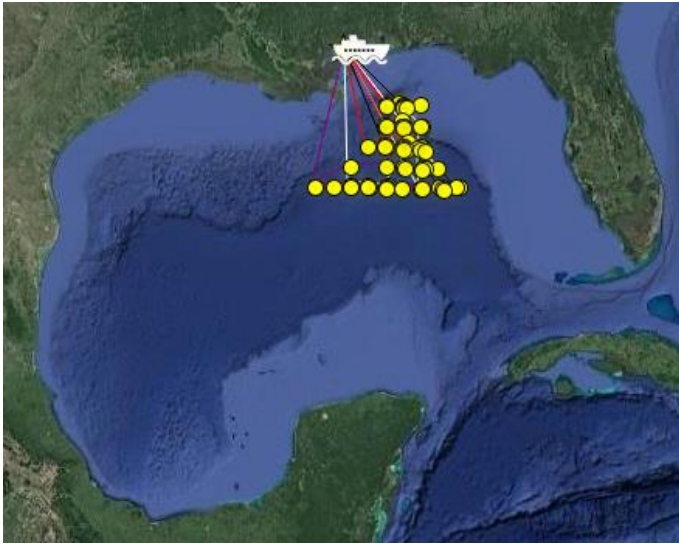


Figure 5

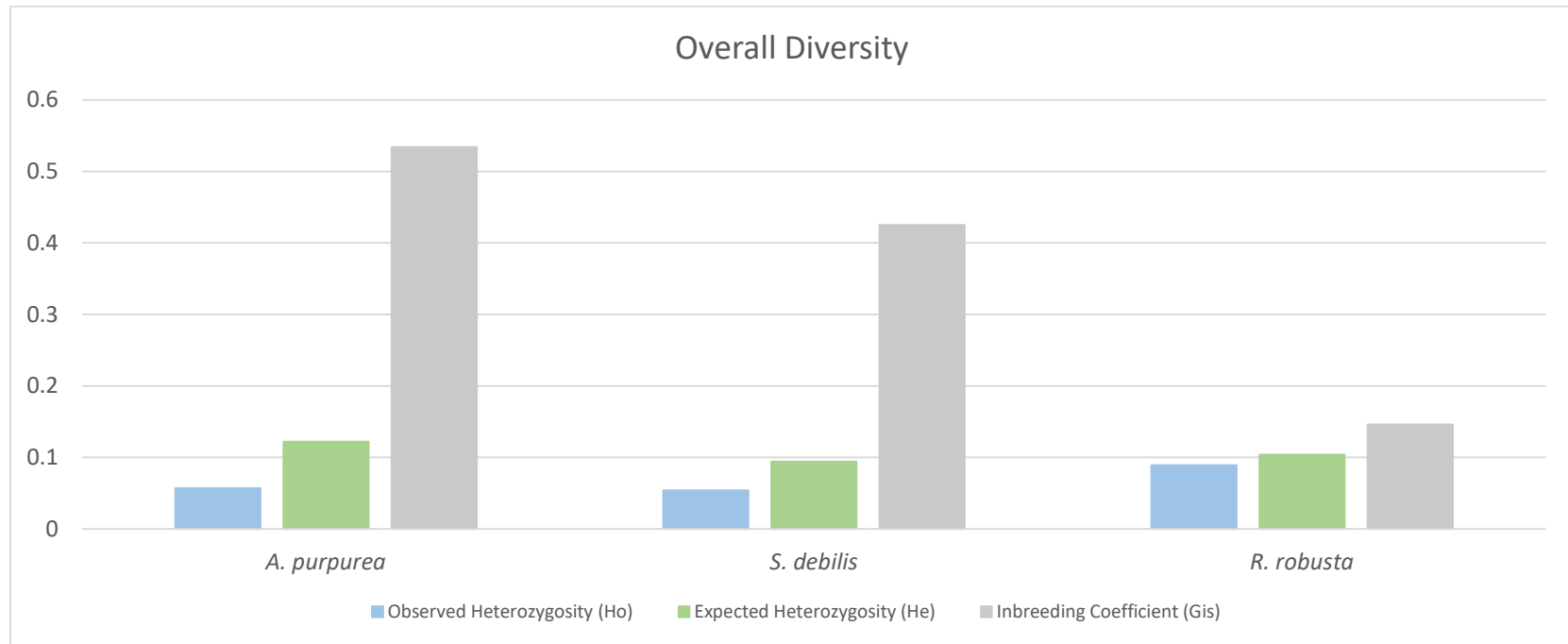


Figure 6

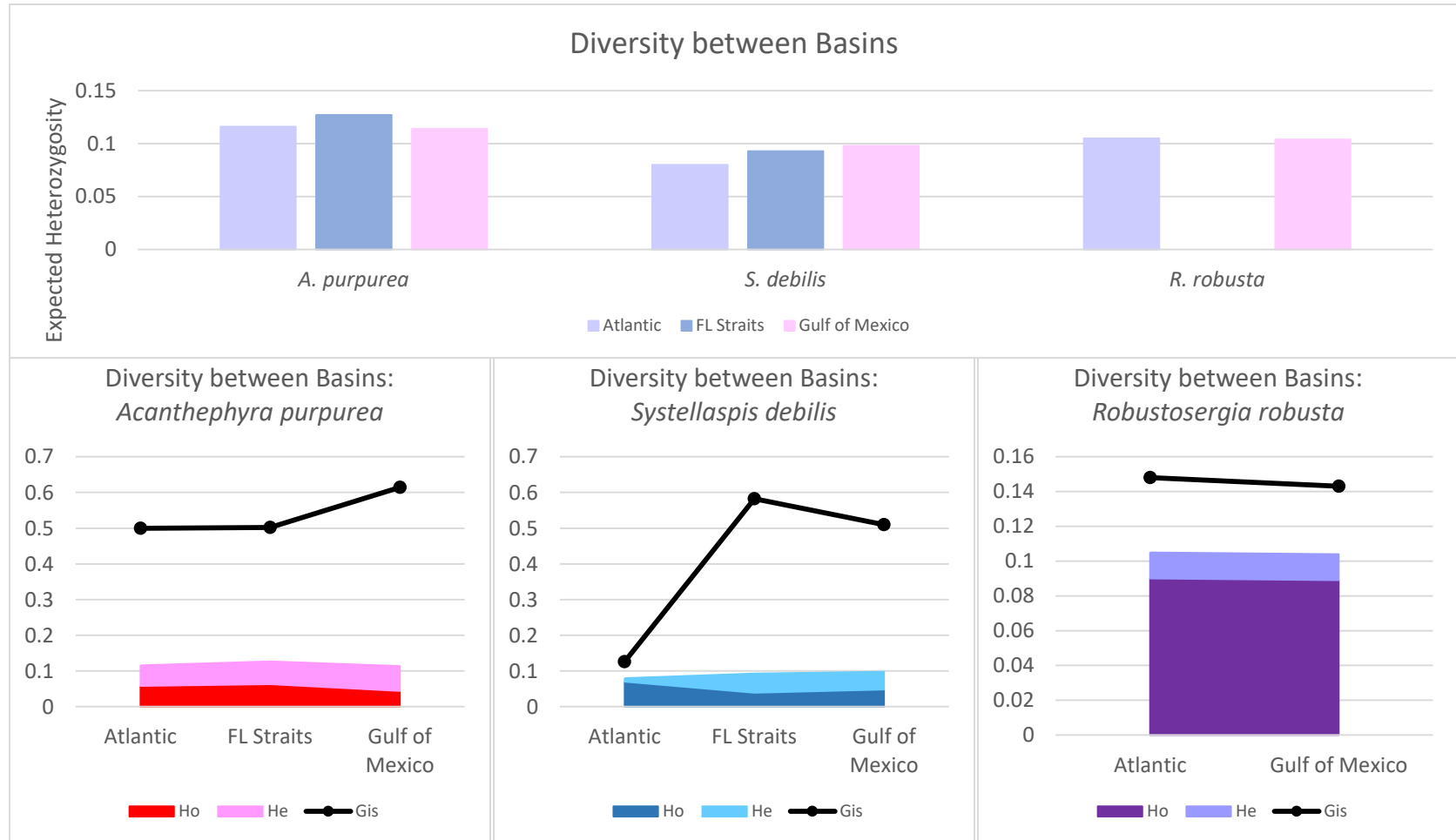


Figure 7

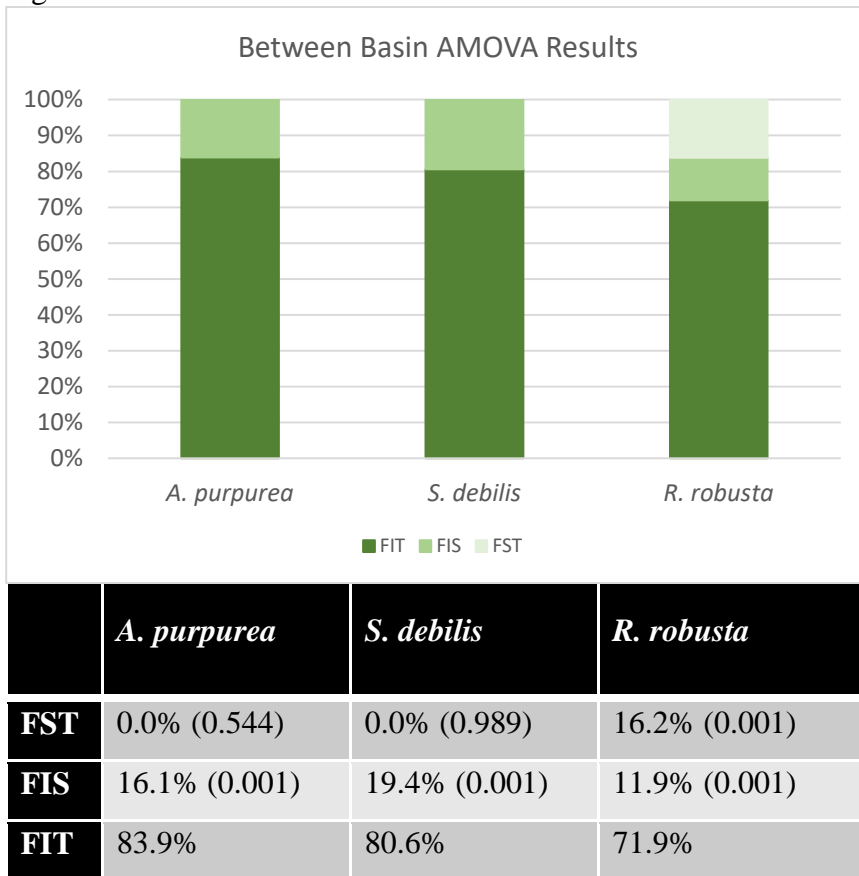


Figure 8

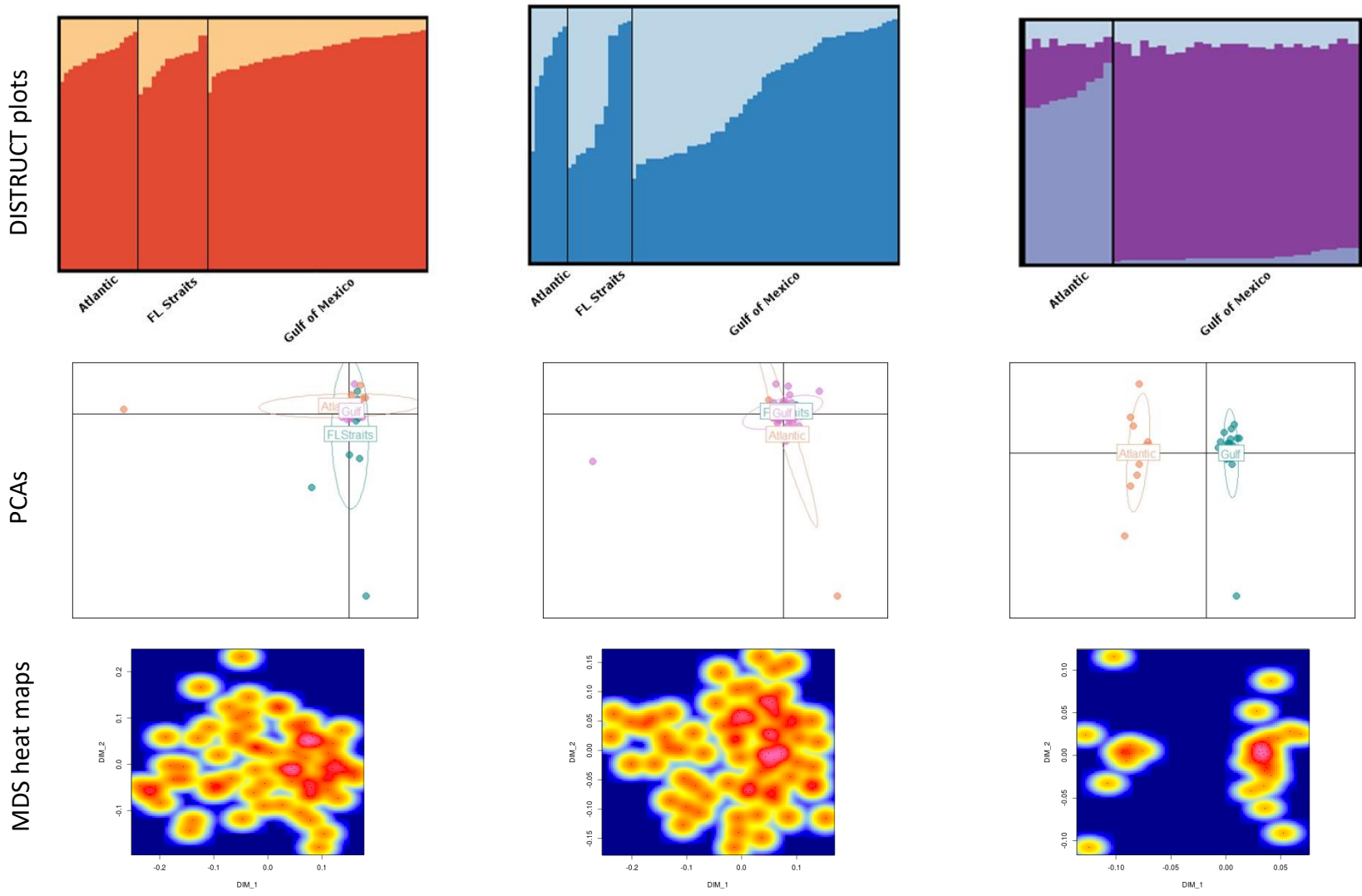
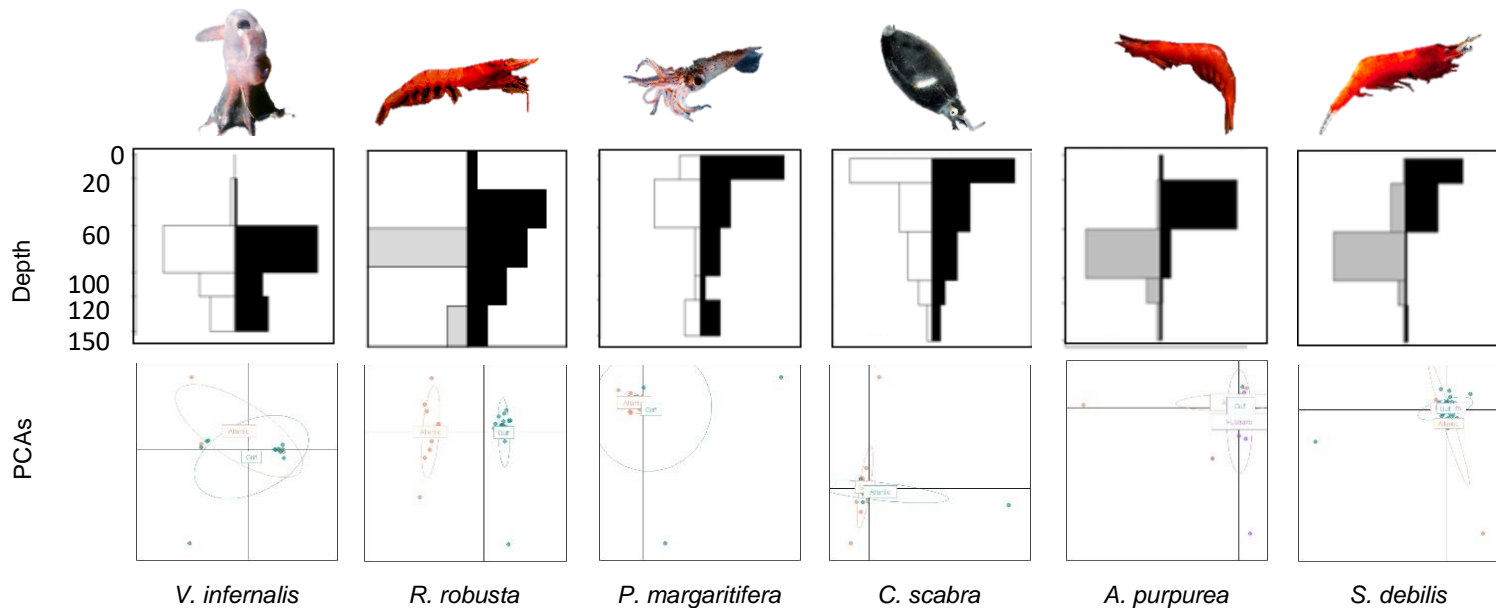
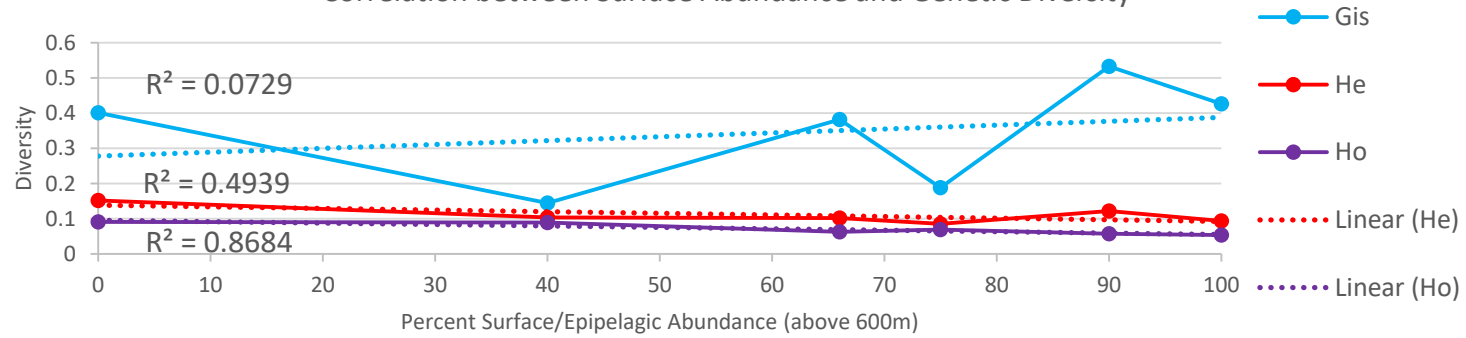


Figure 9



Correlation between Surface Abundance and Genetic Diversity



Appendices Captions

Appendix 1. Metadata for all samples included in this study, including: the Illumina i7 index and custom barcode (see Table 2) combination, listed under “Idx-BC”, HBG number, species, date and basin of collection, as well as the Station ID and coordinates for the collection site, and the depth range from which the sample was collected. The gene targeted for Sanger sequencing, to be used for DNA barcoding to confirm taxonomic identification, was either the 16S small ribosomal subunit (16S) or cytochrome c oxidase subunit I (COI). This is reported under “Gene” and the associated GenBank Accession number is also listed.

Appendices

Appendix 1

Idx-BC	HBG #	Species	Collection Date	Basin	Lat	Lon	Depth (m)	Gene
1-1	HBG5984	<i>A. purpurea</i>	July 18, 2016	Florida Straits	25.42°N	-79.59°W	275 - 250	16S
1-2	HBG5478	<i>A. purpurea</i>	May 2, 2016	Gulf of Mexico	27.99°N	-87.50°W	200 - 600	16S
1-3	HBG6185	<i>A. purpurea</i>	August 16, 2016	Gulf of Mexico	28.01°N	-87.51°W	0 - 1500	16S
1-4	HBG5277	<i>A. purpurea</i>	October 16, 2014	Atlantic Ocean	39.83°N	-67.41°W	2159 - 2731	16S
1-5	HBG4402	<i>A. purpurea</i>	August 14, 2015	Gulf of Mexico	27.91°N	-87.42°W	0 - 1500	16S
1-6	HBG4351	<i>A. purpurea</i>	August 10, 2015	Gulf of Mexico	27.02°N	-89.00°W	600 - 1000	16S
1-7	HBG4313	<i>A. purpurea</i>	August 11, 2015	Gulf of Mexico	27.00°N	-88.00°W	0 - 1500	16S
1-8	HBG3583	<i>A. purpurea</i>	May 1, 2015	Gulf of Mexico	29.00°N	-87.01°W	200 - 600	16S
3-1	HBG3025	<i>A. purpurea</i>	October 23, 2014	Atlantic Ocean	39.79°N	-67.38°W	3041 - 3051	16S
3-2	HBG3481	<i>A. purpurea</i>	May 5, 2015	Gulf of Mexico	28.00°N	-87.46°W	0 - 1500	16S
3-3	HBG4314	<i>A. purpurea</i>	August 11, 2015	Gulf of Mexico	27.00°N	-88.00°W	0 - 1500	16S
3-4	HBG6170	<i>A. purpurea</i>	August 12, 2016	Gulf of Mexico	26.93°N	-89.43°W	0 - 600	16S
3-5	HBG6172	<i>A. purpurea</i>	August 14, 2016	Gulf of Mexico	27.52°N	-89.00°W	0 - 1500	16S
3-6	HBG5287	<i>A. purpurea</i>	October 16, 2014	Atlantic Ocean	39.83°N	-67.41°W	2159 - 2731	16S
3-7	HBG5482	<i>A. purpurea</i>	May 3, 2016	Gulf of Mexico	28.00°N	-87.50°W	0 - 1500	16S
3-8	HBG5985	<i>A. purpurea</i>	July 18, 2016	Florida Straits	25.42°N	-79.59°W	275 - 250	16S
7-1	HBG5986	<i>A. purpurea</i>	July 19, 2016	Florida Straits	25.42°N	-79.59°W	750 - 520	16S
7-2	HBG5289	<i>A. purpurea</i>	October 20, 2014	Atlantic Ocean	39.84°N	-67.36°W	1657 - 2606	16S
7-3	HBG6168	<i>A. purpurea</i>	August 12, 2016	Gulf of Mexico	26.93°N	-89.43°W	0 - 1500	16S
7-4	HBG3537	<i>A. purpurea</i>	May 3, 2015	Gulf of Mexico	28.66°N	-87.55°W	1000 - 1200	16S
7-5	HBG3026	<i>A. purpurea</i>	October 23, 2014	Atlantic Ocean	39.79°N	-67.38°W	3041 - 3051	16S
7-6	HBG4360	<i>A. purpurea</i>	August 10, 2015	Gulf of Mexico	27.01°N	-88.50°W	0 - 1500	16S
7-7	HBG4361	<i>A. purpurea</i>	August 10, 2015	Gulf of Mexico	27.01°N	-88.50°W	600 - 1000	16S

7-8	HBG5487	<i>A. purpurea</i>	May 2, 2016	Gulf of Mexico	27.96°N	-88.00°W	600 - 1000	16S
12-1	HBG3640	<i>A. purpurea</i>	May 7, 2015	Gulf of Mexico	28.00°N	-88.50°W	0 - 1500	16S
12-2	HBG4343	<i>A. purpurea</i>	August 10, 2015	Gulf of Mexico	27.02°N	-89.00°W	0 - 1500	16S
12-3	HBG5290	<i>A. purpurea</i>	October 20, 2014	Atlantic Ocean	39.84°N	-67.36°W	1657 - 2606	16S
12-4	HBG5987	<i>A. purpurea</i>	July 18, 2016	Florida Straits	25.42°N	-79.59°W	275 - 250	16S
12-5	HBG5737	<i>A. purpurea</i>	May 2, 2016	Gulf of Mexico	27.96°N	-87.99°W	0 - 1500	16S
12-6	HBG6178	<i>A. purpurea</i>	August 15, 2016	Gulf of Mexico	27.52°N	-87.98°W	0 - 1500	16S
12-7	HBG6197	<i>A. purpurea</i>	August 18, 2016	Gulf of Mexico	29.02°N	-87.55°W	0 - 1000	16S
12-8	HBG5288	<i>A. purpurea</i>	October 20, 2014	Atlantic Ocean	39.84°N	-67.36°W	1657 - 2606	16S
13-1	HBG5988	<i>A. purpurea</i>	July 18, 2016	Florida Straits	25.42°N	-79.59°W	275 - 250	16S
13-2	HBG5860	<i>A. purpurea</i>	May 8, 2016	Gulf of Mexico	26.97°N	-86.67°W	0 - 1500	16S
13-3	HBG6167	<i>A. purpurea</i>	August 12, 2016	Gulf of Mexico	26.93°N	-89.43°W	0 - 1500	16S
13-4	HBG3603	<i>A. purpurea</i>	May 2, 2015	Gulf of Mexico	29.00°N	-87.01°W	200 - 600	16S
13-5	HBG4368	<i>A. purpurea</i>	August 10, 2015	Gulf of Mexico	27.01°N	-88.50°W	200 - 600	16S
13-6	HBG5274	<i>A. purpurea</i>	October 16, 2014	Atlantic Ocean	39.83°N	-67.41°W	2159 - 2731	16S
13-7	HBG4520	<i>A. purpurea</i>	August 18, 2015	Gulf of Mexico	27.48°N	-87.00°W	0 - 1500	16S
13-8	HBG5291	<i>A. purpurea</i>	October 20, 2014	Atlantic Ocean	39.84°N	-67.36°W	1657 - 2606	16S
16-1	HBG4472	<i>A. purpurea</i>	August 17, 2015	Gulf of Mexico	27.91°N	-86.95°W	200 - 600	16S
16-2	HBG5896	<i>A. purpurea</i>	May 7, 2016	Gulf of Mexico	26.92°N	-86.62°W	602.8 - 197.8	16S
16-3	HBG4304	<i>A. purpurea</i>	August 11, 2015	Gulf of Mexico	27.00°N	-88.00°W	600 - 1000	16S
16-4	HBG4421	<i>A. purpurea</i>	August 13, 2015	Gulf of Mexico	27.46°N	-87.47°W	600 - 1000	16S
16-5	HBG5981	<i>A. purpurea</i>	July 19, 2016	Florida Straits	25.42°N	-79.59°W	750 - 520	16S
16-6	HBG5275	<i>A. purpurea</i>	October 16, 2014	Atlantic Ocean	39.83°N	-67.41°W	2159 - 2731	16S
16-7	HBG5991	<i>A. purpurea</i>	July 20, 2016	Florida Straits	25.38°N	-79.46°W	790 - 500	16S
16-8	HBG6199	<i>A. purpurea</i>	August 18, 2016	Gulf of Mexico	29.04°N	-87.46°W	0 - 1500	16S
21-1	HBG4519	<i>A. purpurea</i>	August 18, 2015	Gulf of Mexico	27.48°N	-87.00°W	0 - 1500	16S
21-2	HBG5445	<i>A. purpurea</i>	May 4, 2016	Gulf of Mexico	27.89°N	-86.88°W	200 - 600	16S

21-3	HBG5982	<i>A. purpurea</i>	July 19, 2016	Florida Straits	25.42°N	-79.59°W	750 - 520	16S
21-4	HBG4390	<i>A. purpurea</i>	August 14, 2015	Gulf of Mexico	28.47°N	-87.46°W	200 - 600	16S
21-5	HBG5989	<i>A. purpurea</i>	July 19, 2016	Florida Straits	25.42°N	-79.59°W	750 - 520	16S
21-6	HBG4453	<i>A. purpurea</i>	August 12, 2015	Gulf of Mexico	27.49°N	-87.49°W	0 - 1500	16S
21-7	HBG5990	<i>A. purpurea</i>	July 19, 2016	Florida Straits	25.42°N	-79.59°W	750 - 520	16S
21-8	HBG5276	<i>A. purpurea</i>	October 16, 2014	Atlantic Ocean	39.83°N	-67.41°W	2159 - 2731	16S
24-1	HBG4454	<i>A. purpurea</i>	August 12, 2015	Gulf of Mexico	27.49°N	-87.49°W	200 - 600	16S
24-2	HBG6174	<i>A. purpurea</i>	August 14, 2016	Gulf of Mexico	27.51°N	-89.01°W	0 - 1500	16S
24-3	HBG4536	<i>A. purpurea</i>	August 20, 2015	Gulf of Mexico	27.47°N	-86.54°W	0 - 1500	16S
24-4	HBG6005	<i>A. purpurea</i>	August 7, 2016	Gulf of Mexico	26.89°N	-89.04°W	0 - 1500	16S
24-5	HBG5994	<i>A. purpurea</i>	July 20, 2016	Florida Straits	25.25°N	-79.48°W	550 - 200	16S
24-7	HBG5995	<i>A. purpurea</i>	July 20, 2016	Florida Straits	25.25°N	-79.48°W	550 - 200	16S
29-1	HBG6000	<i>A. purpurea</i>	August 6, 2016	Gulf of Mexico	26.99°N	-89.99°W	0 - 1500	16S
29-2	HBG6154	<i>A. purpurea</i>	August 10, 2016	Gulf of Mexico	27.01°N	-87.49°W	0 - 1000	16S
29-3	HBG4499	<i>A. purpurea</i>	August 20, 2015	Gulf of Mexico	26.94°N	-87.00°W	0 - 1500	16S
29-5	HBG6186	<i>A. purpurea</i>	August 16, 2016	Gulf of Mexico	28.01°N	-87.51°W	0 - 1500	16S
29-7	HBG5992	<i>A. purpurea</i>	July 20, 2016	Florida Straits	25.25°N	-79.48°W	550 - 200	16S
29-8	HBG4487	<i>A. purpurea</i>	August 19, 2015	Gulf of Mexico	26.93°N	-87.02°W	0 - 1500	16S
37-1	HBG6190	<i>A. purpurea</i>	August 17, 2016	Gulf of Mexico	28.52°N	-87.53°W	0 - 1500	16S
37-2	HBG5283	<i>A. purpurea</i>	October 16, 2014	Atlantic Ocean	39.83°N	-67.41°W	2159 - 2731	16S
37-4	HBG5278	<i>A. purpurea</i>	October 16, 2014	Atlantic Ocean	39.83°N	-67.41°W	2159 - 2731	16S
37-5	HBG6022	<i>A. purpurea</i>	August 9, 2016	Gulf of Mexico	27.01°N	-86.98°W	0 - 1500	16S
37-6	HBG5993	<i>A. purpurea</i>	July 20, 2016	Florida Straits	25.25°N	-79.48°W	550 - 200	16S
37-7	HBG6171	<i>A. purpurea</i>	August 12, 2016	Gulf of Mexico	26.93°N	-89.43°W	0 - 600	16S
37-8	HBG5292	<i>A. purpurea</i>	October 20, 2014	Atlantic Ocean	39.84°N	-67.36°W	1657 - 2606	16S
42-1	HBG6011	<i>A. purpurea</i>	August 8, 2016	Gulf of Mexico	27.02°N	-87.98°W	0 - 1500	16S
42-2	HBG5293	<i>A. purpurea</i>	October 20, 2014	Atlantic Ocean	39.84°N	-67.36°W	1657 - 2606	16S

42-3	HBG6179	<i>A. purpurea</i>	August 15, 2016	Gulf of Mexico	27.52°N	-87.98°W	0 - 1500	16S
42-4	HBG5294	<i>A. purpurea</i>	October 20, 2014	Atlantic Ocean	39.84°N	-67.36°W	1657 - 2606	16S
42-5	HBG6191	<i>A. purpurea</i>	August 17, 2016	Gulf of Mexico	28.52°N	-87.53°W	0 - 1500	16S
42-6	HBG5279	<i>A. purpurea</i>	October 16, 2014	Atlantic Ocean	39.83°N	-67.41°W	2159 - 2731	16S
42-7	HBG4488	<i>A. purpurea</i>	August 19, 2015	Gulf of Mexico	26.93°N	-87.02°W	0 - 1500	16S
43-1	HBG5998	<i>A. purpurea</i>	August 5, 2016	Gulf of Mexico	27.00°N	-90.01°W	0 - 1500	16S
43-2	HBG6160	<i>A. purpurea</i>	August 11, 2016	Gulf of Mexico	27.01°N	-88.46°W	0 - 1200	16S
43-3	HBG6169	<i>A. purpurea</i>	August 12, 2016	Gulf of Mexico	26.93°N	-89.43°W	0 - 600	16S
43-4	HBG4460	<i>A. purpurea</i>	August 17, 2015	Gulf of Mexico	27.91°N	-86.95°W	0 - 1500	16S
43-6	HBG5280	<i>A. purpurea</i>	October 16, 2014	Atlantic Ocean	39.83°N	-67.41°W	2159 - 2731	16S
43-7	HBG5996	<i>A. purpurea</i>	July 20, 2016	Florida Straits	25.25°N	-79.48°W	550 - 200	16S
43-8	HBG5281	<i>A. purpurea</i>	October 16, 2014	Atlantic Ocean	39.83°N	-67.41°W	2159 - 2731	16S
1-1	HBG5999	<i>R. robusta</i>	August 5, 2016	Gulf of Mexico	27.00°N	-90.01°W	0 - 550	COI
1-2	HBG3577	<i>R. robusta</i>	May 2, 2015	Gulf of Mexico	29.00°N	-87.01°W	200 - 600	COI
1-3	HBG4447	<i>R. robusta</i>	August 13, 2015	Gulf of Mexico	27.96°N	-87.49°W	0 - 1500	COI
1-4	HBG5865	<i>R. robusta</i>	May 6, 2016	Gulf of Mexico	27.49°N	-86.96°W	600 - 1000	COI
1-5	HBG6196	<i>R. robusta</i>	August 18, 2016	Gulf of Mexico	29.02°N	-87.55°W	0 - 1500	COI
1-6	HBG5779	<i>R. robusta</i>	May 1, 2016	Gulf of Mexico	27.99°N	-87.99°W	0 - 200	COI
1-7	HBG5474	<i>R. robusta</i>	May 2, 2016	Gulf of Mexico	27.99°N	-87.50°W	0 - 1500	COI
1-8	HBG6195	<i>R. robusta</i>	August 17, 2016	Gulf of Mexico	28.53°N	-87.50°W	0 - 1500	COI
3-1	HBG3472	<i>R. robusta</i>	May 6, 2015	Gulf of Mexico	28.00°N	-88.00°W	0 - 1500	COI
3-2	HBG5475	<i>R. robusta</i>	May 2, 2016	Gulf of Mexico	27.99°N	-87.50°W	0 - 1500	COI
3-3	HBG3473	<i>R. robusta</i>	May 6, 2015	Gulf of Mexico	28.00°N	-88.00°W	0 - 1500	COI
3-4	HBG6189	<i>R. robusta</i>	August 16, 2016	Gulf of Mexico	28.03°N	-87.50°W	0 - 600	COI
3-5	HBG6166	<i>R. robusta</i>	August 12, 2016	Gulf of Mexico	26.93°N	-89.43°W	0 - 1500	COI
3-6	HBG3550	<i>R. robusta</i>	May 3, 2015	Gulf of Mexico	28.66°N	-87.55°W	0 - 1500	COI
3-7	HBG5302	<i>R. robusta</i>	October 25, 2014	Atlantic Ocean	39.91°N	-67.42°W	1125 - 2020	COI

3-8	HBG3536	<i>R. robusta</i>	May 3, 2015	Gulf of Mexico	28.66°N	-87.55°W	200 - 600	COI
7-1	HBG3627	<i>R. robusta</i>	May 7, 2015	Gulf of Mexico	28.00°N	-88.50°W	0 - 1500	COI
7-2	HBG5303	<i>R. robusta</i>	October 25, 2014	Atlantic Ocean	39.91°N	-67.42°W	1125 - 2020	COI
7-3	HBG6007	<i>R. robusta</i>	August 7, 2016	Gulf of Mexico	26.89°N	-89.04°W	0 - 1500	COI
7-4	HBG6153	<i>R. robusta</i>	August 9, 2016	Gulf of Mexico	27.00°N	-86.99°W	0 - 600	COI
7-5	HBG3487	<i>R. robusta</i>	May 5, 2015	Gulf of Mexico	28.00°N	-87.46°W	600 - 1000	COI
7-6	HBG5305	<i>R. robusta</i>	October 25, 2014	Atlantic Ocean	39.91°N	-67.42°W	1125 - 2020	COI
7-7	HBG3504	<i>R. robusta</i>	May 5, 2015	Gulf of Mexico	28.00°N	-87.46°W	0 - 1500	COI
7-8	HBG6198	<i>R. robusta</i>	August 18, 2016	Gulf of Mexico	29.02°N	-87.55°W	0 - 1000	COI
12-1	HBG4531	<i>R. robusta</i>	August 20, 2015	Gulf of Mexico	27.47°N	-86.54°W	0 - 1500	COI
12-2	HBG6545	<i>R. robusta</i>	October 22, 2014	Atlantic Ocean	40.07°N	-67.43°W	2050 - 2070	COI
12-3	HBG5476	<i>R. robusta</i>	May 5, 2016	Gulf of Mexico	28.00°N	-87.00°W	0 - 2000	COI
12-4	HBG6551	<i>R. robusta</i>	October 22, 2014	Atlantic Ocean	40.07°N	-67.46°W	2080 - 2115	COI
12-5	HBG5863	<i>R. robusta</i>	May 9, 2016	Gulf of Mexico	26.97°N	-85.93°W	600 - 1000	COI
12-6	HBG4443	<i>R. robusta</i>	August 13, 2015	Gulf of Mexico	27.96°N	-87.49°W	600 - 1000	COI
12-7	HBG3057	<i>R. robusta</i>	October 23, 2014	Atlantic Ocean	39.79°N	-67.38°W	3040 - 3050	COI
12-8	HBG4438	<i>R. robusta</i>	August 16, 2015	Gulf of Mexico	28.55°N	-87.03°W	600 - 750	COI
13-1	HBG6238	<i>R. robusta</i>	August 18, 2016	Gulf of Mexico	29.04°N	-87.46°W	0 - 1500	COI
13-2	HBG6151	<i>R. robusta</i>	August 9, 2016	Gulf of Mexico	27.00°N	-86.99°W	0 - 1500	COI
13-3	HBG4437	<i>R. robusta</i>	August 16, 2015	Gulf of Mexico	28.55°N	-87.03°W	375 - 600	COI
13-4	HBG6183	<i>R. robusta</i>	August 15, 2016	Gulf of Mexico	27.52°N	-87.98°W	0 - 1500	COI
13-5	HBG3050	<i>R. robusta</i>	October 23, 2014	Atlantic Ocean	39.92°N	-67.41°W	1110 - 1245	COI
13-6	HBG4436	<i>R. robusta</i>	August 16, 2015	Gulf of Mexico	28.55°N	-87.03°W	375 - 600	COI
13-7	HBG5794	<i>R. robusta</i>	May 7, 2016	Gulf of Mexico	26.92°N	-86.37°W	600 - 1000	COI
13-8	HBG6240	<i>R. robusta</i>	August 18, 2016	Gulf of Mexico	29.04°N	-87.46°W	0 - 1500	COI
16-1	HBG6239	<i>R. robusta</i>	August 18, 2016	Gulf of Mexico	29.04°N	-87.46°W	0 - 1500	COI
16-2	HBG4418	<i>R. robusta</i>	August 17, 2015	Gulf of Mexico	28.50°N	-86.96°W	600 - 750	COI

16-3	HBG6008	<i>R. robusta</i>	August 7, 2016	Gulf of Mexico	26.89°N	-89.04°W	0 - 200	COI
16-4	HBG3578	<i>R. robusta</i>	May 3, 2015	Gulf of Mexico	29.00°N	-87.50°W	0 - 1500	COI
16-5	HBG6164	<i>R. robusta</i>	August 11, 2016	Gulf of Mexico	26.89°N	-88.51°W	0 - 1500	COI
16-6	HBG6002	<i>R. robusta</i>	August 7, 2016	Gulf of Mexico	26.97°N	-88.97°W	0 - 1500	COI
16-7	HBG3022	<i>R. robusta</i>	October 20, 2014	Atlantic Ocean	39.80°N	-67.48°W	55 - 100	COI
16-8	HBG6558	<i>R. robusta</i>	October 23, 2014	Atlantic Ocean	39.79°N	-67.38°W	3040 - 3050	COI
21-1	HBG3551	<i>R. robusta</i>	May 3, 2015	Gulf of Mexico	28.66°N	-87.55°W	0 - 1500	COI
21-2	HBG3576	<i>R. robusta</i>	May 2, 2015	Gulf of Mexico	29.00°N	-87.01°W	200 - 600	COI
21-3	HBG6550	<i>R. robusta</i>	October 22, 2014	Atlantic Ocean	39.99°N	-67.42°W	1945 - 2205	COI
21-4	HBG5472	<i>R. robusta</i>	May 3, 2016	Gulf of Mexico	27.94°N	-87.50°W	375 - 550	COI
21-5	HBG6544	<i>R. robusta</i>	October 23, 2014	Atlantic Ocean	39.92°N	-67.41°W	1110 - 1245	COI
21-6	HBG5864	<i>R. robusta</i>	May 8, 2016	Gulf of Mexico	26.96°N	-86.41°W	600 - 1000	COI
21-7	HBG4481	<i>R. robusta</i>	August 19, 2015	Gulf of Mexico	27.42°N	-86.99°W	1200 - 1500	COI
21-8	HBG6553	<i>R. robusta</i>	October 22, 2014	Atlantic Ocean	40.07°N	-67.46°W	2080 - 2115	COI
24-1	HBG6192	<i>R. robusta</i>	August 17, 2016	Gulf of Mexico	28.52°N	-87.53°W	0 - 1000	COI
24-2	HBG6556	<i>R. robusta</i>	October 23, 2014	Atlantic Ocean	39.79°N	-67.38°W	3040 - 3050	COI
24-3	HBG3575	<i>R. robusta</i>	May 2, 2015	Gulf of Mexico	29.00°N	-87.01°W	200 - 600	COI
24-4	HBG5304	<i>R. robusta</i>	October 25, 2014	Atlantic Ocean	39.91°N	-67.42°W	1125 - 2020	COI
24-5	HBG5309	<i>R. robusta</i>	October 20, 2014	Atlantic Ocean	39.80°N	-67.48°W	55 - 100	COI
24-7	HBG6552	<i>R. robusta</i>	October 22, 2014	Atlantic Ocean	40.07°N	-67.46°W	2080 - 2115	COI
29-1	HBG6543	<i>R. robusta</i>	October 23, 2014	Atlantic Ocean	39.92°N	-67.41°W	1110 - 1245	COI
29-3	HBG3059	<i>R. robusta</i>	October 20, 2014	Atlantic Ocean	39.80°N	-67.48°W	55 - 100	COI
29-4	HBG6546	<i>R. robusta</i>	October 22, 2014	Atlantic Ocean	40.07°N	-67.43°W	2050 - 2070	COI
29-5	HBG5308	<i>R. robusta</i>	October 20, 2014	Atlantic Ocean	39.80°N	-67.48°W	55 - 100	COI
29-6	HBG6184	<i>R. robusta</i>	August 15, 2016	Gulf of Mexico	27.49°N	-87.97°W	0 - 1500	COI
29-8	HBG3052	<i>R. robusta</i>	October 22, 2014	Atlantic Ocean	40.07°N	-67.43°W	2050 - 2070	COI
37-2	HBG6548	<i>R. robusta</i>	October 22, 2014	Atlantic Ocean	39.99°N	-67.42°W	1945 - 2205	COI

37-3	HBG3046	<i>R. robusta</i>	October 22, 2014	Atlantic Ocean	39.99°N	-67.42°W	1945 - 2205	COI
37-4	HBG6173	<i>R. robusta</i>	August 14, 2016	Gulf of Mexico	27.52°N	-89.00°W	0 - 1000	COI
37-5	HBG6557	<i>R. robusta</i>	October 23, 2014	Atlantic Ocean	39.79°N	-67.38°W	3040 - 3050	COI
37-6	HBG6555	<i>R. robusta</i>	October 23, 2014	Atlantic Ocean	39.79°N	-67.38°W	3040 - 3050	COI
37-8	HBG6549	<i>R. robusta</i>	October 22, 2014	Atlantic Ocean	39.99°N	-67.42°W	1945 - 2205	COI
42-1	HBG5310	<i>R. robusta</i>	October 25, 2014	Atlantic Ocean	39.91°N	-67.42°W	1125 - 2020	COI
42-3	HBG6165	<i>R. robusta</i>	August 11, 2016	Gulf of Mexico	26.89°N	-88.51°W	0 - 600	COI
42-4	HBG6547	<i>R. robusta</i>	October 22, 2014	Atlantic Ocean	40.07°N	-67.43°W	2050 - 2070	COI
42-5	HBG5306	<i>R. robusta</i>	October 25, 2014	Atlantic Ocean	39.91°N	-67.42°W	1125 - 2020	COI
42-6	HBG6019	<i>R. robusta</i>	August 8, 2016	Gulf of Mexico	26.99°N	-87.95°W	0 - 1500	COI
42-8	HBG5307	<i>R. robusta</i>	October 20, 2014	Atlantic Ocean	39.80°N	-67.48°W	55 - 100	COI
43-1	HBG6560	<i>R. robusta</i>	October 23, 2014	Atlantic Ocean	39.79°N	-67.38°W	3040 - 3050	COI
43-2	HBG6559	<i>R. robusta</i>	October 23, 2014	Atlantic Ocean	39.79°N	-67.38°W	3040 - 3050	COI
43-3	HBG6010	<i>R. robusta</i>	August 8, 2016	Gulf of Mexico	27.02°N	-87.98°W	0 - 1500	COI
43-4	HBG6009	<i>R. robusta</i>	August 8, 2016	Gulf of Mexico	27.02°N	-87.98°W	0 - 1500	COI
43-5	HBG6554	<i>R. robusta</i>	October 22, 2014	Atlantic Ocean	40.07°N	-67.46°W	2080 - 2115	COI
43-6	HBG3044	<i>R. robusta</i>	October 22, 2014	Atlantic Ocean	40.07°N	-67.46°W	2080 - 2115	COI
43-7	HBG3053	<i>R. robusta</i>	October 25, 2014	Atlantic Ocean	39.91°N	-67.42°W	1125 - 2020	COI
1-1	HBG6594	<i>S. debilis</i>	July 19, 2016	Florida Straits	25.42°N	-79.59°W	750 - 520	16S
1-2	HBG6606	<i>S. debilis</i>	July 19, 2016	Florida Straits	25.41°N	-79.67°W	380 - 200	16S
1-3	HBG4323	<i>S. debilis</i>	August 9, 2015	Gulf of Mexico	27.02°N	-89.00°W	200 - 600	16S
1-4	HBG3533	<i>S. debilis</i>	May 3, 2015	Gulf of Mexico	28.66°N	-87.55°W	200 - 600	16S
1-5	HBG3534	<i>S. debilis</i>	May 3, 2015	Gulf of Mexico	28.66°N	-87.55°W	200 - 600	16S
1-6	HBG4365	<i>S. debilis</i>	August 9, 2015	Gulf of Mexico	27.01°N	-89.00°W	0 - 215	16S
1-7	HBG4426	<i>S. debilis</i>	August 13, 2015	Gulf of Mexico	27.46°N	-87.47°W	0 - 1500	16S
1-8	HBG6533	<i>S. debilis</i>	August 5, 2016	Gulf of Mexico	27.00°N	-90.01°W	0 - 1000	16S
3-1	HBG6534	<i>S. debilis</i>	August 5, 2016	Gulf of Mexico	27.00°N	-90.01°W	0 - 1000	16S

3-2	HBG6595	<i>S. debilis</i>	July 20, 2016	Florida Straits	25.25°N	-79.48°W	550 - 200	16S
3-3	HBG6607	<i>S. debilis</i>	July 19, 2016	Florida Straits	25.41°N	-79.67°W	380 - 200	16S
3-4	HBG4324	<i>S. debilis</i>	August 9, 2015	Gulf of Mexico	27.02°N	-89.00°W	200 - 600	16S
3-5	HBG3525	<i>S. debilis</i>	May 5, 2015	Gulf of Mexico	28.00°N	-87.46°W	0 - 1500	16S
3-6	HBG5781	<i>S. debilis</i>	May 7, 2016	Gulf of Mexico	26°92°N	-86.37°W	0 - 1500	16S
3-7	HBG4366	<i>S. debilis</i>	August 9, 2015	Gulf of Mexico	27.01°N	-89.00°W	0 - 215	16S
3-8	HBG4427	<i>S. debilis</i>	August 13, 2015	Gulf of Mexico	27.46°N	-87.47°W	0 - 1500	16S
7-1	HBG4497	<i>S. debilis</i>	August 19, 2015	Gulf of Mexico	26.93°N	-87.02°W	200 - 600	16S
7-2	HBG6535	<i>S. debilis</i>	August 5, 2016	Gulf of Mexico	27.00°N	-90.01°W	0 - 1000	16S
7-3	HBG6596	<i>S. debilis</i>	July 20, 2016	Florida Straits	25.25°N	-79.48°W	550 - 200	16S
7-4	HBG6608	<i>S. debilis</i>	July 19, 2016	Florida Straits	25.41°N	-79.67°W	380 - 200	16S
7-5	HBG4346	<i>S. debilis</i>	August 10, 2015	Gulf of Mexico	27.02°N	-89.00°W	0 - 1500	16S
7-6	HBG3033	<i>S. debilis</i>	October 25, 2014	Atlantic Ocean	39.91°N	-67.42°W	1130 - 2020	16S
7-7	HBG6541	<i>S. debilis</i>	August 7, 2016	Gulf of Mexico	26.97°N	-88.97°W	0 - 600	16S
7-8	HBG4367	<i>S. debilis</i>	August 9, 2015	Gulf of Mexico	27.01°N	-89.00°W	0 - 215	16S
12-1	HBG6536	<i>S. debilis</i>	August 8, 2016	Gulf of Mexico	27.02°N	-87.98°W	0 - 1500	16S
12-2	HBG4306	<i>S. debilis</i>	August 11, 2015	Gulf of Mexico	27.00°N	-88.00°W	0 - 1500	16S
12-3	HBG4498	<i>S. debilis</i>	August 19, 2015	Gulf of Mexico	26.93°N	-87.02°W	200 - 600	16S
12-4	HBG6597	<i>S. debilis</i>	July 20, 2016	Florida Straits	25.25°N	-79.48°W	550 - 200	16S
12-5	HBG6609	<i>S. debilis</i>	July 19, 2016	Florida Straits	25.41°N	-79.67°W	380 - 200	16S
12-6	HBG4347	<i>S. debilis</i>	August 10, 2015	Gulf of Mexico	27.02°N	-89.00°W	0 - 1500	16S
12-7	HBG6381	<i>S. debilis</i>	August 12, 2016	Gulf of Mexico	26.99°N	-89.47°W	0 - 1500	16S
12-8	HBG3401	<i>S. debilis</i>	May 7, 2015	Gulf of Mexico	28.00°N	-88.50°W	0 - 1500	16S
13-1	HBG4399	<i>S. debilis</i>	August 14, 2015	Gulf of Mexico	27.91°N	-87.42°W	0 - 1500	16S
13-2	HBG6531	<i>S. debilis</i>	August 9, 2016	Gulf of Mexico	27.01°N	-86.98°W	0 - 1000	16S
13-3	HBG4307	<i>S. debilis</i>	August 11, 2015	Gulf of Mexico	27.00°N	-88.00°W	0 - 1500	16S
13-4	HBG4505	<i>S. debilis</i>	August 20, 2015	Gulf of Mexico	26.94°N	-87.00°W	1000 - 600	16S

13-5	HBG3414	<i>S. debilis</i>	May 6, 2015	Gulf of Mexico	28.00°N	-88.00°W	200 - 600	16S
13-6	HBG6598	<i>S. debilis</i>	July 20, 2016	Florida Straits	25.25°N	-79.48°W	550 - 200	16S
13-7	HBG6382	<i>S. debilis</i>	August 12, 2016	Gulf of Mexico	26.99°N	-89.47°W	0 - 1500	16S
13-8	HBG3605	<i>S. debilis</i>	May 1, 2015	Gulf of Mexico	29.00°N	-87.01°W	0 - 1500	16S
16-1	HBG3601	<i>S. debilis</i>	May 2, 2015	Gulf of Mexico	28.01°N	-87.01°W	600 - 1000	16S
16-2	HBG4435	<i>S. debilis</i>	August 16, 2015	Gulf of Mexico	28.55°N	-87.03°W	0 - 750	16S
16-3	HBG6468	<i>S. debilis</i>	August 10, 2016	Gulf of Mexico	27.01°N	-87.49°W	0 - 1500	16S
16-4	HBG4308	<i>S. debilis</i>	August 11, 2015	Gulf of Mexico	27.00°N	-88.00°W	0 - 1500	16S
16-5	HBG4506	<i>S. debilis</i>	August 20, 2015	Gulf of Mexico	26.94°N	-87.00°W	1000 - 600	16S
16-6	HBG3034	<i>S. debilis</i>	October 21, 2014	Atlantic Ocean	40.18°N	-67.44°W	1920 - 1940	16S
16-7	HBG6599	<i>S. debilis</i>	July 20, 2016	Florida Straits	25.25°N	-79.48°W	550 - 200	16S
16-8	HBG6383	<i>S. debilis</i>	August 12, 2016	Gulf of Mexico	26.99°N	-89.47°W	0 - 1500	16S
21-1	HBG4322	<i>S. debilis</i>	August 9, 2015	Gulf of Mexico	27.02°N	-89.00°W	200 - 600	16S
21-2	HBG6384	<i>S. debilis</i>	August 12, 2016	Gulf of Mexico	26.99°N	-89.47°W	0 - 1500	16S
21-3	HBG4236	<i>S. debilis</i>	May 2, 2015	Gulf of Mexico	29.00°N	-87.01°W	0 - 200	16S
21-5	HBG6373	<i>S. debilis</i>	August 11, 2016	Gulf of Mexico	27.01°N	-88.46°W	0 - 1500	16S
21-6	HBG4451	<i>S. debilis</i>	August 12, 2015	Gulf of Mexico	27.49°N	-87.49°W	0 - 1500	16S
21-7	HBG3035	<i>S. debilis</i>	October 21, 2014	Atlantic Ocean	40.18°N	-67.44°W	1920 - 1940	16S
21-8	HBG6600	<i>S. debilis</i>	July 21, 2016	Florida Straits	25.16°N	-79.56°W	750 - 550	16S
24-1	HBG6601	<i>S. debilis</i>	July 21, 2016	Florida Straits	25.16°N	-79.56°W	750 - 550	16S
24-2	HBG6286	<i>S. debilis</i>	August 12, 2016	Gulf of Mexico	26.99°N	-89.47°W	0 - 1000	16S
24-4	HBG6472	<i>S. debilis</i>	August 14, 2016	Gulf of Mexico	27.51°N	-89.01°W	0 - 1500	16S
24-6	HBG4419	<i>S. debilis</i>	August 17, 2015	Gulf of Mexico	28.50°N	-86.97°W	380 - 600	16S
24-8	HBG3056	<i>S. debilis</i>	October 20, 2014	Atlantic Ocean	39.80°N	-67.48°W	55 - 100	16S
29-1	HBG6589	<i>S. debilis</i>	October 20, 2014	Atlantic Ocean	39.80°N	-67.48°W	55 - 100	16S
29-2	HBG6602	<i>S. debilis</i>	July 21, 2016	Florida Straits	25.16°N	-79.56°W	750 - 550	16S
29-3	HBG4381	<i>S. debilis</i>	August 18, 2015	Gulf of Mexico	27.93°N	-86.96°W	600 - 850	16S

29-4	HBG5760	<i>S. debilis</i>	May 1, 2016	Gulf of Mexico	27.89°N	-86.87°W	0 - 1500	16S
29-5	HBG6279	<i>S. debilis</i>	August 15, 2016	Gulf of Mexico	27.49°N	-87.97°W	0 - 200	16S
29-8	HBG3585	<i>S. debilis</i>	May 3, 2015	Gulf of Mexico	29.00°N	-87.50°W	0 - 1500	16S
37-2	HBG6590	<i>S. debilis</i>	October 20, 2014	Atlantic Ocean	39.80°N	-67.48°W	55 - 100	16S
37-3	HBG6603	<i>S. debilis</i>	July 19, 2016	Florida Straits	25.42°N	-79.65°W	700 - 500	16S
37-4	HBG4509	<i>S. debilis</i>	August 18, 2015	Gulf of Mexico	27.45°N	-86.99°W	200 - 600	16S
37-5	HBG5761	<i>S. debilis</i>	May 2, 2016	Gulf of Mexico	27°96°N	-87.99°W	600 - 1000	16S
37-6	HBG6227	<i>S. debilis</i>	August 16, 2016	Gulf of Mexico	28.01°N	-87.51°W	0 - 1500	16S
42-3	HBG6591	<i>S. debilis</i>	October 20, 2014	Atlantic Ocean	39.80°N	-67.48°W	55 - 100	16S
42-4	HBG6604	<i>S. debilis</i>	July 18, 2016	Florida Straits	25.42°N	-79.65°W	700 - 500	16S
42-5	HBG4528	<i>S. debilis</i>	August 20, 2015	Gulf of Mexico	27.45°N	-86.54°W	0 - 1500	16S
42-6	HBG5479	<i>S. debilis</i>	May 2, 2016	Gulf of Mexico	27.99°N	-87.50°W	200 - 600	16S
42-7	HBG6428	<i>S. debilis</i>	August 17, 2016	Gulf of Mexico	28.52°N	-87.53°W	0 - 1500	16S
43-1	HBG6394	<i>S. debilis</i>	August 18, 2016	Gulf of Mexico	29.02°N	-87.55°W	0 - 1500	16S
43-2	HBG4459	<i>S. debilis</i>	August 17, 2015	Gulf of Mexico	27.91°N	-86.95°W	200 - 600	16S
43-4	HBG6592	<i>S. debilis</i>	October 20, 2014	Atlantic Ocean	39.80°N	-67.48°W	55 - 100	16S
43-5	HBG6605	<i>S. debilis</i>	July 19, 2016	Florida Straits	25.41°N	-79.67°W	380 - 200	16S
43-7	HBG4529	<i>S. debilis</i>	August 20, 2015	Gulf of Mexico	27.45°N	-86.54°W	0 - 1500	16S
43-8	HBG5442	<i>S. debilis</i>	May 4, 2016	Gulf of Mexico	27.89°N	-86.88°W	0 - 1500	16S

CHAPTER VI
CONCLUSIONS AND FUTURE DIRECTIONS

The series of works I have presented here were completed with the goal of increasing our understanding of crustacean evolution, from one end of the evolutionary spectrum to the other. Beginning with a review of the literature on phylogenetic relationships between decapod infraorders, I continue with a phylogenetic analysis of the genus *Farfantepenaeus*, wherein I also investigate cryptic diversity. In Chapters IV and V, I transitioned to population genetics in two frequently over-looked environments in the Gulf of Mexico: evaluating a potential glacial refugium for *Bathynomus giganteus* in the benthic abyss and establishing biological baselines for three species of mesopelagic shrimp. These studies emphasize the importance of considering the environmental factors that are potentially impacting population dynamics and evolutionary histories of crustaceans.

In the literature review I performed in Chapter II, I recount the history of attempts to classify the infraorders of Decapoda (Timm & Bracken-Grissom, 2015). I find that morphological and molecular phylogenies have generated a suite of evolutionary hypotheses for deep relationships, with some accord reached. The major lineages Dendrobranchiata, Caridea, Stenopodidea, and the “non-swimming” Reptantia, are consistently recovered; with Dendrobranchiata falling as the most ancient lineage and the reptant infraorders (Achelata, Anomura, Astacidea, Axiidea, Brachyura, Gebiidea, Glypheidea, Polychelida) falling as derived lineages. Caridea and Stenopodidea are consistently found to be closely related, sometimes recovered as sisters, sometimes as close relatives. Among the reptant decapods, Anomura and Brachyura are nearly always recovered as sisters in a derived position on the Decapod Tree of Life. However, the lobster and lobster-like lineages Polychelida, Glypheidea, Achelata, and Astacidea are a

source of disagreement, either forming a monophyletic (Bybee et al., 2011; Chu et al., 2009; Qian et al., 2011; Toon et al., 2009; Tsang et al., 2008) or a non-monophyletic clade (Ahyong & Meally, 2004; Bracken-Grissom et al., 2014; Bracken et al., 2009; Bracken et al., 2010; Porter et al., 2005; Shen et al., 2013). Previously classified as the now un-accepted Thalassinidea, ghost shrimp were divided into Axiidea and Gebiidea, but the two infraorders do not consistently fall as sisters (Bracken et al., 2009; Chu et al., 2009, Porter et al., 2005; Shen et al., 2013; Tsang et al., 2008).

In evaluating infraordinal phylogenies for four points of concern (sampling effort, marker selection, data-recycling, and the particulars of phylogenetic analysis procedure) I found that studies have been trending toward consistency in design and execution, making comparison of phylogenies much easier. Perhaps the biggest insight gained from the literature review is the need to carefully consider these four points of concern before the study begins and to detail both study design and the justification for these choices within the manuscript (or supplementary materials).

As in most taxa, the future of phylogenetic studies in decapods lies in next-generation sequencing (NGS). These powerful methods address a consistent challenge in phylogenetic analysis: the need for more molecular markers across a more representative range of the genome. A NGS study can generate hundreds, thousands, even tens of thousands of markers for analysis, in the form of single-nucleotide polymorphisms (SNPs), which are quickly becoming the marker of choice for phylogenetic and population genetic studies (Brito & Edwards, 2009; Brumfield et al., 2003; Morin et al., 2004). However, the field is currently experiencing something of a Red Queen paradox: improvements in marker generation must be paired with models that are capable of

dealing with these vast amounts of data, differentiating noise from signal, and of course recapitulating evolutionary relationships based on this signal.

I put what the knowledge I had gained through the literature review into practice in Chapter III, performing the first comprehensive phylogeny of the genus *Farfantepenaeus*. Despite this difference in species included in the study, the phylogenetic relationships I recovered agreed well with previous molecular studies (Lavery et al. 2004; Voloch et al. 2005). Due to the described biogeographic break between the Gulf of Mexico and the greater Atlantic Ocean, the two species with ranges crossing this break (*F. duorarum* and *F. brasiliensis*) were well represented with individuals from both basins (see review by Avise 1992 and Young et al. 2002 for a decapod-specific example) as I investigated cryptic speciation. My results indicated previously undescribed population structure in *F. brasiliensis*, dividing the species into a northern (Gulf of Mexico and higher latitudes) and southern (latitudes below the Gulf) clade. Further investigation of genetic distance between these clades suggested they may represent distinct sub-species and warrant separate management approaches. I also found a lack of evidence for the species status of *F. notialis*, which was originally described as a sub-species of *F. duorarum*. However, this sister-species relationship may be resolved with the addition of nuclear markers (Timm & Bracken-Grissom, 2015). This could not be achieved in Chapter III due to a lack of voucher specimens.

Future efforts should focus on bolstering genetic markers, both in number and source (nuclear, intronic, etc.), as well as on the discovery and inclusion of diagnostic morphological characters. This approach, commonly referred to as the “total evidence” approach, would likely provide resolution to polytomies within the *Farfantepenaeus* tree

and may allow for time calibration of the phylogeny. Furthermore, thorough sampling along species' ranges would better elucidate the biogeographic factors facilitating speciation in the genus (Ayre et al. 2009). A robust *Farfantepenaeus* phylogeny could be critical to identifying evolutionarily significant units (ESUs) and prioritizing management considerations (Ryder 1986). Historically, ESUs have been defined by reproductive isolation (Waples 1991), but this may result in neglect of other mechanisms maintaining adaptive diversity (Crandall et al. 2000). As such, future research efforts in the realm of farfantepenaeid evolution should focus on characterizing phylogeographic patterns and testing the roles of environmental factors (e.g. currents and geological events) and economic pressures (e.g. fishing pressures and active species management efforts) in establishing and maintaining these patterns.

Such an investigation was undertaken for the giant deep-sea isopod, *Bathynomus giganteus* in Chapter IV. Taking a “hybrid approach”, including traditional Sanger sequencing molecular data as well as a pilot study generating double digest Restriction site-Associated DNA sequencing (ddRADseq) data, this study investigated the role of current and historical environment in maintaining population dynamics of this benthic deep-sea invertebrate through the last glacial maximum (Timm et al., 2018). I specifically investigated De Soto Canyon as a potential glacial refugium and benthic habitat diversity of the substrate in the northern Gulf of Mexico. While population differentiation was low, likely maintained by high connectivity, diversity was lowest in the canyon. This suggests that habitat diversity may be more influential in population dynamics in *B. giganteus*, rather than the presence of a putative glacial refugium in De Soto Canyon. Chapter IV

illuminates population dynamics of a charismatic deep-sea invertebrate in the region and increases our understanding of an often over-looked environment.

In Chapter V, I continued my NGS investigation into the environmental factors that contribute to the state and flux of genetic diversity within the Gulf of Mexico. Here, I turned my attention to another persistently under-studied region: the mesopelagic (200m-1000m). The initial goal of the study was to establish biological baselines for the region and confirm whether the Gulf of Mexico was genetically “open”, that is whether migrants could move freely between the Gulf and the greater Atlantic. However, in describing the natural variability in the region, I uncovered a negative correlation between surface abundance and genetic diversity. This led me to consider the role of the Gulf Loop Current in facilitating gene flow between basins: diel vertical migration, the movement of individuals into shallower epipelagic waters at night, results in substantial surface abundances in mesopelagic species which is likely to expose them to the fastest moving waters of the Gulf Loop Current and increase movement of individuals between basins. This could also maintain a single population spanning the Gulf and Atlantic, homogenizing if not functionally preventing local adaptation and population differentiation.

In many ways, this study only begins to hint at the mechanisms influencing natural variability in the Gulf. The establishment of baselines for genetic diversity and connectivity is crucial to understanding the Gulf and for future appraisal of damages following disturbance events. However in this study, sample sizes of *Robustosergia robusta*, which exhibited lowest surface abundance of the three species included in the study, were small enough to bring the results under heightened scrutiny and required

cautious interpretation. More individuals of these species must be included, as well as additional species from a broader taxonomic distribution.

The evolutionary history of any species in any timeframe is highly dependent on gene flow – the exchange of genetic information within and between groups of conspecific individuals. By better understanding gene flow in marine crustaceans, identifying the environmental factors impacting the state and flux of genetic diversity in these taxa, and seeking to understand the mechanisms by which these relationships are maintained, we gain great insight and substantially increase our knowledge of Crustacea and the evolutionary processes operating therein.

LITERATURE CITED

- Ahyong, S. T., & Meally, D. O. (2004). Phylogeny of the Decapoda Reptantia: resolution using three molecular loci and morphology. *The Raffles Bulletin of Zoology*, 52, 673–693.
- Avise, J. C. (1992). Molecular population structure and the biogeographic history of a regional fauna: a case history with lessons for conservation biology. *Oikos*, 63, 62–76.
- Ayre, D. J., Minchinton, T. E., & Perrin, C. (2009). Does life history predict past and current connectivity for rocky intertidal invertebrates across a marine biogeographic barrier? *Molecular Ecology*, 18, 1887–1903.
- Bracken-Grissom, H. D., Ahyong, S. T., Wilkinson, R. D., Feldmann, R. M., Schweitzer, C. E., Breinholt, J. W., ... Crandall, K. A. (2014). The emergence of the lobsters: phylogenetic relationships, morphological evolution and divergence time comparisons of an ancient group (Decapoda: Achelata, Astacidea, Glypheidea, Polychelida). *Systematic Biology*, 63, 457–479.
- Bracken, H. D., De Grave, S., & Felder, D. L. (2009). Phylogeny of the infraorder Caridea based on mitochondrial and nuclear genes (Crustacea: Decapoda). In *Decapod Crustacean Phylogenetics* (Vol. 18, pp. 281–305).

- Bracken, H. D., De Grave, S., Toon, A., Felder, D. L., & Crandall, K. A. (2010). Phylogenetic position, systematic status, and divergence time of the Procarididea (Crustacea: Decapoda). *Zoologica Scripta*, *39*, 198–212.
- Bracken, H. D., Toon, A., Felder, D. L., Martin, J. W., Finley, M., Rasmussen, J., ... Crandall, K. A. (2009). The decapod tree of life: Compiling the data and moving toward a consensus of decapod evolution. *Arthropod Systematics & Phylogeny*, *67*, 99–116.
- Brito, P. H., & Edwards, S. V. (2009). Multilocus phylogeography and phylogenetics using sequence-based markers. *Genetica*, *135*, 439–455.
- Brumfield, R. T., Beerli, P., Nickerson, D. A., & Edwards, S. V. (2003). The utility of single nucleotide polymorphisms in inferences of population history. *Trends in Ecology and Evolution*, *18*, 249–256.
- Bybee, S. M., Bracken-Grissom, H. D., Hermansen, R. A., Clement, M. J., Crandall, K. A., & Felder, D. L. (2011). Directed next generation sequencing for phylogenetics: An example using Decapoda (Crustacea). *Zoologischer Anzeiger*, *250*, 497–506.
- Chu, K. H., Tsang, L.-M., Ma, K. Y., Chan, T.-Y., & Ng, P. K. L. (2009). Decapod phylogeny: what can protein-coding genes tell us? In *Decapod Crustacean Phylogenetics* (Vol. 18, pp. 89-99).
- Crandall, K. A., Bininda-Emonds, O. R. R., Mace, G. M., & Wayne, R. K. (2000). Considering evolutionary processes in conservation biology. *Trends in Ecology and Evolution*, *15*, 290–295.
- Lavery, S., Chan, T. Y., Tam, Y. K., & Chu, K. H. (2004). Phylogenetic relationships and evolutionary history of the shrimp genus *Penaeus* s.l. derived from mitochondrial DNA. *Molecular Phylogenetics and Evolution*, *31*, 39–49.
- Morin, P. A., Luikart, G., & Wayne, R. K. (2004). SNPs in ecology, evolution and conservation. *Trends in Ecology and Evolution*, *19*, 208–216.
- Porter, M. L., Pérez-Losada, M., & Crandall, K. A. (2005). Model-based multi-locus estimation of decapod phylogeny and divergence times. *Molecular Phylogenetics*
- Qian, G., Zhao, Q., Wang, A. N., Zhu, L., Zhou, K., & Sun, H. (2011). Two new decapod (Crustacea, Malacostraca) complete mitochondrial genomes: bearings on the phylogenetic relationships within the Decapoda. *Zoological Journal of the Linnean Society*, *162*, 471–481.

- Ryder, O. A. (1986). Species conservation and systematics: the dilemma of subspecies. *Trends in Ecology and Evolution*, *1*, 9–10.
- Shen, H., Braband, A., & Scholtz, G. (2013). Mitogenomic analysis of decapod crustacean phylogeny corroborates traditional views on their relationships. *Molecular Phylogenetics and Evolution*, *66*, 776–789.
- Timm, L. E., & Bracken-Grissom, H. D. (2015). The forest for the trees: evaluating molecular phylogenies with an emphasis on higher-level Decapoda. *Journal of Crustacean Biology*, *35*, 577–592.
- Timm, L. E., Moahamed, B., Churchill, D. A., & Bracken-Grissom, H. D. (2018). *Bathynomus giganteus* (Isopoda: Cirolanidae) and the canyon: a population genetics assessment of De Soto Canyon as a glacial refugium for the giant deep-sea isopod. *Hydrobiologia*, 1-15.
- Toon, A., Finley, M., Staples, J., Crandall, K. A., & Koenemann, S. (2009). Decapod phylogenetics and molecular evolution. In *Decapod Crustacean Phylogenetics* (Vol. 18, pp. 15–29).
- Tsang, L. M., Ma, K. Y., Ahyong, S. T., Chan, T. Y., & Chu, K. H. (2008). Phylogeny of Decapoda using two nuclear protein-coding genes: Origin and evolution of the Reptantia. *Molecular Phylogenetics and Evolution*, *48*, 359–368.
- Voloch, C. M., Freire, P. R., & Russo, C. A. M. (2005). Molecular phylogeny of penaeid shrimps inferred from two mitochondrial markers. *Genetics and Molecular Research*, *4*, 668–674.
- Waples, R. S. (1991). Pacific Salmon, *Oncorhynchus spp.*, and the definition of “species” under the Endangered Species Act. *Marine Fisheries Review*, *53*, 11–22.
- Young, A. M., Torres, C., Mack, J. E., & Cunningham, C. W. (2002). Morphological and genetic evidence for vicariance and refugium in Atlantic and Gulf of Mexico populations of the hermit crab *Pagurus longicarpus*. *Marine Biology*, *140*, 1059–1066.

VITA

LAURA E TIMM

2008-2012	B.S., Marine Biology Texas A&M University at Galveston Galveston, Texas
2013-2018	Doctoral Candidate Florida International University Miami, Florida
2013-2016	Presidential Fellow Florida International University Miami, Florida
2016-2017	Doctoral Evidence Acquisition Fellow (awarded twice) Florida International University Miami, Florida
2016	Awarded Scholar Gulf of Mexico Research Initiative
2017	Graduate Student of the Year Award Florida International University Miami, Florida
2017	Masters <i>en route</i> to Ph. D. Florida International University Miami, Florida
2018	Dissertation Year Fellow Florida International University Miami, Florida

PUBLICATIONS AND PRESENTATIONS

Timm, LE, B Moahamed, DA Churchill, HD Bracken-Grissom (2018) *Bathynomus giganteus* (Isopoda: Cirolanidae) and the canyon: a population genetics assessment of Desoto Canyon as a glacial refugium for the giant deep-sea isopod. *Hydrobiologia* Special Issue: Crustacean Genomics. *In Press*.

- Timm, LE and HD Bracken-Grissom (2015) The forest for the trees: evaluating molecular phylogenies with an emphasis on higher-level *Decapoda*. *Journal of Crustacean Biology* 35(5): 577-592.
- Schulze, A, A Maiorova, LE Timm, and ME Rice (2012) Sipunculan larvae and “cosmopolitan” species. *Integrative and Comparative Biology* 52(4): 497-510.
- Schulze A and LE Timm (2011) *Palola* and *un*: distinct clades in the genus *Palola* (Eunicidae, Polychaeta). *Marine Biodiversity* 42(2): 161-171.
- Timm, LE, H Judkins, A Sosnowski, M Vecchione, and HD Bracken-Grissom. DEEPEND: Does the Atlantic serve as a genetic reservoir for the Gulf of Mexico? A comparative population genomics investigation of six midwater invertebrate species. Gulf of Mexico Oil Spill & Ecosystem Science Conference, New Orleans, LA, February 2018 (oral presentation).
- Timm, LE, L Isma, and HD Bracken-Grissom. Population genomics of the mesopelagic shrimp *Sergia robusta* suggests resilience in the Gulf of Mexico following a major anthropogenic disturbance. Crustacean Society Mid-Year Meeting, Barcelona, Spain, June 2017 (invited oral presentation, awarded Best Student Oral Presentation).
- Timm, LE and HD Bracken-Grissom. DEEPEND: Comparative population genomics of mesopelagic shrimp to diagnose long-term changes to ecosystem health and resilience in the Gulf of Mexico. Gulf of Mexico Oil Spill & Ecosystem Science Conference, New Orleans, LA, February 2017 (oral presentation).
- Timm, LE and HD Bracken-Grissom. Diversity and connectivity of mesopelagic shrimp as proxies for ecosystem health and recovery in the Gulf of Mexico. Florida International University Biosymposium, North Miami, FL, February 2016 (poster presentation, awarded 3rd Place in Poster Competition); Gulf of Mexico Oil Spill & Ecosystem Science Conference, Tampa, FL, February 2016 (poster presentation).
- Timm, LE and D Grünbaum. Effects of blastocoel geometry and density on swimming ability in early-stage larvae. Society of Integrative and Comparative Biology Meeting, Charleston, SC, January 2012 (poster presentation).
- Timm, LE and A Schulze. A phylogenetic analysis of *Palola viridis* using cytochrome c oxidase subunit I (COI) and 16S rRNA genes. Texas A&M University at Galveston Student Research Symposium, Galveston, TX, April 2010 (poster presentation, awarded 1st Place in Marine Biology Poster Competition and 3rd Place in Overall Poster Competition); Tri Beta Biological Honors Society Southcentral Regional Conference, Ardmore, OK, May 2010 (poster presentation).